

43  
AFCRL-67-0518  
SEPTEMBER 1967  
SPECIAL REPORTS, NO. 67

AD 662876



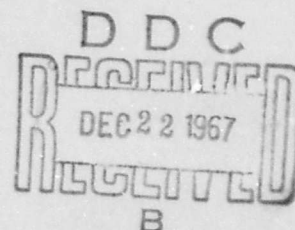
## AIR FORCE CAMBRIDGE RESEARCH LABORATORIES

L. G. HANSCOM FIELD, BEDFORD, MASSACHUSETTS

### Bibliography of Lunar and Planetary Research Supplement No. 2-1966

Editor  
J.W. SALISBURY

Contributors  
J.E.M. ADLER  
J.P. DYBWAD  
G.R. HUNT  
L.B. RONCA  
H.P. ROSS  
J.W. SALISBURY  
W.R. VAN SCHMUS



OFFICE OF AEROSPACE RESEARCH  
United States Air Force



Reproduced by the  
CLEARINGHOUSE  
for Federal Scientific & Technical  
Information Springfield Va. 22151

237

AFCRL-67-0518  
SEPTEMBER 1967  
SPECIAL REPORTS, NO. 67



SPACE PHYSICS LABORATORY PROJECT 8602

**AIR FORCE CAMBRIDGE RESEARCH LABORATORIES**

L. G. HANSCOM FIELD, BEDFORD, MASSACHUSETTS

## **Bibliography of Lunar and Planetary Research Supplement No. 2-1966**

**Editor**

**J.W. SALISBURY**

**Contributors**

**J.E.M. ADLER**

**J.P. DYBWAD**

**G.R. HUNT**

**L.B. RONCA**

**H.P. ROSS**

**J.W. SALISBURY**

**W.R. VAN SCHMUS**

Distribution of this document is unlimited. It may be released to the Clearinghouse, Department of Commerce, for sale to the general public.

**OFFICE OF AEROSPACE RESEARCH**

**United States Air Force**



## **Abstract**

→ A bibliography of lunar and planetary research articles published during 1966 is presented with both subject and author listings. The major subject categories are: astrobiology, comets, meteorite craters and cratering effects, meteors and meteorites, the moon, origin of the solar system, the planets, and tektites. Each article is abstracted. ↑

## **Acknowledgments**

The editor and compilers gratefully acknowledge the assistance of Karen S. Harbert in preparation of the manuscript.

## Contents

1. INTRODUCTION	1
2. ARTICLES LISTED BY AUTHOR	3
3. ARTICLES LISTED BY SUBJECT	47
3.1 Astrobiology	47
3.2 Comets	50
3.3 Meteorite Craters and Cratering Effects	61
3.4 Meteors and Meteorites	68
3.5 Moon	108
3.5.1 General	108
3.5.2 Atmosphere	110
3.5.3 Figure and Internal Structure	111
3.5.4 Changes	115
3.5.5 Surface Features	119
3.5.6 Surface Materials	131
3.5.7 Temperature	154
3.5.8 Topography	159
3.6 Origin of the Solar System	162



## Contents

3.7 Planets	164
3.7.1 General	164
3.7.2 Asteroids	168
3.7.3 Jupiter	169
3.7.4 Mars	183
3.7.5 Mercury	198
3.7.6 Neptune	201
3.7.7 Pluto	202
3.7.8 Saturn	203
3.7.9 Uranus	207
3.7.10 Venus	210
3.8 Tektites	221

## **Bibliography of Lunar and Planetary Research Supplement No. 2-1966**

### **1. Introduction**

Reports of lunar and planetary research are disseminated throughout a large number and wide variety of periodicals, making it difficult for one to be sure that he has read all that has been published, or to start a literature search. This bibliography is intended to provide the best possible coverage of this field for 1966, with the additional benefits of listings by both subject and author, and of complete abstracts.

Similar bibliographies have been published for the years 1960-1965, and a limited number of copies of these bibliographies are available upon request.\* The list of journals regularly searched to compile the bibliography is listed below. Inevitably some articles have been overlooked and, when these are pointed out to the editor, they are added to the following year supplement. It is hoped that the interested reader will feel free to make suggestions to the editor for improving future editions.

---

(Received for publication 14 August 1967)

\* The basic bibliography, for the period 1960-1964 was published in January 1966 as Special Report No. 40(AFCRL-66-42). The first supplement, for 1965, was published in January 1967 as Special Report No. 55(AFCRL-67-0043).

Journals searched during 1966 in compiling this bibliography are:

American Journal of Science  
American Mineralogist  
American Scientist  
Annales d'Astrophysique  
Astronomical Journal  
Astronomische Nachrichten  
Astrophysical Journal  
Australian Journal of Physics  
Bulletin of the Astronomical Institutes of the Netherlands  
Communications of the Lunar and Planetary Laboratory  
Earth and Planetary Science Letters  
Geochemistry International  
Geochimica et Cosmochimica Acta  
Geological Society of America Bulletin  
Geophysical Journal of the Royal Astronomical Society  
Icarus  
Journal of Applied Optics  
Journal of Geophysical Research  
Journal of the Optical Society of America  
Meteoritics  
Mineralogical Magazine  
Monthly Notices of the Royal Astronomical Society  
Nature (London)  
Planetary and Space Science  
Proceedings of the National Academy of Sciences  
Publications of the Astronomical Society of Japan  
Publications of the Astronomical Society of the Pacific  
Quarterly Journal of the Geological Society of London  
Reviews of Geophysics  
Science  
Sky and Telescope  
Smithsonian Astrophysical Observatory Report  
Soviet Astronomy - A.J.  
Tectonophysics  
Transactions of the American Geophysical Union  
Zeitschrift für Astrophysik

## 2. Articles Listed by Author

- A'Hearn, M.F., 1964, C<sub>2</sub> densities in comet Mrkos (1955 III): Publications of the Astronomical Society of the Pacific, V. 76, p. 106-109.
- Akaiwa, H., 1966, Abundances of selenium, tellurium, and indium in meteorites: Journal of Geophysical Research, V. 71, p. 1919-1923.
- Alexander, S.S., 1966 - see Dupee, W.D.
- Alkezweeny, A.J., and Hobbs, P.V., 1966, The reflection spectrum of ice in the near infrared: Journal of Geophysical Research, V. 71, p. 1083-1086.
- Allen, R.O., Jr., 1966 - see Reed, G.W., Jr.
- Allen, R.V., 1966 - see Aronson, J.R.
- Allen, R.V., 1966 - see Vonnegut, B.
- Allen, R.V., 1966 - see Wright, F.W.
- Ananthakrishnan, R., 1966, Meteor luminosity and meteor ionization: Nature, V. 210, p. 402-403.
- Anders, E., 1965, Chemical fractionation in meteorites: Akademia Nauk SSSR Meteoritika, No. 26, p. 17-25.
- Anders, E., and Lipschutz, M.E., 1966, Critique of paper by N.L. Carter and G.C. Kennedy, "Origin of diamonds in the Canyon Diablo and Novo Urei meteorites": Journal of Geophysical Research, V. 71, p. 643-661.
- Anders, E., 1966 - see Haymann, D.
- Anderson, D.L., and Kovach, R.L., 1966, The interiors of the moon and terrestrial planets: Transactions of the American Geophysical Union, V. 47, No. 1, p. 155.
- Anderson, D.L., and Phinney, R.A., 1966, The early thermal history of the earth and the terrestrial planets: Transactions of the American Geophysical Union, V. 47, No. 1, p. 185.

- Annell, C., 1966 - see Chao, E.C.T.
- Anonymous, 1966, Great lakes fireball: Sky and Telescope, V. 31, p. 78-79 and 82.
- Anonymous, 1966, Lunar orbiter photographs earth and moon: Sky and Telescope, V. 32, p. 346-347 and fold out.
- Anonymous, 1966, New comet Kilston (1966b): Sky and Telescope, V. 32, p. 191.
- Anonymous, 1966, Photographs of comet Ikeya-Seki II: Sky and Telescope, V. 31, p. 20-23.
- Anonymous, 1966, Splendid April 25th fireball: Sky and Telescope, V. 31, p. 324-326.
- Anonymous (L.J.R.), 1966, Observers page, Reports of comet Ikeya-Seki (1965f): Sky and Telescope, V. 31, p. 52-56.
- Applebaum, D.C., Harteck, P., Reeves, R.R., Jr., and Thompson, B.A., 1966, Some comments on the Venus temperature: Journal of Geophysical Research, V. 71, p. 5541-5545.
- Arking, A., and Potter, J., 1966, Calculated light curves for models of the Venus atmosphere: The Astronomical Journal, V. 71, p. 154.
- Aronson, J.R., Emslie, A.G., Allen, R.V., and McLinden, H.G., 1966, Far infrared studies of minerals for application in remote compositional mapping of the moon and planets: Transactions of the American Geophysical Union, V. 47, No. 1, p. 155.
- Arthur, D.W.G., Pellicori, R.H., and Wood, C.A., 1966, The system of lunar craters. Quadrant IV: Communications of the Lunar and Planetary Laboratory, V. 5, p. 1-208, +12 pages maps.
- Ash, M.E., 1966 - see Smith, W.B.
- Ashbee, K.H.G., and Vassamillet, L.F., 1966, Dislocation in a Campo del Cielo meteorite: Science, V. 151, p. 1526-1527.
- Ashy, N., 1966, Energy balance on the lunar surface: Publications of the Astronomical Society of the Pacific, V. 78, p. 254-255.
- Bart, E.E., Barrow, C.H., and Lee, R.T., 1966, Burst structure of Jupiter's decametric radiation: The Astronomical Journal, V. 71, p. 377-378.
- Bart, E.E., Barrow, C.H., and Lee, R.T., 1966, Millisecond radio pulses from Jupiter: Nature, V. 211, p. 808.
- Bader, M., Haughney, L.C., and Innes, R.C., 1966, Airborne photographic observations of comet Ikeya-Seki, 1965f: The Astronomical Journal, V. 71, p. 844.
- Baker, G., 1966, External form and structure of some hollow australites: Geochimica et Cosmochimica Acta, V. 30, p. 607-615.
- Baker, G., 1966, Hollow australite button with Flange, Hordern Vale, Otway Peninsula, Western Victoria: Meteoritics, V. 3, p. 35-53.
- Baldwin, R.B., 1966, On the origin of the moon: Journal of Geophysical Research, V. 71, p. 1936-1937.
- Barabashov, N.P., Garazha, V.I., and Dudinov, V.N., 1966, Determination of corrections of corrections to photometric cross sections of planets: Soviet Astronomy - A.J., V. 10, No. 1, p. 113-116.

- Barber, D., 1966, The polarization, periodicity and angular diameter of the radiation from Jupiter at 610 Mc/s: *Monthly Notices of the Royal Astronomical Society*, V. 133, p. 285-308.
- Barnes, V.E., and Russell, R.V., 1966, Devitrification of glass around collapsed bubbles in tektites: *Geochimica et Cosmochimica Acta*, V. 30, p. 143-152.
- Barrett, A.H., 1966 - see Staelin, D.H.
- Barrow, C.H., 1966 - see Baart, E.E.
- Basharinov, A.E., and Kutuza, B.G., 1966, The nature of the cloud layer on Venus from microwave observations: *Soviet Astronomy - A.J.*, V. 10, No. 1, p. 117-120.
- Bastin, J.A., 1966, Small scale lunar roughness: *Nature*, V. 212, p. 171-172.
- Bastin, J.A., 1966 - see Clegg, P.E.
- Beals, C.S., and Innes, M.J.S., 1964, The identification of ancient meteorite craters: *Akademiia Nauk SSSR Meteoritika*, No. 25, p. 3-39.
- Beard, D.B., 1966, The theory of type I comet tails: *Planetary and Space Science*, V. 14, No. 3, p. 303-311.
- Becklin, E.E., and Westphal, J.A., 1966, Infrared observations of comet 1965f: *Astrophysical Journal*, V. 145, p. 445-453.
- Begemann, F., 1966, Tritium content of two chondrites: *Earth and Planetary Science Letters*, V. 1, No. 4, p. 148-150.
- Belton, J.S., and Hunten, D.M., 1966, Abundance and temperature of CO<sub>2</sub> in the Martian atmosphere: *The Astronomical Journal*, V. 71, p. 156.
- Belton, J.S., and Hunten, M., 1966, The abundance and temperature of CO<sub>2</sub> in the Martian atmosphere: *Astrophysical Journal*, V. 71, p. 454-467.
- Belton, M.J.S., and Hunten, D.M., 1966, Water vapor in the atmosphere of Venus: *Astrophysical Journal*, V. 146, p. 307.
- Berge, G.L., 1966, An interferometric study of Jupiter's decimeter radio emission: *Astrophysical Journal*, V. 144, p. 767-798.
- Berikashvili, V.Sh., 1966 - see Zharkov, V.N.
- Berkey, E., and Fisher, D.E., 1966, The chlorine content of iron meteorites: *Transactions of the American Geophysical Union*, V. 47, No. 1, p. 132.
- Boutler, A.E., 1966 - see Smith, N.
- Beyer, M., 1966, Physische Beobachtungen von Kometen XV: *Astronomische Nachrichten*, V. 289, p. 173-180.
- Bigg, E.K., 1966, Periodicities in Jupiter's decametric radiation: *Planetary and Space Science*, V. 14, No. 8, p. 741-758.
- Binder, A.B., 1966, Mariner IV: Analysis of preliminary photographs: *Science*, V. 152, p. 1053-1055.

- Binder, A.B., and Cruikshank, D.P., 1966, Lithological and mineralogical investigation of the surface of Mars: *Icarus*, V. 5, p. 521-525.
- Binder, A.B., and Cruikshank, D.P., 1966, Photometric search for atmospheres on Europa and Ganymede: *Icarus*, V. 5, p. 7-9.
- Binder, A.B., and Cruikshank, D.P., 1966, The composition of the surface layer of Mars: *Communications of the Lunar and Planetary Laboratory*, V. 4, No. 64, p. 111-120 + 2 pages photographs.
- Bingham, E., 1966 - see Nichiporuk, W.
- Blanchard, M.B., 1966 - see Farlow, N.H.
- Blizard, J.B., 1966, Spatial distribution of lunar transient event regions: *Transactions of the American Geophysical Union*, V. 47, No. 3, p. 187.
- Bogard, D.D., and Rowe, M.W., 1966, Anomalous krypton in achondrites: *Transactions of the American Geophysical Union*, V. 47, No. 1, p. 133.
- Bogard, D.D., 1966 - see Rowe, M.W.
- Booker, J.R., and Harrison, C.G.A., 1966, Magnetic properties of tektites: *Transactions of the American Geophysical Union*, V. 47, No. 1, p. 144-145.
- Bouricius, G.M.B., 1966 - see Coulson, K.L.
- Boyce, P.B., Sinton, W.M., 1966, Photometric observations of comet Ikeya-Seki, 1965f, in Na D light: *The Astronomical Journal*, V. 71, p. 847-848.
- Bray, T.A., and Goudas, C.L., 1966, A contour map based on the Selenodetic Control System of ACIC: *Icarus*, V. 5, p. 526-535.
- Brett, R., 1966, Cohenite in meteorites: A proposed origin: *Science*, V. 153, p. 60-62.
- Brett, R., 1966, Metallic spherules in impactite and tektite glasses: *Transactions of the American Geophysical Union*, V. 47, No. 1, p. 145.
- Brinkmann, R.T., 1966, Lunar crater distribution from the Ranger 7 photographs: *Journal of Geophysical Research*, V. 71, p. 340.
- Brockelman, R.A., 1966 - see Evans, J.V.
- Bronner, F.E., 1966 - see Otterman, J.
- Brown, P.L., 1966, The Barwell meteorite: *Sky and Telescope*, V. 32, p. 7-11.
- Brown, R.L., 1966, The acquisition of the solar system: *Transactions of the American Geophysical Union*, V. 47, No. 3, p. 482.
- Brown, T.A., 1966 - see Keay, C.S.L.
- Brown, W.E., Jr., 1966, Surveyor I radar report: *Transactions of the American Geophysical Union*, V. 47, No. 4, p. 616.
- Brownlow, A.E., Hunter, W., and Parkin, D.W., 1966, Cosmic spherules in a Pacific core: *Geophysical Journal of the Royal Astronomical Society*, V. 12, p. 1-12.

- Bühler, F., Geiss, J., Meister, J., Eberhardt, P., Huneke, J.C., and Singer, P., 1966, Trapping of the solar wind in solids. Part I. Trapping probability of low energy He, Ne and Ar ions: *Earth and Planetary Science Letters*, V. 1, No. 5, p. 249-255.
- Bullen, K.E., 1966, On the constitution of Mars III: *Monthly Notices of the Royal Astronomical Society*, V. 133, p. 229-238.
- Bunch, T.E., 1966 - see Park, F.R.
- Burkig, V.W., 1966 - see Greenman, N.N.
- Burley, J., and Middlehurst, B.M., 1966, Apparent lunar activity: *Proceedings of the National Academy of Sciences*, V. 55, p. 1007-1011.
- Burnett, D.S., Lippolt, H.J., and Wasserburg, G.J., 1966, The relative isotopic abundance of  $K^{40}$  in terrestrial and meteoritic samples: *Journal of Geophysical Research*, V. 71, p. 1249-1269.
- Buseck, P.R., 1966, Rutile in meteorites: *Transactions of the American Geophysical Union*, V. 47, No. 3, p. 481.
- Buseck, P.R., and Keil, K., 1964, Meteoritic rutile: *American Mineralogist*, V. 51, p. 1506-1515.
- Buseck, P.R., Mason, B., and Wilk, H.B., 1966, The Farmington meteorite. Mineralogy and chemistry: *Geochimica et Cosmochimica Acta*, V. 30, p. 1-8.
- Butler, C.P., 1966, Temperatures of meteoroids in space: *Meteoritics*, V. 3, p. 59-70.
- Cameron, A.E., 1966 - see Wampler, J.M.
- Cameron, A.G.W., 1966, The accumulation of chondritic material: *Earth and Planetary Science Letters*, V. 1, No. 3, p. 93-96.
- Cameron, E.N., 1966 - see Ramsden, A.R.
- Cameron, W.S., 1966, Operation Moon-Blink: *The Astronomical Journal*, V. 71, p. 379.
- Carpenter, J.W., 1966 - see Davidson, G.
- Carpenter, R.L., 1966, Preliminary results of 12.5 cm radar observations of Venus during its 1966 conjunction: *The Astronomical Journal*, V. 71, p. 848.
- Carpenter, R.L., 1966, Study of Venus by cw radar--1964 results: *The Astronomical Journal*, V. 71, p. 142-152.
- Carpenter, J.W., and Davidson, G., 1966, Feasibility of terrestrial observation of visible radiation associated with meteor impact on the lunar surface: *Transactions of the American Geophysical Union*, V. 47, No. 1, p. 149.
- Carpenter, J.W., 1966 - see Kraner, H.W.
- Carr, T.D., 1966 - see Gulikis, S.
- Carr, T.D., 1966 - see Six, N.F., Jr.
- Carson, D., Davidson, M., Goudas, C.L., Kopel, Z., and Stoddard, L.G., 1966, Lunar profiles determined from annular solar eclipses of 1962 and 1963: *Icarus*, V. 5, p. 334-359.



- Carter, N.L., and Kennedy, G.C., 1966, Origin of diamonds in the Canyon Diablo and Novo Urei meteorites--a reply: *Journal of Geophysical Research*, V. 71, p. 663.
- Cassidy, W., 1966 - see Sanchez, J.
- Centolanzi, F.J., and Chapman, D.R., 1966, Vapor pressure of tektite glass and its bearing on tektite trajectories determined from aerodynamic analysis: *Journal of Geophysical Research*, V. 71, p. 1735-1749.
- Cepiecha, Z., 1965, Investigation of the composition and physical conditions of movement of meteor bodies using analysis of meteor spectrums: *Akademiia Nauk SSSR Meteoritika*, No. 26, p. 66-68.
- Chamberlain, J.W., and McElroy, M.B., 1966, Diffuse reflection by an inhomogeneous planetary atmosphere: *The Astrophysical Journal*, V. 144, p. 1148-1158.
- Chamberlain, J.W., and McElroy, M.B., 1966, Martian atmosphere: The Mariner Occultation Experiment: *Science*, V. 152, p. 21-25.
- Chao, E.C.T., Dwornik, E.J., and Merrill, C.W., 1966, Nickel-iron spherules from Aouelloul glass: *Science*, V. 154, p. 759-765.
- Chao, E.C.T., Merrill, C.W., Cuttitta, F., and Ansell, C., 1966, The Aouelloul crater and the Aouelloul glass of Mauritania, Africa: *Transactions of the American Geophysical Union*, V. 47, No. 1, p. 144.
- Chapman, D., 1966 - see Livingston, W.
- Chapman, D.R., 1966 - see Centolanzi, F.J.
- Charlson, R.J., 1966, Some thoughts on noctilucent clouds: *Transactions of the American Geophysical Union*, V. 47, No. 4, p. 628-629.
- Chebotaiev, G.A., 1966, Cometary motion in the outer solar system: *Soviet Astronomy - A.J.*, V. 10, No. 2, p. 341-344.
- Chessin, H., Hallgren, D.S., and Hemenway, C.L., 1966, Absence of crystal structure in interplanetary dust: *The Astronomical Journal*, V. 71, p. 380.
- Christensen, E.M., 1966, Photo interpretation of Surveyor I interaction with the lunar material: *Transactions of the American Geophysical Union*, V. 47, No. 4, p. 617.
- Clark, T.A., and Dulk, G.A., 1966, Observations of Jupiter at 8.9 and 10 MHz: *The Astronomical Journal*, V. 71, p. 158.
- Clark, T.A., 1966 - see Dulk, G.A.
- Clarke, R.S., Jr., Wosinski, J.F., Marvin, R.F., and Friedman, I., 1966, Potassium-argon ages of artificial tektite glass: *Transactions of the American Geophysical Union*, V. 47, No. 1, p. 144.
- Clegg, P.E., Bastin, J.A., Gear, A.E., 1966, Heat transfer in lunar rock: *Monthly Notices of the Royal Astronomical Society*, V. 133, p. 63-66.
- Cobb, J.C., 1966, A trace element study of tektites: *Transactions of the American Geophysical Union*, V. 47, No. 1, p. 145.
- Cobb, J.C., 1966, Iron meteorites with low cosmic ray exposure ages: *Science*, V. 151, p. 1524.

- Cohen, A.J., 1966, Martian canal system: *The Astronomical Journal*, V. 71, p. 849.
- Cohen, A.J., 1966, Seasonal color changes on Mars: *The Astronomical Journal*, V. 71, p. 849-850.
- Coleman, I., 1966 - see Mertz, L.
- Collins, R.J., 1966 - see Ney, E.P.
- Colombo, G., and Shapiro, I., 1965, The rotation of the planet Mercury: *Astrophysical Journal*, V. 145, p. 296-307.
- Colombo, G., Lautman, D.A., and Shapiro, I.I., 1966, The earth's dust belt: fact or fiction? 2. Gravitational focusing and Jacobi capture: *Journal of Geophysical Research*, V. 71, p. 5705-5717.
- Colombo, G., Shapiro, I.I., and Lautman, D.A., 1966, The earth's dust belt: fact or fiction? 3. Lunar ejecta: *Journal of Geophysical Research*, V. 71, p. 5719-5731.
- Colombo, G., 1966 - see Lautman, D.A.
- Colombo, G., 1966 - see Shapiro, I.I.
- Conel, J., 1966 - see Lucas, J.W.
- Connes, J., Connes, P., and Kaplan, L.D., 1966, Mars: New absorption bands in the spectrum: *Science*, V. 153, p. 739-740.
- Connes, P., 1966 - see Connes, J.
- Cook, A.F., and Franklin, F.A., 1966, Particle sizes in Saturn's rings: *The Astronomical Journal*, V. 71, p. 851.
- Cook, A.F., and Franklin, F.A., 1966, Rediscussion of Maxwell's Adams Prize Essay on the Stability of Saturn's rings. II: *The Astronomical Journal*, V. 71, p. 10-19.
- Cooke, S.R.B., 1966, An unusual lunar dome: *Sky and Telescope*, V. 32, p. 111.
- Copeland, J., 1966, Observations of Venus at 8.6 nm wavelength near inferior conjunction: *Astrophysical Journal*, V. 143, p. 996-1000.
- Copeland, J., 1966, The two-layer model of the lunar surface: *Astrophysical Journal*, V. 145, p. 297-301.
- Coulson, K.L., Gray, E.L., and Bouricius, G.M.B., 1966, Effect of surface reflection on planetary albedo: *Icarus*, V. 5, p. 139-148.
- Cross, C.A., 1966, The size distribution of lunar craters: *Monthly Notices of the Royal Astronomical Society*, V. 134, p. 245-252.
- Crozier, W.D., 1966, Nine years of continuous collection of black, magnetic spherules from the atmosphere: *Journal of Geophysical Research*, V. 71, p. 603-611.
- Cruikshank, D.P., 1966, Possible luminescence events on Mercury: *Nature*, V. 209, p. 701.
- Cruikshank, D.P., 1966 - see Binder, A.B.
- Curtis, G.W., 1966, Daylight observations of the 1965f comet at the Sacramento Peak Observatory: *The Astronomical Journal*, V. 71, p. 194-196.

- Curtis, G.W. and Staff, 1966, Daytime observation of the comet 1965f at the Sacramento Peak Observatory: *The Astronomical Journal*, V. 71, p. 159.
- Cuttitta, F., 1966 - see Chao, E.C.T.
- Danes, Z.F., 1966, Isostatic processes in media of variable viscosity: *Transactions of the American Geophysical Union*, V. 47, No. 4, p. 628.
- Danielson, R.E., 1966, The infrared spectrum of Jupiter: *Astrophysical Journal*, V. 143, p. 949.
- Danielson, R.E., and Solomon, D.M., 1966, Role of collision-induced transitions in the Venus greenhouse effect: *The Astronomical Journal*, V. 71, p. 382-383.
- Danielsson, L.R., and Kasai, G.H., 1966, A model experiment on cometary phenomenon: *Transactions of the American Geophysical Union*, V. 47, No. 3, p. 485.
- David, E., 1966, Meteorite impacts and the ejection mechanism of tektites: *Earth and Planetary Science Letters*, V. 1, No. 2, p. 75-76.
- Davidson, G., Kraner, H.W., Schroeder, G.L., and Carpenter, J.W., 1966, Enhanced radioactivity at the lunar surface: *Transactions of the American Geophysical Union*, V. 47, No. 1, p. 154-155.
- Davidson, G., 1966 - see Carpenter, J.W.
- Davidson, G., 1966 - see Kraner, H.W.
- Davidson, M., 1966 - see Carson, D.
- Davies, R.D., and Gardner, F.F., 1966, Linear polarization of the moon at 6, 11, and 21 cm wavelengths: *Australian Journal of Physics*, V. 19, p. 823-836.
- Davies, R.D., and Williams, D., 1966, Observations of the continuum emission from Venus, Mars, Jupiter, and Saturn at 21.2 cm wavelength: *Planetary and Space Science*, V. 4, No. 1, p. 15-32.
- Davies, J.G., Lovell, B., Pottchard, R.S., and Smith, F.G., 1966, Observation of the Russian Moon Probe Luna 9: *Nature*, V. 209, p. 848, 850.
- Deaton, T.K., 1966 - see Saari, J.M.
- De Marcus, W.C., 1966, Jupiter's Great Red Spot: *Nature*, V. 209, p. 62.
- Dent, W.A., 1966 - see Kuz'min, A.D.
- Derbeneva, A.D., 1966, The luminous efficiency of meteors: *Soviet Astronomy - A.J.*, V. 10, No. 2, p. 355-356.
- Dewey, M.E., and Miller, F.D., 1966, Isophotes of the  $C_2$  distribution in comet Seki (1961 VIII): *The Astrophysical Journal*, V. 144, p. 1170-1173.
- Dews, J.R., 1966, The isotopic composition of lithium in chondrules: *Journal of Geophysical Research*, V. 71, p. 4011-4020.
- Dews, J.R., and Newbury, R.S., 1966, The isotopic composition of silver in the Canyon Diablo meteorite: *Journal of Geophysical Research*, V. 71, p. 3069-3081.
- Dickel, J.R., 1966, Measurement of the temperature of Venus at a wavelength of 3.75 cm for a full cycle of planetary phase angles: *Icarus*, V. 5, p. 305-308.

- Dickel, J.R., 1966, Microwave spectrum of Venus: *The Astronomical Journal*, V. 71, p. 852-853.
- Dickel, J.R., 1966, Observations of Jupiter at a frequency of 610.5 MHz: *The Astronomical Journal*, V. 71, p. 159-160.
- Dietz, R.S., 1966, Shatter cones at the Middlesboro structure, Kentucky: *Meteoritics*, V. 3, p. 27-29.
- Dietz, R.S., 1966, Striated surfaces on meteorites: shock fractures, not slickensides: *Meteoritics*, V. 3, p. 31-33.
- Divari, N.B., 1966, Charged dust particles in interplanetary space: *Soviet Astronomy - A.J.*, V. 10, No. 1, p. 151-155.
- Divoky, D., 1966, The equivalence of mass and energy scaling of crater dimensions: comment on a paper by A.J. Chabai: *Journal of Geophysical Research*, V. 71, p. 2691.
- Dobar, W.I., 1966, Simulated basalt and granite magma upwelled in vacuum: *Icarus*, V. 5, p. 399-405.
- Dodd, R.T., Jr., Van Schmus, W.R., and Marvin, U.B., 1966, Significance of iron-rich silicates in the Mezö-Madaras chondrite: *American Mineralogist*, V. 51, p. 1177-1191.
- Dolginov, A.Z., and Gnedin, Yu.N., 1966, A theory of the atmosphere of a comet: *Icarus*, V. 5, p. 64-74.
- Dolginov, A.Z., 1966 - see Gnedin, Yu.N.
- Donahoe, F.J., 1966, On the abundance of earth-like planets: *Icarus*, V. 5, p. 303-304.
- Donahue, T.M., 1966, Upper atmosphere and ionosphere of Mars: *Science*, V. 152, p. 763-764.
- Donn, B., 1966 - see Jackson, W.M.
- Dossin, F.V., 1966, Emission spectrum of a comet, at large heliocentric distance: *The Astronomical Journal*, V. 71, p. 853-854.
- Drummond, R.R., 1966 - see Kilston, S.D.
- Dryer, M., and Heckman, G.R., 1966, Application of the hypersonic analog to Mars' magnetic field: *Transactions of the American Geophysical Union*, V. 47, No. 1, p. 155-156.
- Dudinov, V.N., 1966 - see Barabashov, N.P.
- Duke, M.B., 1966, The Shergotty meteorite: magmatic and shock metamorphic features: *Transactions of the American Geophysical Union*, V. 47, No. 3, p. 481-482.
- Dulk, G.A., and Clark, T.A., 1966, Almost-continuous radio emission from Jupiter at 8.9 and 10 MHz: *The Astrophysical Journal*, V. 145, p. 945-948.
- Dulk, G.A., and Eddy, J.A., 1966, A new search for visual aurorae on Jupiter: *The Astronomical Journal*, V. 71, p. 160.
- Dulk, G.A., 1966 - see Clark, T.A.
- Duncan, R.A., 1966, Comments on the modulation of Jovian decametric emission by Jupiter's satellites: *Planetary and Space Science*, V. 14, No. 3, p. 173-176.

- Duncan, R.A., 1966, Factors controlling Jovian decametric emission: *Planetary and Space Science*, V. 14, No. 12, p. 1291-1301.
- Dunlap, J.R., 1966 - see Hynek, J.A.
- Dupee, W.D., and Alexander, S.S., 1966, The response of selected rock specimens to vacuum ultraviolet light: *Transactions of the American Geophysical Union*, V. 47, No. 1, p. 150.
- Dupont, E.N., 1966 - see Evans, J.V.
- Dwornik, E.J., 1966 - see Chao, E.C.T.
- D'yakonova, M.I., 1964, Chemical composition of seven stony meteorites of the collection of the Committee on Meteorites of the Academy of Sciences of the USSR: *Akademiia Nauk SSSR Meteoritika*, No. 25, p. 129-133.
- Dyce, R.B., 1966, Radar observations of Mars at 70 cm: *Transactions of the American Geophysical Union*, V. 47, No. 2, p. 427.
- Dyce, R.B., 1966 - see Thompson, T.W.
- Ebeoglu, D.B., 1966, Solar proton induced gamma rays on the lunar surface: *Transactions of the American Geophysical Union*, V. 47, No. 3, p. 487.
- Ebeoglu, D.B., and Wainio, K.M., 1966, Solar proton activation of the lunar surface: *Journal of Geophysical Research*, V. 71, p. 5863-5872.
- Ebeoglu, D.B., and Wainio, K.M., 1966, Solar proton activation on the lunar surface: *Transactions of the American Geophysical Union*, V. 47, No. 1, p. 154.
- Eberhardt, P., and Geiss, J., 1966, On the mass spectrum of fission xenon in the Pasamonte meteorite: *Earth and Planetary Science Letters*, V. 1, No. 3, p. 99-101.
- Eberhardt, P., Geiss, J., and Grögler, N., 1966, Distribution of rare gases in the pyroxene and feldspar of the Khor Temiki meteorite: *Earth and Planetary Science Letters*, V. 1, p. 7-12.
- Eberhardt, P., 1966 - see Bühler, F.
- Eddy, J.A., 1966 - see Dulk, G.A.
- Egan, W.G., and Smith, L.L., 1966, Polarimetric measurements of simulated lunar surfaces: *The Astronomical Journal*, V. 71, p. 383-384.
- Ehmann, W.D., and Tanner, J.T., 1966, The abundance of antimony in meteorites: *Earth and Planetary Science Letters*, V. 1, No. 5, p. 276-279.
- Ekers, R.D., 1966 - see Roberts, J.A.
- El Goresy, A., 1966, Electron microprobe analysis of some rare minerals from Odessa and Toluca iron meteorites: *Transactions of the American Geophysical Union*, V. 47, No. 2, p. 425-426.
- El Goresy, A., 1966, Metallic spherules in Bosumtwi crater glasses: *Earth and Planetary Science Letters*, V. 1, No. 1, p. 23-24.
- Ellis, G.R.A., 1966 - see McCulloch, P.M.

- Ellyett, C.D., 1966 - see Keay, C.S.L.
- Elston, W.E., 1966, Ring-dike complexes: possible analogs of lunar craters: Transactions of the American Geophysical Union, V. 47, No. 1, p. 148.
- Emslie, A.G., 1966 - see Aronson, J.R.
- Epstein, E.E., 1966, Disk temperatures of Mercury and Mars at 3.4 mm: The Astrophysical Journal, V. 143, p. 597.
- Epstein, E.E., 1966, Mercury: Anomalous absence from the 3.4 millimeter radio emission of variation with phase: Science, V. 151, p. 445-447.
- Epstein, E.E., 1966, Mercury: Anomalous absence of a variation with phase in the 3.4 mm radio emission: The Astronomical Journal, V. 71, p. 161.
- Epstein, S., 1966 - see Taylor, H.P., Jr.
- Eshleman, V.R., 1966 - see Fjeldbo, G.
- Evans, J.V., 1966, Radar observations of meteor deceleration: Journal of Geophysical Research, V. 71, p. 171.
- Evans, J.V., and Hagfors, T., 1966, Study of radio echoes from the moon at 23 centimeters wavelength: Journal of Geophysical Research, V. 71, p. 4871-4889.
- Evans, J.V., and Ingalls, R.P., 1966, Radar observations of Venus at 23- and 3.8-cm wavelength: The Astronomical Journal, V. 71, p. 854.
- Evans, J.V., Ingalls, R.P., Rainville, L.P., and Silva, R.R., 1966, Radar observations of Venus at 3.8-cm wavelength: The Astronomical Journal, V. 71, p. 902-915.
- Evans, J.V., Brockelman, R.A., Dupont, E.N., Hanson, L.B., and Reid, W.A., 1966, Radar observations of Venus at 23 cm in 1965/1966: The Astronomical Journal, V. 71, p. 897-901.
- Evans, C., 1966 - see Malville, J.McK.
- Farlow, N.H., and Blanchard, M.B., 1966, Examination of extraterrestrial particles collected by the Luster sounding rocket experiment: Transactions of the American Geophysical Union, V. 47, No. 1, p. 143-144.
- Farlow, N.H., Blanchard, M.B., and Ferry, G.V., 1966, Sampling with a Luster sounding rocket during a Leonid meteor shower: Journal of Geophysical Research, V. 71, p. 5689-5693.
- Faul, H., 1966, Tektites are terrestrial: Science, V. 152, p. 1341-1345.
- Faust, L., 1966 - see Meloy, T.P.
- Feast, W.W., 1966 - see Thackeray, A.D.
- Fechtig, H., Gerloff, U., and Weihrauch, J.H., 1966, Electron microscope and microprobe measurements on Luster-flight samples: Transactions of the American Geophysical Union, V. 47, No. 2, p. 426.
- Fehsenfeld, F.C., 1966 - see Norton, R.B.

- Ferguson, E.E., 1966 - see Norton, R.B.
- Ferry, G.V., 1966 - see Farlow, N.H.
- Fesenkov, V.G., 1965, Advances in meteoritics: *Akademiia Nauk SSSR Meteoritika*, No. 26, p. 3-16.
- Fesenkov, V.G., 1966, A study of the Tunguska meteorite fall: *Soviet Astronomy - A.J.*, V. 10, No. 2, p. 195-213.
- Fesenkov, V.G., 1966, Interplanetary dust matter and methods for its investigation: *Soviet Astronomy - A.J.*, V. 10, No. 3, p. 474-478.
- Fesenkov, V.G., 1964, On the orbit of the Tunguska meteorite: *Akademiia Nauk SSSR Meteoritika*, No. 25, p. 163-167.
- Fesenkov, V.G., 1965, The role of meteorites in solving the problem of the origin of the solar system: *Akademiia Nauk SSSR Meteoritika*, No. 26, p. 69-76.
- Fialko, E.I., 1966, Determination of the absolute magnitude of a meteor from the duration of unstable train echoes: *Soviet Astronomy - A.J.*, V. 10, No. 1, p. 161-164.
- Fielder, G., 1966, Tests for randomness in the distribution of lunar craters: *Monthly Notices of the Royal Astronomical Society*, V. 132, p. 413-422.
- Fielder, G., Wilson, L., and Guest, J.E., 1966, The moon from Luna 9: *Nature*, V. 209, p. 851-853.
- Flink, U., 1966 - see Rank, D.H.
- Fish, F.F., Jr., 1966, The stability of goethite on Mars: *Journal of Geophysical Research*, V. 71, p. 3063-3068.
- Fisher, D.E., 1966, The origin of meteorites: space erosion and cosmic radiation ages: *Journal of Geophysical Research*, V. 71, p. 3251-3259.
- Fisher, D.E., 1966 - see Berkey, E.
- Fjeldbo, G., Fjeldbo, W.C., and Eshleman, V.R., 1966, Models for the atmosphere of Mars based on the Mariner 4 occultation experiment: *Journal of Geophysical Research*, V. 71, p. 2307-2316.
- Fjeldbo, G., Fjeldbo, W.C., and Von Eshleman, R., 1966, Atmosphere of Mars: Mariner IV models compared: *Science*, V. 153, p. 1518-1523.
- Fjeldbo, W.C., 1966 - see Fjeldbo, G.
- Fleischer, R.L., 1966 - see Price, P.B.
- Fleischer, R.L., 1966 - see Walker, R.M.
- Florovskaya, V.N., Vdovykin, G.P., Teplitskaya, T.A., and Zevin, R.B., 1965, Comparative features of polycyclic aromatic hydrocarbons in carbonaceous chondrites and rocks and minerals of endogene origin: *Akademiia Nauk SSSR Meteoritika*, No. 26, p. 169-176.
- Fogel, Ya.M., 1966 - see Koval, A.G.

- Franklin, F.A., 1966 - see Cook, A.F.
- Fredriksson, K., 1966 - see Olsen, E.
- French, B.M., 1966, Some geological implications of equilibrium between graphite and a C-H-O gas phase at high temperatures and pressures: *Reviews of Geophysics*, V. 4, No. 2, p. 223-253.
- Friedman, I., 1966 - see Clarke, R.S., Jr.
- Fronzel, C., 1966 - see Fuchs, L.H.
- Fronzel, C., 1966 - see Meinschein, W.G.
- Fuchs, L.H., 1966, Djerfisherite alkali copper-iron sulfide: A new mineral from Enstatite chondrites: *Science*, V. 153, p. 166-167.
- Fuchs, L.H., Fronzel, C., and Klein, C., Jr., 1966, Roedderite, a new mineral from the Indarch meteorite: *American Mineralogist*, V. 51, p. 949-955.
- Fudali, R.F., 1966, Implications of the non-uniform cooling behavior of the eclipsed moon: *Icarus*, V. 5, p. 536-544.
- Fulmer, C., Saari, J.M., and Shorthill, R.W., 1966, Some physical characteristics of eclipse thermal anomalies in the Apollo band: *Publications of the Astronomical Society of the Pacific*, V. 78, p. 442-444.
- Fulmer, C.V., Saari, J.M., and Shorthill, R.W., 1966, Physical characteristics of some thermally anomalous lunar craters: *Transactions of the American Geophysical Union*, V. 47, No. 4, p. 628.
- Fulmer, C., 1966 - see Oncley, P.B.
- Fung, A.K., and Moore, R.K., 1966, The correlation function in Kirchhoff's method of solution of scattering of waves from statistically rough surfaces: *Journal of Geophysical Research*, V. 71, p. 2939-2943.
- Fung, P.C.W., 1966, Excitation of cyclotron radiation in the forward sublimous mode and its application to Jupiter's decametric emissions: *Planetary and Space Science*, V. 14, No. 6, p. 469-481.
- Gaitskell, J.N., and Gear, A.E., 1966, Solar and lunar observations at submillimeter wavelengths: *Icarus*, V. 5, p. 237-244.
- Gale, N.H., 1966, A potassium-argon age for the Barwell meteorite: *Nature*, V. 210, p. 620.
- Gapcynski, J.P., 1966 - see Michael, W.H., Jr.
- Garazha, V.I., 1966 - see Barabashov, N.P.
- Gardner, F.F., 1966 - see Davies, R.D.
- Garipay, R., 1966 - see Lucas, J.W.
- Gault, D.E., and Quaide, W.L., 1966, Meteoroid erosion and sedimentation on the lunar surface: *Transactions of the American Geophysical Union*, V. 47, No. 1, p. 148.
- Gault, D.E., Quaide, W.L., and Oberbeck, V.R., 1966, Modeling meteorite craters in the laboratory, I, mechanics of formation: *Transactions of the American Geophysical Union*, V. 47, No. 1, p. 148.



- Gault, D.E., Quaide, W.L., Oberbeck, V.R., and Moore, A.J., 1966, Luna 9 photographs: Evidence for a fragmental surface layer: *Science*, V. 153, p. 985-988.
- Gault, D.E., 1966 - see Quaide, W.L.
- Geake, J.E., and Walker, G., 1966, Reply to "Luminescence caused by proton impact with special reference to the Lunar Surface": *Nature*, V. 211, p. 471-472.
- Geake, J.E., and Walker, G., 1966, The luminescence spectra of meteorites: *Geochimica et Cosmochimica Acta*, V. 30, p. 929-937.
- Gear, A.E., 1966 - see Clegg, P.E.
- Gear, A.E., 1966 - see Galtskell, J.N.
- Gehrels, T., 1966, Some comments on Hapke's comments: *Icarus*, V. 5, p. 160-161.
- Geiss, J., 1966 - see Bühler, F.
- Geiss, J., 1966 - see Eberhardt, P.
- Gentry, R.V., 1966, Additional evidence of extinct radioactivity from pleochroic halos and the formation of the lunar crust: *Transactions of the American Geophysical Union*, V. 47, No. 3, p. 487.
- Gentry, R.V., 1966, Anti-matter content of the Tunguska matter: *Nature*, V. 211, p. 1071-1072.
- Gentry, R.V., 1966, Anti-matter meteorite explosions relative to fission track ages of tektites: *Transactions of the American Geophysical Union*, V. 47, No. 4, p. 618.
- Gerloff, U., 1966 - see Fechtig, H.
- Gilpin, C.B., 1966 - see Greenman, N.N.
- Gilvarry, J.J., 1966, Observability of indigenous organic matter on the moon: *Icarus*, V. 5, p. 228-236.
- Ginzburg, I.V., 1964 - see Kvesha, L.G.
- Giver, L.P., and Spinrad, H., 1966, Molecular hydrogen features in the spectra of Saturn and Uranus: *Icarus*, V. 5, p. 586-589.
- Giver, L.P., 1966 - see Spinrad, H.
- Gnedin, Yu.N., and Dolginov, A.Z., 1966, Particle distribution in a comet head: *Soviet Astronomy - A.J.*, V. 10, No. 1, p. 143-150.
- Gnedin, Yu.N., 1966 - see Dolginov, A.Z.
- Gold, T., 1966, Probable mode of landing of Luna 9: *Nature*, V. 210, p. 150.
- Gold, T., and Hapke, B.W., 1966, Implications of the Luna 9 pictures: *Transactions of the American Geophysical Union*, V. 47, No. 2, p. 426.
- Gold, T., 1966 - see Hapke, B.W.
- Gold, T., 1966 - see Werner, M.

- Gold, T., and Hapke, B.W., 1966, Luna 9 pictures: Implications: *Science*, V. 153, p. 290-293.
- Goldreich, P., 1966, Dynamics of planet-satellite system: *Transactions of the American Geophysical Union*, V. 47, No. 1, p. 155.
- Goldreich, P., 1966, Final spin states of planets and satellites: *The Astronomical Journal*, V. 71, p. 1-7.
- Goldreich, P., 1966, History of the lunar orbit: *Reviews of Geophysics*, V. 4, No. 4, p. 411-439.
- Goldreich, P., and Peale, S.J., 1966, Resonant rotation of Venus?: *Nature*, V. 209, p. 1117.
- Goldreich, P., and Peale, S.J., 1966, Resonant spins in the solar systems: *Transactions of the American Geophysical Union*, V. 47, No. 1, p. 155.
- Goldreich, P., and Soter, S., 1966, Q in the solar system: *Icarus*, V. 5, p. 375-389.
- Goldstein, J.I., 1966, Butler, Missouri: An unusual iron meteorite: *Science*, V. 153, p. 975-976.
- Goldstein, J.I., 1966, The distribution of germanium in the metallic phases of some meteorites: *Transactions of the American Geophysical Union*, V. 47, No. 1, p. 134.
- Goldstein, J.I., 1966 - see Short, J.M.
- Goldstein, R.M., 1966 - see Sagan, C.
- Goles, G.G., and Greenland, L.P., 1966, Estimates of primordial halogen abundance ratios from studies of chondritic meteorites: *The Astronomical Journal*, V. 71, p. 162.
- Goles, G.G., 1966 - see Schmitt, R.A.
- Gonzalez, J.L., 1966 - see Sun, K.H.
- Goody, R.M., and Robinson, A.R., 1966, A discussion of the deep circulation of the atmosphere of Venus: *Astrophysical Journal*, V. 146, p. 339-355.
- Gorbunova, T.M., 1964, Preparation of polished slices of large area from iron meteorites: *Akademiia Nauk SSSR Meteoritika*, No. 25, p. 188-191.
- Goudas, C.L., 1966, Note on "Shape and Internal Structure of the Moon" by Lamar and McGann: *Icarus*, V. 5, p. 99-101.
- Goudas, C.L., and Kopal, Z., 1966, Shape of the moon from the orbiter determination of its gravitational field: *Nature*, V. 212, p. 271.
- Goudas, C.L., 1966 - see Carson, D.
- Grasty, R.L., 1966 - see Turner, G.
- Gray, E.L., 1966 - see Coulson, K.L.
- Gray, L.D., 1966, Transmission of the atmosphere of Mars in the region of  $2\mu$ : *Icarus*, V. 5, p. 390-398.
- Green, J., 1966 - see Osgood, J.H.

- Greenland, L.P., 1966 - see Goles, G.G.
- Greenman, N.N., and Gilpin, C.B., 1966, Micrometeorite collectors for high-altitude rockets: Transactions of the American Geophysical Union, V. 47, No. 3, p. 480-481.
- Greenman, N.N., Burkig, V.W., and Young, J.F., 1966, Ultraviolet reflectance measurements of possible lunar silicates: Transactions of the American Geophysical Union, V. 47, No. 1, p. 150.
- Griffin, J., 1966 - see Miller, A.C.
- Grögler, N., 1966 - see Eberhardt, P.
- Gross, S.H., McGovern, W.E., and Rasool, S.I., 1966, Mars: Upper atmosphere: Science, V. 151, p. 1216-1221.
- Groszek, E.J., 1966 - see Wasson, J.T.
- Gruenhagen, G., 1966 - see Huss, G.I.
- Guest, J.E., 1966 - see Fielder, G.
- Gulkis, S., and Carr, T.D., 1966, Asymmetrical stop zones in Jupiter's exosphere: Nature, V. 210, p. 1104-1105.
- Gulkis, S., and Carr, T.D., 1966, Radio rotation period of Jupiter: Science, V. 154, p. 257-259.
- Gulkis, S., and Carr, T.D., 1966, Radio rotation period of Jupiter: The Astronomical Journal, V. 71, p. 856-857.
- Gus'kova, Ye.G., 1965, The nature of the natural remanent, magnetization of meteorites: Akademiia Nauk SSSR Meteoritika, No. 26, p. 60-65.
- Hadjidemetriou, J.D., 1966, Analytic solutions of the two-body problem with variable mass: Icarus, V. 5, p. 34-36.
- Hafner, W., 1966, Report on the lunar geological field conference, Bend, Oregon, August 22-28, 1965: Geophysics, V. 31, No. 4, p. 267-275.
- Hagemeyer, W., 1966 - see Lucas, J.W.
- Hagen, J.P., Jr., 1966 - see Zabriskie, F.R.
- Hagfors, T., 1966, Relationship of geometric optics and autocorrelation approaches to the analysis of lunar and planetary radar: Journal of Geophysical Research, V. 71, p. 379-383.
- Hagfors, T., 1966 - see Evans, J.V.
- Hallgren, D.S., 1966 - see Chessin, H.
- Halliday, I., and Hardie, R.H., 1966, An upper limit for the diameter of Pluto: Publications of the Astronomical Society of the Pacific, V. 78, p. 113-124.
- Hamilton, W.L., and Bull, C., 1966, A comparison of the dust flux in the upper atmosphere and on the polar ice sheets: Journal of Geophysical Research, V. 71, p. 2679-2683.

- Hanson, L.B., 1966 - see Evans, J.V.
- Hapke, B., 1966, An improved theoretical lunar photometric function: *The Astronomical Journal*, V. 71, p. 333-339.
- Hapke, B., 1966, An improved theoretical lunar photometric function: *The Astronomical Journal*, V. 71, p. 386.
- Hapke, B., 1966, Comments on paper by Philip Oetking, "Photometric studies of diffusely reflecting surfaces with applications to the brightness of the moon": *Journal of Geophysical Research*, V. 71, p. 2515.
- Hapke, B., 1966, On the composition of the lunar surface: *Transactions of the American Geophysical Union*, V. 47, No. 1, p. 149-150.
- Hapke, B., 1966, Some comments on Gehrels' model of the lunar surface: *Icarus*, V. 5, p. 154.
- Hapke, B.W., and Gold, T., 1966, Luna 9 pictures and the lunar surface: *The Astronomical Journal*, V. 71, p. 857.
- Hapke, B.W., 1966 - see Gold, T.
- Hapke, B.W., 1966 - see Wattson, R.B.
- Hardie, R.H., 1966 - see Halliday, I.
- Harrington, J.S., 1966, Polycyclic aromatic hydrocarbons in carbonaceous meteorites: *Nature*, V. 212, p. 273-274.
- Harrison, A.E., 1966, Stereo visualization techniques: *Transactions of the American Geophysical Union*, V. 47, No. 4, p. 629.
- Harrison, H., 1966, Metastable oxygen atoms and Martian model atmospheres: *Transactions of the American Geophysical Union*, V. 47, No. 4, p. 629.
- Harrison, C.G.A., 1966 - see Booker, J.R.
- Hartek, P., 1966 - see Applebaum, D.C.
- Hartmann, W.K., 1966, Early lunar cratering: *Icarus*, V. 5, p. 406-418.
- Hartmann, W.K., 1966, Lunar basins, lunar lineaments, and the moon's far side: *Sky and Telescope*, V. 32, p. 128-131.
- Hartmann, W.K., 1966, Martian cratering: *Communications of the Lunar and Planetary Laboratory*, V. 4, No. 65, p. 121-131.
- Hartmann, W.K., 1966, Martian cratering: *Icarus*, V. 5, p. 565-576.
- Harwit, M., 1966, Orbits of sun-grazing comets: *The Astronomical Journal*, V. 71, p. 857.
- Harwit, M., 1966 - see Werner, M.
- Haughney, L.C., 1966 - see Bader, M.
- Hayatsu, R., 1966, Artifacts in polarimetry and optical activity in meteorites: *Science*, V. 153, p. 859-861.

- Heckman, G.R., 1966 - see Dryer, M.
- Hemenway, C.L., 1966 - see Chessin, H.
- Hemenway, C.L., 1966 - see Patashnik, H.
- Herring, A.K., 1966, Observations of comet Ikeya-Seki (1965f) from Mauna Kea, Hawaii: Communications of the Lunar and Planetary Laboratory, V. 4, No. 67, p. 141-144 + 1 color photograph.
- Herring, A.K., 1966, Observing the moon--Beer and Fauillee: Sky and Telescope, V. 31, p. 58.
- Herring, A.K., 1966, Observing the moon--Bessarion B: Sky and Telescope, V. 31, p. 245.
- Herring, A.K., 1966, Observing the moon--Encke: Sky and Telescope, V. 32, p. 239.
- Herring, A.K., 1966, Observing the moon--Jansen B: Sky and Telescope, V. 32, p. 49.
- Herring, A.K., 1966, Preliminary drawings of lunar limb areas, VI: Communications of the Lunar and Planetary Laboratory, V. 4, No. 66, p. 133-140.
- Heymann, D., and Mazor, E., 1966, St. Mesmin, a gas-rich amphoteric chondrite: Journal of Geophysical Research, V. 71, p. 4695-4697.
- Heymann, D., Lipschutz, M.E., Nielsen, B., and Anders, E., 1966, Canyon Diablo meteorite: Metallographic and mass spectrometric study of 56 fragments: Journal of Geophysical Research, V. 71, p. 619-641.
- Hide, R., 1966, On the circulation of the atmospheres of Jupiter and Saturn: Planetary and Space Science, V. 14, No. 8, p. 669-675.
- Hide, R., 1966, Planetary magnetic fields: Planetary and Space Science, V. 14, No. 7, p. 579-586.
- Hide, R., and Ibbotson, A., 1966, An experimental study of "Taylor columns": Icarus, V. 5, p. 279-290.
- Higgins, C.J., 1966 - see Moraski, L.K.
- Higgins, C.S., 1966 - see Slee, O.B.
- Ho, W., Kaufman, I.A., and Thaddeus, P., 1966, Laboratory measurement of microwave absorption in models of the atmosphere of Venus: Journal of Geophysical Research, V. 71, p. 5091-5108.
- Hobbs, P.V., 1966 - see Alkezweeny, A.J.
- Hodge, P.W., 1966 - see Wright, F.W.
- Hohenberg, C.M., 1966 - see Reynolds, J.H.
- Holmes, J.R., 1966 - see Six, N.F., Jr.
- Holt, H.E., 1966 - see Rennilson, J.J.
- Honda, M., 1966 - see Shima, M.

- Hopfield, J.J., 1966, Mechanism of lunar polarization: *Science*, V. 151, p. 1380-1381.
- Horowitz, N.H., 1966, The search for extraterrestrial life: *Science*, V. 151, p. 789-792.
- Houtermans, F.G., and Liener, A., 1966, Thermoluminescence of meteorites: *Journal of Geophysical Research*, V. 71, p. 3387-3396.
- Huebner, W.F., 1966, Diminution of cometary heads during perihelion passage: *The Astronomical Journal*, V. 71, p. 858.
- Huebner, W.F., and Weigert, A., 1966, Eiskörner in der Koma von Kometen: *Zeitschrift für Astrophysik*, V. 64, p. 185-201.
- Hughes, M.P., 1966, Planetary observations at a wavelength of 6 cm: *Planetary and Space Science*, V. 14, No. 10, p. 1017-1022.
- Hulston, J.R., 1966 - see Kaplan, I.R.
- Hunke, J.C., 1966 - see Bühler, F.
- Hunt, G.R., 1966, Rapid remote sensing by a "Spectrum Matching" technique, I, Description and discussion of the method: *Journal of Geophysical Research*, V. 71, p. 2919-2930.
- Hunten, D.M., 1966 - see Belton, M.J.S.
- Hunten, M., 1966 - see Belton, J.S.
- Hunter, W., 1966 - see Brownlow, A.E.
- Hurley, P.M., 1966 - see Shields, R.M.
- Huss, G.I., Moore, C.B., and Busek, P.R., 1966, The Fremont Butte, Washington Co., Colorado, meteorite: *Meteoritics*, V. 3, p. 73-78.
- Huss, G.I., Moore, C.B., and Gruenhagen, G., 1966, The Anoka, Minnesota, iron meteorite: *Meteoritics*, V. 3, p. 83-87.
- Huss, G.I., 1966 - see Nininger, H.H.
- Hyder, C.L., 1966, Polarization of the Na D<sub>2</sub> line and magnetic fields in comet Ikeya-Seki(1965f): *The Astronomical Journal*, V. 71, p. 389.
- Hynek, J.A., and Dunlap, J.R., 1966, A lunar transient phenomena detection program: *The Astronomical Journal*, V. 71, p. 389.
- Ibbetson, A., 1966 - see Hide, R.
- Ingalls, R.P., 1966 - see Evans, J.V.
- Innes, R.C., 1966 - see Bader, M.
- Ioffe, Z.M., 1966, Comets in the solar wind: *Soviet Astronomy - A.J.*, V. 10, No. 1, p. 138-142.
- Ioffe, Z.M., 1966, Comets in the solar wind. II: *Soviet Astronomy - A.J.*, V. 10, No. 3, p. 517-519.

- Irvine, W.M., 1966, The shadowing effect in diffuse reflection: *Journal of Geophysical Research*, V. 71, p. 2931-2937.
- Jackson, W.M., and Donn, B., 1966, Photochemical effects in the formation of cometary radicals and ions: *The Astronomical Journal*, V. 71, p. 859-860.
- Jaeger, R.R., and Schuring, D.J., 1966, Spectrum analysis of terrain of Mare Cognitum: *Journal of Geophysical Research*, V. 71, p. 2023-2028.
- Jaeger, R.R., and Lipschutz, M.E., 1966, X-ray diffraction study of shocked meteoritic minerals: *Transactions of the American Geophysical Union*, V. 47, No. 1, p. 134.
- Jaeger, R.R., 1966 - see Lipschutz, M.E.
- Jaffe, L.D., 1966, Lunar dust depth in Mare Cognitum: *Journal of Geophysical Research*, V. 71, p. 1095-1103.
- Jaffe, L.D., 1966, Lunar overlay depth in Mare Tranquillitatus, Alphonsus, and nearby highlands: *Icarus*, V. 5, p. 545-550.
- Jaffe, L.D., 1966, Scientific results of Surveyor I-summary: *Transactions of the American Geophysical Union*, V. 47, No. 4, p. 617-618.
- Jaffe, L.D., and Scott, R.F., 1966, Lunar surface strength: Implication of Luna 9 landing: *Science*, V. 153, p. 407-408.
- Jarosewich, E., 1966, Chemical analyses of ten stony meteorites: *Geochimica et Cosmochimica Acta*, V. 30, p. 1261-1265.
- Jefferys, W.H., 1966, Rotation of the planet Mercury: *Science*, V. 152, p. 201-202.
- Jobbins, E.A., Dimes, F.G., Binns, R.A., Hey, M.H., and Reed, S.J.B. (1966), The Barwell meteorite: *Mineralogical Magazine*, V. 35, p. 881-902.
- Johnson, R.H., 1966, Flow instabilities relating to the surface markings of tektites: *Journal of Geophysical Research*, V. 71, p. 945-949.
- Johnson, S.W., 1966 - see Moraski, L.K.
- Jones, J., and Kaiser, T.R., 1966, The effects of thermal radiation, conduction and meteoroid heat capacity on meteoric ablation: *Monthly Notices of the Royal Astronomical Society*, V. 133, p. 411-420.
- Jones, R.H., 1966, Surveyor I landing dynamics: *Transactions of the American Geophysical Union*, V. 47, No. 4, p. 617.
- Kaiser, T.R., Poole, L.M.G., Webster, A.R., 1966, Radio-echo observations of the major nighttime meteor streams, I. Perseids: *Monthly Notices of the Royal Astronomical Society*, V. 132, p. 225-237.
- Kaiser, T.R., 1966 - see Jones, J.
- Kaiser, T.R., 1966 - see Webster, H.R.
- Kalinyak, A.A., 1966, Data on the spectra of the Galilean satellites of Jupiter: *Soviet Astronomy - A.J.*, V. 9, p. 824-826.
- Kaplan, I.R., and Hulston, J.R., 1966, The isotopic abundance and content of sulfur in meteorites: *Geochimica et Cosmochimica Acta*, V. 30, p. 479-496.

- Kaplan, L.D., 1966 - see Connes, J.
- Kasai, G.H., 1966 - see Danielsson, L.R.
- Katz, I., 1966, Wavelength dependence of the radar reflectivity of the earth and the moon: *Journal of Geophysical Research*, V. 71, p. 361-366.
- Kaufman, I.A., 1966 - see Ho, W.
- Kearns, C.E., and Rudnicki, K., 1966, 28 photographs of comet Humason (1961e): *Zeitschrift für Astrophysik*, V. 64, p. 337-361.
- Keay, C.S.L., Elliyett, C.D., and Brown, T.A., 1966, Absence of unusual periodicities in radar meteor rates: *Journal of Geophysical Research*, V. 71, p. 1409-1411.
- Keil, K., 1964 - see Buseck, P.R.
- Keil, K., 1966 - see Schmidt, R.A.
- Kellermann, K.I., 1966, The thermal radio emission from Mercury, Venus, Mars, Saturn, and Uranus: *Icarus*, V. 5, p. 478-490.
- Kellermann, K.I., and Pauling-Toth, I.I.K., 1966, Observations of the radio emission of Uranus, Neptune, and other planets at 1.9 cm: *The Astrophysical Journal*, V. 145, p. 954-957.
- Kellermann, K.I., and Pauling-Toth, I.I.K., 1966, The detection of the thermal radio emission from Uranus and Neptune at 1.9 cm: *The Astronomical Journal*, V. 71, p. 390.
- Kelley, A.O., 1966, A water-impact hypothesis for the Sierra Madera structure in Texas: *Meteoritics*, V. 3, p. 79-82.
- Kempe, W., and Zähringer, J., 1966, K-Ar-Altersbestimmungen an Eisenmeteoriten-- I Die Isotopenzusammensetzung des primären Kaliums: *Geochimica et Cosmochimica Acta*, V. 30, p. 1049-1057.
- Kennedy, G.C., 1966 - see Carter, N.L.
- Kern, J.W., 1966 - see Kovar, N.S.
- Kharitonova, V.Ya., 1965, Results of chemical analysis of 10 stone meteorites from the collection of the Academy of Sciences of the U.S.S.R.: *Akademiia Nauk SSSR Meteoritika*, No. 26, p. 146-150.
- Kiang, T., 1966, Bias-free statistics of orbital elements of asteroids: *Icarus*, V. 5, p. 437-449.
- Kilston, S.D., Drummond, R.R., and Sagan, C., 1966, A search for life on earth at kilometer resolution: *Icarus*, V. 5, p. 79-98.
- Kimberlin, J., 1966 - see Wasson, J.T.
- King, E.A., Jr., 1966, Baddeleyite inclusion in a Georgia tektite: *Transactions of the American Geophysical Union*, V. 47, No. 1, p. 145.
- King, E.A., Jr., 1966, Major element composition of Georgia tektites: *Nature*, V. 210, p. 828.



- Klein, M.J., and Selig, T.V., 1966, Radio emission from Uranus at 8 Gc/s: *Astrophysical Journal*, V. 146, p. 599.
- Klein, C., Jr., 1966 - see Fuchs, L.H.
- Kolesov, G.M., 1965 - see Lavrukhina, A.K.
- Kolomenskiy, V.D., 1964 - see Mikheyeva, I.V.
- Kopal, Z., 1966, A possible cause of unequal distribution of the maria on the lunar globe: *Publications of the Astronomical Society of the Pacific*, V. 78, p. 444-445.
- Kopal, Z., 1966, On the possible origin of the lunar maria: *Nature*, V. 210, p. 188.
- Kopal, Z., 1966, The nature of secondary craters photographed by Ranger VII: *Icarus*, V. 5, p. 201-213.
- Kopal, Z., 1966 - see Carson, D.
- Kopal, Z., 1966 - see Goudas, C.L.
- Koppe, V.T., 1966 - see Koval, A.G.
- Kovach, R.L., 1966 - see Anderson, D.L.
- Koval, A.G., Koppe, V.T., and Fogel, Ya.M., 1966, CO, CO<sub>2</sub>, and NO emission spectra excited by 13-keV electrons: *Soviet Astronomy - A.J.*, V. 10, No. 1, p. 165-175.
- Kovar, N.S., Kern, J.W., 1966, Proposed hydromagnetic model for comets: *The Astronomical Journal*, V. 71, p. 861.
- Kovar, N.S., and Kovar, R.P., 1966, I(6300,6363)/I(5577) ratio of [O<sub>1</sub>] in the spectra of comets: *The Astronomical Journal*, V. 71, p. 166.
- Kovar, R.P., 1966 - see Kovar, N.S.
- Kraner, H.W., Schroeder, G.L., Davidson, G., and Carpenter, J.W., 1966, Radioactivity of the lunar surface: *Science*, V. 152, p. 1235-1236.
- Kraner, H.W., 1966 - see Davidson, G.
- Krinov, Ye.L., 1964, Falls and finds of meteorites during the last ten years (from 1953 to 1962): *Akademiia Nauk SSSR Meteoritika*, No. 25, p. 173-177.
- Kuiper, G.P., 1966, Interpretation of Ranger VII records: *Communications of the Lunar and Planetary Laboratory*, V. 4, No. 58, p. 1-70.
- Kumai, M., 1966, Microspherules in snow and ice-fog crystals: *Journal of Geophysical Research*, V. 71, p. 3397-3404.
- Kurbatskiy, N.P., 1964, On forest fire in the area of the Tunguska fall in 1908: *Akademiia Nauk SSSR Meteoritika*, No. 25, p. 168-172.
- Kuroda, P.K., 1966 - see Nix, J.F.
- Kutuza, B.G., Losovskii, B.Ya., and Salomonovich, A.E., 1966, Observations of the radio emission of Mars at 8 mm: *Soviet Astronomy - A.J.*, V. 10, No. 1, p. 190-191.
- Kutuza, B.G., 1966 - see Basharinov, A.E.

- Kuz'min, A.D., 1966, Measurements of the brightness temperature of the illuminated side of Venus at 10.6 cm: *Soviet Astronomy - A.J.*, V. 9, p. 995-998.
- Kuz'min, A.D., and Dent, W.A., 1966, The brightness temperature and polarization of Venus at 3.75-cm wavelength: *Soviet Astronomy - A.J.*, V. 10, No. 3, p. 544-545.
- Kvasha, L.G., 1965, On the structure of chondrules and chondrites: *Akademiia Nauk SSSR Meteoritika*, No. 26, p. 35-59.
- Kvasha, L.G., Sidorenko, G.A., and Ginzburg, I.V., 1964, The pyroxene of the stony meteorite Nakhla: *Akademiia Nauk SSSR Meteoritika*, No. 25, p. 90-95.
- Lamar, D.L., and McGann, J., 1966, Shape and internal structure of the moon: *Icarus*, V. 5, p. 10-23.
- Lamar, D.L., and Merifield, P.M., 1966, Age and origin of earth-moon system revealed by coral growth lines: *Transactions of the American Geophysical Union*, V. 47, No. 3, p. 486.
- Lämmerzahl, P., and Zähringer, J., 1966, K-Ar-Altersbestimmungen an Eisenmeteoriten--II Spallogenes  $Ar^{40}$ - $Ar^{38}$ -Bestrahlungsalter: *Geochimica et Cosmochimica Acta*, V. 30, p. 1059-1074.
- Larson, S.M., 1966, Observations of comet Ikeya-Seki (1965f) from Tucson, Arizona: *Communications of the Lunar and Planetary Laboratory*, V. 4, No. 68, p. 145-156 + 1 color photograph.
- Laslett, L.J., and Sessler, A.M., 1966, Rotation of Mercury: *Science*, V. 151, p. 1384-1385.
- Laur, P., 1966 - see Meinschein, W.G.
- Lautman, D.A., Shapiro, I.I., and Colombo, G., 1966, The earth's dust belt: fact or fiction? 4. Sunlight-pressure air-drag capture: *Journal of Geophysical Research*, V. 71, p. 5733-5741.
- Lautman, D.A., 1966 - see Colombo, G.
- Lautman, D.A., 1966 - see Shapiro, I.I.
- Lavrukhina, A.K., 1965, Study of the spatial and temporal variations of cosmic rays on the basis of the effects of nuclear spallations in meteorites: *Akademiia Nauk SSSR Meteoritika*, No. 26, p. 91-101.
- Lavrukhina, A.K., Vilenskiy, V.D., Kolesov, G.M., Rutkovskiy, V.M., and Yukina, L.V., 1965, Radiochemical investigation of the meteorite Zaysan: *Akademiia Nauk SSSR Meteoritika*, No. 26, p. 102-108.
- Lazarev, R.G., 1966, The frequency of sporadic meteoric bodies: *Soviet Astronomy - A.J.*, V. 9, p. 830-836.
- Le Bas, M.J., 1966, High load-pressure mineralogical relations in chondrites: *Nature*, V. 211, p. 1355-1358.
- Lebo, G.R., 1966 - see Six, N.F., Jr.
- Lee, R.T., 1966 - see Baart, E.E.
- Leftus, V., 1966, Radio emission of Venus at 3 cm and the solar activity: *Nature*, V. 211, p. 176.

- Leighton, R.B., and Murray, B.C., 1966, Behavior of carbon dioxide and other volatiles on Mars: *Science*, V. 153, p. 136-153.
- Leovy, C., 1966, Mars ice caps: *Science*, V. 154, p. 1178-1179.
- Leovy, C., 1966, Note on thermal properties of Mars: *Icarus*, V. 5, p. 1-5.
- Lettau, H.H., 1966, Dust on the moon's surface?: *Journal of Geophysical Research*, V. 71, p. 5469-5470.
- Levengood, W.C., 1966, Internal elastic energy variations in tektites: *Journal of Geophysical Research*, V. 71, p. 613-618.
- Levin, B.Yu., 1966, The structure of the moon: *Soviet Astronomy*, V. 10, No. 3, p. 479-491.
- Levy, P.W., 1966 - see Zeller, E.J.
- Lewis, C.F., 1966 - see Moore, C.B.
- Lienert, A., 1966 - see Houtermans, F.G.
- Lin, S.C., 1966, Cometary impact and the origin of tektites: *Journal of Geophysical*, V. 71, p. 2427-2437.
- Linsky, J., 1966, Models of the lunar surface with temperature-dependent thermal properties: *The Astronomical Journal*, V. 71, p. 168-169.
- Linsky, J.L., 1966, Models of the lunar surface including temperature-dependent thermal properties: *Icarus*, V. 5, p. 606-634.
- Lippolt, H.J., 1966 - see Burnett, D.S.
- Lipschutz, M.E., and Jaeger, R.R., 1966, X-ray diffraction study of minerals from shocked iron meteorites: *Science*, V. 152, p. 1055-1057.
- Lipschutz, M.E., 1966 - see Anders, E.
- Lipschutz, M.E., 1966 - see Heymann, D.
- Lipschutz, M.E., 1966 - see Jaeger, R.R.
- Lipsky, Y.N., 1966, What Luna 9 told us about the moon: *Sky and Telescope*, V. 32, p. 257-260.
- Liu, Han-Shou, 1966, The libration of Mercury: *Journal of Geophysical Research*, V. 71, p. 3099-3100.
- Livingston, W., Roddier, F., Spinrad, H., Slaughter, C., and Chapman, D., 1966, The sodium D lines in comet Ikeya-Seki: *Sky and Telescope*, V. 31, p. 24-25.
- Lloyd, R., 1966 - see Roemer, E.
- Lohman, R., 1966 - see Welch, W.J.
- Losovskii, B.Ya., 1966 - see Kutuza, B.G.
- Lovell, B., 1966 - see Davies, J.G.

- Low, F.J., 1966, Observations of Venus, Jupiter and Saturn at  $\lambda 20\mu$ : The Astronomical Journal, V. 71, p. 191.
- Low, F.J., 1966, The infrared brightness temperature of Uranus: Astrophysical Journal, V. 146, p. 326.
- Lowman, P.D., Jr., and O'Keefe, J.A., 1966, Terrestrial origin of the Igeest objects: Nature, V. 209, p. 67.
- Lucas, J.W., Conel, J., Saari, J., Garipay, R., and Hagemeyer, W., 1966, Some lunar thermal characteristics from Surveyor I data: Transactions of the American Geophysical Union, V. 47, No. 4, p. 616.
- Lunch, J.E., 1966 - see Moraski, L.K.
- Lyttleton, R.A., 1966, The effect on the lunar orbit of meteoritic accretion: Icarus, V. 5, p. 162-164.
- Malsch, W., 1966, Beobachtungen von Planetoiden 1965: Astronomische Nachrichten, V. 289, p. 194.
- Malville, J. McK., and Evans, C., 1966, Observations of comet Ikeya-Seki with the climax coronagraph: The Astronomical Journal, V. 71, p. 169.
- Marcus, A., 1966, Comments on "Distribution of craters on the lunar surface": Monthly Notices of the Royal Astronomical Society, V. 134, p. 269-274.
- Marcus, A.H., 1966, A stochastic model of the formation and survival of lunar craters: Icarus, V. 5, p. 590-605.
- Marcus, A.H., 1966, A stochastic model of the formation and survival of lunar craters II. Approximate distribution of diameter of all observable craters: Icarus, V. 5, p. 165.
- Marcus, A.H., 1966, A stochastic model of the formation and survival of lunar craters III. Filling and disappearance of craters: Icarus, V. 5, p. 178-189.
- Marcus, A.H., 1966, A stochastic model of the formation and survival of lunar craters IV. On the non-randomness of crater centers: Icarus, V. 5, p. 190-200.
- Marsden, B.G., 1966, Evolution of the great sun-grazing comet group: The Astronomical Journal, V. 71, p. 863.
- Marshall, L., 1966, Non-anti-matter nature of the Tunguska meteor: Nature, V. 212, p. 1226.
- Martin, J.J., 1966, Scattering from the moon and other rough surfaces: Journal of Geophysical Research, V. 71, p. 2687-2688.
- Marvin, R.F., 1966 - see Clarke, R.S., Jr.
- Marvin, T.C., 1966 - see Marvin, U.B.
- Marvin, U.B., and Marvin, T.C., 1966, A re-examination of the crater near Crestone, Colorado: Meteoritics, V. 3, p. 1-10.
- Marvin, U.B., 1966 - see Dodd, R.T., Jr.

- Mason, B., 1966, Geochemistry and meteorites: *Geochimica et Cosmochimica Acta*, V. 30, p. 365-374.
- Mason, B., 1966, The enstatite chondrites: *Geochimica et Cosmochimica Acta*, V. 30, p. 23-39.
- Mason, B., 1966 - see Buseck, P.R.
- Massalski, T.B., Park, F.R., and Vassamillet, L.F., 1966, Speculations about plessite: *Geochimica et Cosmochimica Acta*, V. 30, p. 649-662.
- Massalski, T.B., 1966 - see Park, F.R.
- Matsushima, S., 1966, Apparent correlation between the lunar eclipse brightness and the solar wind: *Nature*, V. 211, p. 1027-1028.
- Matsushima, S., 1966, Variation of lunar eclipse brightness and its association with the geomagnetic planetary index  $K_p$ : *The Astronomical Journal*, V. 71, p. 699-705.
- Mattschei, P.K., 1966 - see Wasson, J.T.
- Matveev, Yu.G., Suchkin, G.L., and Troitskii, V.S., 1966, Change of lunite density with depth in the surface layer: *Soviet Astronomy - A.J.*, V. 9, p. 626-630.
- Maurette, M., 1966 - see Walker, R.M.
- Mazor, E., 1966 - see Haymann, D.
- McAdam, W.B., 1966, The extent of the emission region on Jupiter at 408 Mc/s: *Planetary and Space Science*, V. 14, No. 11, p. 1041-1046.
- McCall, G.J.H., 1966, Implication of the Mariner IX photography of Mars: *Nature*, V. 211, p. 1384-1385.
- McCall, G.J.H., 1966, The petrology of the Mount Padbury mesosiderite and its achondrite enclaves: *Mineralogical Magazine*, V. 35, p. 1029-1060.
- McClaine, L.A., 1966 - see McConnell, R.K., Jr.
- McConnell, R.K., Jr., and McClaine, L.A., 1966, Mechanics of magma migration: *Transactions of the American Geophysical Union*, V. 47, No. 1, p. 177.
- McConnell, R.K., Jr., 1966 - see Vonnegut, B.
- McCulloch, P.M., and Ellis, G.R.A., 1966, Observations of Jupiter's decametric radio emissions: *Planetary and Space Science*, V. 14, No. 4, p. 347-359.
- McElroy, M.B., 1966 - see Chamberlain, J.W.
- McGann, J., 1966 - see Lamar, D.L.
- McGovern, W.E., 1966 - see Gross, S.H.
- McLinden, H.G., 1966 - see Aronson, J.R.
- Meadows, A.J., 1966 - see Miles, H.G.
- Megrue, G.H., 1966, Rare-gas chronology of calcium-rich achondrites: *Journal of Geophysical Research*, V. 71, p. 4021-4027.

- Meinschein, W.G., Frondel, C., Laur, P., and Mislow, K., 1966, Meteorites: Optical activity in organic matter: *Science*, V. 154, p. 377-380.
- Meister, J., 1966 - see Bühler, F.
- Meloy, T.P., and Faust, L., 1966, Size and velocity distribution of ejecta from an impact crater: *Transactions of the American Geophysical Union*, V. 47, No. 1, p. 149.
- Meloy, T.P., and Faust, L., 1966, Size distribution and depth of dust on the lunar surface considering impact comminution alone: *Transactions of the American Geophysical Union*, V. 47, No. 1, p. 149.
- Merifield, P.M., 1966 - see Lamar, D.L.
- Merrihue, C., 1966, Xenon and krypton in the Bruderheim meteorite: *Journal of Geophysical Research*, V. 71, p. 263.
- Merrill, C.W., 1966 - see Chao, E.C.T.
- Mertz, L., 1965, Discussion of paper by E.A. Burns and R.J.P. Lyon, "Errors in the Measurement of the Lunar Temperature": *Journal of Geophysical Research*, V. 70, p. 999-1000.
- Mertz, L., and Coleman, I., 1966, Infrared spectrum of Saturn's ring: *The Astronomical Journal*, V. 71, p. 747-748.
- Michael, W.H., Jr., Tolson, R.H., and Gapcynski, J.P., 1966, Lunar orbiter: Tracking data indicate properties of moon's gravitational field: *Science*, V. 153, p. 1102-1103.
- Michelson, I., 1966, Augmented lunar tide heights in barycentric motion: *Monthly Notices of the Royal Astronomical Society*, V. 133, p. 17-20.
- Michelson, I., 1966, Reduced lunar equatorial principal inertia moment difference related to inclination angles: *The Astronomical Journal*, V. 71, p. 171.
- Middlehurst, B.M., 1966, An analysis of lunar events: *Transactions of the American Geophysical Union*, V. 47, No. 1, p. 150.
- Middlehurst, M., 1966, Transient lunar events: possible causes: *Nature*, V. 209, p. 602.
- Middlehurst, B.M., 1966 - see Burley, J.
- Mikhailov, A.A., 1966, Gravitational force and the moon's figure: *Soviet Astronomy - A.J.*, V. 9, p. 819-823.
- Mikheyeva, I.V., and Kolomenskiy, V.D., 1964, Investigation of meteor and industrial dust by the X-ray method: *Akademiia Nauk SSSR Meteoritika*, No. 25, p. 156-162.
- Miles, H.G., and Meadows, A.J., 1966, Fireballs associated with the Barwell meteorite: *Nature*, V. 212, p. 1339.
- Milford, S.N., and Pomilla, F.R., 1966, Contamination of the lunar atmosphere by rocket exhaust gases: *Transactions of the American Geophysical Union*, V. 47, No. 1, p. 155.
- Miller, A.C., and Griffin, J., 1966, 1414 Mc/sec Jupiter observations: *The Astronomical Journal*, V. 71, p. 744-746.

- Miller, F.D., 1966 - see Dewey, M.E.
- Miller, J.A., 1966 - see Turner, G.
- Millman, P.M., 1966, Craters: *Meteoritics*, V. 3, p. 55-57.
- Mislow, K., 1966 - see Meinschein, W.G.
- Miyamoto, S., 1966, Martian atmosphere and crust: *Icarus*, V. 5, p. 360-374.
- Momford, G.S., 1966, Comet Barbon (1966c): *Sky and Telescope*, V. 32, p. 198.
- Moore, A.J., 1966 - see Gault, D.E.
- Moore, C.B., and Lewis, C.F., 1966, The distribution of total carbon content in enstatite chondrites: *Earth and Planetary Science Letters*, V. 1, No. 6, p. 376-378.
- Moore, C.B., 1966 - see Huss, G.I.
- Moore, P., 1966, Origin of the lunar maria: *Nature*, V. 210, p. 1347.
- Moore, R., 1966 - see Spinrad, H.
- Moraski, L.K., Teal, D.J., Lunch, J.E., Higgins, C.J., and Johnson, S.W., 1966, The effects of gravity on shear strength and explosion crater parameters for cohesionless soils: *Transactions of the American Geophysical Union*, V. 47, No. 1, p. 149.
- Morgan, G., 1966 - see Walker, R.M.
- Moron, J.M., Jr., and Staelin, D.H., 1966, Observations of the moon near 1-cm wavelength: *The Astronomical Journal*, V. 71, p. 865.
- Moroz, V.I., 1966, Infrared spectrophotometry of the moon and the Galilean satellites of Jupiter: *Soviet Astronomy - A.J.*, V. 9, p. 999-1006.
- Moroz, V.I., 1966, The spectra of Jupiter and Saturn in the 1.0-2.5 $\mu$  region: *Soviet Astronomy - A.J.*, V. 10, No. 3, p. 457-468.
- Morris, E.C., and Shoemaker, E.M., 1966, Craters and fragmental debris of the lunar surface around Surveyor 1: *Transactions of the American Geophysical Union*, V. 47, No. 4, p. 617.
- Morris, E.C., 1966 - see Shoemaker, E.M.
- Mueller, G., 1966, Origin of meteorites, in the light of recent rocket photography of the moon and Mars: *Nature*, V. 211, p. 1134-1135.
- Mueller, G., 1966, Significance of inclusions in carbonaceous meteorites: *Nature*, V. 210, p. 151-155.
- Müller, O., and Zähringer, J., 1966, Chemische Unterschiede bei uredelgashaltigen steinmeteoriten: *Earth and Planetary Science Letters*, V. 1, No. 1, p. 25-29.
- Müller, O., and Zähringer, J., 1966, K-Ar-Altersbestimmungen an Eisenmeteoriten-- III Kalium- und Argon-Bestimmungen: *Geochimica et Cosmochimica Acta*, V. 30, p. 1075-1092.

- Münch, G., 1966 - see Younkin, R.L.
- Munk, M.N., 1966 - see Reynolds, J.H.
- Murray, B.C., 1966 - see Leighton, R.B.
- Mutch, T.A., 1966, Abundances of magnetic spherules in Silurian and Permian salt samples: *Earth and Planetary Science Letters*, V. 1, No. 5, p. 325-329.
- Nagy, B., 1966, A study of the optical rotation of lipids extracted from soils, sediments, and the Orgueil carbonaceous meteorite: *Proceedings of the National Academy of Sciences*, V. 56, p. 339-398.
- Nash, D.B., 1966, Proton-excited luminescence of silicates: experimental results and lunar implications: *Journal of Geophysical Research*, V. 71, p. 2517-2534.
- Nash, D.B., 1966, Proton luminescence of feldspars and silica polymorphs and lunar applications: *Transactions of the American Geophysical Union*, V. 47, No. 1, p. 150.
- Nazarkina, G.B., 1965 - see Surkov, Yu.A.
- Neal, R.W., 1966 - see Steelin, D.H.
- Neubauer, F.M., 1966, Thermal convection in the Martian atmosphere: *Journal of Geophysical Research*, V. 71, p. 2419-2426.
- Newbury, R.S., 1966 - see Dews, J.R.
- Ney, E.P., Woolf, N.J., and Collins, R.J., 1966, Mechanisms for lunar luminescence: *Journal of Geophysical Research*, V. 71, p. 1787-1793.
- Nichiporuk, W., and Bingham, E., 1966, Copper and vanadium in stony meteorites: *Transactions of the American Geophysical Union*, V. 47, No. 1, p. 131.
- Nielsen, B., 1966 - see Heymann, D.
- Nininger, H.H., and Huss, G.I., 1966, Free copper in the Odessa, Texas, siderite: *Meteoritics*, V. 3, p. 71-72.
- Nix, J.F., and Kuroda, P.K., 1966, A neutron activation analysis of uranium in stone meteorites: *Transactions of the American Geophysical Union*, V. 47, No. 1, p. 133.
- Norton, R.B., Ferguson, E.E., Fehsenfeld, F.C., and Schmeltekopf, A.L., 1966, Ion-neutral reactions in the Martian ionosphere: *Planetary and Space Science*, V. 14, No. 10, p. 969-978.
- Oberbeck, V.R., 1966 - see Gault, D.E.
- Oberbeck, V.R., 1966 - see Quaide, W.L.
- Oetking, P., 1966, Photometric studies of diffusely reflecting surfaces with applications to the brightness of the moon: *Journal of Geophysical Research*, V. 71, p. 2505-2513.
- Ohring, G., 1966, Water-vapor mixing ratios near the cloudtops of Venus: *Icarus*, V. 5, p. 329-333.
- O'Keefe, J.A., 1966, Lunar questions discussed at Pasadena: *Sky and Telescope*, V. 31, p. 10-12.



- O'Keefe, J.A., 1966, Muong Nong tektites and lunar ash flows: *The Astronomical Journal*, V. 71, p. 393-394.
- O'Keefe, J.A., 1966 - see Lowman, P.D., Jr.
- Oleak, H., 1966, Die streifende Feuerkugel vom 14. Jan '65 *Astronomische Nachrichten*, V. 289, p. 71-79.
- O'Leary, B.T., 1966, On the occurrence and nature of planets outside the solar system: *Icarus*, V. 5, p. 419-436.
- O'Leary, B.T., 1966, Photometry of a Venus halo effect: *Transactions of the American Geophysical Union*, V. 47, No. 1, p. 156.
- O'Leary, B.T., 1966, The presence of ice in the Venus atmosphere as inferred from a halo effect: *Publications of the Astronomical Society of the Pacific*, V. 78, p. 447-448.
- O'Leary, T.O., 1966, The presence of ice in the Venus atmosphere as inferred from a halo effect: *Astrophysical Journal*, V. 144, p. 754-766.
- Olivarez, J., 1966, Unusual widespread colors on Jupiter: *Sky and Telescope*, V. 31, p. 306-307.
- Olsen, E., and Fredriksson, K., 1966, Phosphates in iron and pallasite meteorites: *Geochimica et Cosmochimica Acta*, V. 30, p. 459-470.
- Olsson, C.N., and Smith, A.G., 1966, Decametric radio pulses from Jupiter: *Characteristics*: *Science*, V. 153, p. 289-290.
- Oncley, P.B., and Fulmer, C., 1966, The Martian "Canali" as meteoritic crater rays: *Transactions of the American Geophysical Union*, V. 47, No. 3, p. 482.
- Opik, E.J., 1966, The Martian surface: *Science*, V. 153, p. 255-265.
- Osgood, J.H., and Green, J., 1966, Sonic velocity and penetrability of simulated lunar rock dust: *Geophysics*, V. 31, No. 3, p. 536-561.
- Osnach, A.I., 1966 - see Zharkov, V.N.
- Ostic, R.G., 1966, The concentration and isotopic composition of lead in Toluca Iron Meteorite: *Journal of Geophysical Research*, V. 71, p. 4060-4063.
- Ottermann, J., and Bronner, F.E., 1966, Martian wave of darkening: A frost phenomenon: *Science*, V. 153, p. 56-60.
- Owen, T., 1966, An identification of the 6800-Å methane band in the spectrum of Uranus and a determination of atmospheric temperature: *Astrophysical Journal*, V. 146, p. 611.
- Owen, T., 1966, The composition and surface pressure of the Martian atmosphere: results from the 1965 opposition: *Astrophysical Journal*, V. 146, p. 259-270.
- Park, F.P., Bunch, T.E., and Massalski, T.B., 1966, A study of the silicate inclusions and other phases in the Campo del Cielo meteorite: *Geochimica et Cosmochimica Acta*, V. 30, p. 399-414.
- Park, F.R., 1966 - see Massalski, T.B.

- Parkin, D.W., 1966 - see Brownlow, A.E.
- Patashnik, H., and Hemenway, C.L., 1966, Mass and density measurements of micro-meteorites: *The Astronomical Journal*, V. 71, p. 866.
- Pauling-Toth, I.I.K., 1966 - see Kellermann, K.I.
- Peale, S.J., 1966, Dust belt of the earth: *Journal of Geophysical Research*, V. 71, p. 911-933.
- Peale, S.J., 1966 - see Goldreich, P.
- Pellicori, R.H., 1966 - see Arthur, D.W.G.
- Pepin, R.O., 1966, Heavy rare gases in silicates from the Estherville mesosiderite: *Journal of Geophysical Research*, V. 71, p. 2815-2829.
- Petrova, N.N., 1966, Spectrophotometric study of the lunar surface: *Soviet Astronomy - A.J.*, V. 10, No. 1, p. 128-135.
- Philpotts, J.A., and Pinson, W.H., Jr., 1966, New data on the chemical composition and origin of moldavites: *Geochimica et Cosmochimica Acta*, V. 30, p. 253-266.
- Phinney, R.A., 1966 - see Anderson, D.L.
- Pinson, W.H., Jr., 1966 - see Philpotts, J.A.
- Pinson, W.H., Jr., 1966 - see Shields, R.M.
- Plagemann, S., 1965, A model of the internal constitution and temperature of the planet Mercury: *Journal of Geophysical Research*, V. 70, p. 985-993.
- Plechkov, V.M., 1966, Observations of the June 1964 lunar eclipse at 1.8 cm at Gor'Kii: *Soviet Astronomy - A.J.*, V. 10, No. 1, p. 136-137.
- Plummer, W., and Strong, J., 1966, A new estimate of the surface temperatures of Venus: *The Astrophysical Journal*, V. 144, p. 423.
- Plummer, W.T., and Strong, J., 1966, Conditions on the planet Venus: *Transactions of the American Geophysical Union*, V. 47, No. 1, p. 156.
- Pollack, J.B., 1966 - see Sagan, C.
- Pollack, S.S., 1966, Disordered orthopyroxene in meteorites: *American Mineralogist*, V. 51, p. 1722-1726.
- Pomilla, F.R., 1966 - see Milford, S.N.
- Ponnamperuma, C., 1966, Some recent work on prebiological synthesis of organic compounds: *Icarus*, V. 5, p. 450-454.
- Poole, L.M.G., 1966 - see Kaiser, T.R.
- Poole, L.M.G., 1966 - see Webster, H.R.
- Popov, N.M., 1965 - see Vinogradov, A.P.
- Portnov, A.M., 1964, On the crater on the Potomsk Upland: *Akademiia Nauk SSSR Meteoritika*, No. 25, p. 194-197.

- Pottchard, R.S., 1966 - see Davies, J.G.
- Potter, J., 1966 - see Arking, A.
- Price, P.B., Walker, R.M., and Fleischer, R.L., 1966, The use of plutonium fission tracks to measure the cooling of meteoritic bodies following the formation of the solar system: *Transactions of the American Geophysical Union*, V. 47, No. 1, p. 132.
- Price, P.B., 1966 - see Walker, R.M.
- Qualde, W.L., Oberbeck, V.R., and Gault, D.E., 1966, Modeling meteorite craters in the laboratory, 2, deformational structures: *Transactions of the American Geophysical Union*, V. 47, No. 1, p. 148.
- Qualde, W.L., 1966 - see Gault, D.E.
- Rainville, L.P., 1966 - see Evans, J.V.
- Ramovich, M., 1965, On the significance of the study of geoelectric pulsations for the problem of the origin of meteorites: *Akademiia Nauk SSSR Meteoritika*, No. 26, p. 109-111.
- Ramsden, A.R., and Cameron, E.N., 1966, Kamacite and taenite superstructures and a metastable tetragonal phase in iron meteorites: *American Mineralogist*, V. 51, p. 37-55, p. 1544.
- Rank, D.H., Fink, U., and Wiggins, T.A., 1966, Measurements on spectra of gases of planetary interest II.  $H_2$ ,  $CO_2$ ,  $NH_3$ , and  $CH_4$ : *Astrophysical Journal*, V. 143, p. 980.
- Rasool, S.I., 1966 - see Gross, S.H.
- Read, G.W., Jr., and Allen, R.O., Jr., 1966, Halogens in chondrites: *Geochimica et Cosmochimica Acta*, V. 30, p. 779-800.
- Reese, E.J., and Smith, B.A., 1966, A rapidly moving spot on Jupiter's North Temperate Belt: *Icarus*, V. 5, p. 248-257.
- Reese, E.J., and Solberg, H.G., Jr., 1966, Recent measures of the latitude and longitude of Jupiter's Red Spot: *Icarus*, V. 5, p. 266-273.
- Reeves, R.R., Jr., 1966 - see Applebaum, D.C.
- Reid, W.A., 1966 - see Evans, J.V.
- Rennilson, J.J., 1966, Selected colorimetric results from Surveyor I television: *Transactions of the American Geophysical Union*, V. 47, No. 4, p. 616.
- Rennilson, J.J., and Holt, H.E., 1966, Photometric properties and photoclinometry of the lunar surface from Surveyor I television: *Transactions of the American Geophysical Union*, V. 47, No. 4, p. 616.
- Rennilson, J.J., 1966 - see Turkevich, A.
- Reynolds, J.H., Honenberg, C.M., and Munk, M.N., 1966, The case for  $Pu^{244}$  in the Pasamonte achondrite: *Transactions of the American Geophysical Union*, V. 47, No. 1, p. 133.
- Righini, A., Jr., and Rigutti, N., 1966, Some results of research on lunar luminescence: *Icarus*, V. 5, p. 258-265.

- Rigutti, M., 1966 - see Righini, A., Jr.
- Riihimaa, J.J., 1966, High-resolution spectra of decametric radio bursts from Jupiter: *Nature*, V. 209, p. 387-388.
- Riihimaa, J.J., 1966, Spectral types of decametric radiation from Jupiter: *Nature*, V. 212, p. 1338-1339.
- Rindfleisch, T., 1966, Photometric method for lunar topography: *Photogrammetric Engineering*, V. 32, No. 2, p. 262-276.
- Ringwood, A.E., 1966, Chemical evolution of the terrestrial planets: *Geochimica et Cosmochimica Acta*, V. 30, p. 41-104.
- Ringwood, A.E., 1966, Genesis of chondritic meteorites: *Reviews of Geophysics*, V. 4, No. 2, p. 113-175.
- Roberts, G.L., 1966, Three-color photoelectric photometry of the moon: *Icarus*, V. 5, p. 555-564.
- Roberts, W.A., 1966, Lunar surface characteristics: A contemporary view: *Publications of the Astronomical Society of the Pacific*, V. 78, p. 448-449.
- Roberts, W.A., 1966, Shock--a process in extraterrestrial sedimentology: *Icarus*, V. 5, p. 459-477.
- Roberts, J.A., and Ekers, R.D., 1966, The position of Jupiter's Van Allen belt: *Icarus*, V. 5, p. 149-153.
- Robinson, J.C., 1966, Ground-based photography of the Mariner IV region of Mars: *Icarus*, V. 5, p. 245-247.
- Robinson, A.R., 1966 - see Goody, R.M.
- Roddier, F., 1966 - see Livingston, W.
- Roddy, D.J., 1966, Carbonate deformation at a probable impact crater at Flynn Creek, Tennessee: *Transactions of the American Geophysical Union*, V. 47, No. 3, p. 493-494.
- Roddy, D.J., 1966, Minimum energy of formation for a probable impact crater at Flynn Creek, Tennessee: *Transactions of the American Geophysical Union*, V. 47, No. 3, p. 482.
- Roemer, E., 1966, Comet notes: *Publications of the Astronomical Society of the Pacific*, V. 78, p. 83-91.
- Roemer, E., 1966, Comet notes: *Publications of the Astronomical Society of the Pacific*, V. 78, p. 178-179.
- Roemer, E., 1966, Comet notes: *Publications of the Astronomical Society of the Pacific*, V. 78, p. 348-350.
- Roemer, E., 1966, Comet notes: *Publications of the Astronomical Society of the Pacific*, V. 78, p. 488-490.
- Roemer, E., and Lloyd, R.E., 1966, Observations of comets, minor planets, and satellites: *The Astronomical Journal*, V. 71, p. 433-457.

- Roemer, E., Thomas, M., and Lloyd, R., 1966, Observations of comets, minor planets, and Jupiter VIII: *The Astronomical Journal*, V. 71, p. 591-601.
- Romig, M.F., 1966, The scientific study of meteors in the 19th century: *Meteoritics*, V. 3, p. 11-25.
- Ronca, L.B., 1966, Meteoritic impact and volcanism: *Icarus*, V. 5, p. 515-520.
- Ronca, L.B., 1966, Structure of the crater Alphonsus: *Science*, V. 209, p. 182.
- Ronca, L.B., and Salisbury, J.W., 1966, Lunar history as suggested by the circularity index of lunar craters: *Icarus*, V. 5, p. 130-138.
- Ronca, L.B., 1966 - see Salisbury, J.W.
- Ronca, L.B., 1966 - see Zeller, E.J.
- Roper, R.G., 1966, Atmospheric turbulence in the meteor region: *Journal of Geophysical Research*, V. 71, p. 5785-5792.
- Rosenberg, D.L., 1966, Modification of optical properties of the lunar surface by solar wind bombardment: *Transactions of the American Geophysical Union*, V. 47, No. 3, p. 486-487.
- Rowe, M.W., 1966, Solar nucleosynthesis of extinct <sup>129</sup>I: *Earth and Planetary Science Letters*, V. 1, No. 3, p. 97-98.
- Rowe, M.W., and Bogard, D.D., 1966, Isotopic composition of xenon from Ca-poor achondrites: *Journal of Geophysical Research*, V. 71, p. 4183-4191.
- Rowe, M.W., and Bogard, D.D., 1966, Xenon anomalies in the Pasamonte meteorite: *Journal of Geophysical Research*, V. 71, p. 686-687.
- Rowe, M.W., and Bogard, D.D., 1966, Xenon from achondrites: *Transactions of the American Geophysical Union*, V. 47, No. 1, p. 133.
- Rowe, M.W., 1966 - see Bogard, D.D.
- Rubashevskii, A.E., 1966, A method for determining the diameter of Pluto from occultation observations (remarks of Halliday's paper): *Soviet Astronomy - A.J.*, V. 10, No. 1, p. 124-127.
- Rudnicki, K., 1966 - see Kearns, C.E.
- Runcorn, S.K., 1966, The figure of the moon: *Transactions of the American Geophysical Union*, V. 47, No. 3, p. 486.
- Ruskol, E.L., 1966, On the past history of the earth-moon system: *Icarus*, V. 5, p. 221-227.
- Russell, R.V., 1966 - see Barnes, V.E.
- Rutkovskiy, V.M., 1965 - see Lavrukhina, A.K.
- Ryan, J.A., 1966, Adhesion of silicates in ultrahigh vacuum: *Journal of Geophysical Research*, V. 71, p. 4413-4425.
- Saari, J.M., and Shorthill, R.W., 1966, Hot spots on the moon: *Sky and Telescope*, V. 31, p. 327-331.

- Saari, J.M., and Shorthill, R.W., 1966, Studies of thermal features on the eclipsed moon: Publications of the Astronomical Society of the Pacific, V. 78, p. 451-453.
- Saari, J.M., Shorthill, R.W., and Deaton, T.K., 1966, Infrared and visible images of the eclipsed moon: Icarus, V. 5, p. 635-659.
- Saari, J., 1966 - see Lucas, J.W.
- Saari, J.M., 1966 - see Fulmer, C.
- Saari, J.M., 1966 - see Fulmer, C.V.
- Safronov, V.S., 1966, Sizes of the largest bodies falling onto the planets during their formation: Soviet Astronomy - A.J., V. 9, p. 987-994.
- Sagan, C., 1966, The photometric properties of Mercury: The Astrophysical Journal, V. 144, p. 1218, 1221.
- Sagan, C., and Pollack, J.B., 1966, An inorganic model of Martian phenomena: The Astronomical Journal, V. 71, p. 178.
- Sagan, C., and Pollack, J.B., 1966, Elevation differences on Mars: Special Report No. 224, Smithsonian Astrophysical Observatory, Cambridge, Massachusetts.
- Sagan, C., and Pollack, J.B., 1966, Elevation differences on Mars: The Astronomical Journal, V. 71, p. 869.
- Sagan, C., and Pollack, J.B., 1966, On the nature of the canals of Mars: Nature, V. 212, p. 117-121.
- Sagan, C., and Pollack, J.B., 1966, On the nature of the clouds and the origin of the surface temperature of Venus: The Astronomical Journal, V. 71, p. 178-179.
- Sagan, C., Pollack, J.B., and Goldstein, R.M., 1966, Radar doppler spectroscopy of Mars. I. Elevation differences between bright and dark areas: Special Report No. 221, Smithsonian Astrophysical Observatory, Cambridge, Massachusetts.
- Sagan, C., 1966 - see Kilston, S.D.
- Sagan, C., 1966 - see Walker, R.G.
- Salisbury, J.W., 1966, The light and dark areas of Mars: Icarus, V. 5, p. 291-298.
- Salisbury, J.W., and Ronca, L.B., 1966, The origin of continents: Nature, V. 210, p. 669-670.
- Salisbury, J.W., 1966 - see Ronca, L.B.
- Salisbury, W.W., 1966, A method of translunar radio communication: Nature, V. 211, p. 950-951.
- Salomonovich, A.E., 1966 - see Kutuza, B.G.
- Samuelson, R.E., 1966, Greenhouse effect in semi-infinite scattering atmospheres: The Astronomical Journal, V. 71, p. 179.
- Sanchez, J., and Cassidy, W., 1966, A previously undescribed meteorite crater in Chile: Journal of Geophysical Research, V. 71, p. 4891-4895.

- Sanchez, J., and Cassidy, W., 1966, A previously undescribed meteorite crater in Chile: Transactions of the American Geophysical Union, V. 47, No. 1, p. 144.
- Sastry, Ch.V., 1966, Short-term correlations of decameter radio emission from Jupiter and solar activity: The Astronomical Journal, V. 71, p. 179.
- Schmeltekopf, A.L., 1966 - see Norton, R.B.
- Schmidt, R.A., and Keil, K., 1966, Electron microprobe study of spherules from Atlantic Ocean sediments: Geochimica et Cosmochimica Acta, V. 30, p. 471-478.
- Schmitt, R.A., Smith, R.H., and Goles, G.G., 1966, Chainpur-like chondrites: Primitive precursors of ordinary chondrites: Science, V. 153, p. 644-646.
- Schorn, R.A., 1966 - see Spinrad, H.
- Schröder, W., 1966, Additional note of noctilucent clouds over Germany: Journal of Geophysical Research, V. 71, p. 5185.
- Schroeder, G.L., 1966 - see Davidson, G.
- Schroeder, G.L., 1966 - see Kraner, H.W.
- Schuring, D.J., 1966 - see Jaeger, R.M.
- Schutten, J., and Van Dijk, Th., 1966, Luminescence caused by proton impact with special reference to the lunar surface: Nature, V. 211, n. 470-471.
- Scott, R.F., 1966, Symposium on Surveyor I results: soil mechanics results: Transactions of the American Geophysical Union, V. 47, No. 4, p. 617.
- Scott, R.F., 1966 - see Jaffe, L.D.
- Seeger, C.R., 1966, Sound wave velocities in some tektites and natural glasses: Transactions of the American Geophysical Union, V. 47, No. 1, p. 144.
- Sekania, Z., 1966, Dynamical effect of explosive phenomena in comet Halley and its nuclear rotation: Zeitschrift für Astrophysik, V. 64, p. 465-471.
- Sekera, Z., 1966, Recent developments in the theory of radiative transfer in planetary atmospheres: Review of Geophysics, V. 4, No. 1, p. 101-111.
- Selling, T.W., 1966, Observations of total eclipses of the moon at a wavelength of 1.82 centimeters: Journal of Geophysical Research, V. 71, p. 3339-3343.
- Sessler, A.M., 1966 - see Laslett, L.J.
- Selling, T.V., 1966 - see Klein, M.J.
- Shapiro, I.I., Lautman, D.A., and Colombo, G., 1966, The earth's dust belt: fact or fiction?: Journal of Geophysical Research, V. 71, p. 5696-5704.
- Shapiro, I., 1965 - see Colombo, G.
- Shapiro, I.I., 1966 - see Lautman, D.A.
- Shapiro, I.I., 1966 - see Smith, W.B.
- Shawhan, S.D., 1966, Ionization rate and electron density profile for the Martian ionosphere based on Mariner 4 observations: Transactions of the American Geophysical Union, V. 47, No. 2, p. 427.

- Shaw, S.J., 1966 - see Spinrad, H.
- Shields, R.M., Pinson, W.H., Jr., and Hurley, P.M., 1966, Rubidium-strontium analyses of the Bjurböle chondrite: *Journal of Geophysical Research*, V. 71, p. 2163-2167.
- Shima, M., 1966, Glassy spherules (microtektites?) found in ice at Scott Base, Antarctica: *Journal of Geophysical Research*, V. 71, p. 3595-3596.
- Shima, M., and Honda, M., 1966, Distribution of spallation produced chromium between alloys in iron meteorites: *Earth and Planetary Science Letters*, V. 1, No. 2, p. 65-74.
- Shimazu, Y., 1966, Survival time of lunar surface irregularities and viscosity distribution within the moon: *Icarus*, V. 5, p. 455-458.
- Shoemaker, E.M., and Morris, E.C., 1966, Fine structure of the lunar surface at the Surveyor I landing site: *Transactions of the American Geophysical Union*, V. 47, No. 4, p. 617.
- Shoemaker, E.M., 1966 - see Morris, E.C.
- Short, J.M., and Goldstein, J.I., 1966, The cooling history of meteorite parent bodies: *Transactions of the American Geophysical Union*, V. 47, No. 2, p. 425.
- Short, N.M., 1966, Shock-lithification of unconsolidated rock materials: *Science*, V. 154, p. 382-384.
- Shorthill, R.W., 1966 - see Fulmer, C.
- Shorthill, R.W., 1966 - see Fulmer, C.V.
- Shorthill, R.W., 1966 - see Saari, J.M.
- Shute, B.E., 1966, Geocentric initial conditions of trajectories originating at the moon's surface: *The Astronomical Journal*, V. 71, p. 602-609.
- Shute, B.E., 1966, Geocentric initial conditions of trajectories originating at the moon's surface: *The Astronomical Journal*, V. 71, p. 870-871.
- Shute, B.E., 1966, Moon-to-earth trajectories and the origin of tektites: *Transactions of the American Geophysical Union*, V. 47, No. 3, p. 486.
- Sidorenko, G.A., 1964 - see Kvashe, L.G.
- Silva, R.R., 1966 - see Evans, J.V.
- Simpson, J.F., 1966, Additional evidence for the volcanic origin of lunar and Martian craters: *Earth and Planetary Science Letters*, V. 1, No. 3, p. 132-134.
- Simpson, J.F., 1966, Evidence for the volcanic origin of lunar and Martian craters: *Earth and Planetary Science Letters*, V. 1, No. 3, p. 130-131.
- Singer, P., 1966 - see Bühler, F.
- Singer, S.F., 1966, Does the earth have a dust belt?: *Transactions of the American Geophysical Union*, V. 47, No. 3, p. 481.
- Sinton, W.M., 1966 - see Boyce, P.B.



- Six, N.F., Jr., Holmes, J.R., Lebo, G.R., Smith, A.G., and Carr, T.D., 1966, Periodicities in the Jovian decametric radio emission: *The Astronomical Journal*, V. 71, p. 398.
- Slaughter, C., 1966 - see Livingston, W.
- Slee, O.B., and Higgins, C.S., 1966, The apparent sizes of the Jovian decametric radio sources: *Australian Journal of Physics*, V. 19, p. 167-180.
- Smalley, V.G., 1966, Time variance of the earth-moon distance: *Icarus*, V. 5, p. 491-504.
- Smith, N., and Beutler, A.E., 1966, A model Martian atmosphere and ionosphere: *Transactions of the American Geophysical Union*, V. 47, No. 1, p. 156.
- Smith, W.B., Shapiro, I.I., and Ash, M.E., 1966, Preliminary results from processing radar and optical planetary observations: *The Astronomical Journal*, V. 71, p. 871-872.
- Smith, A.G., 1966 - see Olsson, C.N.
- Smith, A.G., 1966 - see Six, N.F., Jr.
- Smith, B.A., 1966 - see Reese, E.J.
- Smith, D.H., 1966 - see Wampler, J.M.
- Smith, F.G., 1966 - see Davies, J.G.
- Smith, J.H., 1966 - see Spinrad, H.
- Smith, L.L., 1966 - see Egan, W.G.
- Smith, R.H., 1966 - see Schmitt, R.A.
- Smoluchowski, R., 1966, Structure and coherency of the lunar dust layer: *Journal of Geophysical Research*, V. 71, p. 1569-1574.
- Smyshlyayev, S.I., and Yudin, I.A., 1964, Chemical-mineragraphic investigation of the opaque minerals of the Holbrook chondrite: *Akademiia Nauk SSSR Meteoritika*, No. 25, p. 121-128.
- Smyshlyayev, S.I., 1964 - see Yudin, I.A.
- Sobotovich, Ye.V., 1964, Radiogenic and cosmogenic isotopes in meteorites and cosmo-chronology: *Akademiia Nauk SSSR Meteoritika*, No. 25, p. 40-74.
- Solberg, H.G., Jr., 1966 - see Reese, E.J.
- Solomon, D.M., 1966 - see Danielson, R.E.
- Solomon, W.A., 1966 - see Zabriskie, F.R.
- Soter, S.L., 1966, Mercury: Infrared evidence of non-synchronous rotation: *Science*, V. 153, p. 1112-1113.
- Soter, S., 1966 - see Goldreich, P.
- Spiegel, M.S., 1966, Solar flare induced neutrons at the surface of the moon: *Transactions of the American Geophysical Union*, V. 47, No. 1, p. 154.

- Spinrad, H., 1966, Resolution of the CO<sub>2</sub> "hot band" in the Venus spectrum: *The Astrophysical Journal*, V. 145, p. 943-945.
- Spinrad, H., and Giver, L.P., 1966, Jupiter and Saturn: Plane.  $\gamma$  line inclinations: *Publications of the Astronomical Society of the Pacific*, V. 78, p. 175-177.
- Spinrad, H., and Shawl, S.J., 1966, Water vapor on Venus--a confirmation: *Astrophysical Journal*, V. 146, p. 328.
- Spinrad, H., Schorn, R.A., Moore, R., Giver, L.P., and Smith, J.H., 1966, High-dispersion spectroscopic observations of Mars I. The CO<sub>2</sub> content and surface pressure: *Astrophysical Journal*, V. 146, p. 331-338.
- Spinrad, H., 1966 - see Giver, L.P.
- Spinrad, H., 1966 - see Livingston, W.
- Staelin, D.H., and Barrett, A.H., 1966, Spectral observations of Venus near 1-centimeter wavelength: *The Astrophysical Journal*, V. 144, p. 352.
- Staelin, D.H., and Neal, R.W., 1966, Observations of Venus and Jupiter near 1-cm wavelength: *The Astronomical Journal*, V. 71, p. 872.
- Staelin, D.H., 1966 - see Moron, J.M., Jr.
- Staley, D.O., 1966, Temperatures of meteoroids and meteorites: *Journal of Geophysical Research*, V. 71, p. 5681-5687.
- Stoddaro, L.G., 1966 - see Carson, D.
- Strong, J., 1966 - Plummer, W.
- Strong, J., 1966 - see Plummer, W.T.
- Suchkin, G.L., 1966 - see Matveev, Yu.G.
- Sun, K.H., and Gonzalez, J.L., 1966, Thermoluminescence of the moon: *Nature*, V. 212, p. 23-25.
- Surkov, Yu.A., and Nazarkina, G.B., 1965, Nuclear reactions in meteorites: *Geochemistry International*, V. 2, p. 689. (Translated from *Geokhimiya*, No. 8, p. 918-935, 1965; translation not published but may be ordered).
- Surveyor Scientific Evaluation and Analysis Team, 1966, Surveyor I: Preliminary results: *Science*, V. 152, p. 1737-1750.
- Tanner, J.T., 1966 - see Ehmann, W.D.
- Tatlock, D.B., 1966, Some alkali and titania analyses of tektites before and after G-1 precision monitoring: *Geochimica et Cosmochimica Acta*, V. 30, p. 123-128.
- Tatsch, J.H., 1966, Certain correlations between selenophysical observations and deductions arrived at from applying a dual primeval planet model to the earth-moon system: *Transactions of the American Geophysical Union*, V. 47, No. 3, p. 486.
- Taylor, H.P., Jr., and Epstein, S., 1966, Oxygen isotope studies of Ivory Coast tektites and impactite glass from the Bosumtwi Crater, Ghana: *Science*, V. 153, p. 173-175.

- Taylor, S.R., 1966, Australites, Henbury impact glass and subgreywacke: a comparison of the abundances of 51 elements: *Geochimica et Cosmochimica Acta*, V. 30, p. 1121-1136.
- Teal, D.J., 1966 - see Moraski, L.K.
- Telfel, V.S., 1966, Spectrophotometry of the methane absorption bands at  $0.7-1.0 \mu$  on the disk of Jupiter: *Soviet Astronomy - A.J.*, V. 10, No. 1, p. 121-123.
- Teplitzskaya, T.A., 1965 - see Florovskaya, V.N.
- Thackeray, A.D., Feast, W.W., and Warner, B., 1966, Daytime spectra of comet Ikeya-Seki near perihelion: *The Astrophysical Journal*, V. 143, p. 276.
- Thaddeus, P., 1966 - see Ho, W.
- Thomas, M., 1966 - see Roemer, E.
- Thompson, B.A., 1966 - see Applebaum, D.C.
- Thompson, T.W., and Dyce, R.B., 1966, Mapping of lunar radar reflectivity at 70 centimeters: *Journal of Geophysical Research*, V. 71, p. 4843-4853.
- Thornton, D.D., 1966 - see Welch, W.J.
- Titulaer, C., 1966, Isophotes of the Aristarchus region of the moon: *Bulletin of the Astronomical Institutes of the Netherlands*, V. 18, p. 167-169.
- Tolbert, C.W., 1966, Observed millimeter wavelength brightness temperatures of Mars, Jupiter, and Saturn: *The Astronomical Journal*, V. 71, p. 30-32.
- Tolson, R.H., 1966 - see Michael, W.H., Jr.
- Tombaugh, C.W., 1966, Evidence that the dark areas on Mars are elevated mountain ridges: *Nature*, V. 209, p. 1338.
- Trafton, L., 1966, Model atmospheres of the major planets: *The Astronomical Journal*, V. 71, p. 183.
- Troitskii, V.S., 1966, Radio emission of the eclipsed moon: *Soviet Astronomy - A.J.*, V. 9, p. 1007-1019.
- Troitskii, V.S., 1966 - see Matveev, Yu.G.
- Tuchek, D., 1965, Two recent meteorite falls in Czechoslovakia: *Akademiia Nauk SSSR Meteoritika*, No. 26, p. 112-118.
- Tull, R.G., 1966, The reflectivity spectrum of Mars in the near-infrared: *Icarus*, V. 5, p. 505-514.
- Turkevich, A., and Rennilson, J.J., 1966, Location and altitude of Surveyor I on the lunar surface: *Transactions of the American Geophysical Union*, V. 47, No. 4, p. 616.
- Turner, G., Miller, J.A., and Grasty, R.L., 1966, The thermal history of the Bruderheim meteorite: *Earth and Planetary Science Letters*, V. 1, No. 4, p. 155-157.
- Tyler, G.L., 1966, The bistatic, continuous-wave radar method for the study of planetary surfaces: *Journal of Geophysical Research*, V. 71, p. 1559-1567.

- Urey, H.C., 1966, Biological material in meteorites: A review: *Science*, V. 151, p. 157-166.
- Vand, V., 1966, Monro jets and the origin of tektites: *Nature*, V. 209, p. 496.
- van Diggelen, J., 1966, The linear network of lunar surface features: *Bulletin of the Astronomical Institutes of the Netherlands*, V. 18, p. 311-322.
- Van Dijk, Th., 1966 - see Schutten, J.
- van Houten, C.J., and van Houten-Groeneveld, I., 1966, A new periodic comet, observed in 1960: *Bulletin of the Astronomical Institutes of the Netherlands*, V. 18, p. 441, note.
- van Houten-Groeneveld, I., 1966 - see van Houten, C.J.
- Van Schmus, W.R., 1966 - see Dodd, R.T., Jr.
- Vassamillet, L.F., 1966 - see Ashbee, K.H.G.
- Vassamillet, L.F., 1966 - see Massalski, T.B.
- Vdovykin, G.P., 1964, Some results of the study of the mineral composition of 12 carbon-bearing meteorites: *Akademiia Nauk SSSR Meteoritika*, No. 25, p. 134-155.
- Vdovykin, G.P., 1965, On the origin of the carbonaceous chondrites: *Akademiia Nauk SSSR Meteoritika*, No. 26, p. 151-168.
- Vdovykin, G.P., 1965 - see Florovskaya, V.N.
- Vdovykin, G.P., 1965 - see Vinogradov, A.P.
- Verniani, F., 1966, Meteor masses and luminosity: Special Report No. 219, Smithsonian Astrophysical Observatory, Cambridge, Massachusetts.
- Verniani, F., 1966, Physical characteristics of 320 faint radio meteors: *Journal of Geophysical Research*, V. 71, p. 2749-2761.
- Viiding, H.A., 1965, Meteoritic dust at the base of Cambrian sandstones of Estonia: *Akademiia Nauk SSSR Meteoritika*, No. 26, p. 132-139.
- Vilenskiy, V.D., 1965 - see Lavrukhina, A.K.
- Vinogradov, A.P., and Zadorozhnyy, I.K., 1965, Cosmogenic, radiogenic, and primordial inert gases in stone meteorites: *Akademiia Nauk SSSR Meteoritika*, No. 26, p. 77-90.
- Vinogradov, A.P., Vdovykin, G.P., and Popov, N.M., 1965, Investigation of the carbonaceous matter of meteorites by microdiffraction with ultra-fast electrons: *Geochemistry International*, V. 2, p. 249-253 (english translation from *Geokhimiya*, No. 4, p. 387-389, 1965).
- Vogel, U., 1966, Molecular fluxes in the lunar atmosphere: *Planetary and Space Science*, V. 14, No. 12, p. 1233-1252.
- Von Eshleman, R., 1966 - see Fjeldbo, G.
- Vonnegut, B., McConnell, R.K., Jr., and Allen, R.V., 1966, Evaporation of lava and its condensation from the vapour phase in terrestrial and lunar volcanism: *Nature*, V. 209, p. 445-448.

- Vorob'yev, G.G., 1964, New finds and new tektite deposits in southern Bohemia: *Akademiia Nauk SSSR Meteoritika*, No. 25, p. 178-187.
- Wainio, K.M., 1966 - see Ebeoglu, D.B.
- Walker, E.H., 1966, Comments on paper by L.D. Jaffe, "Depth of the Lunar Dust": *Journal of Geophysical Research*, V. 71, p. 5007-5010.
- Walker, G., 1966 - see Geake, J.E.
- Walker, R.G., and Sagan, C., 1966, The ionospheric model of the Venus microwave emission: An obituary: *Icarus*, V. 5, p. 105-123.
- Walker, R.M., Fleischer, R.L., Price, P.B., Maurette, M., and Morgan, G., 1966, Study of very heavy cosmic-ray primaries using nuclear tracks in meteorites: *Transactions of the American Geophysical Union*, V. 47, No. 1, p. 132.
- Walker, R.M., 1966 - see Price, P.B.
- Wampler, J.M., Smith, D.H., and Cameron, A.E., 1966, Isotopic comparison of lead from Ivory Coast tektites and Bosumtwi Crater materials: *Transactions of the American Geophysical Union*, V. 47, No. 1, p. 145.
- Warner, B., 1966 - see Thackeray, A.D.
- Warwick, J.W., 1966, New information on Jupiter's magnetic field: *Transactions of the American Geophysical Union*, V. 47, No. 1, p. 44.
- Wasserburg, G.J., 1966 - see Burnett, D.S.
- Wasson, J.T., 1966, Butler, Missouri: An iron meteorite with extremely high germanium content: *Science*, V. 153, p. 976-978.
- Wasson, J.T., 1966, Some geochemical considerations regarding the concentrations of siderophilic elements in meteorites: *Transactions of the American Geophysical Union*, V. 47, No. 3, p. 497.
- Wasson, J.T., Kimberlin, J., Mattschei, P.K., and Groszek, E.J., 1966, Ga, Ge, and other siderophilic elements in iron meteorites: *Transactions of the American Geophysical Union*, V. 47, No. 1, p. 131.
- Watts, R.N., Jr., 1966, Lunar orbiter surveys the moon: *Sky and Telescope*, V. 32, p. 192-197.
- Watts, R.N., Jr., 1966, Pictures from the moon: *Sky and Telescope*, V. 32, p. 16-20.
- Wattson, R.B., and Hapke, B.W., 1966, A comparison of the infrared spectra of the moon and simulated lunar surface materials: *The Astrophysical Journal*, V. 144, p. 364-368.
- Webster, H.R., Kaiser, T.R., Poole, L.M.G., 1966, Radio-echo observations of the major nighttime meteor streams, II. Geminids: *Monthly Notices of the Royal Astronomical Society*, V. 133, p. 309-319.
- Webster, A.R., 1966 - see Kaiser, T.R.
- Weigert, A., 1966 - see Huebner, W.F.
- Weihrauch, J.H., 1966 - see Fechtig, H.

- Weinberg, J.L., 1966, Photoelectric polarimetry of comet 1965f: *The Astronomical Journal*, V. 71, p. 875.
- Welch, W.J., Thornton, D.D., and Lohman, R., 1966, Observations of Jupiter, Saturn, and Mercury: *Astrophysical Journal*, V. 144, p. 799-809.
- Werner, M., Gold, T., and Harwit, M., 1966, Detection of water on the moon: *The Astronomical Journal*, V. 71, p. 875-876.
- Westphal, J.A., 1966, The 10-micron limb darkening of Venus: *Journal of Geophysical Research*, V. 71, p. 2693-2696.
- Westphal, J.A., 1966 - see Becklin, E.E.
- Whipple, F.L., 1966, Chondrules: Suggestion concerning the origin: *Science*, V. 153, p. 54-56.
- Whitaker, E.A., 1966, Further observations on the Ranger VII records: *Communications of the Lunar and Planetary Laboratory*, V. 4, No. 59, p. 71-76.
- Wiggins, T.A., 1966 - see Rank, D.H.
- Wilk, H.B., 1966 - see Buseck, P.R.
- Wildt, R., 1966, The greenhouse effect in a gray planetary atmosphere: *Icarus*, V. 5, p. 24-33.
- Williams, D., 1966 - see Davies, R.D.
- Wilson, L., 1966 - see Fielder, G.
- Winter, D.F., 1966, Note on the non-uniform cooling behavior of the eclipsed moon: *Icarus*, V. 5, p. 551-553.
- Witting, J., 1966, Satellite roles in radio emission from Jupiter: *The Astronomical Journal*, V. 71, p. 187.
- Wood, C.A., 1966 - see Arthur, D.W.G.
- Woolf, N.J., 1966 - see Ney, E.P.
- Wosinski, J.F., 1966 - see Clarke, R.S., Jr.
- Wright, F.W., Hodge, P.W., and Allen, R.V., 1966, Electron-probe analysis of interiors of microscopic spheroids from eruptions of the Mt. Aso, Surtsey, and Kilauea Iki volcanoes: Special Report No. 228, Smithsonian Astrophysical Observatory, Cambridge, Massachusetts.
- Yabushita, S., 1966, Stability analysis of Saturn's rings with differential rotation: *Monthly Notices of the Royal Astronomical Society*, V. 133, p. 247-263.
- Yagi, K., 1966, Discussion of paper by J.A. O'Keefe and E.W. Adams, "Tektite structure and lunar ash flows": *Journal of Geophysical Research*, V. 71, p. 5492-5493.
- Yavnel, A.A., 1964, On the abundance of elements in the metallic phase of iron meteorites and in chondrites: *Akademiia Nauk SSSR Meteoritika*, No. 25, p. 75-89.
- Yavnel, A.A., 1965, On the classification of iron meteorites by structure: *Akademiia Nauk SSSR Meteoritika*, No. 26, p. 140-145.

- Yavnel, A.A., 1965, Regularities in the composition and structure of meteorites and the problem of their origin: *Akademiia Nauk SSSR Meteoritika*, No. 26, p. 26-34.
- Yavnel, A.A., 1966, The origin of meteorites (an outline): *Soviet Astronomy - A.J.*, V. 10, No. 3, p. 511-516.
- Young, J.F., 1966 - see Greenman, N.N.
- Younkin, R.L., 1966, A search for limonite near-infrared spectral features on Mars: *The Astrophysical Journal*, V. 144, p. 809, 818.
- Younkin, R.L., and Münch, G., 1966, Visible and near-infrared spectrophotometry of Saturn's rings: *The Astronomical Journal*, V. 71, p. 188.
- Yudin, I.A., 1964, On the problem of collecting and studying meteor dust: *Akademiia Nauk SSSR Meteoritika*, No. 25, p. 192-193.
- Yudin, I.A., 1964 - see Smyshlyayev, S.I.
- Yudin, I.A., and Smyshlyayev, S.I., 1964, Chemical-mineragraphic investigation of the opaque minerals of the Norton County and Staroye Pes'yanoye achondrites: *Akademiia Nauk SSSR Meteoritika*, No. 25, p. 96-120.
- Yukina, L.V., 1965 - see Lavrukhina, A.K.
- Zabriskie, F.R., Solomon, W.A., and Hagen, J.P., Jr., 1966, Radiation from Jupiter at long wavelengths: *The Astronomical Journal*, V. 71, p. 877.
- Zadorozhnyy, I.K., 1965 - see Vinogradov, A.P.
- Zähringer, J., 1966, Primordial argon and the metamorphism of chondrites: *Earth and Planetary Science Letters*, V. 1, No. 6, p. 379-382.
- Zähringer, J., 1966, Primordial He distribution by microprobe technique: *Transactions of the American Geophysical Union*, V. 47, No. 2, p. 425.
- Zähringer, J., 1966, Primordial helium detection by microprobe technique: *Earth and Planetary Science Letters*, V. 1, p. 20-22.
- Zähringer, J., 1966 - see Kempe, W.
- Zähringer, J., 1966 - see Lämmerzahl, P.
- Zähringer, J., 1966 - see Müller, O.
- Zander, R., 1966, Spectral scattering properties of ice clouds and hoarfrost: *Journal of Geophysical Research*, V. 71, p. 375-378.
- Zeller, E.J., Ronca, L.B., and Levy, P.W., 1966, Proton-induced hydroxyl formation on the lunar surface: *Journal of Geophysical Research*, V. 71, p. 4855-4860.
- Zezin, R.B., 1965 - see Florovskaya, V.N.
- Zharkov, V.N., Berikashvili, V.Sh., and Osnach, A.I., 1966, Geophysical problems and lunar investigations: *Soviet Astronomy*, V. 10, No. 3, p. 492-510.
- Zheleznyakov, V.V., 1966, The origin of Jovian radio emission: *Soviet Astronomy - A.J.*, V. 9, p. 617-625.

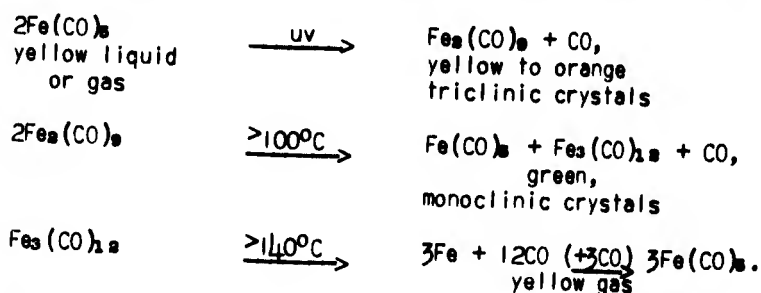
### 3. Articles Listed by Subject

#### 3.1 Astrobiology

Cohen, A.J., 1966, Seasonal color changes on Mars: The Astronomical Journal, V. 71, p. 849-850.

The atmosphere seasonal color changes, polar ice caps, and "dust storms" on the Martian surface may be all explained by various molecules, compounds and complexes of permutations among iron, carbon, and oxygen. The atmosphere is almost certainly made of carbon dioxide along with dissociation products.

A seasonal chemical cycle closely explaining Lowell's color changes observed in 1903 as well as the "yellow dust clouds" may be written as follows:



This model is capable of laboratory test and would preclude even the most rudimentary life of Mars. (Abstract of a paper presented at the July 1966 meeting of the American Astronomical Society).

Florovskaya, V.N., Vdovkin, G.P., Teplitskaya, T.A., and Zevin, R.B., 1965, Comparative features of polycyclic aromatic hydrocarbons in carbonaceous chondrites and rocks and minerals of endogene origin: Akademiia Nauk SSSR Meteoritika, No. 26, p. 169-176.



Aromatic hydrocarbons in carbonaceous chondrites and in rock and minerals of endogene origin are compared. In very high temperature formations (rocks and minerals of the Ilmen alkaline massif and meteorites), the predominant components are anthracene and 3,4-benzpyrene, whereas in lower temperature hydrothermal formations (pegmatites of the Khibin massif and deposits of the Armenian S.S.R.), 1,12-benzpyrene predominates and coronene appears. (From Geophysical Abstracts, No. 236).

Gilvarry, J.J., 1966, Observability of indigenous organic matter on the moon: *Icarus*, V. 5, p. 228-236.

The theories of Gilvarry and Sagan implying the presence of indigenous organic matter on the moon are reviewed briefly, for comparison. The former postulates the presence in the lunar maria of organic remains derived from a pristine biota in a hydrosphere formed by exudation from the moon's interior and lasting several billion years. The latter assumes the presence of organic matter on the lunar highlands, now covered by meteoritic infall, formed by the action of solar ultraviolet light and other agencies on a reducing proto-atmosphere lasting significantly less than a billion years. However, the fact that meteoritic infall on a moon without an atmosphere causes a net loss of mass from that body is determinative for observability in the Surveyor and Apollo missions of the organic vestiges postulated in the two theories. On Gilvarry's model, a loss of mass from the lunar surface of at least 7 meters in depth is found for the effects of meteoritic impact and sputtering action (by the particles of the solar wind and flares) over the period of several billion years since the atmosphere and hydrosphere vanished.

Harrington, J.S., 1966, Polycyclic aromatic hydrocarbons in carbonaceous meteorites: *Nature*, V. 212, p. 273-274.

The presence of hydrocarbons in several meteorites has been confirmed, but insufficient evidence is available to allow a determination as to whether they derived as contamination from the soil in which the meteorites were found or whether they were present in the chondrites before entering the terrestrial atmosphere.

Hayatsu, R., 1966, Artifacts in polarimetry and optical activity in meteorites: *Science*, V. 153, p. 859-861.

Commercial polarimeters may produce spurious optical rotation. This effect may explain the optical activity reported in the Orgueil meteorite.

Horowitz, N.H., 1966, The search for extraterrestrial life: *Science*, V. 151, p. 789-792.

Present knowledge on the Martian environment and on the origin of the planet does not preclude the possibility of Martian life.

Kaplan, I.R., and Hulston, J.R., 1966, The isotopic abundance and content of sulfur in meteorites: *Geochimica et Cosmochimica Acta*, V. 30, p. 479-496.

Twenty meteorites were studied in the iron (hexahedrites and octahedrites) and stony (enstatite achondrite, carbonaceous, enstatite, bronzite and hypersthene chondrites) families. Troilite is the chief sulfur component of iron meteorites and the  $\delta S^{34}$  ranges from 0 to +0.6 per mil with respect to Canyon Diablo troilite. Stony meteorites contain a wide variety of sulfur compounds including water and acid soluble sulfides, elemental sulfur, water and acid soluble sulfates and unidentified components soluble only in aqua regia. The  $\delta S^{34}$  content of the isolated compounds varies from +2.5 to -5.5 per mil with

respect to Canyon Diablo. The weighted average for all components of each meteorite, however, falls within  $\pm 1$  per mil of Canyon Diablo. The  $S^{34}$  distribution closely follows  $S^{34}$ . The data strongly suggest that differentiations have occurred in a closed system, corresponding to the meteorites or their parent body, and starting from a single source of sulfur. There is no evidence for biological activity having occurred in the meteorites, either from the distribution of sulfur compounds or from the isotope abundance data.

Kilston, S.D., Drummond, R.R., and Sagan, C., 1966, A search for life on earth at kilometer resolution: *Icarus*, V. 5, p. 79-98.

A search for life on earth at kilometer resolution, using several thousand photographs obtained by the Tiros and Nimbus meteorological satellites, has been undertaken. No sign of life can be discovered on the vast majority of these photographs. No seasonal variations in the contrast of vegetation could be detected. Of several thousand photographs of essentially cloudfree terrains, one feature was found indicative of a technical civilization on earth--a recently completed interstate highway--and another suggestive feature was discovered, possibly a jet contrail. A striking rectilinear feature was found on the Moroccan coast; however, it appears to be a natural peninsula. An orthogonal grid is due to the activities of Canadian loggers, and is a clear sign of life. It appears that several thousand photographs, each with a resolution of a few tenths of a kilometer, are required before any sign of intelligent life can be found with reasonable reliability. An equivalent Mariner 4 system would not detect any sign of life on earth, intelligent or otherwise.

Meinschein, W.G., Frondel, C., Laur, P., and Mislav, K., 1966, Meteorites: Optical activity in organic matter: *Science*, V. 154, p. 377-380.

A low-amplitude Cotton effect has been measured in organic extracts of samples from non-carbonaceous chondrites. It is likely that they are due to contamination on earth.

Nagy, B., 1966, A study of the optical rotation of lipids extracted from soils, sediments, and the Orgueil carbonaceous meteorite: *Proceedings of the National Academy of Sciences*, V. 56, p. 389-398.

Low real values of optical rotation have been found for lipids extracted from the Orgueil meteorite. Four samples of the meteorite were found to contain several different kinds of anaerobic non-spore forming bacteria. There was no way to determine if the optically active material and bacteria were terrestrial contaminants.

Öpik, E.J., 1966, The Martian surface: *Science*, V. 153, p. 255-265.

A volcanic origin of the Martian crater is to be completely excluded. Craters larger than 20 km survived erosion from the beginning of the Martian surface, therefore a dense atmosphere never existed. The large amplitude in temperature indicates that the upper soil is of a porous, unconsolidated structure. Survival of vegetation, if it exists, must depend on the low nighttime temperature and deposition of hoarfrost, which could melt to droplets after sunrise, before evaporating. The "canals" may be cracks in the crust, radiating from the point of impact. Limb darkening of the planet in green, yellow and red light indicates absorption by atmospheric haze, aerosols, and dust.

Ponnamperuma, C., 1966, Some recent work on prebiological synthesis of organic compounds: *Icarus*, V. 5, p. 450-454.

The experimental approach to the question of the origin of life is based on the Oparin-Haldane hypothesis that life is a special property of matter which arose at a particular period in the existence of our planet and resulted from its orderly development. The simple working hypothesis has been adopted that the molecules which are important now were important at the time of the origin of life. Starting with the earth's primordial atmosphere and the various forms of energy which may have existed at the time, we are endeavoring to retrace the origin of the constituents of the nucleic acid and protein molecules.

Sagar, C., and Pollack, J.B., 1966, An inorganic model of Martian phenomena: The Astronomical Journal, V. 71, p. 178.

Recent work showing that the optical detection of life on earth over interplanetary distances is extremely difficult has led the authors to re-examine the Martian seasonal changes and related phenomena, to see whether plausible inorganic models explaining these observations can be devised. They assume that the entire planet, except for the polar caps, is covered with a layer of pulverized limonite, with mean particle dimensions  $\sim 0.1$  mm, in accordance with polarimetric and spectrometric observations. Elevation differences will lead to a particle size segregation, as suggested by Rea. The smaller particles will be preferentially present in the lowlands. The visible reflectivity of the highlands, with relatively more large particles, will be less. If the lowlands have mean particle sizes  $\sim 0.3$  that of the highlands, the average reflectivity differences between Martian bright and dark areas can be understood; but the dark areas must have systematically higher elevations. Wind patterns, which are expected to change markedly with the seasons, will force greater periodic variations in mean particle size for the windswept highlands than for the lowlands, as is the case in some terrestrial deserts. This particle size modulation can account quantitatively for the observed seasonal variation in albedo and polarization. The model also explains in a straightforward manner the secular changes, the "blue haze," the blue clearings, and the relatively high radar reflectivity of the Martian dark areas. Since it assumes only winds, pulverized limonite, elevation differences and dust storms, we believe the model is promising; but while providing an inorganic explanation of gross Martian phenomena previously attributed to life, it does not, of course, in any way exclude life on Mars. (Abstract of a paper presented at the December 1965 meeting of the American Astronomical Society).

Urey, H.C., 1966, Biological material in meteorites: A review: Science, V. 151, p. 157-166.

A complete review of the present stage of knowledge of organic material in meteorites is presented. The most acceptable hypothesis at present is contamination of the lunar surface with terrestrial water and primitive organic matter and subsequent impact ejection from the lunar gravity field to land on the earth's surface.

### 3.2 Comets

A'Hearn, M.F., 1964, Ca densities in comet Mrkos (1955 III): Publications of the Astronomical Society of the Pacific, V. 76, p. 106-109.

The author has estimated the densities of Ca in comet Mrkos (1955 III) by photometric analysis of photographs. He finds that the densities are comparable with those in other comets, but considerably lower than Wurm's estimate for the brightest known comets.

Anonymous, 1966, New comet Kilston (1966b): *Sky and Telescope*, V. 32, p. 191.

The discovery of a new comet is reported. A spectrum and photographs are presented.

Anonymous, 1966, Photographs of comet Ikeya-Seki II: *Sky and Telescope*, V. 31, p. 20-23.

Thirteen photographs of the comet taken by different observers are presented with photographic notes.

Anonymous (L.J.R.), 1966, Observers page: Reports of comet Ikeya-Seki (1965f): *Sky and Telescope*, V. 31, p. 52-56.

Several drawings and photographs are presented with observers notes.

Bader, M., Haughney, L.C., and Innes, R.C., 1966, Airborne photographic observations of comet Ikeya-Seki, 1965f: *The Astronomical Journal*, V. 71, p. 844.

A photographic history of comet Ikeya-Seki, 1965f, was obtained for the days 23 to 26 October 1965. The photographs, taken from a NASA jet airplane at 40 000 ft. over the Pacific Ocean, show the development of the tail in the post-perihelion period.

The minimum length of the tail at 15<sup>h</sup>38<sup>m</sup>35<sup>s</sup> UT, 23 October, was 2°; at 15<sup>h</sup>23<sup>m</sup>47<sup>s</sup> UT, 24 October, it was at least 51/30°. Grids of right ascension and declination were computed and superposed on the photographs of 25 and 26 October, thus permitting measurements of the tail's length and curvature and of the movement of features in the tail. The end point of the tail is defined at a specified point where the photographic tail begins to merge into the sky background. The length of the tail is then measured along the great circle arc between this end point and the head. On 25 October, 15<sup>h</sup>11<sup>m</sup>10<sup>s</sup> UT, the length of the tail was 10° 50'; on 26 October, 14<sup>h</sup>39<sup>m</sup>40<sup>s</sup> UT, it was 13° 50'.

The curvature of the tail is indicated by the deviation of the tail's center from the midpoint of the great circle arc between the end and the head. For the times given above, this deviation was 0°75 and 1°0, respectively.

The movement of a dark band in the midtail was followed between 15<sup>h</sup>14<sup>m</sup>20<sup>s</sup> UT, 25 October, and 15<sup>h</sup>11<sup>m</sup>55<sup>s</sup> UT, 26 October. The point where this band intersects the outer edge of the tail was 6° 30' from the head on the earlier date and 8° 50' at the later date as measured along the great circle arc between the head and the specified point in the feature. (Abstract of a paper presented at the July 1966 meeting of the American Astronomical Society).

Beard, D.B., 1966, The theory of type I comet tails: *Planetary and Space Science*, V. 14, No. 3, p. 303-311.

Type I comet tails are shown to arise from the energetic electrons in the shock structure surrounding the head of a comet once sufficient ionization of cometary gases has occurred to slow the magnetic lines of force trapped in the solar wind. The theory of the evolution of comet gases and the density distribution in the head is used to describe the inertial slowing down of the interplanetary field lines due to ionization of cometary molecules while in the magnetic field. The subsequent establishment of the ray structure by energetic electrons is shown quantitatively to follow very simply from energetic electrons resulting from the charge separation layer created by the shock structure on the comet head.

Becklin, E.E., and Westphal, J.A., 1966, Infrared observations of comet 1965f: *Astrophysical Journal*, V. 145, p. 445-453.

Infrared photometric measurements of comet 1965f were made on 19 days during October and November, 1965. Absolute intensities as a function of the comet's distance to the sun were measured in a region centered on the cometary nucleus at wavelengths near 1.65, 2.2, 3.4, and 10 $\mu$ . On three days the intensity in the tail was measured. Color temperatures were calculated in both the head and tail region from these absolute intensities. From the color temperatures the nature of the emissivity of the emitting particles is derived and the nature of the possible materials is discussed.

Bayer, M., 1966, *Physische Beobachtungen von Kometen XV: Astronomische Nachrichten*, V. 289, p. 177-180.

Visual observations of the comets 1964h and 1965h and of the last phase of a light burst on comet 1925 II. (In German).

Boyce, P.B., and Sinton, W.M., 1966, Photometric observations of comet Ikeya-Seki, 1965, in Na D Light: *The Astronomical Journal*, V. 71, p. 847-848.

Measurements were made of the flux from Ikeya-Seki, 1965f, using a spectrum scanner with a 12-Å bandpass fixed on the sodium D lines in a grid of points at precise off-sets from the nucleus during the period 19 to 22 October 1965. Observations were also made each day of  $\alpha$  Lyr to calibrate the instrumental sensitivity. From these measurements were constructed four isophotal maps of the sodium light intensity corresponding to different times before and after perihelion passage. The highest sodium intensity in the 1 min diameter entrance aperture was found in the map made at 18<sup>h</sup> UT 20 October. The amount of flux was  $8.5 \times 10^{-10}$  ergs sec<sup>-1</sup> cm<sup>-2</sup> min<sup>-1</sup> above the earth's atmosphere. The sodium was weaker in a map made later on this same day. The two maps on this day show a trident structure of rays extending 4 to 5 min from the nucleus. By 22 October the sodium was much weaker and the authors were unable to map its intensity. (Abstract of a paper presented at the July 1966 meeting of the American Astronomical Society).

Chebotaiev, G.A., 1966, Cometary motion in the outer solar system: *Soviet Astronomy - A.J.*, V. 10, p. 341-344.

The motion of a body of infinitesimal mass (a "comet") in the outer regions of the solar system is investigated. The galactic nucleus is taken as the perturbing body. Stable cometary motion (for  $e_0 = 0.6$ ) is possible 80,000 a.u. from the sun. The "comet cloud" extends from about 60,000 to 100,000 a.u.

Curtis, G.W., 1966, Daylight observations of the 1965f comet at the Sacramento Peak Observatory: *The Astronomical Journal*, V. 71, p. 194-196.

The comet 1965f was seen and observed from the Sacramento Peak Observatory during the daylight hours from 16:22 to 23:19 UT on 20 October 1965 and from 15:56 to 17:42 UT on 21 October 1965. During these periods a coordinate effort was made by the entire staff to utilize a maximum of the solar instruments on the comet. A list of all the solar and comet observations is presented. The former, mostly coronal, were made in an attempt to detect any influence of the comet on the corona; the latter to gather data on the comet itself. Coronal green line movies and coronal spectra around  $\lambda 6564$  and  $\lambda 5303$  were taken with dispersion of 9.2 and 2.2 Å/mm. Similar spectra were taken of the comet's head and tail.



The Sacramento Peak Observatory (SPO) 16-in. coronagraph, in combination with a small universal spectrograph (3600-8000 Å; 2.5 Å/mm) was used to obtain spectra of both the head and the tail of the comet. Polarization measurements were made by placing a polaroid in front of the spectrograph slit. Finally, photoelectric scans (dispersion of 5 mm/Å) were taken in the sodium D lines region and color photographs of the comet were taken on 35 mm film.

A table of the most conspicuous lines appearing in the comet spectra is presented as well as the results of an analysis of the Na D lines profiles obtained photoelectrically. The emission redshift and absorption blueshift of the Na D lines are discussed.

Curtis, G.W., and Staff, 1966, Daytime observation of the comet 1965f at the Sacramento Peak Observatory: *The Astronomical Journal*, V. 71, p. 159.

The comet 1965f was seen and observed from the Sacramento Peak Observatory during the daylight hours from 16:22 to 23:19 UT on 20 October 1965 and from 15:56 to 17:42 UT on 21 October 1965. During these periods a coordinated effort was made to utilize a maximum of the solar instruments on the comet.

A first study of the spectra shows that strong lines such as the D lines are shifted to the red in emission and to the blue in absorption. The shifts indicate velocities of at least 100 km/sec. The most conspicuous emission lines besides the Na D lines and Ca II H and K lines are the Fe I lines arising from transitions to terms within one volt of the ground state. These and other results are presented and discussed. (Abstract of a paper presented at the December 1965 meeting of the American Astronomical Society).

Danielsson, L.R., and Kasai, G.H., 1966, A model experiment on cometary phenomena: *Transactions of the American Geophysical Union*, V. 47, No. 3, p. 485.

In a laboratory experiment the situation in a cometary atmosphere under the influence of the solar wind is simulated. The model comet is a piece of dry ice inserted into a plasma wind tunnel. The velocity and density of the plasma flow are 10<sup>7</sup> cm/sec and about 10<sup>-8</sup> cm<sup>-3</sup>. The plasma stream is interacting with CO<sub>2</sub> gas released from the surface of the piece of ice. Account is taken of the fact that interparticle collisions must play a very minor role for the interaction. The mean free paths for elastic collisions, as well as charge transfer between protons and gas molecules, are estimated to be long compared with the dimension of the gas cloud. Photographs reveal, however, that the interaction is strong and that a tendency toward tail formation is evident. The importance of magnetic fields frozen into the plasma is considered. (Abstract of a paper presented at the September 1966 meeting of the American Geophysical Union).

Dewey, M.E., and Miller, F.D., 1966, Isophotes of the Ca distribution in comet Seki (1961 VIII): *The Astrophysical Journal*, V. 144, p. 1170-1173.

Isophotes of comet Seki (1961 VIII) show an asymmetry of the coma which may be accounted for by a simple variation of desorption over the cometary nucleus. Intensity contours derived from these isophotes indicate a Ca lifetime in interplanetary space about one-half as long as for normal comets and a longer lifetime (by a factor of about 2) of the "parent molecules."

Dolginov, A.Z., and Gnedin, Yu.N., 1966, A theory of the atmosphere of a comet: *Icarus*, V. 5, p. 64-74.

The formulas for the distribution of neutral particles in the head of a comet are obtained. The distribution of the particles produced by dissociation is

considered. The brightness of different parts of the head in different lines of the spectrum is determined. The observed brightness of the comet Burnham (1959 k) is explained.

Dossin, F.V., 1966, Emission spectrum of a comet, at large heliocentric distance: The Astronomical Journal, V. 71, p. 853-854.

The spectrum of comet Humason 1961e was photographed at McDonald Observatory, in February 1964. In addition to a faint continuum, confined to the central region, the picture shows several emission features, extending on both sides, along the slit image. The following transitions are easily identified:

$\text{CO}^+$  bands: 3-0; 2-0; 1-0; 4-2; 2-1, (intense)  
 4-0; 3-2, (faint); 1-1 (trace).  
 $\text{Na}^+$  band: 0-0, (moderately intense).  
 CN band: 0-0, (faint, but definitely present).

The same emission bands, and a few more, had been observed when the comet was near perihelion (Greenstein, Astrophys. J. 136, 1962; Dossin and Rousseau, Compt. Rend. 255, 1962). But, in February 1964, the heliocentric distance of the comet was 5 a.u.

At the request of the author, another spectrogram of comet 1961e was obtained by Fehrenbach at Haute Provence Observatory at the same period. The exposure was shorter and the quality of the sky was not as good as it was in Texas; nevertheless, a few bands of  $\text{CO}^+$  appear clearly. In the discussion of the spectrographic results, two points must be stressed: On the one hand, it was the first time a spectrum of a comet at large heliocentric distance could be observed, in spite of a reported magnitude of about 17 for the object. On the other hand, the spectrum showed emissions, intense relative to the continuum, and mostly of ionized radicals.

In conclusion, the author suggests that every effort should be made to observe more often the spectrum of faint or distant comets. The increasing number of large telescopes and fast nebular spectrographs could provide new and important observational data about some cometary problems which are not well understood. Strong emissions from ionized molecules in a comet at 5 a.u. from the sun are a puzzling phenomenon. (Abstract of a paper presented at the July 1966 meeting of the American Astronomical Society).

Dulk, G.A., and Clark, T.A., 1966, Almost-continuous radio emission from Jupiter at 8.9 and 10 MHz: The Astrophysical Journal, V. 145, p. 945-948.

During the apparition of 1964, radiation from Jupiter at 8.9 and 10 MHz was recorded almost every night with large antenna arrays located near Boulder, Colorado. This report describes the observations and shows how the emission depends on Jupiter's longitude and Io's position.

Fesenkov, V.G., 1964, On the orbit of the Tunguska meteorite: Akademiia Nauk SSSR Meteoritika, No. 25, p. 163-167.

Possible orbits of the Tunguska meteorite of 1908 are worked out from the conflicting reports of the event. The elements of circular and parabolic orbits (inclination to plane of ecliptic, perihelion distance, eccentricity, major semi-axis, and relative impact velocity) are tabulated for three azimuths ( $0^\circ$ ,  $20^\circ$ ,  $40^\circ$ ) of visible radiant. For all these variants, one of which should be the true orbit, the motion is not characteristic of ordinary meteorites representing the product of breakup of asteroids, but is normal for the case of a comet. (From Geophysical Abstracts, No. 217).

Gnedin, Yu.N., and Dolginov, A.Z., 1966, Particle distribution in a comet head: Soviet Astronomy - A.J., V. 10, p. 143-150.

Formulas are obtained for the distribution of atoms and molecules in a comet head. The possibility of production and decay of particles in processes of dissociation and ionization is taken into account. The radiant flux in spectral lines observed for individual parts of the coma is determined.

Harwit, M., 1966, Orbits of sun-grazing comets: The Astronomical Journal, V. 71, p. 857.

Comet Ikeya-Seki (1965f) was part of a family, all of whose members come very close to the sun. A number of these comets have broken into fragments and this has led to the belief that all family members are descendants of a single progenitor. If this idea is correct, one should be able to account for observed differences in the orbital parameters of fragments. We evaluate the possible changes caused by the breakup process and find that one cannot account for some of the orbital differences in this way. Planetary perturbations then are evaluated. The results allow one to decide whether or not certain doubtful family members should be considered true members of the group. (Abstract of a paper presented at the July 1966 meeting of the American Astronomical Society).

Herring, A.K., 1966, Observations of comet Ikeya-Seki (1965f) from Mauna Kea, Hawaii: Communications of the Lunar and Planetary Laboratory, V. 4, No. 67, p. 141-144 + 1 color photograph.

Visual and photographic observations and a noon-time observation at perihelion.

Huebner, W.F., 1966, Diminution of cometary heads during perihelion passage: The Astronomical Journal, V. 71, p. 858.

The amount of icy conglomerate that is sublimated from the surface of a cometary nucleus is calculated from the time integral of the sublimation rate. The sublimation rate used (Huebner, W.F., Z. Astrophys. 63, 22, 1965) gives general agreement with estimates made by Biermann and Trefftz (Z. Astrophys. 59, 1, 1964) for gas productivities for comets in which the forbidden [O I] lines have been observed, and is by powers of 10 higher than the estimates based on the intensity of observed molecular bands. The amount of sublimation is correlated with data reduced from observations of some comets. The mass loss calculated for comet Encke agrees with that from Whipple's "pinwheel" effect. The calculated mass loss for comet Halley is larger than the one estimated from intensities of molecular bands in the tail, and suggest that there are more non-luminous molecules in the tail than had been assumed. The average reduction of reduced brightness per perihelion passage for the above comets cannot be explained to be due to the reduction of gas producing surface area; the reduction being caused by the sublimation of a layer of ice. The gas production rate itself must decrease, presumably through the accumulation of meteoritic material acting as an insulation layer on the surface. On the other hand, for sun-grazing comets, the reduction of gas producing surface area is an important factor in explaining the reduction of reduced brightness after perihelion passage as compared to that before perihelion passage. This work was performed under the auspices of the U.S. Atomic Energy Commission. (Abstract of a paper presented at the July 1966 meeting of the American Astronomical Society).

Huebner, W.F., and Weigert, A., 1966, Eiskörner in der Koma von Kometen: Zeitschrift für Astrophysik, V. 64, p. 185-201.



The size and number of particles which are dragged into cometary atmospheres are determined by the balance of energy and of momentum. It is proposed that the activity observed in some comets (for instance 1925 II) at large heliocentric distances could be explained through disturbances in the balance of the ice halo. (In German).

Hyder, C.L., 1966, Polarization of the Na D<sub>1</sub> line and magnetic fields in the comet Ikeya-Seki (1965f): *The Astronomical Journal*, V. 71, p. 389.

The linear polarization in optically thin cometary Na D<sub>1</sub> and D<sub>2</sub> lines was measured in three regions of the comet Ikeya-Seki on 20, 21 October 1965. The polarization observed for the D<sub>1</sub> line (which cannot be polarized in the comet) was used to calibrate the Sacramento Peak coronagraph-universal spectrograph system, and the D<sub>2</sub> line polarization was corrected accordingly. The resulting planes of polarization in the D<sub>2</sub> line were always perpendicular to the line joining the comet and the sun (the normal direction). The degrees of polarization in the three regions were 4.5%, 5.5% and 7%, and the angles of deviation from the normal were 30°, 33°, and 19°, respectively.

The observed polarizations are uniquely explained by cometary magnetic fields parallel to the cometary velocity vectors. I believe that the cometary magnetic fields are parallel to the Type I tail of the comet (not observed visually or photographically for this comet).

Upper limits of 175 and 36 km/sec were found for the solar wind speeds at the comet for the two times of observation. These speeds are theoretically compatible with values somewhat less than the 260 km/sec observed at 1 a.u. on a quiet solar day. The theoretical solar wind values for the cometary distances are given by Parker for an isothermal corona less than  $0.5 \times 10^6$  °K. (Abstract of a paper presented at the March 1966 meeting of the American Astronomical Society).

Ioffe, Z.M., 1966, Comets in the solar wind: *Soviet Astronomy - A.J.*, V. 10, p. 138-142.

A comet nucleus is treated as a source, in the hydrodynamic sense, located in a supersonic, stationary, solar plasma stream. Newton's formula yields the pressure at the source-stream interface. The plasma-head configuration and the cylindrical shape of a type I tail can be explained. The recession distance of the shock wave is estimated by comparison with the solution for a source in an incompressible medium.

Ioffe, Z.M., 1966, Comets in the solar wind. II: *Soviet Astronomy - A.J.*, V. 10, p. 517-519.

A comet is treated as a source embedded in a supersonic stream. The problem of stationary supersonic flow of a compressible gas stream around a subsonic source is formulated. The stream-source interface approaches a cylinder at infinity. The minimum source radius  $r_{min}$  characterizing the ionization region is found. The asymptotic values of the thermodynamic parameters yield the parameters near the sphere  $r_{min}$ .

Jackson, W.M., and Donn, B., 1966, Photochemical effects in the formation of cometary radicals and ions: *The Astronomical Journal*, V. 71, p. 859-860.

Calculations of the photochemical yield of radicals and ions for a region within 5000 km of the nucleus have been carried out. In this region the photochemical loss of daughter molecules can be neglected. The theoretical basis for the determination of the density of the parent species is the continuity equation in which we include a term to account for photodissociation or

ionization. The variation of life-time for these processes with nuclear distance because of changing optical depth within the coma was allowed for.

The solution of the equation yielded equidensity contours for both radicals and ions for nuclear radii of 0.5, 1, and 5 km. The  $C_2$  radical density was calculated to be  $2 \times 10^9/\text{cm}^3 \text{ km}$ , for a 0.5 km comet radius, a relative abundance of  $10^{-4}$  for the  $C_2$  parent molecule, and a dissociation cross section of  $10^{-17} \text{ cm}^2$ .  $CO^+$  densities at 1000 km were of the order of  $10^4/\text{cm}^3$  for relative, CO concentrations of about 0.5. The ion distributions were strongly concentrated in the sunward direction for nuclear radii greater than 1 km. As  $CO^+$  and  $C_2$  have comparable  $f$  values,  $CO^+$  will be visible near the nucleus.

The density of the observed species depends directly upon the corresponding parent densities and the flux of solar radiation. Rapid changes in either of these quantities will cause rapid changes in the densities and hence luminosities of these ions and radicals.

The present calculations are based upon a reasonable model of the composition of the nucleus of a comet and show that the parents of the observed radicals represent only a minor constituent. The large CO concentration in some comets is consistent with molecular equilibrium calculations for the primordial solar nebula. (Abstract of a paper presented at the July 1966 meeting of the American Astronomical Society).

Kearns, C.E., and Rudnicki, K., 1966, 28 photographs of comet Humason (1961e): *Zeitschrift für Astrophysik*, V. 64, p. 337-361.

23 blue and 5 yellow photographs of comet Humason (1961e) were obtained with the 48" Schmidt Telescope of Mt. Palomar Observatory.

Kovar, N.S., and Kern, J.W., 1966, Proposed hydromagnetic model for comets: *The Astronomical Journal*, V. 71, p. 861.

Today it is widely thought that Type I comet tails are caused by an interaction between the solar wind and cometary molecules evaporated from the nucleus. Here loading of the solar wind by ionization of neutral cometary molecules is calculated. Four ionization mechanisms are considered: collisional ionization by solar-wind protons and neutral comet molecules; photo-ionization; and cascade ionization by cometary ions accelerated by the solar plasma flow.

Equations for continuity of energy, momentum, mass, and solar-wind electron flux are formulated and an adiabatic relation between the solar wind pressure and the density of original solar-wind electrons is assumed. Expressions are obtained for the velocity, mass density, and Mach number of the flow. The distance at which pressure and density go to zero is calculated.

Several conclusions are drawn. The momentum flux density is reduced in the comet head, especially in the vicinity of the nucleus. The distances at which the momentum flux density goes to zero for reasonable solar-wind parameters are in accord with Wurm's observation that the tail ions are limited to a distance of less than 10 000 km centered on the nucleus. The derived comet ions that load the solar wind have number densities which may be too small to be observed--of the order of  $0.01 \text{ cm}^{-3}$  or less. The Mach number of the flow is found to increase in the vicinity of the nucleus, making the presence of a shock upstream unlikely. For radial distances larger than the characteristic size of the ion coma, the most important loading mechanism is found to be charge exchange between neutral cometary molecules and solar-wind protons. (Abstract of a paper presented at the July 1966 meeting of the American Astronomical Society).

Kovar, N.S., and Kovar, R.P., 1966,  $I(6300,6363)/I(5577)$  ratio of  $[O_I]$  in the spectra of comets: *The Astronomical Journal*, V. 71, p. 166.

It is not possible to explain the variation in the intensity ratio of the  $\lambda 5577$  and  $\lambda 6300, 6363$  lines of  $[O_I]$  in comets in terms of the fluorescence process or electron collisions. By considering the contributions of various atomic and molecular processes (such as dissociation, recombination, etc.) to the above processes, the various observed intensity ratios can be explained simply in terms of the electron density and temperature within the coma. Reasonable electron densities for the coma suggest that an electron temperature in the  $10^3$ - $5 \times 10^4$  K range would best produce the conditions necessary for an understanding of the observed intensity ratios of  $[O_I]$ . (Abstract of a paper presented at the December 1965 meeting of the American Astronomical Society).

Larson, S.M., 1966, Observations of comet Ikeya-Seki (1965f) from Tucson, Arizona: *Communications of the Lunar and Planetary Laboratory*, V. 4, No. 68, p. 145-156 + 1 color photograph.

Visual and photographic observations were made to determine positions, size, color and apparent visual magnitudes, September 22 to December 4, 1965.

Livingston, W., Roddier, F., Spinrad, H., Slaughter, C., and Chapman, D., 1966, The sodium D lines in comet Ikeya-Seki: *Sky and Telescope*, V. 31, p. 24-25.

A spectrum of the comet between 5890 and 5896 angstroms is presented and explained in terms of the structure of the comet.

Malville, J. McK., and Evans, C., 1966, Observations of comet Ikeya-Seki with the climax coronagraph: *The Astronomical Journal*, V. 71, p. 169.

Slitless spectra obtained on 20 October are used to obtain relative intensities of sodium D<sub>1</sub> and D<sub>2</sub> throughout the head and tail. The D<sub>2</sub>/D<sub>1</sub> intensity ratio in the cometary head decreased from 1.7 at 2100 UT to 1.3 at 2330 UT indicating a steady increase in the optical depth of sodium. The ratio was consistently larger in the tail than in the head; at 2140 UT the ratio increased from 1.4 in the head to 1.95 in the tail. The ratio of the intensities of the D lines to the intensity of the neighboring continuum in the head decreased by a factor of more than 5 between 2100 and 2300 UT suggesting a more rapid expulsion of gas than of dust. At 2100 UT a sunward spike of sodium gas was present. By 2240 UT the spike had disappeared and a bright sodium condensation had appeared in the tail. Slit spectra show a red-shift of the lines in emission in the head by 2.4 Å at 2226 UT and a blue-shift of the D lines in absorption by 1.4 Å. (Abstract of a paper presented at the December 1965 meeting of the American Astronomical Society).

Marsden, B.G., 1966, Evolution of the great sun-grazing comet group: *The Astronomical Journal*, V. 71, p. 863.

The apparent distribution of the times of perihelion passage of the known members of the sun-grazing comet group is far from uniform. There are good reasons for including comets 1689, 1695, 1702a and Tefvik (the eclipse comet of 17 May 1882) among the group, and then the three clusters, separated in time by a century or two, are even more obvious. In view of this, it is reasonable to suppose that, if the observed comets are indeed returning fragments of a larger comet that broke up at its perihelion passage, then that breakup took place the last time around. It is tempting to identify the parent comet with the enigmatic comet of 1106, and then with an alleged daylight comet of 368 and the celebrated comet of -371, described by Aristotle. There is some observational evidence that all but possibly the principal fragments of a comet that has split

do not survive more than one or two further returns to perihelion. The clusters would be associated with multiple nuclei similar to those observed in comets 1882 $\eta$  and 1965f, and the individual comets would have been indistinguishable even if present observing techniques had been available. It has been found that the orbital elements of the best observed comets may be represented very closely by

$$\begin{aligned} a &= 689.4 & +17987 & \sin(\lambda' + 99.18) \\ \tau &= 246.84 & +20.75 & \sin(\lambda' + 100.81) \\ i &= 142.23 & +2.50 & \sin(\lambda' + 108.15) \\ q &= 0.007487 - 0.002307 \sin(\lambda' + 105.98) \text{ (a.u.)}, \end{aligned}$$

where  $\lambda'$  is the longitude of Jupiter when the comets are at perihelion. Assuming that the orbits of the fragments differed at the breakup only in semi-major axis (and hence revolution period), expressions similar to the above arise from the subsequent differential attraction of Jupiter, except that the calculated coefficients are about an order of magnitude smaller than those observed. Since this result has been obtained both by a simple general theory and by direct numerical integration of typical orbits, it is hard to believe it is incorrect. One concludes that the differences among the orbital elements of the members of the group cannot be explained by planetary perturbation and that the apparent dependence upon the position of Jupiter is probably fortuitous. (Abstract of a paper presented at the July 1966 meeting of the American Astronomical Society).

Momford, G.S., 1966, Comet Barbon (1966c): *Sky and Telescope*, V. 32, p. 198.

The discovery of a faint comet is reported.

Roemer, E., 1966, Comet notes: *Publications of the Astronomical Society of the Pacific*, V. 78, p. 83-91.

Principally a discussion of comet 1965 Ikeya-Seki observations, including three photographs taken at Flagstaff, Arizona in October and November 1965.

Roemer, E., 1966, Comet notes: *Publications of the Astronomical Society of the Pacific*, V. 78, p. 178-179.

Astrometric observations of the double nuclei of comet Ikeya-Seki are reported, together with brief references to comet Klamola, 1965j; comet Alcock, 1965h; and comet Humason, 1961e.

Roemer, E., 1966, Comet notes: *Publications of the Astronomical Society of the Pacific*, V. 78, p. 348-350.

Comet Ikeya-Seki is reported to have faded out by mid March. The observed and predicted appearances of several periodic comets are presented.

Roemer, E., 1966, Comet notes: *Publications of the Astronomical Society of the Pacific*, V. 78, p. 488-490.

The discovery and orbits of comets Kilston, 1966b and Barbon, 1966c are described. Observations and predicted appearances of several periodic comets are presented.

Roemer, E., and Lloyd, R.E., 1966, Observations of comets, minor planets, and satellites: *The Astronomical Journal*, V. 71, p. 433-457.

Accurate positions and descriptive notes are presented for 38 comets, 33 minor planets, 5 faint natural satellites, and Pluto, for which astrometric reduction of the series of Flagstaff observations has been completed.

Roemer, E., Thomas, M., and Lloyd, R., 1966, Observations of comets, minor planets, and Jupiter VIII: *The Astronomical Journal*, V. 71, p. 591-601.

Accurate positions and descriptive notes are presented for 24 comets, 11 minor planets, and the eighth satellite of Jupiter.

Sekanina, Z., 1966, Dynamical effect of explosive phenomena in comet Halley and its nuclear rotation: *Zeitschrift für Astrophysik*, V. 64, p. 465-471.

Changes in the daily motion and in the orbital elements of comet Halley, caused by a non-gravitational mechanism have been investigated in the period of the comet's latest apparition during 1909-1911 based on a new orbit derived by Zadunsky. Full agreement is reached if explosions of solid matter from the nucleus are assumed, thereby exerting a push on the comet's nucleus on about May 14 or 15, 1910, coinciding with the time of maximum activity of comet Halley.

Thackeray, A.D., Feast, W.W., and Warner, B., 1966, Daytime spectra of comet Ikeya-Seki near perihelion: *The Astrophysical Journal*, V. 143, p. 276.

Spectra of the comet were recorded on October 20, 1965 at the Radcliffe Observatory using a stopped down 72" telescope. The spectra show a) emission lines from the nucleus of the comet, b) a Fraunhofer spectrum scattered by the nucleus and c) a Fraunhofer spectrum due to scattering in the atmosphere. The emission spectrum from the comet shows FeI, CaI (H and K) and CaI  $\lambda 46226$  concentrated at the nucleus, plus weak emission of H, SrII, FeII  $\lambda 4233$  and MgI. Also NaD-lines and CN emission appear from a larger volume than the metallic emissions.

van Houten, C.J., and van Houten-Groeneveld, I., 1966, A new periodic comet, observed in 1960: *Bulletin of the Astronomical Institutes of the Netherlands*, V. 18, p. 441 note.

The comet, not occurring in the latest list by Porter (1961) was found during the blinking of plates taken in September and October 1960 with the 48 inch Schmidt camera of the Mt. Palomar Observatory. Orbiting elements have been computed and are given.

Weinberg, J.L., 1966, Photoelectric polarimetry of comet 1965f: *The Astronomical Journal*, V. 71, p. 875.

Multicolor observations were taken of the principal Stokes parameters of the night-sky radiation over a  $9 \times 20$  deg section of the sky containing comet 1965f. The total and polarized components of radiance, the degree of polarization, and the orientation of the plane of polarization are derived (at  $5300\text{\AA}$ ) both along and normal to the axis throughout the tail of the comet, and a preliminary interpretation is given on the implications in terms of the nature and distribution of the particles.

Preliminary results are also presented on fluctuations in the zodiacal light resulting from the presence of the newly injected cometary material. (Abstract of a paper presented at the July 1966 meeting of the American Astronomical Society).

### 3.3 Meteorite Craters and Cratering Effects

Beals, C.S., and Innes, M.J.S., 1964, The identification of ancient meteorite craters: *Akademiia Nauk SSSR Meteoritika*, No. 25, p. 3-39.

The most important results of the study of ancient craters is the fact that their underground structure can be predicted from Rottenberg's model; this was confirmed by geophysical observations and diamond drilling on the Brent, Holleford, and Deep Bay craters in Canada, results of which are discussed. Inasmuch as these craters are of different age (Precambrian to Mesozoic), it is reasonable to conclude that a sufficiently thorough search might reveal a considerably larger number of craters. In addition to these three, there are about 10 cryptovolcanic structures in the United States and Europe for which current studies indicate a possible impact origin. Adding to these the 20 known craters or crater groups, it would appear that large meteor impacts can no longer be considered to be particularly rare. The question is raised whether these processes have played the same role in earth history as on the moon. It is hoped that all countries will make the most of the possibilities of aerial photography for this purpose. (From *Geophysical Abstracts*, No. 217).

Brett, R., 1966, Metallic spherules in impactite and tektite glasses: *Transactions of the American Geophysical Union*, V. 47, No. 1, p. 145.

Electron-microprobe analyses indicate that Ni-Fe spherules within impactite glass bombs from the Canyon Diablo area, Arizona, contain from 20 to 65 weight % Ni. Spherules from impactite glass at Wabar, Saudi Arabia, contain 12-41 weight % Ni. The parent meteorites contain 7-8 weight % Ni. Microprobe analysis indicates that the glass surrounding the spherules is enriched in iron. The glass surrounding tektite spherules is not enriched in Fe. Therefore, some mechanism is considerably enriching the metal and glass in nickel and iron, respectively, in impactites, but not in tektites. It is proposed that spherules in impactite glasses were partially oxidized before incorporation into impactite bombs. After incorporation, the almost Ni-free Fe oxide diffused into the glass, thus enriching it in Fe. Spherules in tektites were not oxidized because the tektites were formed in an atmosphere with extremely low fugacity of oxygen. A less likely alternative is that the spherules were incorporated into the tektite glass instantaneously so that oxidation was prevented. (Abstract of a paper presented at the April 1966 meeting of the American Geophysical Union).

Carpenter, J.W., and Davidson, G., 1966, Feasibility of terrestrial observation of visible radiation associated with meteor impact on the lunar surface: *Transactions of the American Geophysical Union*, V. 47, No. 1, p. 149.

The possibility of observation of meteors impacting the lunar surface has been considered many times. In light of recent estimates of the density of the lunar atmosphere, no energy will be dissipated by the meteor before it strikes the surface. The radiation emitted will be that associated with hypervelocity impact. Laboratory results on hypervelocity impact phenomena generally yield visible light flashes having decay times of the order of a few microseconds. The limiting backgrounds for observations using photoelectric techniques and ground-based telescopes are earthlight and scattering of light from the sunlit portion of the lunar disc. A proposed technique for definitive observations of lunar meteor impacts utilizing two widely spaced telescopes is discussed. It is estimated that, using two 26-inch telescopes and viewing a large fraction of the lunar disc near new moon, meteors with  $m \geq 6.5$  grams will be observed at a rate of 1 in 20 minutes. (Abstract of a paper presented at the April 1966 meeting of the American Geophysical Union).

- Chao, E.C.T., Dwornik, E.J., and Merrill, C.W., 1966, Nickel-iron spherules from Aouelloul glass: *Science*, V. 154, p. 759-765.

Nickel-iron spherules were found in glass associated with the Aouelloul crater. It is concluded that the glass is of terrestrial origin.

- Chao, E.C.T., Merrill, C.W., Cuttitta, F., and Ansell, C., 1966, The Aouelloul crater and the Aouelloul glass of Mauritania, Africa: *Transactions of the American Geophysical Union*, V. 47, No. 1, p. 144.

The Aouelloul crater, 250 meters in diameter, is located at 20°15'N and 12°41'W about 50 km southeast of Atar. It is in the gently dipping Ordovician Oujf quartzite and the micaceous Zli sandstone. Shocked sandstone was not found. The Aouelloul glass occurs both within and outside the crater. The Aouelloul glass shows pronounced flow structures. It contains abundant inclusions of lechatellierite and incompletely digested mixtures of quartz and vesicular silica glass. Ni is not detected in the Zli sandstone and the Oujf quartzite, whereas the Aouelloul glass contains 330-430 ppm Ni. The data suggest that the Aouelloul glass is derived from the Zli sandstone and that a part of the discrepancy in Fe and Ni content may be attributed to the addition of a minute fraction of the impacting body. The new evidence gathered is consistent with an impact origin of the crater. The absence or rarity of shocked sandstone is not unique. (Abstract of a paper presented at the April 1966 meeting of the American Geophysical Union).

- Danes, Z.F., 1966, Isostatic processes in media of variable viscosity: *Transactions of the American Geophysical Union*, V. 47, No. 4, p. 628.

The analysis of rebound processes in large craters, reported previously, has been extended to media in which viscosity is a linear function of depth. Solutions are given as infinite series of confluent hypergeometric functions, and are easily amenable to computer techniques. (Abstract of a paper presented at the September 1966 meeting of the American Geophysical Union).

- David, E., 1966, Meteorite impacts and the ejection mechanism of tektites: *Earth and Planetary Science Letters*, V. 1, No. 2, p. 75-76.

The possibility that tektites could be formed by meteorite impact on the surface of the earth has been frequently rejected because no mechanism has been found which explains the large distances over which the tektites appear to travel. This paper presents a description of meteoritic impact according to which the ejection of collision fragment out of the atmosphere is possible, and which therefore can explain the large distances of tektite travel. The horizontal expansion of the compressed, overheated impact vapor against the air of normal density stops within ten kilometers. Vertically the barometric decrease of air density soon exceeds the pressure decrease of the expanding rock vapor which shoots out into free space in a large cone, with a streaming velocity of at least 3 km/s. Fortuitously favorable injection conditions combined with an event which needs not surpass the Reis event in order of magnitude might have given rise to the enormous quantity of the southeast Asian-Australian tektites.

- Dietz, R.S., 1966, Shatter cones at the Middlesboro structure, Kentucky: *Meteoritics*, V. 3, p. 27-29.

Shatter cones have been discovered in two residual boulders in the central uplift eye of the Middlesboro structure, Kentucky. This finding gives additional support to the interpretation of Englund and Roen that this is probably an astrobleme, i.e., an ancient meteorite impact scar.



Divoky, D., 1966, The equivalence of mass and energy scaling of crater dimensions: comment on a paper by A.J. Chabal: *Journal of Geophysical Research*, V. 71, p. 2691.

In a recent paper by Chabal (1965), four distinct scaling laws for the determination of crater dimensions are derived: mass and energy scaling and mass, energy, and gravity scaling for variable gravity. These four scaling laws present a paradox, for it appears that, in general, mass and energy relations do not result in equivalent crater predictions.

The author demonstrates that mass and energy scaling laws are, in fact, equivalent.

El Goresy, A., 1966, Metallic spherules in Bosumtwi crater glasses: *Earth and Planetary Science Letters*, V. 1, No. 1, p. 23-24.

Several metallic spherules were discovered in some new glass specimens from the Bosumtwi crater in Ghana. The microprobe analysis indicated 95.4% Fe, 5.2% Ni and 0.6% Co. Pyrrhotite spherules present also contain Ni up to 0.3%. The presence of Ni and Co in the metallic spherules is in agreement with the impact origin of the glasses.

Faul, H., 1966, Tektites are terrestrial: *Science*, V. 152, p. 1341-1345.

Geochronologic evidence is presented in favor of the theory of terrestrial origin of tektites from large impact craters. Ivory Coast tektites are related to the Bosumtwi crater, and Moldavites to the Ries crater. No crater has been found for the North American and Australasian tektites.

Fesenkov, V.G., 1966, A study of the Tunguska meteorite fall: *Soviet Astronomy - A.J.*, V. 10, p. 195-213.

An interpretation is offered of all available information on the fall of the Tunguska meteorite in an effort to understand the nature of the phenomenon. Eyewitness accounts and the falling of trees yield the probable trajectory of the meteorite in the atmosphere. Several cases are treated for the space orbit, the position of the apex, and the geocentric approach velocity. Fourteen sets of orbital elements are recomputed; in all cases the orbit is dissimilar to that of normal meteorites. The distinctive properties of the abnormal night-sky glow associated with the Tunguska fall are discussed. The probability is computed for penetration of a comet's dust tail into the upper atmosphere. The range of dust dispersal and the total amount of dust are estimated. The searing of trees near the epicenter of the fall and the height of the explosion deduced from observations yield a probable size and a mean density well below unity for the head of the Tunguska comet. Several cases are treated for the motion of the comet nucleus in the atmosphere, with initial approach velocities of 30 and 40 km/sec. A nucleus of density considerably less than unity, treated as solid, furnishes the most probable interpretation of the phenomena observed. All the results support a cometary origin for the Tunguska meteorite.

Fesenkov, V.G., 1964, On the orbit of the Tunguska meteorite: *Akademiia Nauk SSSR Meteoritika*, No. 25, p. 163-167.

Possible orbits of the Tunguska meteorite of 1908 are worked out from the conflicting reports of the event. The elements of circular and parabolic orbits (inclination to plane of ecliptic, perihelion distance, eccentricity, major semi-axis, and relative impact velocity) are tabulated for three azimuths ( $0^\circ$ ,  $20^\circ$ ,  $40^\circ$ ) of visible radiant. For all these variants, one of which should be the true orbit, the motion is not characteristic of ordinary meteorites.



representing the product of breakup of asteroids, but is normal for the case of a comet. (From Geophysical Abstracts, No. 217).

Gault, D.E., Quaide, W.L., and Oberbeck, V.R., 1966, Modeling meteorite craters in the laboratory, I. Mechanics of formation: Transactions of the American Geophysical Union, V. 47, No. 1, p. 148.

Impact craters formed in the laboratory in low- and variable-strength materials have been studied to gain insight into the mechanics of the formation and structure of meteorite craters. High-speed framing camera records and stereo-photographs of the developing cavity, together with terminal structure geometry, indicate that craters are produced primarily as the result of shearing deformations. Basic differences in the mechanics of impact- and explosion-crater formation caution against the general application of explosive data to meteorite craters. (Abstract of a paper presented at the April 1966 meeting of the American Geophysical Union).

Gentry, R.V., 1966, Anti-matter meteorite explosions relative to fission track ages of tektites: Transactions of the American Geophysical Union, V. 47, No. 4, p. 618.

Previous attempts to account for the considerable variation of fission track ages in the Georgia and Australian tektite fields have been on the basis of post-arrival heating events. If tektites are assumed to have originated with anti-matter meteorite explosions (lunar or terrestrial), then another source of error in fission track ages is possible. Using nuclear explosion data, calculations show that small but significant amounts of certain short half-life spontaneous fissionable nuclides may be produced by the interaction of the high neutron flux from an anti-matter burst with the U <sup>238</sup> fraction in the vaporized material. Subsequent incorporation of these short half-life nuclides into molten tektites material would then produce large background fission track densities. Thus, anomalously high fission track ages would result in some tektites. If this hypothesis is correct, it would tend to support geological evidence of recent tektite infalls. Electron microprobe analysis of several unusual structures in biotite is discussed relative to anti-matter burst phenomena. (Abstract of a paper presented at the September 1966 meeting of the American Geophysical Union).

Kelley, A.O., 1966, A water-impact hypothesis for the Sierra Madera structure in Texas: Meteoritics, V. 3, p. 79-82.

It is proposed that the Sierra Madera structure was formed by meteorite impact while the area was submerged under pre-historic seas. The water would cause modification of the shock waves resulting from the cosmic impact in order to account for the atypical structures at Sierra Madera.

Kurbatskiy, N.P., 1964, On forest fire in the area of the Tunguska fall in 1908: Akademiia Nauk SSSR Meteoritika, No. 25, p. 168-172.

It is pointed out that the forest blown down by the Tunguska fall might have been already dead and decayed due to forest fires; this possibility should be taken into account in calculating the violence of the ballistic and explosive waves from the extent of flattened forest. Moreover, a great forest fire creates strong convection currents of air and winds near the ground, which can fell trees in the direction of movement of the front of the fire. (From Geophysical Abstracts, No. 217).

Lin, S.C., 1966, Cometary impact and the origin of tektites: Journal of Geophysical Research, V. 71, p. 2427-2437.

The possibility of a terrestrial origin of tektites is re-examined in the light of recent aerodynamic evidence presented by Chapman, Larson, and Anderson. It is found that even though existing evidence points strongly toward a lunar origin as most probable for Australasian tektites, there still exists the possibility that these small glassy objects originated on the earth. In particular, it is conceivable that a sufficiently energetic cometary collision of the type hypothesized earlier by Urey could momentarily blow a bubble through the earth's atmosphere and hence propel small objects over inter-continental distances. The minimum mass of a comet head required to accomplish such a feat is estimated to be about  $5 \times 10^{17}$  grams. Some obvious questions which remain to be answered in order to support such a model of tektite origin are discussed.

Marshall, L., 1966, Non-anti-matter nature of the Tunguska meteor: *Nature*, V. 212, p. 1226.

The mechanisms involved in an anti-matter explosion are discussed to support the assumption of Cowar *et al.* that there are about  $8 \pm$  neutrons per nucleon-anti-nucleon annihilation, and reaffirms the validity of their conclusion.

Marvin, U.B., and Marvin, T.C., 1966, A re-examination of the crater near Crestone, Colorado: *Meteoritics*, V. 3, p. 1-10.

The Crestone crater is an elliptical bowl measuring 355 feet by 246 feet with a mean depth of 23 feet. It lies in unconsolidated sand on the surface of an alluvial fan at the base of the Sangre de Cristo Mountain Range in the San Luis Valley, Colorado ( $37^{\circ}54'N$ ,  $105^{\circ}39'W$ ). Aerial photographs show the crater as a striking feature in its setting on a gently undulating terrain.

The crater is less than half as deep relative to its diameter as known meteorite explosion craters. Furthermore, topographic profiles indicate that the crater does not form a depression in the land surface. The crater rim is a positive feature enclosing a basin that has a floor approximately level with the surface of the alluvial fan on which it lies. In the absence of any mineralogic or topographic evidence of impact or explosion, it is concluded that this landform is not meteoritic or cometary in origin.

Maloy, T.P., and Faust, L., 1966, Size and velocity distribution of ejecta from an impact crater: *Transactions of the American Geophysical Union*, V. 47, No. 1, p. 149.

A rotationally symmetric model of an impact crater was considered. It was assumed that the partition of energy in the compressional wave through the substrate was proportional to the energy in the wave. The Gaudin-Maloy size distribution law was used to compute the size distribution of the daughter fragments resulting from comminution of the rock substrate. The velocity of the ejecta particles was assumed to be proportional to the energy in the compressional wave and to the surface area of the particles. Integrating over the crater volume yields a size distribution and a velocity distribution of the fragment. This result is used to predict size distribution of fragments as a function of distance from the crater. (Abstract of a paper presented at the April 1966 meeting of the American Geophysical Union).

Millman, P.M., 1966, Craters: *Meteoritics*, V. 3, p. 55-57.

Recent observational evidence emphasizes the importance of craters as a prominent surface characteristic of the smaller planetary bodies in the solar system. Craters of similar appearance may have very diverse origins. An initial assumption as to the type of origin should not influence an impartial and detailed physical study of any given crater.

- Moraski, L.K., Teal, D.J., Lunch, J.E., Higgins, C.J., and Johnson, S.W., 1966, The effects of gravity on shear strength and explosion crater parameters for cohesionless soils: Transactions of the American Geophysical Union, V. 47, No. 1, p. 149.

The effects of gravity on shear strength and explosion crater parameters for cohesionless granular media have been determined experimentally using apparatus flown in the JC-131B and the KC-135 aircraft. These aircrafts permitted tests to be run using first a penetrometer in media of various mass densities and later 6.0 grain squibs detonated at various depths in Ottawa sand. That gravity does affect explosion crater parameters is shown by the tests, the results of which are plotted and subjected to statistical analysis. Crater dimensions were found to vary inversely with gravity. Experimental and analytical work in this study verify that the shear strength of a cohesionless medium varies directly with gravity. Cratering processes such as compaction, scouring, spalling, and gas acceleration are influenced by changes in shear strength and weight of overburden. Hence, crater dimensions are expected to be gravity dependent, as observed. (Abstract of a paper presented at the April 1966 meeting of the American Geophysical Union).

- Portnov, A.M., 1964, On the crater on the Potomsk Upland: Akademiia Nauk SSSR Meteoritika, No. 25, p. 194-197.

A crater about 86 m in diameter that occurs on the Potomsk Upland, about 50 km west of Perevoz settlement in the Badaybinsk area of the Irkutsk Region, is described. The external aspect, regular shape, presence of a ring wall and central hill, and shattered and pulverized but not altered rocks, all indicate an explosive, possibly meteoritic, origin. (From Geophysical Abstracts, No. 217).

- Quaide, W.L., Oberbeck, V.R., and Gault, D.E., 1966, Modeling meteorite craters in the laboratory. 2. Deformational structures: Transactions of the American Geophysical Union, V. 47, No. 1, p. 148.

Numerous structures produced in the laboratory by impacting spherical models into low strength targets are identical to those found in large meteorite craters. Structures produced include upwarped rims with inverted stratigraphy, near surface overthrusts, stratigraphically deep underthrusts, and polygonal craters. All structures observed are compatible with particle motions outlined in the paper describing the mechanics of formation of impact craters. (Abstract of a paper presented at the April 1966 meeting of the American Geophysical Union).

- Roberts, W.A., 1966, Shock--a process in extraterrestrial sedimentology: Icarus, V. 5, p. 459-477.

Impact-induced shock is an operative process on planetary surfaces and provides the mechanism for comminution transport by ballistic ejection, and deposition in regions adjacent to the shock focus. Deposits of ejecta thin radially outward with a probable general decrease in median grain size with increasing radial distance from the crater and upward from the base of the ejecta deposit. Some of the ejected material travels outward with densities high enough, or porosity low enough, that winnowing action by an atmosphere does not occur. Other material, generally that ejected at higher velocities and angles, is winnowed and sorted by the atmosphere during ballistic flight. Fallback in the crater is composed of this latter material as well as material from the rim which slides back into the crater depths. Range of ejecta deposits is a function of ejection angles and velocities, gravity, and drag by the atmosphere. The unwinnowed material, called bulk ejecta, is deposited in an order the inverse of the preshock vertical sequence.

Roddy, D.J., 1966, Carbonate deformation at a probable impact crater at Flynn Creek, Tennessee: Transactions of the American Geophysical Union, V. 47, No. 3, p. 493-494.

A partly buried crater about 3.5 km in diameter and 110 meters deep is exposed in an area of flat-lying carbonates in north-central Tennessee. Current studies indicate the crater was formed in Middle or Late Devonian time, probably by impact of an extraterrestrial body. In the rim of the crater, limestones of Middle and Upper Ordovician age are folded, faulted, and brecciated in an irregular band up to several hundred meters wide. An irregular, apparently discontinuous zone a few meters to several hundred meters wide adjacent to the crater wall contains extensive fractures, microfractures, and calcite twin lamellas. Micro-twinning becomes prominent near the crater wall in crystals as small as  $20\mu$ , and kink bands occur in some larger calcite crystals ( $>100\mu$ ). These patterns of deformation for the calcite appear consistent with patterns described by Short for explosive shock loading and are interpreted as caused by high stress imposed during the passage of a shock front(s) produced during impact. (Abstract of a paper presented at the September 1966 meeting of the American Geophysical Union).

Roddy, D.J., 1966, Minimum energy of formation for a probable impact crater at Flynn Creek, Tennessee: Transactions of the American Geophysical Union, V. 47, No. 3, p. 482.

The Flynn Creek structure in north-central Tennessee consists of a partly buried crater 3.5 km in diameter and 110 meters deep. Detailed field and laboratory studies suggest formation by impact of an extraterrestrial body in Middle or Late Devonian time. Evaluation of pre-crater breccia and in the central uplift indicates a minimum volume of  $4 \times 10^{12}$  cm<sup>3</sup> of disrupted rock (mass of  $10^{16}$  grams). The energy necessary to fracture this volume of rock is estimated to be  $10^{22}$ - $10^{24}$  ergs based on reported comminution studies. Energy scaling from the "Jangle U" nuclear explosion crater and the 500-ton TNT explosion crater at the Suffield Experimental Station, Canada, indicates an energy of formation of  $10^{24}$ - $10^{26}$  ergs for the Flynn Creek crater. It is estimated that an impacting body with these kinetic energies traveling at 30 km/sec would have a diameter of about 80 meters, assuming  $\rho = 3.3$  g/cm<sup>3</sup>. (Abstract of a paper presented at the September 1966 meeting of the American Geophysical Union).

Ronca, L.B., 1966, Meteoritic impact and volcanism: Icarus, V. 5, p. 515-520.

The possibility of volcanism triggered by meteoritic impact is analyzed theoretically by comparing volcanological and impact data. Field data on some terrestrial craters are also discussed. The conclusion is that volcanism triggered or localized by impact is possible. The hypothesis is proposed that lunar craters represent a spectrum of craters ranging from completely meteoritic craters, through meteoritic craters modified by volcanism, to completely volcanic craters. The data on Mars are meager, but suggest that Martian craters may owe their origin to the same processes.

Salisbury, J.W., and Ronca, L.B., 1966, The origin of continents: Nature, V. 210, p. 669-670.

The possible role of the impact of large meteorites or asteroids in the production of terrestrial continental nuclei is examined. It is suggested that the localized addition of energy to the earth's crust is the key to continent formation. Convection currents and/or the migration of a phase change boundary would assist in the formation of a nucleus, as well as in subsequent continental growth. Other mechanisms could, however, function just as well in continent formation, given the initial localized addition of energy resulting from an impact.

Sanchez, J., and Cassidy, W., 1966, A previously undescribed meteorite crater in Chile: *Journal of Geophysical Research*, V. 71, p. 4891-4895.

A previously undescribed meteorite crater having dimensions of 455 m average diameter and 31 m average depth has been discovered in northern Chile at  $23^{\circ}55.6'S$ ,  $68^{\circ}16.7'W$ . Meteorites have not been recovered, but iron shale and impactite material verify its meteoritic origin. The crater is emplaced in granite, overlain by a thin ignimbrite sheet. From the apparent disruption of the local Pleistocene drainage pattern, the age of formation of the crater must be Pleistocene or Recent. It may have been formed by the same meteoroid that created the Campo del Cielo craters in Argentina. The name Monturaqui crater is proposed.

Sanchez, J., and Cassidy, W., 1966, A previously undescribed meteorite crater in Chile: *Transactions of the American Geophysical Union*, V. 47, No. 1, p. 144.

The crater has been located in the Atacama Desert region of northern Chile. It is 450 m in diameter and 31 m deep, and is emplaced in granite. Age of the crater is Pleistocene or Recent. Meteoritic iron shale and cindery impactites were collected at points on the rim crest and flanks. (Abstract of a paper presented at the April 1966 meeting of the American Geophysical Union).

Short, N.M., 1966, Shock-lithification of unconsolidated rock materials: *Science*, V. 154, p. 382-384.

Loose quartz grains are lithified around chemical explosive craters. Similar phenomena are found at the Wabar (Arabia) meteorite crater.

Taylor, H.P., Jr., and Epstein, S., 1966, Oxygen isotope studies of Ivory Coast tektites and impactite glass from the Bosumtwi Crater, Ghana: *Science*, V. 153, p. 173-175.

Comparison between oxygen isotope ratios of Ivory Coast tektites and Bosumtwi Crater glass suggests a terrestrial origin of these tektites.

Wampler, J.M., Smith, D.H., and Cameron, A.E., 1966, Isotopic comparison of lead from Ivory Coast tektites and Bosumtwi Crater materials: *Transactions of the American Geophysical Union*, V. 47, No. 1, p. 145.

Lead from samples of two Ivory Coast tektites has the isotopic composition:  $Pb^{208}/Pb^{207} = 1.184$ ,  $Pb^{208}/Pb^{206} = 0.494$ ,  $Pb^{208}/Pb^{204} = 18.1$ . Whereas lead from tektites of other groups is quite similar to relatively young terrestrial lead samples, the Ivory Coast tektite lead is slightly higher in  $Pb^{204}$  and lower in  $Pb^{206}$  than most terrestrial lead samples with a similar  $Pb^{208}/Pb^{207}$  ratio. The hypothesis that Ivory Coast tektites are derived from terrestrial materials at Lake Bosumtwi, Ghana, is examined. Although none of the Lake Bosumtwi samples contained lead identical to that of the tektites, the qualitative similarities support the hypothesis that the tektite material is of terrestrial origin. (Abstract of a paper presented at the April 1966 meeting of the American Geophysical Union).

### 3.4 Meteors and Meteorites

Akaiwa, H., 1966, Abundances of selenium, tellurium, and indium in meteorites: *Journal of Geophysical Research*, V. 71, p. 1919-1923.

The following abundances (atoms per  $10^6$  Si atoms) were measured by neutron activation analysis in three carbonaceous chondrites of types I, II, II, and

one enstatite chondrite of type 1. Se: 53, 15.2, 6.4; Te: 6.9, 3.2, 1.67, 4.1; In: 0.26, 0.094, 0.049, and 0.19. This abundance pattern supports the view that chondrites are a blend of two types of material: a high-temperature fraction (chondrules plus metal) from which the volatiles were lost, and low-temperature fraction (matrix), which retained its volatiles. The data also suggest that the cosmic abundance curve in the Cd-I region may have to be raised by a factor of 2 over previous estimates. The abundances of Ga and In in the chondrite Renazzo are 11.9 and 0.036 on the Si = 10<sup>6</sup> scale. These figures, together with other compositional data, suggest that Renazzo occupies an intermediate position between the carbonaceous and bronzite chondrites, rather than belongs to either class.

Ananthakrishnan, R., 1966, Meteor luminosity and meteor ionization: *Nature*, V. 210, p. 402-403.

It is suggested that the major discrepancy which existed between theory and observation in respect to meteor luminosity/ionization can be explained in terms of the assumption that the heat transfer coefficient is dependent upon the atmospheric density, (which is plausible on physical grounds), and so displaces the earlier theory based on an efficiency factor. This determines what fraction of the kinetic energy of ablated atoms is converted into luminous/ionization energy, being dependent on the atmospheric density.

Anders, E., 1965, Chemical fractionation in meteorites: *Akademiia Nauk SSSR Meteoritika*, No. 26, p. 17-25.

The simplest model fitting available data on the distribution of the elements in chondrites proposes that meteorites (and the planets) are a mixture of two types of material, fraction A, undepleted of its volatiles, and fraction B, from which the volatiles have been lost. The first evidently separated from a complex of cosmic gases at a low temperature, the second at a high temperature. Theoretically, the A and B fractions can be identified with the low- and high-temperature minerals in primary, unmetamorphosed chondrites; they also correspond approximately to the matrix and to the chondrules + metal fractions of chondrites. With minor changes, Wood's (1963) theory provides a satisfactory explanation of the origin of the A and B fractions: A is unheated or slightly heated primordial dust, while B is primordial dust that was vaporized and recondensed upon passage of a shock wave through the solar nebula. (From *Geophysical Abstracts*, No. 237).

Anders, E., and Lipschutz, M.E., 1966, Critique of paper by N.L. Carter and G.C. Kennedy, "Origin of diamonds in the Canyon Diablo and Novo Urei meteorites:" *Journal of Geophysical Research*, V. 71, p. 643-661.

Carter and Kennedy claim to have found convincing evidence against a shock origin of meteoritic diamonds and suggest, that they formed under high hydrostatic pressures instead. Their key exhibit, an "unheated," diamond-bearing Canyon Diablo specimen, was examined. It contains ample evidence of shock in the range of 400-750 kb, and there are good reasons to believe that the diamonds were, in fact, formed as a result of this shock.

Anonymous, 1966, Great lakes fireball: *Sky and Telescope*, V. 31, p. 78-79 and 82.

A collection of reports concerning the fireball of 9 December 1965 and attempts to locate the meteoritic mass, if any.

Anonymous, 1966, Splendid April 25th fireball: *Sky and Telescope*, V. 31, p. 324-326.

Several observers reports of the fireball are presented together with frames from an amateur movie of the event.

Ashbee, K.H.G., and Vassamillet, L.F., 1966, Dislocation in a Campo del Cielo meteorite: *Science*, V. 151, p. 1526-1527.

Thin-film transmission electron microscopy showed an immobile dislocation network of high density in a Campo del Cielo meteorite.

Begemann, F., 1966, Tritium content of two chondrites: *Earth and Planetary Science Letters*, V. 1, No. 4, p. 148-150.

The tritium content of the chondrites Kiel and Pantar has been measured to be  $(450 \pm 30)$  and  $(580 \pm 60)$  dpm/kg, respectively. As Kiel has an exceptionally high ratio  $^3\text{He}/^{21}\text{Ne} = 10.3$ , its normal tritium activity represents further evidence that the variable  $^3\text{He}/^{21}\text{Ne}$  ratios found in chondrites are not caused predominantly by a variation of the  $^3\text{He}$  production rate.

Berkey, E., and Fisher, D.E., 1966, The chlorine content of iron meteorites: *Transactions of the American Geophysical Union*, V. 47, No. 1, p. 132.

The abundance and distribution of chlorine in some iron meteorites have been determined by neutron activation analysis. Contamination by terrestrial chlorine generally overwhelms the primordial abundances, although it is not always possible to differentiate clearly between the two. The chlorine which is presumably primordial seems to be associated with inclusions and grain boundaries, whereas the terrestrial chlorine seems to concentrate along Neumann lines and grain boundaries as well as along cracks. The following average numbers in ppm indicate the range of values found for primordial chlorine: Ni-poor ataxite,  $<0.01$ ; Ni-rich ataxite, 0.02; hexahedrites,  $<0.005-10$ ; octahedrites, 1-300. The octahedrite values may be altered by contamination. (Abstract of a paper presented at the April 1966 meeting of the American Geophysical Union).

Bogard, D.D., and Rowe, M.W., 1966, Anomalous krypton in achondrites: *Transactions of the American Geophysical Union*, V. 47, No. 1, p. 133.

The abundance and isotopic composition of krypton have been determined in five calcium-rich achondrites (eucrites) and in five calcium-poor achondrites (representing various classes). When the isotopic abundances are normalized to  $\text{Kr}^{86}$ , these meteorites exhibit a  $\text{Kr}^{78}$ ,  $\text{Kr}^{80}$ ,  $\text{Kr}^{82}$ ,  $\text{Kr}^{83}$ , and  $\text{Kr}^{84}$  excess as compared with the atmosphere. When the isotopic excess is plotted against the cosmic-ray exposure ages of these meteorites, a linear relation is noted. The isotopic excess is also found to increase from the low krypton masses to  $\text{Kr}^{84}$ . It is suggested that this excess krypton is formed as a cosmic-ray spallation product from strontium and heavier elements. For the calcium-poor achondrites excess krypton was also found, although the isotopic relationships are not as apparent. This interpretation of the excess krypton in achondrites agrees quite well with the explanation given for the excess light xenon isotopes found in these same meteorites. (Abstract of a paper presented at the April 1966 meeting of the American Geophysical Union).

Brett, R., 1966, Cohenite in meteorites: A proposed origin: *Science*, V. 153, p. 60-62.

Cohenite  $[(\text{Fe}, \text{Ni})_3\text{C}]$  occurs in meteorites containing from 6 to 8 percent nickel. It is shown from iron-nickel-carbon phase diagrams that the formation of cohenite means low pressure during cooling.



Brown, P.L., 1966, The Barwell meteorite: *Sky and Telescope*, V. 32, p. 7-11.

A description of the fall and recovery of the Barwell, England, olivine hypersthene-chondrite.

Brownlow, A.E., Hunter, W., and Parkin, D.W., 1966, Cosmic spherules in a Pacific core: *Geophysical Journal of the Royal Astronomical Society*, V. 12, p. 1-12.

The concentration of black magnetic spherules is plotted in an 8 meter core from the North Pacific. The size distribution of the small spherules is similar to the particles of the zodiacal cloud. Larger spherules depart from this because of ablation by the atmosphere.

Bühler, F., Geiss, J., Meister, J., Eberhardt, P., Huneke, J.C., and Singer, P., 1966, Trapping of the solar wind in solids. Part I. Trapping probability of low energy He, Ne and Ar ions: *Earth and Planetary Science Letters*, V. 1, No. 5, p. 249-255.

The trapping probability in Al foils of He, Ne and Ar ions with energies between 0.46 and 7 KeV has been determined. Argon is trapped quantitatively for ion energies higher than 2.5 KeV. At 2.5 KeV the trapping probabilities of neon and helium are about 0.6, decreasing rapidly for lower energies with argon. The trapped gases are held quite firmly. These results show that an Al foil exposed to the solar wind would trap and retain a large fraction of these solar wind ions. There is little doubt that the solar wind will also be trapped in interplanetary dust grains and in the surface layers of asteroids and moons provided these have no atmosphere or magnetic field.

Burnett, D.S., Lippolt, H.J., and Wasserburg, G.J., 1966, The relative isotopic abundance of  $K^{40}$  in terrestrial and meteoritic samples: *Journal of Geophysical Research*, V. 71, p. 1249-1269.

Fowler, Greenstein, and Hoyle have proposed that the inner solar system was heavily irradiated during its formation. A consequence of this proposal is that sizeable differences in meteoritic and terrestrial  $K^{41}/K^{40}$  ratios are possible if the fraction of material which was irradiated was different in the two cases. The isotopic composition of potassium was measured by mass spectrometry for nine stone meteorites, silicates from the Vaca Muerta mesosiderite and the Weekeroo Station iron meteorite, and four terrestrial samples. Measurements on enriched standards showed that any variations greater than 1% would certainly have been detected, and variations greater than  $\frac{1}{2}\%$  would probably have been detected with replicate analyses. Within these limits, no variations in the  $K^{40}$  abundance between the terrestrial and meteoritic samples could be found which could be ascribed to particle irradiation in the early history of the solar system.

Buseck, P.R., 1966, Rutile in meteorites: *Transactions of the American Geophysical Union*, V. 47, No. 3, p. 481.

Although it is not widely recognized as a meteoritic phase, rutile is a reasonably widespread but minor mineral in meteorites. Optical studies indicate that rutile occurs in L group chondrites, H group chondrites, mesosiderites, and octahedrites. In most cases the rutile is associated with ilmenite or chromite; only in Bondoc and Allegan does it occur as individual grains free of these minerals. It probably has several corresponding origins: by exsolution where it occurs with chromite, by reduction where with ilmenite, and by primary crystallization as a minor accessory mineral where it occurs with neither. Free energy calculations for the ilmenite reaction, assuming ideality, indicate upper limits for the oxygen fugacities of  $10^{-14.6}$  atm at  $800^{\circ}$  and  $1100^{\circ}\text{C}$ , respectively; these values need apply to only very small areas within the meteorites because



there is surely insufficient rutile and ilmenite to have suffered the entire meteorite. (Abstract of a paper presented at the September 1966 meeting of the American Geophysical Union).

Buseck, P.R., and Keil, K., 1964, Meteoritic rutile: *American Mineralogist*, V. 51, p. 1506-1515.

Rutile has not been widely recognized as a meteoritic constituent. Recent microscopic and electron microprobe studies show, however, that  $\text{TiO}_2$  is a reasonably widespread phase, albeit in minor amounts. X-ray diffraction studies confirm the  $\text{TiO}_2$  to be rutile. It was observed in the following meteorites--Allegan, Bondoc, Estherville, Farmington, and Vaca Muerta. The rutile is associated primarily with ilmenite and chromite, in some cases as exsolution lamellae.

Buseck, P.R., Mason, B., and Wiik, H.B., 1966, The Farmington meteorite: *Mineralogy and chemistry: Geochimica et Cosmochimica Acta*, V. 30, p. 1-8.

The Farmington hypersthene chondrite is a dense, black meteorite that has been shocked and partly brecciated. It contains olivine (23% Fa), hypersthene (21% Fs), plagioclase ( $\text{An}_{50}$ ), kamacite, taenite, troilite, chromite, ilmenite and possibly clinohypersthene or pigeonite, merrillite and/or apatite and a titanium dioxide mineral.

Some kamacite grains, sheathed by troilite, have globular shapes suggesting that they may have been molten. As temperatures decreased sulfur was introduced and reacted with the metal to form the troilite rims. Following this the meteorite was shocked, producing the black "breccia fragment" as well as the metal veins in the fragment.

The electron microprobe analyzer indicates the metal throughout the meteorite is compositionally inhomogeneous, raising the possibility that it may not be indigenous. A chemical analysis, indicating that Farmington belongs to the L-group of chondrites, shows the following results: Fe 64.0, Ni 1.06, Co 0.09, FeS 4.79,  $\text{SiO}_2$  40.79,  $\text{TiO}_2$  0.17,  $\text{Al}_2\text{O}_3$  1.75, FeO 15.15, MnO 0.28, MgO 21.84, CaO 1.92,  $\text{Na}_2\text{O}$  0.96,  $\text{K}_2\text{O}$  0.13,  $\text{P}_2\text{O}_5$  0.30,  $\text{H}_2\text{O} +$  0.09,  $\text{H}_2\text{O} -$  0.00,  $\text{Cr}_2\text{O}_3$  0.55; total 99.27.

Butler, C.P., 1966, Temperatures of meteoroids in space: *Meteoritics*, V. 3, p. 59-70.

On the basis of reported optical measurements of iron and stony meteorites, upper and lower limits for solar absorptance and hemispherical emittance of the surfaces of meteoroids have been established. Temperatures of three classes of meteoroids, none larger than approximately 10 meters in radius, have been calculated for various orbits and a/e ratios. These classes are light chondrites, dark chondrites and the irons. Temperatures for a meteoroid in a Mercury orbit range from 100°C for a light chondrite to 400°C for an iron.

Cameron, A.G.W., 1966, The accumulation of chondritic material: *Earth and Planetary Science Letters*, V. 1, No. 3, p. 93-96.

Whipple's suggestion that chondrules are melted in lightning flashes is examined in the context of models of the primordial solar nebula previously proposed by the writer. It is shown that solid bodies in the chondrule size range can be melted, but much larger bodies cannot be melted and much smaller bodies will be vaporized. Accumulation mechanisms involving electrostatic acceleration and gas motions are discussed.

Carter, N.L., and Kennedy, G.C., 1966, Origin of diamonds in the Canyon Diablo and Novo Urei meteorites--a reply: *Journal of Geophysical Research*, V. 71, p. 663.

In a reply to the paper of Heymann et al. (1966) and the critique of Anders and Lipschutz, Carter and Kennedy maintain that there are good reasons to believe that the meteoritic diamonds formed by normal static processes, rather than by shock.

In a following reply to the reply of Carter and Kennedy, Anders and Lipschutz debate the issues.

Caplecha, Z., 1965, Investigation of the composition and physical conditions of movement of meteor bodies using analysis of meteor spectrums: *Akademiia Nauk SSSR Meteoritika*, No. 26, p. 66-68.

Both the chemical composition and physical conditions of excitation of the spectral lines can be determined from the spectrums of meteors in flight, using the method of growth curves described earlier by the author. (From *Geophysical Abstracts*, No. 237).

Chessin, H., Hallgren, D.S., and Hemenway, C.L., 1966, Absence of crystal structure in interplanetary dust: *The Astronomical Journal*, V. 71, p. 380.

Previously particles collected by the Venus Flytrap experiment were studied by electron diffraction techniques. Of the 254 particles examined, only two particles exhibited diffraction patterns. However, patterns could be obtained if the particles were heated.

In the present work hard x-rays were employed to obtain x-ray scattering diagrams using standard precession and oscillation techniques.

The cosmic dust particles, which we have examined by x-ray techniques, were collected during meteor shower activity by a balloon-top collection system described previously (Coon, Dugan, Hallgren, and Hemenway, *Astron. J.* 70, 671, 1965). The particles, all irregular in shape, ranged in size from 20-130  $\mu$ . Only one of the 14 particles studied thus far has shown a detectable diffraction pattern, although 24-h exposures were made. Thus far it has been impossible to identify this pattern.

Four cosmic dust particles were observed by low-angle x-ray scattering techniques. No inhomogeneities in electron or mass densities were found. The techniques employed should reveal regularity greater than 10  $\text{\AA}$ .

Thus, it appears that cosmic dust particles are amorphous. At present it is not known if their lack of crystal structure is the result of the method of formation of these particles or the result of cosmic ray proton bombardment in space. In any case, our surprisingly large particles have not been annealed by heating during entry into the earth's atmosphere. The theory describing their entry may require further consideration (Whipple, F.L., *Proc. Nat'l. Acad. Sci.* 36, 687, 1950). (Abstract of a paper presented at the March 1966 meeting of the American Astronomical Society).

Cobb, J.C., 1966, Iron meteorites with low cosmic ray exposure ages: *Science*, V. 151, p. 1524.

It is suggested that perhaps 20 percent of the iron meteorites have exposure times shorter by one or two orders of magnitude than the average.

Colombo, G., Lautman, D.A., and Shapiro, I.I., 1966, The earth's dust belt: fact or fiction? 2. Gravitational focusing and Jacobi capture: *Journal of Geophysical Research*, V. 71, p. 5705-5717.

The effectiveness of the gravitational attraction of the earth in increasing the near-earth dust concentration over its interplanetary value is reassessed in this paper. This increase is a maximum for particles entering the earth's sphere of influence with a speed of about 0.1 km/sec. The corresponding near-earth enhancement is of the order of  $10^2$  and reaches this maximum at an altitude of about 0.5 earth radii. However, for a realistic distribution of dust-particle speeds at the boundary of the earth's sphere of influence, the enhancement is negligible. In addition to considering purely gravitational focusing, the restricted three-body problem, including sunlight pressure has been analyzed. The results indicate that the Jacobi capture of dust particles into temporary geocentric orbits is so rare that its effect on the near-earth dust concentration may be neglected.

Colombo, G., Shapiro, I.I., and Lautman, D.A., 1966, The earth's dust belt: fact or fiction? 3. Lunar ejecta: *Journal of Geophysical Research*, V. 71, p. 5719-5731.

The orbits of small dust particles ejected from the lunar surface during meteorite-moon collisions have been studied. Only a small percentage enter into geocentric orbits; of these, almost none remains in such an orbit for more than one year. Using an upper-bound estimate on the amount of dust that the moon might supply to cislunar space, it is concluded that lunar ejecta do not cause an appreciable enhancement of the near-earth dust concentration.

Crozier, W.D., 1966, Nine years of continuous collection of black, magnetic spherules from the atmosphere: *Journal of Geophysical Research*, V. 71, p. 603-611.

Data on the deposition of black, magnetic spherules from the atmosphere, at two stations in central New Mexico, have accumulated for the 9-year period 1956-1964. These spherules, which appear to be similar to those recovered from various sedimentary rocks and to those recovered from ice in Antarctica and Greenland and from Paleozoic salts, are believed to be of extraterrestrial origin. The 9-year average of the annual rate of mass accretion to the earth, for spherules in the diameter range of 5 to  $60\mu$ , was approximately  $1.04 \times 10^{11}$  grams. The size distributions show fluctuations but, in general, are similar to those previously reported. The rate of deposition decreased from 1956 to 1962, and high peaks occasionally occurred. Interesting seasonal and biennial patterns appear in the rate of deposition, and there seems to be a degree of correlation between the spherule rates and radar meteor rates, the spherule rates leading the radar rates by about 6 weeks. In 1963, high rates of spherule deposition coincided with unusually high radar meteor rates.

Derbeneva, A.D., 1966, The luminous efficiency of meteors: *Soviet Astronomy - A.J.*, V. 10, No. 2, p. 355-356.

The luminous efficiency of a meteor is derived from collisional cross sections. Numerical estimates are obtained for the luminous efficiency, using experimental values for excitation cross sections, and gas-kinetic and theoretical momentum-transfer cross sections, and gas-kinetic and theoretical momentum-transfer cross sections for collision of Ca and Na atoms with N molecules. The estimates are compared with values derived from meteor observations.

Dews, J.R., 1966, The isotopic composition of lithium in chondrules: *Journal of Geophysical Research*, V. 71, p. 4011-4020.

Trace quantities of Li in chondrules from the Bruderheim and Bjurböle meteorites were isolated by chemical procedures that yielded more than 90% of the Li in the sample. The isotopic composition of Li in two samples of Bruderheim chondrules and one sample of Bjurböle chondrules was measured on a 9-inch-radius-of-curvature, single-focusing mass spectrometer. The problem of mass fractionation which occurs

during the mass analysis was solved by an integration procedure. The isotopic composition of Li from two samples of "whole-rock" Bruderheim and one sample of the granite G-1 was also measured for comparison. The  $Li^7/Li^6$  ratios for the chondrules, whole-rock Bruderheim, and G-1 were found to be identical within 3.3% (at the 95% confidence level). We are unable to confirm a previous report of a 15% excess of  $Li^6$  in the Bruderheim meteorite.

Dews, J.R., and Newbury, R.S., 1966, The isotopic composition of silver in the Canyon Diablo meteorite: *Journal of Geophysical Research*, V. 71, p. 3069-3081.

Trace quantities of silver in the iron meteorite Canyon Diablo were isolated by chemical procedures with an average yield of 80%. The isotopic composition of 5 samples of silver from the meteorite was measured on a 12-inch radius of curvature, double-focusing, fast-sweep mass spectrometer. The isotopic composition of 18 samples of terrestrial silver was measured for comparison. The meteoritic and terrestrial ratios of  $Ag^{107}/Ag^{109}$  were found to be identical to within 1%. The silver content of Canyon Diablo is 58 parts per billion from isotopic dilution analyses of aliquots of the meteorite samples. Blanks were less than 10% of the sample size in our analyses. We are thus unable to confirm a previous report of a 4% excess of  $Ag^{107}$  for Canyon Diablo.

Dietz, R.S., 1966, Striated surfaces on meteorites: shock fractures, not slickensides: *Meteoritics*, V. 3, p. 31-33.

Veined and brecciated chondrites commonly display striated fractures which have been interpreted as slickensides (fault dislocations). Observations on several such fractures in various collections suggest they are not true slickensides but, instead, are probably shock features related to shatter coning.

Divari, N.B., 1966, Charged dust particles in interplanetary space: *Soviet Astronomy - A.J.*, V. 10, No. 1, p. 151-155.

Implications of the assumption that the dust particles in interplanetary space bear an electric charge are discussed. Several effects observed in the zodiacal light, the Gegenschein, the twilight glow, and noctilucent clouds can then be explained naturally. The earth and moon may have dust tails. Submicron particles are captured by the geomagnetic field, forming the most stable component of the earth's dust cloud. Interplanetary space may be replenished by submicron dust blown from near the moon by the solar wind.

Dodd, R.T., Jr., Van Schmus, W.R., and Marvin, U.B., 1966, Significance of iron-rich silicates in the Mezo-Madaras chondrite: *American Mineralogist*, V. 51, p. 1177-1191.

Several chondrules in the Mezo-Madaras chondrite contain the disequilibrium mineral assemblage: ferrous olivine--magnesian pyroxene--merrihueite (approximately  $(K \geq Na)_2 (Fe \geq Mg)_2 Si_{12}O_{30}$ ) + metallic nickel-iron. The ferrous silicates in this assemblage were probably formed by introduction of FeO into an earlier igneous assemblage which consisted of enstatite or clinoenstatite, a magnesian analogue of merrihueite, and silica. Textural and chemical evidence indicate that this alteration of the chondrules took place before they were incorporated in the chondrite.

Duke, M.B., 1966, The Shergotty meteorite: magmatic and shock metamorphic features: *Transactions of the American Geophysical Union*, V. 47, No. 3, p. 481-482.

Petrographic features of the Shergotty, India, meteorite indicate that it formed as part of a diabasic intrusion and was later subjected to strong shock while at low temperature. The Shergotty meteorite resembles terrestrial basalts or

diabases more closely than any other meteorite. It is compositionally distinct from typical basaltic meteorites in its more sodic feldspar ( $Ab_{80}$  instead of  $Ab_{10}$ ), higher proportion of augite to pigeonite (about 1:1 instead of 1:4), primary magnetite instead of metallic iron, and the presence of whitlockite (calcium phosphate). Free silica and minor iron sulfide are present. Brown interstitial material is amorphous or gives cristobalite X-ray patterns. These transformations, which are best interpreted as being due to shock metamorphism, are superimposed on the magmatic features. A series of time-temperature curves for individual maskelynite grains allows limits to be placed on the thermal history of the meteorite following maskelynite formation. The data indicate that the meteorite was essentially below  $450^{\circ}\text{C}$  immediately after maskelynite was formed. (Abstract of a paper presented at the September 1966 meeting of the American Geophysical Union).

D'yakonova, M.I., 1964, Chemical composition of seven stony meteorites of the collection of the Committee on Meteorites of the Academy of Sciences of the USSR: *Akademiya Nauk SSSR Meteoritika*, No. 25, p. 129-133.

Results of chemical analysis of the Kainsaz, Kul'p, Manych, Sungach, Khmelevka, and Chuvashskiy Kissy chondrites and Novyye Urey ureilite are tabulated. Each meteorite is discussed briefly. (From *Geophysical Abstracts*, No. 217).

Eberhardt, P., and Geiss, J., 1966, On the mass spectrum of fission xenon in the Pasamonte meteorite: *Earth and Planetary Science Letters*, V. 1, No. 3, p. 99-101.

The xenon abundances determined by Rowe and Bogard in Pasamonte II are corrected for trapped as well as for spallation xenon, and the following mass spectrum for the fission component is obtained:  $^{131}\text{Xe} = 33.5 \pm 3$ ;  $^{132}\text{Xe} = 95 \pm 9$ ;  $^{134}\text{Xe} = 91 \pm 2.5$ ;  $^{136}\text{Xe} = 100$ . The correction for spallation xenon increases the  $^{132}\text{Xe}$  yield considerably. The Pasamonte II fission spectrum differs from the spontaneous  $^{235}\text{U}$  and thermal neutron  $^{235}\text{U}$  fission spectrum, indicating that long-lived transuranic elements have contributed to the fission xenon.

Eberhardt, P., Geiss, J., and Grögler, N., 1966, Distribution of rare gases in the pyroxene and feldspar of the Khor Temiki meteorite: *Earth and Planetary Science Letters*, V. 1, p. 7-12.

From the matrix of the Khor Temiki aubrite three grain size fractions ( $2.9\mu$ ,  $6.2\mu$ ,  $11.1\mu$ ) highly enriched in feldspar and three corresponding pyroxene grain size fractions were prepared. The concentrations and isotopic compositions of He, Ne and Ar were measured in these six fractions. Diffusion loss of radiogenic, spallation and trapped rare gases in the feldspar is evident. The pyroxene shows no diffusion loss of spallation produced isotopes, even in micron sized grains. In the feldspar  $^{39}\text{Ar}_{\text{spall}}$  is not lost; up to 50% of the  $^{21}\text{Ne}_{\text{spall}}$  may have been lost; and virtually no  $^{20}\text{Ne}_{\text{spall}}$  is retained.  $^{40}\text{Ar}$  is partially lost in the finest ( $2.9\mu$ ) feldspar fraction. The trapped gases in the pyroxene show again a strong anti-correlation with the grain size. The feldspar contains less than 10% as much trapped  $^4\text{He}$  as the corresponding pyroxene, approximately 30% trapped  $^{20}\text{Ne}$  and between 60 to 80% trapped  $^{39}\text{Ar}$ .

Enmann, W.D., and Tanner, J.T., 1966, The abundance of antimony in meteorites: *Earth and Planetary Science Letters*, V. 1, No. 5, p. 276-279.

The abundance of antimony in various classes of meteorites has been determined by neutron activation analysis. A specific radiochemical separation procedure was used to obtain antimony samples of high radiochemical purity. Experimental cosmic abundances of antimony based on several different models have been calculated.

- El Goresy, A., 1966, Electron microprobe analysis of some rare minerals from Odessa and Toluca iron meteorites: Transactions of the American Geophysical Union, V. 47, No. 2, p. 425-426.

Quantitative microprobe analyses have been carried out on several rare mineral phases from Odessa and Toluca meteorites. Before analysis, meteoritic polished sections were studied in detail in reflected light. Microprobe analysis of many grains from several nodules indicated a constant Fe content between 3.1% and 4.9%. In Odessa a new Cu, Fe, Cr sulfide was discovered. Microprobe analysis indicated 28.3% Cu, 9.1% Fe, 31.4% Cr, and 32.6% S. Several sphalerite grains were discovered as inclusions in kamacite of Toluca and Canyon Diablo meteorites. Quantitative microprobe analysis indicated a maximum Fe content of 17%. Nodules in the neighborhood of these grains were found to be barren of sphalerite. (Abstract of a paper presented at the April 1966 meeting of the American Geophysical Union).

- Evans, J.V., 1966, Radar observations of meteor deceleration: Journal of Geophysical Research, V. 71, p. 171.

By using a narrow-beam high-power radar operating at 68 cm it has been possible to detect meteors traveling radially toward the radar. In these observations the antenna is directed at the radiant point of an intense meteor shower, and the receiver is tuned to the expected Doppler-shifted signal. Because the actual Doppler shift can be measured with precision, both the velocity and the deceleration of the approaching meteor can be determined. The behavior of the velocity is compared with the theory for a solid particle entering the earth's atmosphere at heights where no air cap is formed. Anomalous behavior was occasionally observed, but the height at which it appears to begin is too great to be accounted for by cap formation. We conclude that errors in the computed height of the meteor may be responsible for the anomalies. A mean value for the effective ablation energy of  $15.4 \text{ km}^2/\text{sec}^2$  was obtained, but individual meteors showed wide departures from this value. The mean mass of the meteors is estimated to be in the range  $10^{-2}$ - $10^{-3}$  gram, corresponding to a visual magnitude of +5.

- Farlow, N.H., and Blanchard, M.B., 1966, Examination of extraterrestrial particles collected by the Luster sounding rocket experiment: Transactions of the American Geophysical Union, V. 47, No. 1, p. 143-144.

The Luster micrometeoroid sampling instrument was carried by an Aerobee 150 sounding rocket to an altitude of 144 km during the November 1965 Leonids meteor shower. Pre-evacuated sealed modules on the instrument carried sampling surfaces provided by eight U.S. and five European experimenters. The instrument opened and exposed 1 square meter of sampling surface vertically and another square meter horizontally, for 206 seconds, above an altitude of 63 km. After reclosing, the instrument was parachuted to earth. Vacuum sealed modules containing the samples were removed to the laboratory for analysis. An extensive contamination control program was utilized to exclude terrestrial material from the flight instrument and samples. Microscopic examinations were made of the sampling surfaces using optical and electron microscopes. (Abstract of a paper presented at the April 1966 meeting of the American Geophysical Union).

- Farlow, N.H., Blanchard, M.B., and Ferry, G.V., 1966, Sampling with a Luster sounding rocket during a Leonid meteor shower: Journal of Geophysical Research, V. 71, p. 5689-5693.

A Luster micrometeoroid sampling payload was successfully launched and recovered during the Leonid meteor shower November 16, 1965, at White Sands Missile Range, New Mexico. The instrument opened at an altitude of 63 km and exposed  $2 \text{ m}^2$  of sampling surface area. The rocket carried the exposed sampling surfaces to a

height of 145 km. The instrument reclosed at 116 km after 206 sec of sampling time and was parachuted to earth after severance from the rocket. An extensive contamination control program using laminar flow clean rooms was applied to all phases of the experiment in an attempt to exclude contaminating particles larger than  $0.5 \mu$ . About 3% (264  $\text{cm}^2$ ) of the sampling area has been surveyed with the optical microscope. Every particle larger than  $4 \mu$ , which could not be recognized as a known contaminant, has been removed and examined with an electron microprobe X-ray analyzer. On the basis of morphology and chemical composition, each particle has been categorized as to possible origin. Results to date indicate that the number of particles found on this area, which may have an extraterrestrial origin, is much smaller than predictions based on measurements from artificial earth satellites and other sounding rocket collections.

Fechtig, H., Gerloff, U., and Weihrauch, J.H., 1966, Electron microscope and microprobe measurements on Luster-flight samples: Transactions of the American Geophysical Union, V. 47, No. 2, p. 426.

The National Aeronautics and Space Administration (NASA) has given permission to expose several types of micrometeorite detectors on the Luster-flight of November 16, 1965, at White Sands Missile Range, New Mexico. Three  $\text{cm}^2$  open area of nitrocellulose films were evaluated with electron microscope and microprobe methods. Pictures were taken of all particles larger than  $0.2 \mu$  diameter and of several holes probably produced by particle impacts. The size distribution of the different types of the particles was determined. Particles larger than  $0.5 \mu$  were submitted to chemical analyses, using both non-dispersive and dispersive methods for elements heavier than magnesium. (Abstract of a paper presented at the April 1966 meeting of the American Geophysical Union).

Fesenkov, V.G., 1964, On the orbit of the Tunguska meteorite: Akademiia Nauk SSSR Meteoritika, No. 25, p. 163-167.

Possible orbits of the Tunguska meteorite of 1908 are worked out from the conflicting reports of the event. The elements of circular and parabolic orbits (inclination to plane of ecliptic, perihelion distance, eccentricity, major semi-axis, and relative impact velocity) are tabulated for three azimuths ( $0^\circ$ ,  $20^\circ$ ,  $40^\circ$ ) of visible radiant. For all these variants, one of which should be the true orbit, the motion is not characteristic of ordinary meteorites representing the product of breakup of asteroids, but is normal for the case of a comet. (From Geophysical Abstracts, No. 217).

Fesenkov, V.G., 1965, Advances in meteoritics: Akademiia Nauk SSSR Meteoritika, No. 26, p. 3-16.

It is shown how in recent years the study of meteorite composition and circumstances of their fall to earth have become of interest in connection with important problems of geochemistry, astronomy, physics, and even biology. (From Geophysical Abstracts, No. 237).

Fesenkov, V.G., 1965, The role of meteorites in solving the problem of the origin of the solar system: Akademiia Nauk SSSR Meteoritika, No. 26, p. 69-76.

It is shown that the constitution of meteorites indicates that the solar system formed as a result of nucleogenesis (explosion of a supernova star) that took place about 5 b.y. ago. Any reasonable theory concerning the origin of the solar system should be based on this important conclusion.

Fesenkov, V.G., 1966, Interplanetary dust matter and methods for its investigation: Soviet Astronomy - A.J., V. 10, No. 3, p. 474-478.

This paper discusses the photometric method of investigating the interplanetary dust matter which manifests itself as the zodiacal cloud. The zodiacal isophotes have been obtained with atmospheric scattering taken into account and checked by means of the brightness and degree of polarization at the ecliptic pole. These isophotes lead us to the conclusion that the main source of replenishment of interplanetary matter is the disintegration of comets and not the fragmentation of asteroids. The "twilight method" is useful for the detection of the circum-terrestrial dust cloud, at least in its inner parts. Two methods for taking into account the tropospheric component, so that the primary twilight can be estimated from the observations, are given. It is shown that when the angular distance of the sun below the horizon is greater than  $10^\circ$ , the observed twilight segment is completely determined by the cosmic dust cloud.

Fialko, E.I., 1966, Determination of the absolute magnitude of a meteor from the duration of unstable trail echoes: *Soviet Astronomy - A.J.*, V. 10, No. 1, p. 161-164.

A method is developed for determining the absolute magnitude of a meteor from the duration of the radar echoes received from an unstable meteor trail. An example illustrates the method.

Fisher, D.E., 1966, The origin of meteorites: space erosion and cosmic radiation ages: *Journal of Geophysical Research*, V. 71, p. 3251-3259.

It is suggested that the erosion of chondritic meteorites by interplanetary dust is a mechanism that can account satisfactorily for the cutoff in radiation ages at  $55 \times 10^6$  years, if the meteorites have an asteroidal origin. Spectra of chondritic radiation ages are calculated, based on a model involving continuous meteorite creation in the asteroidal belt and coupled with several erosion rates, and are compared to experimental results. The calculated and experimental spectra are in good agreement.

Florovskaya, V.N., Vdovkin, G.P., Teplitskaya, T.A., and Zezin, R.B., 1965, Comparative features of polycyclic aromatic hydrocarbons in carbonaceous chondrites and rocks and minerals of endogene origin: *Akademiia Nauk SSSR Meteoritika*, No. 26, p. 169-176.

Aromatic hydrocarbons in carbonaceous chondrites and in rocks and minerals of endogene origin are compared. In very high temperature formations (rocks and minerals of the Ilmen alkaline massif and meteorites), the predominant components are anthracene and 3,4-benzpyrene, whereas in lower temperature hydrothermal formations (pegmatites of the Khibin massif and deposits of the Armenian S.S.R.), 1,12-benzpyrene predominates and coronene appears. (From *Geophysical Abstracts*, No. 236).

French, B.M., 1966, Some geological implications of equilibrium between graphite and a C-H-O gas phase at high temperatures and pressures: *Reviews of Geophysics*, V. 4, No. 2, p. 223-253.

The occurrence of graphite as a common accessory mineral in meteorites and in terrestrial metamorphic and igneous rocks gives particular importance to the study of equilibrium between graphite and a co-existing gas phase. By using a simplified model in which  $T$ ,  $P_{\text{gas}}$ , and  $F_{\text{O}_2}$  are independently specified for the system C-H-O, values of  $P_{\text{CO}}$ ,  $P_{\text{CO}_2}$ ,  $P_{\text{H}_2\text{O}}$ ,  $P_{\text{H}_2}$ , and  $P_{\text{CH}_4}$  in a gas phase in equilibrium with graphite have been calculated for a wide range of geologically possible conditions by means of a high-speed computer. The numerical results support several general conclusions, including: (1) The assumption that  $P_{\text{gas}} = P_{\text{H}_2\text{O}} + P_{\text{CO}_2}$  is significantly in error for many graphite bearing mineral



assemblages. (2) It is possible that the terrestrial atmosphere could have evolved by conversion of original methane to water and  $\text{CO}_2$  by reaction with graphite and other accessory minerals within the primordial earth at temperatures of  $600^\circ$  to  $1000^\circ\text{C}$ . Material requirements for such a conversion are not unreasonable, and the process itself is consistent with many proposed models for the origin of the earth.

Fuchs, L.H., 1966, Djerfisherite alkali copper-iron sulfide: A new mineral from enstatite chondrites: *Science*, V. 153, p. 166-167.

The new mineral was discovered in the following chondrites: Kota Kota, St. Marks, and Pena Blanca.

Fuchs, L.H., Frondel, C., and Klein, C., Jr., 1966, Roedderite, a new mineral from the Indarch meteorite: *American Mineralogist*, V. 51, p. 949-955.

The new mineral roedderite,  $(\text{Na}_{1.30}\text{K}_{0.69})_{1.99}(\text{Mg}_{4.98}\text{Fe}_{0.02})_{5.00}(\text{Si}_{11.00}\text{Al}_{0.07})_{11.07}\text{O}_{30}$  has been found as an accessory in the enstatite chondrite, Indarch. The assemblage in which it occurs consists of enstatite, clinoenstatite, troilite, nickel-iron and small amounts of schreibersite, plagioclase ( $\text{Ab}_{90}\text{An}_{10}$ ), tridymite, oldhamite, glass, and carbon. X-ray studies of the roedderite established it to be isostructural with osumilite and merrihueite as well as synthetic  $\text{K}_2\text{O} \cdot 5\text{MgO} \cdot 12\text{SiO}_2$  and  $\text{Na}_2\text{O} \cdot 5\text{MgO} \cdot 12\text{SiO}_2$ . Electron probe analyses, an indexed x-ray diffraction pattern, unit cell dimensions ( $a=10.139 \pm 0.01$ ;  $c=14.275 \pm 0.01$  Å) and optical data ( $n=1.537$ ;  $e=1.542$ ) for roedderite are presented.

Gale, N.H., 1966, A potassium-argon age for the Barwell meteorite: *Nature*, V. 210, p. 620.

Neutron activation analysis as well as flame photometry were used to determine the potassium content of the olivine-hyperthene chondrite which fell at Barwell in 1965, and the argon content was determined by mass spectrometry. The Meteorite Age was determined to be  $3.49$  to  $3.50 \times 10^9$  years, which is appreciably shorter than the usual range of from  $3.5$  to  $4.5 \times 10^9$  years.

Geake, J.E., and Walker, G., 1966, The luminescence spectra of meteorites: *Geochimica et Cosmochimica Acta*, V. 30, p. 929-937.

The luminescence spectra of 20 stony meteorites of several different classes are given. Proton excitation was used, as UV radiation was found to be ineffective. Estimates of radiation conversion efficiency are given, and found to fall into three groups. Changes in the luminescence spectra after proton damage are shown; the spectra and the changes are both shown to be characteristic of the class of meteorite.

Gentry, R.V., 1966, Additional evidence of extinct radioactivity from pleochroic halos and the formation of the lunar crust: *Transactions of the American Geophysical Union*, V. 47, No. 3, p. 487.

Dwarf radioactive halos similar to the small bleached halos reported by Joly have been found in the Ytterby mica. The  $5.2\text{-}\mu$  radius halo was heretofore attributed to  $\text{Sm}^{147}$ , but energy considerations do not exclude the presently extinct isotope  $\text{Sm}^{148}$  as a parent nuclide of this halo. The  $8.6\text{-}\mu$  radius halo is attributed to the  $3.18\text{-Mev}$  alpha from  $\text{Gd}^{148}$ , and a bleached ring halo of about  $20\text{-}\mu$  radius corresponds to an alpha emitter of about  $5.5\text{ Mev}$ . This bleached ring has also been observed in certain polonium halos. Electron microprobe analysis of the central inclusions of some of these halos together with autoradiographic and fission track studies provide substantial evidence for naturally occurring extinct radioactivity. If similar radioactive halos

are found in lunar crustal material, there will be a method for determining the maximum time period between nucleosynthesis and formation of the lunar crust. (Abstract of a paper presented at the September 1966 meeting of the American Geophysical Union).

Gentry, R.V., 1966, Anti-matter content of the Tunguska matter: *Nature*, V. 211, p. 1071-1072.

The mechanisms which initiate thermonuclear and anti-matter explosions are discussed and calculations are performed which permit a comparison to be made of the energy distribution between an ordinary nuclear explosion and an anti-matter explosion. In an air burst of a fission-fusion device roughly 50 per cent of the energy is dissipated in blast and shock effects, 35 per cent of the total yield appears as thermal radiation, 5 per cent as initial nuclear radiation, and 10 per cent as residual radioactivity. These percentages are of course dependent on altitude. The significant point for this type of explosion is that a major proportion of the particles emitted in the fission-fusion reactions dissipate their energy within a short distance, thus producing conditions favourable for the formation of a fireball.

It appears that the relatively short duration fireball is reasonable evidence against the Tunguska explosion being thermonuclear in nature, and it seems possible that it was due to an anti-matter explosion.

Goldstein, J.I., 1966, Butler, Missouri: An unusual iron meteorite: *Science*, V. 153, p. 975-976.

This meteorite has been found to contain an unusual high content of cobalt (1.4 percent) and of germanium in the kamacite and taenite phases. Also the cooling rate was unusually low ( $0.5^{\circ}\text{C} \times 10^{-6}$  years).

Goldstein, J.I., 1966, The distribution of germanium in the metallic phases of some meteorites: *Transactions of the American Geophysical Union*, V. 47, No. 1, p. 134.

Measurements of the Ge distribution in a number of meteorites were made by means of an electron probe microanalyzer. Meteorites classified by Lovering into Ge groups I, II, and III were measured, the detectability limit being 10 ppm. Most of the Ge is located in the taenite phase. Within this phase the Ge follows the Ni content. The maximum Ge content is 500 ppm, at the kamacite/taenite interface. The Ge content in kamacite varies directly with the width of the phase, as does the average Ni content. The variations of Ge concentrations in the metal phases are explained (1) by the decreasing solubilities of Ge in the kamacite phase and a solubility of greater than 500 ppm in the taenite phase as cooling proceeds, and (2) by the decreasing diffusion rates of Ge in the metal phases as cooling proceeds. At low temperatures ( $<500^{\circ}\text{C}$ ) the Ge will not be able to diffuse out of the kamacite phase into the taenite phase in order to satisfy the solubility requirements in kamacite within the available cooling times. (Abstract of a paper presented at the April 1966 meeting of the American Geophysical Union).

Goles, G.G., and Greenland, L.P., 1966, Estimates of primordial halogen abundance ratios from studies of chondritic meteorites: *The Astronomical Journal*, V. 71, p. 162.

Neutron activation analyses of Cl, Br, and I in meteorites indicate that these halogens are geochemically coherent in most carbonaceous and enstatite chondrites. There is some evidence that whatever fractionation process has operated on the parent materials of these meteorites, has left halogen abundance ratios unchanged. Thus, the present mean abundance ratios ( $\text{Cl}/\text{Br}=4.10$ ,  $\text{Cl}/\text{I}=4.500$ ,  $\text{Br}/\text{I}=1.1$ , all in atoms per atom) are probably good approximations to the abundance ratios in the primordial solar nebula. These ratios may be used as additional boundary condi-

tions on nucleosynthetic models. (Abstract of a paper presented at the December 1965 meeting of the American Astronomical Society).

Gorbunova, T.M., 1964, Preparation of polished slices of large area from iron meteorites: *Akademiia Nauk SSSR Meteoritika*, No. 25, p. 188-191.

The preparation of polished slices of iron meteorites 10 x 15 cm or more in size, suitable for macroscopic examination and etching, is described. These slices do not require as careful polishing as specimens to be studied under the microscope. Two examples are cited to show the time required for preparation. (From *Geophysical Abstracts*, No. 217).

Greenman, N.N., and Gilpin, C.B., 1966, Micrometeorite collectors for high-altitude rockets: *Transactions of the American Geophysical Union*, V. 47, No. 3, p. 480-481.

If solar and galactic cosmic rays are effective in producing radiation damage in micrometeorites, the detection of such damage offers a promising means for distinguishing micrometeorites from contaminants in rocks and other particle collections. In earlier studies, the failure of Venus Flytrap particles to yield electron diffraction patterns suggested the possible existence of radiation damage. A heat-resistant collector was designed and tested for use on future collection flights. This assembly proved to have adequate collection efficiency and was able to withstand heating to 950°C without damage or distortion. Collectors of this type were flown on a series of high-altitude rocket collection flights in 1965 (Venus Flytrap and Lusier). Studies of the collections are now in progress. (Abstract of a paper presented at the September 1966 meeting of the American Geophysical Union).

Gus'kova, Ye.G., 1965, The nature of the natural remanent magnetization of meteorites: *Akademiia Nauk SSSR Meteoritika*, No. 26, p. 60-65.

Investigations of the remanent magnetization of several stone and iron meteorites show that between the time of their formation and their fall on earth, the meteorites did not encounter ambient magnetic fields of more than a few oersteds, or temperatures high enough to affect their magnetization. These data should be taken into account in constructing any scheme of the origin of meteorites of different types. (From *Geophysical Abstracts*, No. 236).

Hamilton, W.L., and Bull, C., 1966, A comparison of the dust flux in the upper atmosphere and on the polar ice sheets: *Journal of Geophysical Research*, V. 71, p. 2679-2683.

The number of particles in specified volumes of meltwater are counted in eight size intervals between 0.72 and 3.57  $\mu$  diameter. For two consecutive annual layers of Greenland ice deposited about 1740 A.D. and for the South Pole 1958 annual layer, the number of microparticles larger than the specified diameter, falling per square meter per second, is plotted versus the diameter. The results of Soberman and Hemenway are added for comparison.

The good agreement between the upper-atmosphere dust flux and that on the ice sheets, both with respect to slopes of the distributions and magnitudes of the annual fluxes, leads the authors to conclude that, especially for diameters larger than 1.5  $\mu$ , the proportion of meteoritic material in fallout on the high polar ice sheets is large.

Hapke, B., 1966, On the composition of the lunar surface: *Transactions of the American Geophysical Union*, V. 47, No. 1, p. 149-150.

A large number of igneous rocks and meteoritic material were pulverized and irradiated by hydrogen ions to simulate the effects of meteorite and solar wind bombardment of the lunar surface. The optical properties of these materials were then studied and compared with those of the moon. Several varieties of basic rock powders duplicated lunar optical characteristics after irradiation, including certain ultrabasic rocks, basalts, and diorites. Highly acidic rocks, such as granites, syenites, and granodiorites, do not match the moon, nor do chondritic meteorites. From these observations, the following deductions can be made about the composition of the surface of the moon: (1) The lunar crust appears to be largely basic in composition. (2) The lunar surface apparently is not chondritic; hence, chondrites probably do not come from the moon, although achondrites may. The southern highland areas of the moon appear to be the unaltered remnants of the last stages of accretion, implying that at least part of the material from which the moon was accreted probably contained less Fe than chondrites, which is consistent with the density of the moon. (Abstract of a paper presented at the April 1966 meeting of the American Geophysical Union).

Harrington, J.S., 1966, Polycyclic aromatic hydrocarbons in carbonaceous meteorites: *Nature*, V. 212, p. 273-274.

The presence of hydrocarbons in several meteorites has been confirmed, but insufficient evidence is available to allow a determination as to whether they derived as contamination from the soil in which the meteorites were found or whether they were present in the chondrites before entering the terrestrial atmosphere.

Hayatsu, R., 1966, Artifacts in polarimetry and optical activity in meteorites: *Science*, v. 153, p. 859-861.

Commercial polarimeters may produce spurious optical rotation. This effect may explain the optical activity reported in the Orgueil meteorite.

Heymann, D., and Mazor, E., 1966, St. Mesmin, a gas-rich amphoteric chondrite: *Journal of Geophysical Research*, V. 71, p. 4695-4697.

Mass spectrometer analysis of the light and dark portions of the amphoteric chondrite, St. Mesmin, has shown that it is gas-rich, the primordial gases being associated with the dark portion.

Heymann, D., Lipschutz, M.E., Nielsen, B., and Anders, E., 1966, Canyon Diablo meteorite: Metallographic and mass spectrometric study of 56 fragments: *Journal of Geophysical Research*, V. 71, p. 619-641.

In an attempt to reconstruct the history of the surviving Canyon Diablo fragments, 56 specimens were studied by metallography and mass spectrometry and 5 others by metallography only. Of these, 25 came from the rim of the crater, and 36 from the plains. Fifteen contained diamonds. On the basis of metallographically observable reheating effects, the samples were classified as strongly, moderately, and lightly shocked, corresponding to shock pressures of  $\geq 750$  kb, 130-750 kb, and  $< 130$  kb. The division among these categories was as follows: Plains: 0, 14, and 86%; rim: 72, 28, and 0%; diamond-bearing: 67, 33, and 0%. This bears out earlier observations by Nininger and the authors that rim (and diamond-bearing) specimens tend to be much more strongly reheated than plains specimens. Diamond-bearing and rim specimens also come from greater mean depths: 135 and 127 cm, in contrast to the depth of the plains specimens (81 cm). The throwout pattern for shocked material seems to have been highly directional, like the lunar ray craters.

Houtermans, F.G., and Liener, A., 1966, Thermoluminescence of meteorites: *Journal of Geophysical Research*, V. 71, p. 3387-3396.

The experimental techniques used for measuring thermoluminescence are described. The glow curves of achondrites differ markedly from subclass to subclass in their artificially excited glow curves. A fair correlation exists between the radiation ages and the luminescence intensity. The olivine components of pallasites yield very low luminescence whereas the silicate components of mesosiderites (with the exception of Weatherford) exhibit distinct peaks at about 90°C. To a good approximation the luminescence intensity of the chondrites is proportional to their radiation ages. If a correction for the radiogenic part of the thermoluminescence is applied, approximate radiation ages can be estimated from thermoluminescence data.

Huss, G.I., Moore, C.B., and Busek, P.R., 1966, The Fremont Butte, Washington Co., Colorado, meteorite: *Meteoritics*, V. 3, p. 73-78.

The Fremont Butte meteorite was found near Fremont Butte, Colorado, in 1963. A single individual was found weighing 6.6 kg. It is an olivine-hypersthene or L group chondrite showing brecciation and a small number of well formed chondrules and olivine phenocrysts.

Huss, G.I., Moore, C.B., and Gruenhagen, G., 1966, The Anoka, Minnesota, iron meteorite: *Meteoritics*, V. 3, p. 83-87.

The Anoka, Minnesota, meteorite was found on the Joe Fields Farm at location co-ordinates 45° 12' N, 92° 51' W. It is a fine octahedrite distinguished by large fields of dense plate. The chemical analysis of the meteorite is 84.9 percent iron, 11.75 nickel, 0.51 cobalt.

Jaeger, R.R., and Lipschutz, M.E., 1966, X-ray diffraction study of shocked meteoritic minerals: *Transactions of the American Geophysical Union*, V. 47, No. 1, p. 134.

A number of recent metallographic studies have shown that the microstructure of meteorites is affected by shock waves. Qualitatively these changes can be used to classify iron meteorites only into lightly (<80 kb), moderately (130-750 kb), and strongly (>750 kb) shocked groups. We have discovered that such shocks also alter the crystallographic structure of a number of common meteoritic minerals. By comparison with suitable standards, these alterations can be related in a semi-quantitative fashion to the shock magnitude and can therefore serve as pressure indicators over the 0- to 1000-kb range. Thus far kamacite, schreibersite, and cohenite have been studied in some detail. For these minerals observations are consistent with the interpretation that the crystallographic alterations are progressive steps in the minerals' recrystallization. For the case of cohenite, at least no reasonable natural process other than shock can account for the effects that were observed. It is demonstrated that the recrystallization of cohenite occurred during the pressure pulse and not subsequently as a result of the high after-shock, residual temperature. (Abstract of a paper presented at the April 1966 meeting of the American Geophysical Union).

Jarosewich, E., 1966, Chemical analyses of ten stony meteorites: *Geochimica et Cosmochimica Acta*, V. 30, p. 1261-1265.

A group of stony meteorites, mainly unequilibrated chondrites has been analyzed chemically. The chemical analyses of ten meteorites (Bishunpur, Bonita Springs, Clovis I, Coolidge, Ehole, Hallingberg, Ioka, Karatu, Khohar, Semarkona) are given in this paper.

- Jobbins, E.A., Dimes, F.G., Binns, R.A., Hey, M.H., and Reed, S.J.B., 1966, The Barwell meteorite: *Mineralogical Magazine*, V. 35, p. 881-902.

Part of a meteorite was seen to fall on a road ( $52^{\circ} 33' 55''$  N.,  $1^{\circ} 20' 23''$  W) in the village of Barwell, Leicestershire, England, at about 16:20 hours G.M.T. on 24 December 1965. Fragments have been found over an area some  $3/4$  mile long by  $1/2$  mile across, and appear to have been part of a single stone, of which 44 kg. (97 lb) have been recovered. The distribution, impact effects and crustal morphology of the recovered fragments are described. Barwell is a moderately metamorphosed white olivine-hypersthene chondrite; a chemical analysis, with derived Wahl norm, and a modal analysis are given, together with optical data and electron-probe analyses of the principal constituent minerals.

- Jones, J., and Kaiser, T.R., 1966, The effects of thermal radiation, conduction and meteoroid heat capacity on meteoric ablation: *Monthly Notices of the Royal Astronomical Society*, V. 133, p. 411-420.

The classical theory of meteoric ablation is generalized to include the effects of thermal radiation, thermal conduction and heat capacity of the impinging meteoroid, which is assumed to be a solid stone particle.

In the magnitude range  $+3 < M < +10$ , which embraces the bulk of radio meteors, it is shown that thermal radiation may be neglected but that the onset of ablation is delayed due to the finite heat capacity of the meteoroids. This results in evaporation profiles significantly shorter than predicted by the classical theory. Particles of radius greater than 0.1 cm ( $M < +3$ ) develop a marked radial thermal gradient and the stresses due to this thermal shock are sufficient to cause fracture before ablation commences. The smallest fragments will be the first to ablate and the theory predicts that for fragments smaller than 0.01 cm radius, this will occur at an atmospheric density  $\rho_a = 9 \times 10^9 v^{-2}$  where  $v$  is the meteoric velocity. This is in close agreement with the experimental result of Jacchia et al. (1965) for photographic meteors observed with the Harvard Baker-Super-Schmidt cameras.

- Kaiser, T.R., Poole, L.M.G., and Webster, A.R., 1966, Radio-echo observations of the major nighttime meteor streams, I. Perseids: *Monthly Notices of the Royal Astronomical Society*, V. 132, p. 225-237.

Observations of the Perseid shower of August 1964 are presented, an attempt has been made to interpret the observed activity in terms of a radiant model comprising an intensive discrete center of activity, and a more diffuse component. The distribution in radio-magnitude in the range +8.4 to +6.8 of the shower meteors has been studied as a function of solar longitude, and significant systematic variations, especially for the discrete component are indicated.

- Kaplan, I.R., and Hulston, J.R., 1966, The isotopic abundance and content of sulfur in meteorites: *Geochimica et Cosmochimica Acta*, V. 30, p. 479-496.

Twenty meteorites were studied in the iron (hexahedrites and octahedrites) and stony (enstatite achondrite, carbonaceous, enstatite, bronzite and hypersthene chondrite) families. Troilite is the chief sulfur component of iron meteorites and the  $\delta S^{34}$  ranges from 0 to +0.6 per mil with respect to Canyon Diablo troilite. Stony meteorites contain a wide variety of sulfur compounds including water and acid soluble sulfides, elemental sulfur, water and acid soluble sulfates and unidentified components soluble only in aqua regia. The  $\delta S^{34}$  content of the isolated compounds varies from +2.5 to -5.5 per mil with respect to Canyon Diablo. The weighted average for all components of each meteorite, however, falls within  $\pm 1$  per mil of Canyon Diablo. The  $S^{33}$  distribution closely

follows  $S^{34}$ . The data strongly suggest that differentiations have occurred in a closed system, corresponding to the meteorites or their parent body, and starting from a single source of sulfur. There is no evidence for biological activity having occurred in the meteorites, either from the distribution of sulfur compounds or from the isotope abundance data.

Keay, C.S.L., Ellyett, C.D., and Brown, T.A., 1966, Absence of unusual periodicities in radar meteor rates: *Journal of Geophysical Research*, V. 71, p. 1409-1411.

A spectral analysis of extensive meteor rate data obtained at Christchurch, New Zealand, reveals no evidence of a lunar influence or of any other unusual periodicities.

Kelley, A.O., 1966, A water-impact hypothesis for the Sierra Madera structure in Texas: *Meteoritica*, V. 3, p. 79-82.

It is proposed that the Sierra Madera structure was formed by meteorite impact while the area was submerged under pre-historic seas. The water would cause modification of the shock waves resulting from the cosmic impact in order to account for the atypical structures at Sierra Madera.

Kempe, W., and Zähringer, J., 1966, K-Ar-Altersbestimmungen an Eisenmeteoriten--I Die Isotopenzusammensetzung des primären Kaliums: *Geochimica et Cosmochimica Acta*, V. 30, p. 1049-1057.

The isotopic composition of primordial potassium has been determined in inclusions of five iron meteorites and in one stone meteorite and was compared with terrestrial standards. In iron meteorites with low spallation content, the same isotopic abundance has been found for  $K^{40}$  as in terrestrial samples. In the Treysa meteorite spallation-produced  $K^{40}$  could be detected.

For the calculation of radiogenic ages of iron meteorites the same  $K^{40}$  abundance of 0.012 per cent can be used as for terrestrial material.

From the  $K^{40}$  abundance one can estimate the maximal difference in proton irradiation of some  $10^{17}$  p/cm<sup>2</sup> between terrestrial and meteoritic matter during the early history of the solar system. Iron meteorites are especially interesting, since their origin might have been different from that of terrestrial matter and even from stone meteorites. (Text in German).

Kharitonova, V.Ya., 1965, Results of chemical analysis of 10 stone meteorites from the collection of the Academy of Sciences of the U.S.S.R.: *Akademiia Nauk SSSR Meteoritika*, No. 26, p. 146-150.

Results are presented of chemical analyses of 10 meteorites from the collection of the Academy of Sciences of the U.S.S.R. Seven of these are analyzed for the first time: Berdyansk, Bolshaya Korta, Bochechki, Yerofeyevka, Ichkala, Kagarlyk, and Pribram. The other three (Zhemaytkemis, Stavropol, and Mocs) are re-analysed. (From *Geophysical Abstracts*, No. 236).

Krinov, Ye.L., 1964, Falls and finds of meteorites during the last ten years (from 1953 to 1962): *Akademiia Nauk SSSR Meteoritika*, No. 25, p. 173-177.

The 64 meteorites that fell or were found in 1953-1962 are tabulated by year and class. Falls included 3 irons, 1 stone-iron, and 27 stones; finds included 16 irons, 4 stone-irons, and 13 stones. Their weight and distribution by year and by country are given. These bring the total number of known meteorites to 1,684 (744 falls, 940 finds). (From *Geophysical Abstracts*, No. 217).

Kumai, M., 1966, Microspherules in snow and ice-fog crystals: *Journal of Geophysical Research*, V. 71, p. 3397-3404.

Spherules found in snow crystals, ice-fog crystals, fallout particles, and fly ash were studied with an electron microscope using the electron diffraction method. The central part of the residues of 1004 specimens of natural snow crystals from Greenland, the United States, and Japan were examined; 14 spherules 0.1 to 1.5  $\mu$  in radius were found among them. The residues of 658 artificial ice-fog crystals formed from water vapor in flue gases of coal-burning electric power plants at Fairbanks, Alaska, were also examined; 9 spherules were found. Spherules similar to those found in ice-fog residues were found in furnace-produced fly ash fallout. Electron and optical microscope examination of spherules found in Greenland snow reveals a size distribution of the form  $dN/d(\log r) = Cr^{-B}$  where  $B \approx 3$ . The properties of spherules and mean mass of snow crystals in Greenland are described. The electron microscope study indicated that less than 0.7% of the 1004 snow crystals contained spherules of possibly extraterrestrial origin and that snow crystals are formed mainly on clay mineral particles by heterogeneous nucleation.

Kurbatskiy, N.P., 1964, On forest fire in the area of the Tunguska fall in 1908: *Akademiia Nauk SSSR Meteoritika*, No. 25, p. 168-172.

It is pointed out that the forest blown down by the Tunguska fall might have been already dead and decayed due to forest fires; this possibility should be taken into account in calculating the violence of the ballistic and explosive waves from the extent of flattened forest. Moreover, a great forest fire creates strong convection currents of air and winds near the ground, which can fell trees in the direction of movement of the front of the fire. (From *Geophysical Abstracts*, No. 217).

Kvasha, L.G., 1965, On the structure of chondrules and chondrites: *Akademiia Nauk SSSR Meteoritika*, No. 26, p. 35-59.

Results of an exhaustive investigation of the structure of chondrules and chondrites lead to the conclusion that chondrules crystallized as independent bodies from a solution of certain composition and volume. Chondrules are porous, as lavas or crystalline rocks are porous; chondrites as a whole are porous in the same sense as pyroclastic rocks. The pyroxene chondrules solidified somewhat later than the others. Chondrules and chondrites appear to have formed at about the same time. Sulfides and other admixed minerals were formed after consolidation of the chondrules and facilitated sintering of the aggregate. The origin of the liquid droplets from which the chondrules were formed is not yet clear. (From *Geophysical Abstracts*, No. 237).

Kvasha, L.G., Sidorenko, G.A., and Ginzburg, I.V., 1964, The pyroxene of the stony meteorite Nakhla: *Akademiia Nauk SSSR Meteoritika*, No. 25, p. 90-95.

Results of petrographic, chemical, and X-ray study of the pyroxene in the Nakhla meteorite are presented. This pyroxene, called nakhlite, is an augite that apparently crystallized from a silicate melt somewhat more basic than a basaltic lava. The absence among terrestrial volcanic rocks of types similar to the Nakhla meteorite is indicative not only of different conditions of formation but also of some differences in chemical composition. (From *Geophysical Abstracts*, No. 217).

Lammerzahl, P., and Zähringer, J., 1966, K-Ar-Altersbestimmungen an Eisenmeteoriten--II Spallogenes  $Ar^{40}$ - $Ar^{38}$ -Bestrahlungsalter: *Geochimica et Cosmochimica Acta*, V. 30, p. 1059-1074.



A first attempt to determine the spallation  $\text{Ar}^{40}$  in iron meteorites is reported. A new extraction technique for metallic samples with atmospheric contamination as low as  $10^{-9}$  cm<sup>3</sup> S.T.P.  $\text{Ar}^{40}$  was developed to determine the spallation-produced  $\text{Ar}^{40}$  in iron meteorites. The samples were degassed in steps with increasing temperature. The atmospheric and radiogenic components were released at low temperatures. At higher temperature the  $\text{Ar}^{40}/\text{Ar}^{39}$  values remain constant and give an upper limit of the spallation ratio.

The spallation-produced  $\text{Ar}^{40}$  is mainly important as a correction in the determination of the radiogenic  $\text{Ar}^{40}$  content. The precision achieved is, however, high enough to determine also cosmic ray exposure ages.

The measured  $\text{Ar}^{40}/\text{Ar}^{39}$  spallation ratios range from 0.188 to 0.226 and depend on the time of the decay of the cosmic-ray-produced  $\text{K}^{40}$ . By comparison with exposure ages deduced from other isotopes relative production rates of  $\text{Ar}^{40}/\text{Ar}^{39} = 0.186 \pm 0.005$  and of  $\text{K}^{40}/\text{Ar}^{39} = 0.97 \pm 0.05$  are derived. The production cross sections of  $\text{K}^{39}$ ,  $\text{K}^{40}$  and  $\text{K}^{41}$  in iron targets bombarded with 575 MeV protons were also measured. For  $\text{K}^{40}$   $9.2 \pm 0.8$  mbarn have been obtained. This value is in agreement with the  $\text{K}^{40}$  spallation yield calculated from the cosmic-ray-produced K isotopes in iron meteorites.

The  $\text{Ar}^{40}/\text{Ar}^{39}$  determinations of this work give cosmic ray exposure ages which are in good agreement with the ages obtained from the  $\text{K}^{40}$ - $\text{K}^{41}$  method. (In German).

Lautman, D.A., Shapiro, I.I., and Colombo, G., 1966, The earth's dust belt: fact or fiction? 4. Sunlight-pressure air-drag capture: *Journal of Geophysical Research*, V. 71, p. 5733-5741.

The contribution to the earth's dust belt that stems from the trapping of particles into long lifetime bound geocentric orbits by the combined action of air drag and sunlight pressure has been investigated. This concentration mechanism is of significance only if the speed of a substantial fraction of the dust particles entering the earth's sphere of influence is of the order of 1 km/sec or less. The dust-particle flux will then exhibit a broad peak at an altitude of about 0.5 earth radii and will be of the order of  $10^9$  or more times greater than the flux at the boundary of the earth's sphere of influence. By considering a more realistic initial distribution of dust-particle orbits, the theoretical analyses lend little support to the supposition that the earth is a very effective entity for concentrating interplanetary dust particles.

Lavrukhina, A.K., 1965, Study of the spatial and temporal variations of cosmic rays on the basis of the effects of nuclear spallations in meteorites: *Akademiia Nauk SSSR Meteoritika*, No. 26, p. 91-101.

The evidence in meteorites suggests that (1) cosmic ray intensity varies as a function of intensity of solar activity even at considerable distances from the sun (several astronomical units); (2) cosmic ray intensity is about twice as great in the region of meteorite orbits as in the vicinity of the earth. At first sight the latter conclusion contradicts the constancy of cosmic ray intensity claimed by many investigators on the basis of  $\text{Ar}^{37}/\text{Ar}^{39}$  values. The data on cosmic ray intensity and its distribution in the solar system are still not sufficiently accurate or complete; further investigations are recommended. (From *Geophysical Abstracts*, No. 236).

Lavrukhina, A.K., Vilenskiy, V.D., Kolesov, G.M., Rutkovskiy, V.M., and Yukina, L.V., 1965, Radiochemical investigation of the meteorite Zaysan: *Akademiia Nauk SSSR Meteoritika*, No. 26, p. 102-108.

The contents of Sc, Ce, Eu, Ba, U, P, and Ti in the Zaysan stone meteorite are reported. All are somewhat higher than the average for ordinary chondrites. The Be-10, Al-26, Cl-36, and Mn-54 contents are also reported (in disintegrations per minute per kg):  $38 \pm 11$ ,  $240 \pm 60$ ,  $10 \pm 10$ , and  $<1,000$ , respectively. (From *Geophysical Abstracts*, No. 2367).

Lazarev, R.G., 1966, The frequency of sporadic meteoric bodies: *Soviet Astronomy - A.J.*, V. 9, p. 830-836.

An elliptical model of the true-radiant distribution in the ecliptic plane and the exponential distribution with ecliptic latitude is discussed. The Stauder-Hoffmeister integral is generalized. A formula for the frequency of meteoric bodies is obtained, from which follows an elliptical value for the mean heliocentric velocity of meteors. The relative numbers of meteoric particles encountering and overtaking a body moving in interplanetary space is estimated.

Le Bas, M.J., 1966, High load-pressure mineralogical relations in chondrites: *Nature*, V. 211, p. 1355-1358.

The data presented suggest that it may be possible to distinguish chondrites formed at high load-pressure environments from those formed at lower load-pressures. In this way a model might be constructed of the original body or bodies. It would also contribute to the solution of the problem of whether or not the H and L chondrites might have come from different bodies, possibly of different sizes, which came close enough to each other to cause their disintegration.

Lipschutz, M.E., and Jaeger, R.R., 1966, X-ray diffraction study of minerals from shocked iron meteorites: *Science*, V. 152, p. 1055-1057.

A pronounced shock-induced alteration is indicated by the X-ray analyses.

Lowman, P.D., Jr., and O'Keefe, J.A., 1966, Terrestrial origin of the Igast objects: *Nature*, V. 209, p. 67.

By analysis of an Igast object which fell from the sky at Igast, Etonia, in 1855, and by comparison with other meteorites, the authors conclude that the objects are of terrestrial origin, and were probably pseudoseorias formed by burning coals.

Mason, B., 1966, Geochemistry and meteorites: *Geochimica et Cosmochimica Acta*, V. 30, p. 365-374.

Goldschmidt's (1923) geochemical classification of the elements into siderophile, chalcophile, lithophile and atmophile groups is reviewed, and the pertinence of this classification in meteorite research is emphasized. The occurrence and distribution in meteorites of nitrogen, magnesium, silicon, phosphorus, calcium, titanium, vanadium, chromium, manganese, iron, nickel and copper are discussed. Of these elements, the normally lithophile calcium, titanium, chromium and manganese became chalcophile in meteorites showing a very high degree of reduction (the enstatite chondrites and enstatite achondrites).

Mason, B., 1966, The enstatite chondrites: *Geochimica et Cosmochimica Acta*, V. 30, p. 23-39.

Fifteen enstatite chondrites have been recognized: Abee, Adhi Kot, Atlanta, Bethune, Blithfield, Daniel's Kuil, Hvittis, Indarch, Jajh deh Kot Lalu, Khairpur, Kota-Kota, Pillistfer, St. Mark's, Saint-Sauveur and Ufana. Their essential minerals are enstatite and/or clinoenstatite (40-60%), kamacite (20-28%), troilite (7-15%), and sometimes plagioclase (5-10%). A considerable number

of accessory minerals, some of them unique to this group, have been recorded. Chondritic structure is seldom well developed, and some of these meteorites appear to be completely recrystallized and lack chondrules entirely. Their bulk chemical composition is similar throughout, the principal variable being total Fe, which ranges from 20.71 in Blithfield to 35.02 in Saint-Sauveur. Some trace elements, however, show remarkable variation between the individual meteorites. Geochemically the enstatite chondrites are characterized by a high degree of reduction, Fe, Ni, Co, Cr, Mn and Ti being present in metal and/or sulfide phases, and some Si being in solid solution in the nickel-iron.

Massalski, T.B., Park, F.R., and Vessamillet, L.F., 1966, Speculations about plessite: *Geochimica et Cosmochimica Acta*, V. 30, p. 649-662.

Plessite, a component of most metallic meteorites, is discussed in terms of its composition and texture. The variations in texture and composition indicate that more than one mechanism may be responsible for plessite formation. Without an unambiguous origin for plessite, interpretation of the compositional variations within plessite in terms of the thermal history of the meteorite can only be tentative.

McCall, G.J.H., 1966, The petrology of the Mount Padbury mesosiderite and its achondrite enclaves: *Mineralogical Magazine*, V. 35, p. 1029-1060.

The petrography of the Mount Padbury meteorite is described in detail. Eucrite, brecciated eucrite, and a peculiar "shocked" form of eucrite are the calcium-rich achondrite types represented; hypersthene achondrite (including typical diogenite material and unfamiliar material) and olivine achondrite (granular aggregates of olivine not entirely similar to the unique chassignite and single crystals up to 4 in. in length) are the calcium-poor achondrite types represented. The eucrite displays more or less uniform mineralogy, but the mineral constituents are present in varying proportions, and there is a wide range of textural variations recognized. The silicate grain fragments enclosed in the metallic reticulation to form the mesosiderite host material are, significantly, entirely of minerals seen within the achondrite enclaves--plagioclase, hypersthene, pigeonite, olivine, and tridymite.

These results include microscopic analysis of thin sections and polished sections, X-ray diffraction studies, optical determination of refractive indices using mineral grain mounts, and chemical analyses.

Mcgrue, G.H., 1966, Rare-gas chronology of calcium-rich achondrites: *Journal of Geophysical Research*, V. 71, p. 4021-4027.

The isotopes of He, Ne, and Ar from pyroxene and feldspar concentrates of the Estherville mesosiderite and Haraia, Juvinas, Shergotty, and Stannern achondrites were analyzed. Concordant K-Ar ages of  $3.6 \times 10^9$  years (Haraia) and  $4.0 \times 10^9$  years (Estherville, Juvinas, Shergotty, Stannern) indicate that diffusion of radiogenic Ar after crystallization has been negligible. One separate of the severely shocked Shergotty meteorite gave an age of  $2.2 \times 10^9$  years, which may represent the time at which the meteorites broke up. Cosmic ray exposure ages have been calculated from the  $\text{He}^3$  and  $\text{Ne}^{21}$  content of the pyroxene separates and production rates derived from the pyroxene data of the Estherville mesosiderite. The radiation ages vary between 10 m.y. (Juvinas) and 60 m.y. (Shergotty). Haraia and Stannern have similar radiation ages of 32 m.y. The age values of Juvinas and Stannern are greater than were found in previous determinations made on the entire meteorite. This is primarily the result of recent  $\text{He}^3$  and Ne diffusion from feldspar. U and  $\text{He}^4$  concentrations from pyroxene and feldspar concentrates of the Estherville mesosiderite can be altered by simple leaching. This suggests that U is associated with a highly soluble mineral such as whitlockite. Interpretation of the thermal history of the parent body from (U, Th)-He ages may be incorrect.

because the loss of radiogenic  $\text{He}^4$  accompanying the recent diffusion of cosmogenic  $\text{He}^3$  and  $\text{Ne}$  is unknown.

Meinschein, W.G., Frondel, C., Laur, P., and Mislow, K., 1966, Meteorites: Optical activity in organic matter: *Science*, V. 154, p. 377-380.

A low-amplitude Cotton effect has been measured in organic extracts of samples from non-carbonaceous chondrites. It is likely that they are due to contamination on earth.

Merrihue, C., 1966, Xenon and krypton in the Bruderheim meteorite: *Journal of Geophysical Research*, V. 71, p. 263.

In a series of heating experiments, xenon, radiogenic  $\text{Xe}^{129}\text{R}$ , and krypton contents, and the xenon and krypton isotopic composition of the Bruderheim meteorite were studied for the separated minerals feldspar, pyroxene, olivine, and troilite and for numerous chondrule fractions. Important differences among the individual minerals and between minerals and chondrules were observed.

Mikheyeva, I.V., and Kolomenskiy, V.D., 1964, Investigation of meteor and industrial dust by the X-ray method: *Akademiia Nauk SSSR Meteoritika*, No. 25, p. 156-162.

X-ray studies show that oxymagnetite is the main component of meteoric and industrial dust. In the latter the oxidation of divalent iron to trivalent goes somewhat further, but the difference is so close to the limit of accuracy of determination that further investigation is necessary before the two types of dust can be distinguished by X-ray methods. (From *Geophysical Abstracts*, No. 217).

Miles, H.G., and Meadows, A.J., 1966, Fireballs associated with the Barwell meteorite: *Nature*, V. 212, p. 1339.

Additional data now available imply the existence of a third fireball associated with the meteorite fall at Barwell on December 24, 1965. The track of the third fireball was approximately parallel to the other two and 30 km west, thus passing over Bristol. No sound effects accompanied its passage.

Moore, C.B., and Lewis, C.F., 1966, The distribution of total carbon content in enstatite chondrites: *Earth and Planetary Science Letters*, V. 1, No. 6, p. 376-378.

Total carbon abundances in thirteen enstatite chondrites range from 0.056 wt% in Khairpur to 0.56 wt% in Kota Kota. The enstatite chondrites cannot be subdivided into two groups on the basis of their carbon contents.

Mueller, G., 1966, Origin of meteorites, in the light of recent rocket photography of the moon and Mars: *Nature*, V. 211, p. 1134-1135.

The aim of the article is to create interest in the interpretation of rocket photographs of the moon and other celestial bodies, in considering the problem of the origin of meteorites. It is suggested that the petrography and other geological aspects of celestial bodies may prove to depend essentially on a few parameters such as mass, temperature and other properties of the material in the course of condensation. Additional clues must be sought in the specification of the parent bodies of meteorites to help establish the main laws governing the condensation of matter.

Mueller, G., 1966, Significance of inclusions in carbonaceous meteorites: *Nature*, V. 210, p. 151-155.

This article describes some recently observed examples of inhomogeneities, inclusions, and interbrecciation in meteoritic materials of which at least one sample belongs to the "carbon-rich" groups.

The observations and considerations presented seem to indicate that the very broad range of sulphur: carbon ratios of meteorites can be derived through devolatilization of primordial matter (cosmic dust) of approximately uniform composition under differing temperatures and reducing or oxidizing conditions.

Müller, O., and Zähringer, J., 1966, Chemische Unterschiede bei uredelgashaltigen steinmeteoriten: *Earth and Planetary Science Letters*, V. 1, No. 1, p. 25-29.

So far differences in the chemical composition of meteorites with light-dark structure have only been found for the trace elements, C, Bi and primordial rare gases. In this work further chemical analyses of stony meteorites with sharp boundaries between the light and dark structure have been performed. Large differences have been found in the achondrites Kapoeta and Staroe Pesjanoe. Chondrites show this difference to a smaller extent. In all cases, however, C is enriched in the dark phases by a factor of 2 to 3. The primordial rare gases show a similar behavior. It is difficult to interpret the chemical differences by the shock and solar wind hypothesis alone. The dark phases have specific similarities with carbonaceous chondrites and can rather be understood as an admixture of carbonaceous chondritic material to the light phases. (In German).

Müller, O., and Zähringer, J., 1966, K-Ar-Altersbestimmungen an Eisenmeteoriten--III Kalium- und Argon-Bestimmungen: *Geochimica et Cosmochimica Acta*, V. 30, p. 1075-1092.

The K-Ar age of iron meteorites has been investigated. Neutron activation analysis has been applied for the determination of the total  $\text{Ar}^{40}$  and  $\text{K}^{41}$  content. The spallation-produced  $\text{Ar}^{40}$  could be corrected by means of mass spectrometric analysis. After irradiation the surfaces of the samples were filed off to avoid potassium contamination. Atmospheric argon could be removed by fractionated degassing at increasing temperatures. The potassium content ranges from less than one ppb to several ppm and the radiogenic  $\text{Ar}^{40}$  from  $10^{-9}$  to  $10^{-7}$   $\text{cm}^3/\text{g}$ . By dissolving the inclusions before evaporating the specimens, fractions of high and low potassium content were obtained. Thus, Ar/K ratios for single fractions could be determined separately. Usually this ratio is much lower for inclusions than for the metal phase and is most likely due to diffusion losses. Meteorites with very low potassium content are difficult to date due to argon of other than radiogenic origin. For five iron meteorites with potassium content larger than about 100 ppb, however, the radiogenic  $\text{Ar}^{40}$  is proportional to K and reliable K-Ar ages of  $6.3 \pm 0.4$  b.y. were obtained. Although the cosmic and terrestrial history of these meteorites were quite different, the ages lie within a narrow range. (In German).

Mutch, T.A., 1966, Abundances of magnetic spherules in Silurian and Permian salt samples: *Earth and Planetary Science Letters*, V. 1, No. 5, p. 325-329.

Abundances of magnetic spherules in 26 Silurian and Permian salt samples are very similar to abundances in recent collections from the atmosphere. This suggests that meteoritic influx has been constant for the three periods of time sampled.

Nagy, B., 1966, A study of the optical rotation of lipids extracted from soils, sediments, and the Orgueil carbonaceous meteorite: *Proceedings of the National Academy of Sciences*, V. 56, p. 389-398.

Low real values of optical rotation have been found for lipids extracted from the Orgueil meteorite. Four samples of the meteorite were found to contain several

different kinds of anaerobic non-spore forming bacteria. There was no way to determine if the optically active material and bacteria were terrestrial contaminants.

Nichiporuk, W., and Bingham, E., 1966, Copper and vanadium in stony meteorites: Transactions of the American Geophysical Union, V. 47, No. 1, p. 131.

The concentrations of copper and vanadium have been determined spectrographically in fifty-seven ordinary chondrites, seven carbonaceous chondrites, three enstatite chondrites, and the olivine phase of two pallasites. Values determined the range for Cu from a low of 12 ppm in the basaltic achondrite Pasamonte to a high of 212 ppm in the enstatite chondrite Abee. In the same way, the V values obtained a range from a low of 14 ppm in the enstatite chondrite Cumberland Falls to a high of 263 ppm in the basaltic achondrite La Fayette. The ordinary chondrites investigated appear to constitute the least differentiated meteorite group with average concentrations of Cu = 133 ppm and V = 60 ppm. The best value of the ratio Cu/V for those chondrites is 2.2. (Abstract of a paper presented at the April 1966 meeting of the American Geophysical Union).

Nininger, H.H., and Huss, G.I., 1966, Free copper in the Odessa, Texas, siderite: Meteoritics, V. 3, p. 71-72.

A grain of free copper is reported from the Odessa octahedrite. It is in the schreibersite surrounding a nodule of troilite. Free copper is now known in three nickel-iron meteorites.

Nix, J.F., and Kuroda, P.K., 1966, A neutron activation analysis of uranium in stone meteorites: Transactions of the American Geophysical Union, V. 47, No. 1, p. 133.

The uranium content of Pasamonte meteorite and the light and dark parts of the Fayetteville meteorite were determined by means of a neutron activation technique. The primary purpose of this work was to determine the  $Pu^{244}$  age or the time interval ( $T$ ) between the cessation of nucleosynthesis and formation of the meteorite. The meteorite samples were irradiated,  $Np^{239}$  was isolated from the irradiated samples, exhaustively purified, and beta counted. The  $Pu^{244}$  age of the meteorite was calculated by means of the continuous nucleosynthesis model. A value of  $72 \times 10^8$  years was obtained for the Fayetteville meteorite, whereas a value of  $385 \times 10^8$  years was obtained for the Pasamonte meteorite. The apparent difference in the  $Pu^{244}$  ages for these meteorites thus obtained may be due to some unknown nuclear process taking place during the time interval  $T$ . The uranium content of the Bruderheim meteorite was also determined. (Abstract of a paper presented at the April 1966 meeting of the American Geophysical Union).

Oleak, H., 1966, Die streifende Feuerkugel vom 14. January 1965: Astronomische Nachrichten, V. 289, p. 71-79.

Orbiting elements deduced from 1000 eyewitness accounts are given for a meteor visible as a bright fireball in Poland and the German Democratic Republic. (In German).

Olsen, E., and Fredriksson, K., 1966, Phosphates in iron and pallasite meteorites: Geochimica et Cosmochimica Acta, V. 30, p. 459-470.

The ferrous (manganous) orthophosphates, sarcopside and graffonite (both calcium-free) have been found in four fine octahedrites (Bella Roca, Chupaderos, Sam's Valley, Verkhne Dnieprovsk). They co-exist with schreibersite, troilite and metal. Calculations of  $P(O_2) - T$  for reactions relating these phases show that the presence of these phosphates presents no inconsistency with respect to the degree of reduction encountered in iron meteorites. Similar calculations for

magnesium orthophosphate (farringtonite) indicate that the pallasite in which it occurs is somewhat more reduced than the octahedrites. These phosphate-bearing irons suggest a degree of oxidation close to that of common chondrites.

Ostic, R.G., 1966, The concentration and isotopic composition of lead in Toluca Iron Meteorite: *Journal of Geophysical Research*, V. 71, p. 4060-4063.

Examination of the lead content of two troilite-graphite nodules showed that it was of primordial composition, and not radiogenic as reported by previous workers.

Park, F.R., Bunch, T.E., and Massalski, T.B., 1966, A study of the silicate inclusions and other phases in the Campo del Cielo meteorite: *Geochimica et Cosmochimica Acta*, V. 30, p. 399-414.

The material occurring as inclusions and the surrounding metallic matrix of a specimen of the Campo del Cielo meteorite have been examined in detail. The association of phases and the structure of the metallic portion indicate that the meteorite may be designated as a hexahedrite, or a very coarse octahedrite and that the samples examined had been severely deformed. The particular inclusions examined are composed of silicates associated with a large amount of opaque minerals and are separated from the metallic matrix by a complex interface region. Schreibersite, troilite, and graphite are the principal components of the interface region, which contains, in addition, chromite, sphalerite, and a calcium-rich phosphate. The texture of the minerals of the interface region indicates non-equilibrium conditions; in particular, an initial heating, and then a relatively rapid cooling. Petrographic modal analyses of the silicates indicate an average of 37.9 volume per cent forsterite, 35.3 vol. per cent chrome-diopside, 18.4 vol. per cent enstatite and 8.4 vol. per cent oligoclase. A mineral suite so composed is comparable to similar silicate inclusions occurring in predominantly metallic meteorites and also to some terrestrial rocks, but is not comparable to other known silicate meteorite assemblages.

Patashnik, H., and Hemenway, C.L., 1966, Mass and density measurements of micrometeorites: *The Astronomical Journal*, V. 71, p. 866.

A new instrument has been developed and employed to make direct measurements of the masses of micrometeorites.

Preliminary results indicate sensitivity approaching  $10^{-10}$  g and further refinements are expected to increase this sensitivity. Calibration has been accomplished through the use of aluminum and nickel microspheres of known diameter and density. Initial measurements of the masses and densities of micrometeorites are given. (Abstract of a paper presented at the July 1966 meeting of the American Astronomical Society).

Peale, S.J., 1966, Dust belt of the earth: *Journal of Geophysical Research*, V. 71, p. 911-933.

The dynamical and light-scattering properties of small dust grains that orbit the earth are investigated. It is shown that the radiation pressure will cause a diffuse concentration of dust particles near the ecliptic plane. The ecliptic symmetry of the orbiting dust implies that all the zodiacal light might be due to dust on such geocentric orbits rather than on heliocentric ones as is commonly believed. Observational evidence currently available does not distinguish between these possibilities. In an appendix a new method of estimating the photoelectron contribution to the electrostatic potential of a dust grain is used in determining the charged-particle drag as a function of plasma temperature and density.

Pepin, R.O., 1966, Heavy rare gases in silicates from the Estherville mesosiderite: *Journal of Geophysical Research*, V. 71, p. 2815-2829.

Krypton in Estherville silicates is shown to be a mixture of primordial and spallation-produced components, and xenon a mixture of primordial, spallation, and fission components. Small amounts of radiogenic  $\text{Xe}^{136}$  may also be present. An average isotopic composition for Estherville spallation xenon is  $\text{Xe}^{124}:\text{Xe}^{130}:\text{Xe}^{132}:\text{Xe}^{134}:\text{Xe}^{136} = .34: .62: 1.00: 1.05: 4.80: 3.3$ . This composition is compared with theoretical isobaric production rates calculated from a model of cosmic-ray spallation in meteoritic material. The relative abundance of  $\text{Xe}^{131}$  is found to be significantly higher than predicted: whether this implies either thermal neutron irradiation or a departure from a simple cosmic-ray irradiation history is at present uncertain. The possible presence of a spallation component in carbonaceous chondrite xenon is considered. Extinct radioactivity chronologies and the question of concordant formation intervals are examined for Estherville and for the Pasamonte achondrite. I-Xe and Pu-Xe formation intervals for Pasamonte are probably concordant at  $\sim 220 \pm 40$  million years. The isotopic composition of Pasamonte fission xenon, after correction for spallation contributions, is estimated as  $\text{Xe}^{131}:\text{Xe}^{132}:\text{Xe}^{134}:\text{Xe}^{136} = 0.18: 0.91: 0.97: 1.00$ .

Pollack, S.S., 1966, Disordered orthopyroxene in meteorites: *American Mineralogist*, V. 51, p. 1722-1726.

Disordered orthorhombic pyroxene, which was first found in meteorites by Brown and Smith (1963), and later by Pollack and Ruble (1964), has now been found in all the enstatite achondrites except Shallowater. It has also been found in the Stannern (eucrite), Abee (enstatite chondrite) and Hugoton (olivine-bronzite chondrite).

Portnov, A.M., 1964, On the crater on the Potomsk Upland: *Akademiia Nauk SSSR Meteoritika*, No. 25, p. 194-197.

A crater about 86 m in diameter that occurs on the Potomsk Upland, about 50 km west of Perevoz settlement in the Badaybinsk area of the Irkutsk Region, is described. The external aspect, regular shape, presence of a ring wall and central hill, and shattered and pulverized but not altered rocks, all indicate an explosive, possibly meteoritic, origin. (From *Geophysical Abstracts*, No. 217).

Price, P.B., Walker, R.M., and Fleischer, R.L., 1966, The use of plutonium fission tracks to measure the cooling of meteoritic bodies following the formation of the solar system: *Transactions of the American Geophysical Union*, V. 47, No. 1, p. 132.

Meteoritic minerals that were formed and cooled soon after the beginning of the solar system should contain tracks from the spontaneous fission of primordial plutonium. In silicate minerals from certain iron meteorites we observe densities of natural fission tracks with densities that are far too high to be accounted for by spontaneous fission of  $\text{U}^{238}$ . The reasonable explanation for these tracks is spontaneous fission of  $\text{Pu}^{244}$ . Alternative explanations are discussed and shown to be highly improbable. We find increasing track abundances in the sequence enstatite-albite-diopside that corresponds to extrapolated 100 m.y. track-annealing temperatures of 550°, 750°, and 950°K. These data allow a cooling rate of 1.3°C/m.y. to be determined for the parent body of the meteorite toluca. This value is independent of the original  $\text{U}^{238}/\text{Pu}^{244}$  ratio and is in agreement with independent values obtained from electron probe studies of the metallic phases in this same meteorite. (Abstract of a paper presented at the April 1966 meeting of the American Geophysical Union).

Ramovich, M., 1965, On the significance of the study of geoelectric pulsations for the problem of the origin of meteorites: *Akademiia Nauk SSSR Meteoritika*, No. 26, p. 109-111.

It must be assumed that there have been pulsations of energy in the endosphere below the earth's mantle; the phenomena governed by the manifestations of maximum



energy are recorded in the rocks in the form of the acid granites, which have no counterparts among the stony meteorites. The difference in activity between earlier and later geomagnetic cycles has been noted by many; the later cycles have been shorter and less active. Since the Silurian there have been four intervals when rocks similar in some respects to the stony meteorites have formed--Devonian-early Carboniferous, Triassic-Early Jurassic, Late Cretaceous Paleogene, and Pliocene-Anthropogene. (From Geophysical Abstracts, No. 236).

Ramsden, A.R., and Cameron, E.N., 1966, Kamacite and taenite superstructures and a metastable tetragonal phase in iron meteorites: *American Mineralogist*, V. 51, p. 37-55.

Kamacite and taenite in iron meteorites have cubic superstructures in which the unit cell edges are respectively three times and two times those of the disordered phases. Certain iron meteorites also contain a tetragonal phase that seemingly has the same chemical composition as kamacite. This is considered to be a transitional state in the transformation of  $\gamma$ -phase alloy into  $\alpha$ -phase alloy (kamacite). \*The identification of the kamacite and taenite structures was in error.

\*p. 1544 (A correction).

Reed, G.W., Jr., and Allen, R.O., Jr., 1966, Halogens in chondrites: *Geochimica et Cosmochimica Acta*, V. 30, p. 779-800.

Cl, Br and I contents in samples of the several classes of chondrites have been simultaneously measured by activation analysis. Auxiliary information derived from this work confirms U and Te concentrations and I/Te ratios reported in the literature. For the ordinary (bronzite and hypersthene), pigeonite, enstatite and carbonaceous chondrites the respective Cl contents are 4-90, 120, 516 and 280 ppm; the Br contents are 0.05-0.08, 0.16, 0.07-0.47 and 0.23-1.21 ppm.

Cl and Br are positively correlated; most chondrites fall on correlation lines with Cl/Br weight ratios between 20 and 100. Br and I exhibit a simple correlation; most meteorites fall near a line with a Br/I weight ratio of about 1.

Leaching experiments yielded results that supported these interhalogen relations, and also gave the degree of water solubility of the halogens:  $\text{Cl} < \text{Br} \sim \text{I} \sim \text{Te}$ . Abundances derived from the data support current thinking that the Type I carbonaceous chondrites have best retained a primordial complement of solar system matter. The astrophysical and meteoritic abundances of chlorine based on oxygen agree reasonably well, 22 vs.  $\sim 9$  atom Cl/ $10^6$  atom O; whereas the abundance based on Si differ greatly,  $1.5 \times 10^6$  vs. 2800 atom Cl/ $10^6$  atom Si.

Reynolds, J.H., Hohenberg, C.M., and Munk, M.N., 1966, The case for  $\text{Pu}^{244}$  in the Pasamonte achondrite: *Transactions of the American Geophysical Union*, V. 47, No. 1, p. 133.

Following the discovery by Rowe and Kuroda that there are striking excesses of the xenon ratios  $^{134}/^{132}$  and  $^{136}/^{132}$  in the Pasamonte achondrite, we performed stepwise heating experiments with this meteorite. Xenon results from three experimental systems were concordant. The ratio  $^{124}/^{130}$  is linearly correlated with the ratio  $^{126}/^{130}$ , showing a (cosmogenic) spallation component. Ratios reported for total xenon from other achondrites and a mesosiderite all fall on this correlation line. The ratio  $^{134}/^{132}$  is linearly correlated with the ratio  $^{136}/^{132}$ , showing a fission component. The Pasamonte data permit calculation of the isotopic compositions of the fission and spallation components. Krypton data from the stepwise heating experiment provide ratios  $^{80}/^{84}$ ,  $^{82}/^{84}$ ,  $^{83}/^{84}$ , which are linearly correlated, showing a spallation component. The case for  $\text{Pu}^{244}$  rests on the evidence: (1) the fission component differs isotopically

from spontaneous or neutron induced fission xenon in uranium; (2) the concentration of fission  $Xe^{136}$  ( $7.9 \times 10^{-12}$  cc STP/g) exceeds that attributable to uranium in Pasamonte by a factor of 46. Eventually data on fission krypton should provide additional surety, but even now the evidence for  $Pu^{244}$  in the early solar system seems conclusive. (Abstract of a paper presented at the April 1966 meeting of the American Geophysical Union).

Ringwood, A.E., 1966, Chemical evolution of the terrestrial planets: *Geochimica et Cosmochimica Acta*, V. 30, p. 41-104.

The terrestrial planets are believed to have formed by accretion from an initially cold and chemically homogeneous cloud of dust and gas. The iron occurring in the dust particles of the cloud was present in a completely oxidized form. Either before or during accretion of dust into planets, partial reduction of oxidized iron to metal occurred. The role of oxidation-reduction equilibria during the formation of terrestrial planets is discussed and it is concluded that the differing zero-pressure densities of the planets are caused dominantly by differing mean states of oxidation which were established during the primary accretion processes. This interpretation avoids the necessity for assuming the occurrence of physical fractionation of metal from silicates in the solar nebula before accretion.

A detailed study is made of the evidence shed by chondritic meteorites upon oxidation-reduction equilibria occurring early in the history of the solar system. It is concluded that the different classes of chondrites have formed by an autoreduction process operating upon primitive material similar in composition to the Type I carbonaceous chondrites. Reduction occurred when this material accreted into parent bodies which were heated internally, perhaps by extinct radio-activities. Under these conditions, trapped carbonaceous material reacted with oxidized iron to produce a metallic phase in situ. The chemistry of the reduction process which operated in chondrites is studied. The evidence strongly indicates that the principal reducing agent was carbon and not hydrogen. Furthermore, reduction occurred in a condensed environment and not in the dispersed solar nebula. The origins and chemical evolution of other terrestrial planets are discussed in the light of evidence yielded by the chondrites. The hypothesis is advanced that each of the terrestrial planets formed by a single-stage autoreduction process operating upon primitive material similar to the Type I carbonaceous chondrites. The origins of the Moon, Earth, Mars, Venus, and Mercury are developed in detail.

Ringwood, A.E., 1966, Genesis of chondritic meteorites: *Reviews of Geophysics*, V. 4, No. 2, p. 113-175.

The abundances of elements in the major classes of chondrites are discussed, and the major abundance patterns defined. The chemical compositions of Type I carbonaceous chondrites are uniquely related to those of other classes of chondrites, the compositions of which can be obtained solely by the removal of appropriate amounts of trace and minor elements from Type I carbonaceous chondrites by appropriate chemical and physical processes. Evidence suggests that these chondrites are extremely primitive in nature and may be closely related to the primordial dust of the parental solar nebula. The mineralogy of the different classes of chondrites is reviewed. Types II and III carbonaceous chondrites represent a physical mixture of high-temperature minerals with primitive material similar to Type I carbonaceous chondrites. The significance of these mineral assemblages is discussed. A detailed review of oxidation-reduction relationships in chondrites is given, particularly with respect to "Pior's rule." It is concluded from mineralogical and chemical evidence that the metal in chondrites was produced by a carbon-reduction process operating on primitive oxidized material in an essentially condensed system at high temperatures.

rather than by hydrogen reduction in a highly dispersed system. Hypotheses relating to the origin of chondrules and chondritic structures are reviewed. Chondrules may have formed during volcanic processes on a parent body or by impact phenomena during collisions of planetesimals with one or more parent bodies. There is evidence that chondrites have evolved in a substantial gravitational field. The three major theories of origin of chondrites are considered.

Romig, M.F., 1966, The scientific study of meteors in the 19th century: *Meteoritics*, V. 3, p. 11-25.

A review, with references, of the development of the study of meteors.

Roper, R.G., 1966, Atmospheric turbulence in the meteor region: *Journal of Geophysical Research*, V. 71, p. 5785-5792.

In 1961 at Adelaide the atmospheric turbulence near 90 km was measured month by month using a spaced-station radio meteor technique. The characteristics of the large-scale turbulent motions are found to be similar to those observed in the northern hemisphere.

Rowe, M.W., 1966, Solar nucleosynthesis of extinct  $^{129}\text{I}$ : *Earth and Planetary Science Letters*, V. 1, No. 3, p. 97-98.

This paper presents additional data which appear to be consistent with the idea of a solar synthesis of  $^{129}\text{I}$ , as advanced by Rowe and Kuroda, in addition to the galactic event. Using essentially non-fissiogenic xenon extracted from two Ca-rich achondrites, an attempt was made to derive a "pure" cosmic ray spallation xenon spectrum. The lack of fission-produced xenon cannot be attributed to a low uranium concentration and hence low initial  $^{244}\text{Pu}$  content in these meteorites. It is pointed out that the view that the  $^{244}\text{Pu}$  and  $^{129}\text{I}$  are produced in two different nucleosynthesis events, (the  $^{244}\text{Pu}$  only in galactic nucleosynthesis and the  $^{129}\text{I}$  from both galactic and solar nucleosynthesis) appears consistent with the observation of a  $^{129}\text{Xe}$  excess with no measurable fission anomaly. It appears that the  $^{244}\text{Pu}$  and  $^{129}\text{I}$  may have been incorporated into the Nakhilitic meteorite parent material and decayed there. The material was then outgassed to such an extent that virtually all the excess fissiogenic xenon was lost.

Rowe, M.W., and Bogard, D.D., 1966, Isotopic composition of xenon from Ca-poor achondrites: *Journal of Geophysical Research*, V. 71, p. 4183-4191.

The isotopic composition of xenon extracted from six samples of five Ca-poor achondrites is presented. The data suggest that the principal component in all the samples studied here (except Shallowater) is probably atmospheric xenon, which is simply adsorbed onto the meteorite, presumably during the terrestrial life of the sample. A quite high  $\text{Xe}^{129}/\text{Xe}^{130}$  ratio is observed in xenon from the Shallowater enstatite achondrite, which contained relatively large amounts of primordial xenon compared to the other Ca-poor achondrites. The large spectral anomaly is thought to imply a genetic relationship between the enstatite achondrites and enstatite chondrites.

Rowe, M.W., and Bogard, D.D., 1966, Xenon anomalies in the Pasamonte meteorite: *Journal of Geophysical Research*, V. 71, p. 686-687.

The largest anomalies ever observed in the mass region 131 to 136 are seen in the xenon from Pasamonte II. The results of this second analysis of Pasamonte have confirmed the data reported by Rowe and Kuroda (1965).

Rowe, M.W., and Bogard, D.D., 1966, Xenon from achondrites: *Transactions of the American Geophysical Union*, V. 47, No. 1, p. 133.

Measurement of the abundance and isotopic composition of xenon extracted from several Ca-rich and several Ca-poor achondrites is reported. The xenon in these meteorites is apparently due to a mixture of four components: primordial, radiogenic, fissionogenic, and spallogenic. The spallation component is shown to be due to recent cosmic-ray bombardment of the meteorite. The fission-produced xenon, which caused large enrichments of the heavier isotopes, is presumed to be from the spontaneous fission of extinct  $\text{Pu}^{244}$ . A large  $\text{Xe}^{136}$  anomaly was found in only one case, from the Shallowater achondrite. Primordial xenon in achondrites is apparently similar to xenon from the Murray carbonaceous meteorite as determined by Reynolds. (Abstract of a paper presented at the April 1966 meeting of the American Geophysical Union).

Safronov, V.S., 1966, Sizes of the largest bodies falling onto the planets during their formation: *Soviet Astronomy - A.J.*, V. 9, p. 987-994.

Application of co-agulation theory to the process of accumulation of the planets from solid matter leads to the conclusion that this matter was in the form of particles and bodies of different sizes. Falling onto the planets, the bodies imparted to them a rotational moment consisting of two components of different nature: a regular component ("direct" rotation), related to rotation of the system as a whole, and a random component, related to the random direction of velocity of the falling bodies relative to the planet and manifested in the inclinations of the axes of rotation of the planets. The largest bodies made the principal contribution to the random component of rotation. This article gives the derivation of expressions relating the values of the random component of rotation to the masses  $m_1$  of the largest bodies falling onto a planet of mass  $m$  on the assumption of an exponential distribution function of the sizes of the bodies. Table I gives the values  $m_1/m$  determined from a comparison of the theoretically computed angles of inclination of the axes of rotation of the planets and the observed values. The largest bodies falling onto the earth had masses of about  $10^{-3}$  of the earth's mass; that is, they were of the size of the largest asteroids. This same mechanism makes it possible to explain the anomalous rotation of Uranus if it is assumed that the random component of the rotation of Uranus was greater than the systematic component. The mass of the largest body falling onto the surface of Uranus in this case would have to be 0.05 of the mass of that planet.

Schmidt, R.A., and Keil, K., 1966, Electron microprobe study of spherules from Atlantic Ocean sediments: *Geochimica et Cosmochimica Acta*, V. 30, p. 471-478.

Spherules recovered by K. Utech from Atlantic Ocean sediments (Albatross expedition, lat.  $23^{\circ} 58'$  N, long.  $38^{\circ} 56'$  W) were studied by means of electron microprobe techniques. Unlike the analyses of spherule surfaces reported by Wright et al. (1963); Langway (1963); Schmidt (1964); Hodge et al. (1964); Mutch (1964); and Langway and Marvin (1964), those in the present study were performed on polished sections of the spherules. Apparent terrestrial alteration of particle surfaces and the introduction of contaminants suggest that analyses limited to surfaces cannot be regarded as representative of entire spherules. Thirteen spherules ranging from 60-450  $\mu$  in diameter were classed into four groups based on their textures and compositions; Group 1: magnetite laths containing Ni and Co, surrounded by Si-rich films at grain boundaries. Occasionally, an off-center, circular area of metallic Ni-Fe-Co and/or trevorite ( $\text{NiFe}_2\text{O}_4$ ) is present. Group 2: homogeneous magnetite, with small amounts of Ni and Co. Group 3: magnetite with Si-rich lamellae in a dendritic intergrowth. Group 4: irregular particles commonly with low Fe content, but occasionally with minute Ni-rich flakes embedded in a granular matrix. Each particle shows effects of alteration, ranging from a narrow rim at the circumference on most to essentially complete corrosion of others. Lesser amounts of major constituents were present in alteration zones; in addition, minor amounts of Si, Al, P, Ca,

Mg, Mn, Cr, and Ti were noted there. Where metallic Ni-Fe-Co areas were altered, trevorite with traces of V was formed. The data suggest that spherules in Groups 1 and perhaps 2 are of meteoritic origin, representing ablation droplets swept from meteorites during passage through the earth's atmosphere. No definite conclusions were derived as to the origin of particles in Groups 3 and 4.

Schmitt, R.A., Smith, R.H., and Goles, G.G., 1966, Chainpur-like chondrites: Primitive precursors of ordinary chondrites: *Science*, V. 153, p. 644-646.

Chainpur and similar chondritic meteorites could be precursors of ordinary chondrites.

Schröder, W., 1966, Additional note of noctilucent clouds over Germany: *Journal of Geophysical Research*, V. 71, p. 5185.

In a recent letter the author (Schröder, 1966b) presented some statistics on the occurrence of noctilucent clouds over Germany ( $\phi:50-54^{\circ}\text{N}$ ). A careful search made recently through German astronomical journals uncovered 21 additional records of German sightings of noctilucent clouds during the years 1884-1964.

Shapiro, I.I., Lautman, D.A., and Colombo, G., 1966, The earth's dust belt: fact or fiction? I. Forces perturbing dust particle motion: *Journal of Geophysical Research*, V. 71, p. 5695-5704.

The forces influencing the motion of small dust particles orbiting near the earth and in interplanetary space have been studied. The predominant non-gravitational force is that of sunlight whose effects may be quite varied depending on the shape, orientation, and constitution of a dust particle. Far from the earth the only other force that may be of significance is the Lorentz force, whereas near the earth all the usual forces included in analyzing satellite orbits become important.

Shields, R.M., Pinson, W.H., Jr., and Hurley, P.M., 1966, Rubidium-strontium analyses of the Bjurböle chondrite: *Journal of Geophysical Research*, V. 71, p. 2163-2167.

The Bjurböle chondrite and several separated phases were analyzed for Rb-Sr ages. The chondrule age lies within two standard deviations of our recently established 4.45 billion year Rb-Sr stony meteorite isochron ( $\lambda_{\text{Rb}} = 1.39 \times 10^{-11} \text{ year}^{-1}$ ). The whole meteorite, two magnetically separated phases, and the matrix material all lie far off the isochron. It is concluded that the Bjurböle chondrite is hopelessly contaminated by terrestrial minerals and is not a satisfactory sample for testing for possible Rb-Sr age differences between chondrules and matrix. This is unfortunate because the Bjurböle sample is one of the few chondrites from which chondrules can be easily separated.

Shima, M., 1966, Glassy spherules (microtektites?) found in ice at Scott Base, Antarctica: *Journal of Geophysical Research*, V. 71, p. 3595-3596.

In the precipitate of melted ice collected on December 20, 1964, near Scott Base, Antarctica, glassy spherules were found under the microscope. The composition, shape, and refractive index of some of these spherules suggest that they are microtektites.

Shima, M., and Honda, M., 1966, Distribution of spallation produced chromium between alloys in iron meteorites: *Earth and Planetary Science Letters*, V. 1, No. 2, p. 65-74.

Chromium nuclides produced by cosmic rays were measured mass spectrometrically in iron meteorites. A marked enrichment due to cosmic ray products of  $^{54}\text{Cr}$  and  $^{53}\text{Cr}$  could be observed in the samples obtained by fractional dissolution with dilute sulfuric acid. The overall contents of  $^{54}\text{Cr}$  were found to be in the range of 13-25 ppb in several meteorites, and the ratios of the products,  $^{50}\text{Cr}$ : $^{53}\text{Cr}$ : $^{54}\text{Cr}$  were always found to be approximately 0.2: 1: 1 respectively. The enrichment of these chromium nuclides in taenite was confirmed by several methods. The interpretation of this phenomenon is discussed from a cosmochemical viewpoint.

Short, J.M., and Goldstein, J.I., 1966, The cooling history of meteorite parent bodies: Transactions of the American Geophysical Union, V. 47, No. 2, p. 425.

The cooling rates during formation of the Widmanstätten pattern have been determined for several iron and stony-iron meteorites by matching the Ni concentration gradients in the metal phases as measured by electron probe micro-analysis to theoretical diffusion gradients calculated by a comprehensive computer growth-analysis. The results indicate that in iron and stony-iron meteorites the Widmanstätten pattern developed within the parent bodies before their breakup under probable static pressures of less than 4 kb. However, definite differences were found in the cooling rates at 500°C of the meteorites studied, ranging from 0.8 to 7°C per million years. Two possible causes of the differences in cooling rates are variations in location of the meteorites within the parent body or variable parent body sizes. These differences can also account for deviations from the rough correlation between kamacite bandwidths and bulk Ni content and for the existence of meteorites with different structures but identical bulk Ni content. (Abstract of a paper presented at the April 1966 meeting of the American Geophysical Union).

Singer, S.F., 1966, Does the earth have a dust belt? Transactions of the American Geophysical Union, V. 47, No. 3, p. 481.

A measurement of concentration (particles per cubic centimeter) will show only a modest increase as one approaches the earth, with a maximum at about 2000 km above sea level. A detector that measures a simple flux, i.e., the number of particles crossing a square centimeter per second, will show an increase between an order of magnitude or somewhat more. An impact detector that counts the flux of particles having a momentum greater than a certain minimum value, will, however, show increases of two orders of magnitude or more. We have now calculated the expected impact rate for a detector mounted in an orbiting satellite and can reproduce the large differences in rates, first pointed out by Shipple on the basis of the data of Alexander, Dubin, and McCracken. It is not necessary to invoke trapped dust particles, only the particles of the zodiacal cloud and the earth's gravitational field. (Abstract of a paper presented at the September 1966 meeting of the American Geophysical Union).

Smyshlyayev, S.I., and Yudin, I.A., 1964, Chemical-mineragraphic investigation of the opaque minerals of the Holbrook chondrite: Akademiia Nauk SSSR Meteoritika, No. 25, p. 121-128.

Results of study of the opaque minerals in the Holbrook chondrite show that (1) the taenite, which is present in considerable quantity (up to 1 percent by volume), is rich in nickel (31.3 percent Ni); (2) taenite and kamacite usually occur as plessite; (3) schreibersite is rare; (4) native copper is observed in the nickel-iron together with corroded grains of troilite; (5) the composition of the troilite is Fe = 64.0 percent, Si = 36.0 percent, Ni not detected; (6) ilmenite is very rare; and (7) as in other chondrites, the nickel-iron, troilite, and chromite occur in three main forms--large particles (segregations) of irregular shape, chondrules, and dust grains. (From Geophysical Abstracts, No. 217).



Sobotovitch, Ye.V., 1964, Radiogenic and cosmogenic isotopes in meteorites and cosmo-chronology: *Akademiia Nauk SSSR Meteoritika*, No. 25, p. 40-74.

On the basis of a review of present knowledge on radiogenic and cosmogenic isotopes in meteorites, the chronology of the evolution of meteoritic matter is outlined. (From *Geophysical Abstracts*, No. 217).

Staley, D.O., 1966, Temperatures of meteoroids and meteorites: *Journal of Geophysical Research*, V. 71, p. 5681-5687.

The effects of emissivity, absorptivity, and thermal inertia are taken into account in the calculation of meteoroid temperatures at the earth's distance from the sun. Iron meteoroids at 1 AU with equivalent sphere radii in excess of about 1.5 meters may have temperatures departing substantially from radiative equilibrium temperatures as they move toward or away from the sun in highly eccentric orbits. The radiative equilibrium temperature of stone meteoroids is less than 0°C. These results are consistent with observed temperatures of newly fallen meteorites.

Surkov, Yu.A., and Nazarkina, G.B., 1965, Nuclear reactions in meteorites: *Geochemistry International*, V. 2, p. 689. (Translated from *Geokhimiya*, No. 8, p. 918-935, 1965; translation not published but may be ordered).

A review with 135 references.

Tuchek, D., 1965, Two recent meteorite falls in Czechoslovakia: *Akademiia Nauk SSSR Meteoritika*, No. 26, p. 112-118.

In the Pribram meteor shower of April 7, 1959, a bolide was observed over south-eastern Bohemia whose entire trajectory was photographed by two observatories. At an altitude of 25-44 km it apparently consisted of 16 fragments; at 13.3 km it disappeared and fell to earth. Four pieces totalling 5.695 kg have been recovered; the largest piece, estimated to weight about 100 kg, has not yet been found. The meteorite is a fine-grained, holocrystalline, porphyroblastic chondrite. The chondrules, about 15-20 percent of the meteorite, are mostly of enstatite but some are of olivine and a few are mixed. The mineralogy is described. The Usti nad Orlici chondrite, weighing 1.26 kg, fell on June 12, 1963, in a garden in eastern Bohemia, forming a crater 30 cm across and 40 cm deep. Mineralogical and chemical studies are not yet completed. (From *Geophysical Abstracts*, No. 236).

Turner, G., Miller, J.A., and Grasty, R.L., 1966, The thermal history of the Bruderheim meteorite: *Earth and Planetary Science Letters*, V. 1, No. 4, p. 155-157.

Using an activation technique it is possible to show that the spatial distributions of K and radiogenic  $^{40}\text{Ar}$  in the meteorite Bruderheim are different and to conclude that Bruderheim was heated  $495 \pm 30$  m.y. ago at which time it lost around 90% of its radiogenic  $^{40}\text{Ar}$ .

Urey, H.C., 1966, Biological material in meteorites: a review: *Science*, V. 151, p. 157-166.

A complete review of the present stage of knowledge of organic material in meteorites is presented. The most acceptable hypothesis at present is contamination of the lunar surface with terrestrial water and primitive organic matter and later impact ejection from the lunar gravity field to land on the earth's surface.

Vdovykin, G.P., 1964, Some results of the study of the mineral composition of 12 carbon-bearing meteorites: *Akademiia Nauk SSSR Meteoritika*, No. 25, p. 134-155.

Results of X-ray investigations of 12 carbon-bearing meteorites are presented. These include the Murray and Mighei carbonaceous chondrites, the Ghubara chondrite, the unaltered chondrites Kainsaz, Krymka, Sevryukova, and Farmington, the crystalline chondrites Kul'p and Gilgoin, the Dyalpur ureilite, and carbonaceous globules from the Yarymlinskiy (Arus) and Burgavli meteorites; diamonds from Novyy Urey and Goalpara are also discussed. (From Geophysical Abstracts, No. 217).

Vdovykin, G.P., 1965, On the origin of the carbonaceous chondrites: *Akademiia Nauk SSSR Meteoritika*, No. 26, p. 151-168.

It is argued that the carbonaceous chondrites, like the other types of meteorites, are fragments of asteroid bodies which had become somewhat differentiated at an earlier stage of their development; they come from the outer zones of the parent asteroids. (From Geophysical Abstracts, No. 236).

Verniani, F., 1966, Meteor masses and luminosity: Special Report No. 219, Smithsonian Astrophysical Observatory, Cambridge, Massachusetts.

In 1961 the author published a study of the meteor luminous efficiency based on Harvard's photographic data. This paper presents a more sophisticated analysis of the same data since it takes better into account the effects of fragmentation. The luminous efficiency  $\tau_p$  can be expressed as a function of velocity simply as  $\tau_p = 1.0 \times 10^{-10} v$ , with  $v$  in  $\text{cm sec}^{-1}$  and the luminosity expressed in units of 0-mag stars. The uncertainty is  $\pm 0.1$  in the velocity exponent and about 40 percent in the coefficient. In the mass range  $10^{-2}$  - 30 g, the luminous efficiency does not depend either on mass or on brightness, nor does it show any appreciable variation in the course of the trajectory. The coefficient,  $\tau_{\text{top}} = 1 \times 10^{-10} \text{ 0 mag g}^{-1} \text{ cm}^3 \text{ sec}^4$ , has been established by means of the data on three asteroidal meteors. Most meteors, both sporadic and shower, have an average density in the vicinity of  $0.2 \text{ g cm}^{-3}$ . It appears, however, that a small group of sporadic meteors in very short orbits exists, with higher densities of the order of  $1 \text{ g cm}^{-3}$ . Because of selection effects, it is impossible to estimate the actual consistency of this group; it is clear, however, that it must represent a very small minority of cometary meteors.

Verniani, F., 1966, Physical characteristics of 320 faint radio meteors: *Journal of Geophysical Research*, V. 71, p. 2749-2761.

Results are presented of an analysis of the physical characteristics of 320 very small meteors (mean mass:  $\sim 10^{-4}$  g) observed under the Harvard Radio Meteor Project. The meteors have been detected from at least three different stations. Each station yields instantaneous values of the velocity  $v$  and of the electron line density  $q$  in the trail that permit the determination of the mean deceleration and a sketch of the ionization curve. In turn, from the determination of the total ionization produced by the meteor its initial mass  $m_0$  is computed. It is therefore possible for the first time to derive values for the density and ablation coefficient of radio meteors. Analysis of the magnitudes and heights reveals the common occurrence of fragmentation among the meteors of the sample. The maximum electron line density  $q_m$  is found to be proportional to  $m_0^{0.7} v^{0.3}$  instead of to  $m_0 v^4$ , as predicted by the classical theory. Moreover, the observed  $q_m$  is systematically larger than its theoretical value by a factor of 2. Consequently, the observed magnitudes are 0.8 magnitude brighter than theoretically expected. The height of maximum ionization is 2.5 km higher than the theoretical value; its dependence on velocity is not too anomalous. The average length (10 km) and duration (0.3 sec) of the meteors of the present sample are only 40% of the expected theoretical values. The computed densities are affected by large random errors, due principally to the inaccuracy of the heights. The median value,  $0.8 \text{ g/cm}^3$ , confirms the fragile structure of these particles. The ablation



coefficients are remarkably lower than those of faint photographic meteors and show a strong dependence on velocity.

Vliding, H.A., 1965, Meteoritic dust at the base of Cambrian sandstones of Estonia: *Akademiia Nauk SSSR Meteoritika*, No. 26, p. 132-139.

In investigations of the minerals of the heavy fraction of Paleozoic and Quaternary clastic rocks from Estonia, individual magnetic spherules have occasionally been encountered which resemble meteorite dust, but their rarity has precluded detailed analysis. In 1963 a considerable number of such particles were found in a terrigenous Cambrian sandstone recovered from 324-326 m depth in a borehole, directly overlying the weathered Precambrian surface. These particles are described. They comprise about 0.2 percent by weight of the rock, from which it is estimated that more than 5 kg of meteoritic particles fell per sq m. It is believed that they were formed upon pulverization of a single giant meteorite, in late Precambrian or Early Cambrian time, rather than by concentration of slowly accumulated extraterrestrial dust. Their preservation is attributed to quick burial. (From *Geophysical Abstracts*, No. 236).

Vinogradov, A.P., and Zadorozhnyy, I.K., 1965, Cosmogenic, radiogenic, and primordial inert gases in stone meteorites: *Akademiia Nauk SSSR Meteoritika*, No. 26, p. 77-90.

Most stone meteorites contain inert gases of three different origins--primordial, cosmogenic, and radiogenic--and may also absorb small amounts of atmospheric argon. The primordial gases usually are argon and the heavier inert gases, very rarely He and Ne. The content and isotopic composition of the cosmogenic gases depends on the intensity and energy spectrum of cosmic radiation, duration of exposure, and shielding effect and chemical composition of the meteorites. The radiogenic ages determined from the  $\text{He}^3\text{-H}^3$  and  $\text{Ne}^{21}\text{-Na}^{22}$  isotopes correspond to within 30 percent. There is no clustering of radiogenic ages, but they generally tend to be low; about 73 percent are  $<10$  m.y. The bronzite and hypersthene chondrites are distinctly different; the lower radiogenic ages of the latter could be due to greater loss of radiogenic gases. The mechanism of formation of both groups is discussed. (From *Geophysical Abstracts*, No. 237).

Vinogradov, A.P., Vdovkin, G.P., and Popov, N.M., 1965, Investigation of the carbonaceous matter of meteorites by microdiffraction with ultra-fast electrons: *Geochemistry International*, V. 2, p. 249-253 (English translation from *Geokhimiya*, No. 4, p. 387-389, 1965).

An electron microscope using 557 Kev electrons was used to determine that the carbonaceous fraction of the carbonaceous chondrites Mighei, Cold Bokkeveld, and Staroe Boriskino, as well as the Novyi Urei and Burgavli meteorites, is principally a mixture of amorphous and crystalline polymers of high molecular weight. Dispersed partially graphitized carbon is also present. The ureilites contain much graphite and some diamond. Photomicrographs and electron diffraction patterns are given. Data on the chemical composition of the carbon-bearing phases will be given later.

Walker, R.M., Fleischer, R.L., Price, P.B., Maurette, M., and Morgan, G., 1966, Study of very heavy cosmic-ray primaries using nuclear tracks in meteorites: *Transactions of the American Geophysical Union*, V. 47, No. 1, p. 132.

Fossil nuclear particle tracks have been found in the silicate phases of some forty meteorites. In most of these meteorites, the fossil tracks are due to slowed down, very heavy cosmic-ray primaries of the iron group. The identification of the tracks with heavy primaries has been made partly from finding positive identifying characteristics expected for heavy ions. Theoretical calculations show

that the observable track length for a stopping heavy ion increases rapidly with increasing mass for ions heavier than a threshold value that lies close to iron. Small numbers of very long tracks have been found, constituting positive evidence for the existence of extremely heavy ions in the primary beam. Preliminary analysis of these results indicates that the abundance of extremely heavy primaries relative to hydrogen is no greater than the universal abundances. (Abstract of a paper presented at the April 1966 meeting of the American Geophysical Union).

Wasson, J.T., 1966, Butler, Missouri: An iron meteorite with extremely high germanium content: *Science*, V. 153, p. 976-978.

This meteorite is found to contain germanium in a concentration 5 times higher than the highest concentration previously measured. The gallium content is also very high.

Wasson, J.T., 1966, Some geochemical considerations regarding the concentrations of siderophilic elements in meteorites: *Transactions of the American Geophysical Union*, V. 47, No. 3, p. 497.

Nickel is the only major element that is always found to be in the metal phase in reduced meteoritic matter. Owing to this fact, the best way to express concentration data for the siderophilic elements is in terms of metal/nickel ratios. When concentration data for the iron meteorites are expressed in this way, the maximum metal/nickel ratios found in the irons are consistently larger than the mean ratios found in the ordinary chondrites but are about the same as the few ratios available for Type I carbonaceous chondrites. This result is interpreted to mean that (1) the parent material for these irons was more rich in siderophilic elements than are the ordinary chondrites; and (2) fractional crystallization within the metal region of the iron-meteorite parent bodies has been of no consequence. (Abstract of a paper presented at the September 1966 meeting of the American Geophysical Union).

Wasson, J.T., Kimberlin, J., Mattschei, P.K., and Groszek, E.J., 1966, Ga, Ge, and other siderophilic elements in iron meteorites: *Transactions of the American Geophysical Union*, V. 47, No. 1, p. 131.

New measurements of Ga, Ge, Ni, Re, Os, and Ir in iron meteorites have been made on members of Ga-Ge groups III and IVa. Neutron activation followed by radiochemical separation has been used in the analysis of all elements except Ni, which was determined by atomic absorption spectrometry. The data will be employed to test the hypothesis that a fully resolved Ga-Ge group will show only a small range of concentration for elements that tend to concentrate in the kamacite and taenite phases. This hypothesis has a strong bearing on the possible origin of the Ga-Ge groups in separate parent bodies. (Abstract of a paper presented at the April 1966 meeting of the American Geophysical Union).

Webster, H.R., Kaiser, T.R., Poole, L.M.G., 1966, Radio-echo observations of the major nighttime meteor streams; II. Geminids: *Monthly Notices of the Royal Astronomical Society*, V. 133, p. 309-319.

Observations of the Geminid meteor shower during December 1962 and 1963 are presented. In addition to the expected Geminid shower on additional activity peak indicating a second active radiant was observed in 1962. Radio magnitude distributions in the range +8.3m to +6.8m were determined as a function of solar longitude for meteors associated with both the true radiant and the second radiant.

Whipple, F.L., 1966, Chondrules: Suggestion concerning the origin: *Science*, V. 153, p. 54-56.

The origin of the chondrules is attributed to lightning in the primitive Laplacian-type nebula.

- Wright, F.W., Hodge, P.W., and Allen, R.V., 1966, Electron-probe analysis of interiors of microscopic spheroids from eruptions of the Mt. Aso, Surtsey, and Kilauea Iki volcanoes: Special Report No. 228, Smithsonian Astrophysical Observatory, Cambridge, Massachusetts.

Interiors of particles collected from fresh volcanic deposits have been analyzed with a microprobe to allow comparison of them with dust of a possibly extraterrestrial origin. We find support for the argument that the majority of the possibly extraterrestrial particles collected in old Greenland ice deposits are not volcanic in origin.

- Yavnel, A.A., 1964, On the abundance of elements in the metallic phase of iron meteorites and in chondrites: Akademiia Nauk SSSR Meteoritika, No. 25, p. 75-89.

All available results of determinations of the abundance (in weight percent) of the elements in iron meteorites and chondrites are compiled in a table; method of analysis and author are indicated for each determination. The elemental concentrations in the two types of meteorites are also plotted as a function of atomic number. The distribution of elements in the metallic phases is governed by their siderophile properties. (From Geophysical Abstracts, No. 217).

- Yavnel, A.A., 1965, On the classification of iron meteorites by structure: Akademiia Nauk SSSR Meteoritika, No. 26, p. 140-145.

A classification of iron meteorites is proposed, based on their primary structure; hexahedrites (with average maximum grain diameter of the  $\alpha$ -phase much more than 50 mm); hexaoctahedrites (10-50 mm); coarse-structured octahedrites (2-10 mm); medium-structured octahedrites (0.5-2.0 mm); fine-structured octahedrites (0.05-0.5 mm); and ataxites (less than 0.05 mm). (From Geophysical Abstracts, No. 236).

- Yavnel, A.A., 1965, Regularities in the composition and structure of meteorites and the problem of their origin: Akademiia Nauk SSSR Meteoritika, No. 26, p. 26-34.

The composition and structure of different types of meteorites, reviewed here, reflect the complex processes of formation of meteorite matter. The regularities noted should be taken into account in formulating hypotheses of the origin of meteorites. (From Geophysical Abstracts, No. 237).

- Yavnel, A.A., 1966, The origin of meteorites (an outline): Soviet Astronomy - A.J., V. 10, No. 3, p. 511-516.

Precise orbit determinations for iron and stony meteorites indicate a relationship with asteroidals, probably with families intersecting Mars' orbit. Various methods of meteorite age determination imply that meteoritic material first formed in the solar system 4.5-4.8 billion years ago. From regularities of chemical composition, structure, gas-retention age, and cosmic age, meteorites may be divided into several groups formed under differing conditions, apparently in several parent bodies. Computations of the cooling rate in these bodies and the occurrence of minerals as pressure indicators in meteorites confirm that the bodies measured only a few hundred kilometers across. Meteorites are considered fragments resulting from mutual collisions of the parent bodies.

- Yudin, I.A., 1964, On the problem of collecting and studying meteor dust: Akademiia Nauk SSSR Meteoritika, No. 25, p. 192-193.

Observational data suggest that meteor dust should be identical in mineral composition and microstructure with the outer melted crust of meteorites. The main methods of distinguishing meteor dust from industrial dust are mineragraphic, spectral, X-ray, and microchemical. Mineragraphic study of silicate meteor dust (the most widespread) can determine its microstructure and the nature and content of opaque minerals; knowing the amount of ore minerals, the percentage of Fe, Ni, and Co in them can be determined by microchemical and spectral analysis, thus indicating whether the origin is meteoric or not. (From Geophysical Abstracts, No. 217).

Yudin, I.A., and Smyshlyayev, S.I., 1964, Chemical-mineragraphic investigation of the opaque minerals of the Norton County and Staroye Pes'yanoye achondrites: *Akademiia Nauk SSSR Meteoritika*, No. 25, p. 96-120.

Results of chemical and mineragraphic study of the Norton County and Staroye Pes'yanoye achondrites are presented. These meteorites were already known to contain kamacite, schreibersite, rhodite, and troilite; taenite, pyrrhotite, daubreelite, osbornite, oldhamite, and chromite are reported for the first time for these meteorites, and ferro-alabandite for the first time in any meteorite. Staroye Pes'yanoye also contains magnomagnetite, goethite, and hydrogoethite as secondary minerals in its outer melted zone. The micro-structures observed in these meteorites belong to five groups: those of brittle deformation, plastic deformation, break-up of solid solutions, replacement textures, and collomorphic textures (in the goethite and hydrogoethite).

Zähringer, J., 1966, Primordial argon and the metamorphism of chondrites: *Earth and Planetary Science Letters*, V. 1, No. 6, p. 379-382.

Carbonaceous and enstatite chondrites contain relatively high amounts of heavy primordial rare gases. The carbonaceous chondrites show a clear correlation between the  $^{36}\text{Ar}$  content and the mineralogical texture as classified by Van Schmus and Wood. The trend of decreasing  $^{36}\text{Ar}$  with increasing degree of metamorphism is also clearly established for the H, L-, and LL- chondrites, but not for the enstatite chondrites. This supports the author's earlier conclusion that all chondrites originally had similar amounts of primordial gases.

Zähringer, J., 1966, Primordial helium detection by microprobe technique: *Earth and Planetary Science Letters*, V. 1, p. 20-22.

The location of primordial rare gases has some important bearings on the trapping mechanism. A microprobe technique was developed to extract the gases in small dimensions; the gases then were detected by a sensitive mass spectrometer behind the diffusion pump of the microprobe. The resultant method has a high sensitivity and shortened delay time between extraction and detection. In preliminary work, 21 mm of the dark phase of the Fayetteville bronzite chondrite has been scanned, yielding a total of 310 He peaks. An interpretation of the data to date indicate it is unlikely that the grains have directly trapped solar wind particles. A shock phenomenon and addition of other less fractionated material, such as a cometary impact, seems to be more favorable to explain the results of this work.

Zähringer, J., 1966, Primordial He distribution by microprobe technique: *Transactions of the American Geophysical Union*, V. 47, No. 2, p. 425.

A new technique is described to study the distribution of He in primordial gas-rich meteorites. A microprobe is used to degas small volumes of the sample. Simultaneously, the He release and the Fe concentration, which gives the composition and the boundaries of the grains, are detected by a sensitive mass spectrometer. Preliminary results obtained from Fayetteville and Kapoeta meteorites show that the He is mainly concentrated at the surfaces of the grains. In addition, however, it was observed that about 40% of the He peaks appeared when the electron beam hit the

inner planes of those grains. The mechanism suggested for the incorporation of the rare gases is discussed in the light of these new results. (Abstract of a paper presented at the April 1966 meeting of the American Geophysical Union).

### 3.5 Moon

#### 3.5.1 General

Goldreich, P., 1966, Dynamics of planet-satellite system: Transactions of the American Geophysical Union, V. 47, No. 1, p. 155.

The origin of natural satellites is discussed as a part of a general dynamical theory of planets and satellites. New calculations of the evolution of the earth-moon system are described. The tidal effective  $Q$ 's of the major planets are shown to be several orders of magnitude larger than that of the earth. (Abstract of a paper presented at the April 1966 meeting of the American Geophysical Union).

Goldreich, P., 1966, Final spin states of planets and satellites: The Astronomical Journal, V. 71, p. 1-7.

The spin of a planet or satellite which is losing angular momentum through tidal friction may approach one of at least two distinct final states. We derive a criterion which determines whether or not the final state will be one of synchronous rotation. If the tidal phase lag is independent of the amplitude and frequency of the tide, then synchronous rotation will result when  $[3(B-A)/CT^2 > (9.5ne^2)]$ . If this inequality is not satisfied, the body will end up spinning with a mean angular velocity which is somewhat larger than its orbital mean motion. This criterion is only slightly altered if the phase lag varies with amplitude and/or frequency. It is easily seen that the moon fails to satisfy the condition for synchronous rotation with the present value of its orbital eccentricity. However, the moon could have attained synchronous rotation if its mean orbital eccentricity was less than 0.041 at some time in the past.

No analytical treatment of commensurate spin states other than synchronous rotation is included in the present investigation. However, the results of a separate study of these commensurate spins are briefly described.

Goldreich, P., 1966, History of the lunar orbit: Reviews of Geophysics, V. 4, No. 4, p. 411-439.

A method of calculating the past states of the earth-moon system is developed. The method is based on the existence of three distinct time scales for dynamical change. The short time scale is determined by the revolution periods of the sun and moon about the earth and the intermediate scale by the precessional motions of the lunar orbit plane and the earth's equator plane. The long time scale is defined by the rate at which tidal friction alters the state of the earth-moon system. The equations of motion governing the earth-moon system are successively averaged over the short and then the intermediate time scales. These averaged equations are then integrated back a short interval on the long time scale. At present, the inclination of the lunar orbit plane to the ecliptic remains nearly constant during the precessional motion. This investigation shows that this inclination could never have been less than  $10^\circ$  and, therefore, that the moon could never have moved on an equatorial orbit. This result contradicts theories that postulate fission of the earth to form the moon and also those which propose that the moon formed by accretion within 10 earth radii.



Soldraich, F., and Peale, S.J., 1966, Resonant spins in the solar system: Transactions of the American Geophysical Union, V. 47, No. 1, p. 154.

The effects of gravitational torques on spinning non-axisymmetric planets and satellites are investigated in detail. A stability criterion is derived for the maintenance of a planetary or satellite spin angular velocity, which is commensurate with its mean motion. Spin angular velocities that are half and whole integral multiples of orbital angular velocities are shown to be stable for even very slight deviations from axial symmetry. An analytical method is developed for determining the probability of a planet's or satellite's being captured into such a resonant spin state, as the spin is decreased by tidal friction. The dependence of this capture probability on orbital eccentricity is also discussed. Numerical results are given for Mercury and the moon. A similar analysis gives a stability criterion for a Venusian spin that is resonant with the synodic motion of Venus. (Abstract of a paper presented at the April 1966 meeting of the American Geophysical Union).

Hide, R., 1966, Planetary magnetic fields: Planetary and Space Science, V. 14, No. 7, p. 179-186.

Present knowledge and modern theories of the earth's main magnetic field are outlined and the state of knowledge of the magnetic fields of the other planets is sketched. Little is known of planetary magnetic fields other than for the earth and Jupiter, although magnetometer data from Mariner II and Mariner IV may set an upper limit to the magnetic fields of Venus and Mars, respectively. Lunick II data indicates the surface magnetic field of the moon may be less than  $10^{-8}$  G. Decameter wavelength radiation has been observed from Jupiter and Saturn only. The effect of the solar wind interacting with planetary magnetic fields is briefly mentioned.

Lamar, D.L., and Merrill, P.M., 1966, Age and origin of earth-moon system revealed by coral growth lines: Transactions of the American Geophysical Union, V. 47, No. 3, p. 1186.

Groupings of diurnal growth lines on Middle Devonian corals have been related to monthly and annual periodicities by paleontologists. Assuming conservation of angular momentum and no change in the mass of the earth and moon and earth's moment of inertia, the length of the Middle Devonian day (20.9 to 21.7 hours) is determined from counts of the number of days in the synodic month and application of Kepler's third law. The growth line studies are consistent with an intermediate value of the lunar torque and tidal friction divided equally between ocean currents and body tides since Middle Devonian and suggest that the earth-moon system originated between 0.7 and 1.0 billion years ago. The absence of evidence of a catastrophic event in late Precambrian rocks favors the aggregation-of-many-moons and capture-at-a-distance theories of lunar origin rather than the fission or close-capture theories. (Abstract of a paper presented at the September 1966 meeting of the American Geophysical Union).

Levin, B.Yu., 1966, The structure of the moon: Soviet Astronomy - A.J., V. 10, No. 3, p. 479-491.

This paper presents a survey dealing with the origin of the moon, the tidal evolution of the earth-moon system, the history of bombardment of the lunar surface and the thermal history of its interior, the figure of the moon, the density distribution along its radius, the composition of the moon, and the history of its atmosphere.

O'Keefe, J.A., 1966, Lunar questions discussed at Pasadena: Sky and Telescope, V. 31, p. 10-12.

A popular summary of a conference held in September 1965: Various authors discussed the origin of the craters, the heat balance of the moon, the origin of tektites and other lunar problems.

Smith, W.B., Shapiro, I.I., and Ash, M.E., 1966, Preliminary results from processing radar and optical planetary observations: *The Astronomical Journal*, V. 71, p. 871-872.

Preliminary values of a number of astronomical constants have been obtained from the simultaneous processing of planetary radar data spanning the interval from 1959 to July 1966 and of U.S. Naval Observatory optical data extending from 1950 to 1965. Results obtained using general relativity (Newtonian) theory with their formal standard errors are: a.u., 499.004786 (499.004785) + 0.000005 light-sec; Mercury radius, 2434 (2440) + 2 km; Venus radius, 6056 (6056) + 1 km; Mercury mass, 6021000 (6029000) + 53000; Venus mass, 408250 (408450) + 120; earth plus moon mass, 328900 (328950) + 60; Mars mass, 3111000 (3107000) + 9000; earth-moon mass ratio, 81.3030 (81.3024) + 0.005. The planetary masses are given as inverses in terms of the solar mass. (Abstract of a paper presented at the July 1966 meeting of the American Astronomical Society).

Tatsch, J.H., 1966, Certain correlations between selenophysical observations and deductions arrived at from applying a dual primeval planet model to the earth-moon system: *Transactions of the American Geophysical Union*, V. 47, No. 3, p. 486.

A dual primeval planet model was developed in 1959 for the purpose of attempting to explain the retrograde motion of Jupiter's outer satellites and the anomalous behavior of certain other planetary satellites. The basic model has been extended, both in depth and on regional bases, to certain selected areas of the earth and to the earth-moon system. This paper describes the specific correlations found between selenophysical observations and deductions arrived at from applying a dual primeval planet model to the earth-moon system. (Abstract of a paper presented at the September 1966 meeting of the American Geophysical Union).

### 3.5.2 Atmosphere

Cameron, W.S., 1966, Operation Moon-Blink: *The Astronomical Journal*, V. 71, p. 379.

Operation Moon-Blink is a project to develop, fabricate, and test James Edson's concept of using a blink technique to detect lunar color phenomena with a rotating two-color filter wheel. The filtered transmission is passed onto an image-converter tube whose face may be viewed or photographed directly. The whole unit is attached to the telescope at its focus. A color phenomenon is seen as a black, blinking area. In progress is the development of a multi-purpose detector, composed of a camera, polarimeter, spectrograph, and infrared detector, each to be successively rotated into the focal plane during an event. When completed, it will give the first multifaceted assault on the nature of these phenomena.

Many other reports of transient phenomena have been received, details of which are presented in tabular form. The last Moon-Blink observation was made on 15 November 1965. It marked the first completely successful Confirmation Network alert; two visual partial confirmations were received. Also, photographs and radio data were obtained. These observations are discussed in some detail. Other groups on the Moon-Blink Network have also been successful in photographing transitory phenomena in the Aristarchus region. (Abstract of a paper presented at the March 1966 meeting of the American Astronomical Society).

Milford, S.N., and Pomilla, F.R., 1966, Contamination of the lunar atmosphere by rocket exhaust gases: Transactions of the American Geophysical Union, V. 47, No. 1, p. 155.

During the lunar landing phase of the Apollo mission, the exhaust gases from the lunar excursion module (LEM) will be distributed in the lunar atmosphere and interplanetary space, as well as on the lunar surface. Estimates are being made of the contamination of the ambient lunar atmosphere by the exhaust gases. During the LEM stay time the contamination of the atmosphere is shown to be both appreciable and non-uniform in distribution, with the subsequent trend toward a uniform distribution proceeding at different rates for different exhaust gas species. (Abstract of a paper presented at the April 1966 meeting of the American Geophysical Union).

Vogel, U., 1966, Molecular fluxes in the lunar atmosphere: Planetary and Space Science, V. 14, No. 12, p. 1233-1252.

The properties of a neutral lunar atmosphere are investigated theoretically. A non-uniformity is shown to result from the temperature variations and non-uniform gas source distribution on the surface of the moon. An integral equation governing the distribution of molecular fluxes, in the steady state, is formulated. This equation is solved by computer and analytical methods. Solutions are obtained and discussed for mass numbers ranging from hydrogen to the heavy gases. It is concluded that in all cases a marked anisotropy of molecular fluxes can be expected. By measuring these fluxes, conclusions can be drawn about the distribution of gas sources, the physical properties of the surface and the composition of the lunar atmosphere.

Werner, M., Gold, T., and Harwit, M., 1966, Detection of water on the moon: The Astronomical Journal, V. 71, p. 875-876.

If water percolates up from the interior of the moon and evaporates from its surface it may be indirectly detected by coronagraphic observations. The technique we propose involves a search for the OH radical produced by the dissociation of lunar  $H_2O$ . One should be able to observe the O-O and I-I vibrational bands covering the range from 3075 to 3105 Å and 3135 to 3160 Å, respectively, provided OH is sufficiently abundant. Both these bands are observed in cometary spectra. In computing the minimum detectable amount of OH we have made use of published figures on (a) the night sky brightness at 3100 Å, and (b) atmospheric light scattering coefficients obtained from solar coronagraphic work. The minimum detectable value of OH is found to be of the order of  $5 \times 10^4/cm^2$  under the most favorable observing conditions. We have computed the dissociation rate of  $H_2O$  and the mean life of the OH radical in the vicinity of the moon.

For a given rate of outgassing of water out of the moon the amount of OH to be expected depends upon the unknown probabilities for the formation of  $H_2O$  at each contact of an OH molecule with the lunar surface. Outgassing rates similar to those appropriate for the earth may lead to observable results. (Abstract of a paper presented at the July 1966 meeting of the American Astronomical Society).

### 3.5.3 Figure and Internal Structure

Anderson, D.L., and Kovach, R.L., 1966, The interiors of the moon and terrestrial planets: Transactions of the American Geophysical Union, V. 47, No. 1, p. 155.

Present information regarding the composition and strength of the interior of the earth is used to discuss the interiors of the moon and terrestrial planets. Results strongly suggest homogeneity of the Fe/Si ratio in the inner part of the solar system. The mass versus density function is determined for iron-rich



silicate planets with different degrees of oxidation, and the results are compared with the terrestrial planets. The properties of Mars, Venus, and the earth are all consistent with the assumption of early uniformity of the solar system. The data for Mars slightly favor the hypothesis that Mars is more oxidized than the earth, but the uncertainty in the radius of Mars also allows the composition to be the same as the earth's. Contrary to current thoughts, the shape of the moon implies that it is weaker than the earth; this is consistent with thermal calculations. Using the earth's mantle as a model, the density and elastic properties are calculated for the interior of the moon. Density and velocity decrease with depth throughout most of the moon. (Abstract of a paper presented at the April 1966 meeting of the American Geophysical Union).

Bray, T.A., and Goudas, C.L., 1966, A contour map based on the Selenodetic Control System of ACIC: *Icarus*, V. 5, p. 526-535.

The control system published in 1965 by ACIC has recently been augmented by more than 100 points. The analysis has led to no improvement in regard to the values of the two known harmonic coefficients of second order. This is probably caused by the uneven distribution of the additional data. Nevertheless, the contour map constructed on their basis exhibits substantial consistence with the one constructed from only the 196 points of the original system.

Carson, D., Davidson, M., Goudas, C.L., Kopal, Z., and Stoddard, L.G., 1966, Lunar profiles determined from annular solar eclipses of 1962 and 1963: *Icarus*, V. 5, p. 334-359.

The present paper contains a discussion of the techniques of measurements and the result of reductions of the photographs of the annular solar eclipses observed on July 31, 1962. The lunar profile deduced from the 1962 eclipse plates was found to be insufficiently well defined due to the effects of irradiation. The 1963 eclipse plates were, however, largely free from this defect, and their analysis led to satisfactory results.

The outcome of the reductions revealed that the deviations of the lunar profile from a circle were of the form  $+0.54 \sin 2\beta - 0.16 \cos 2\beta + 0.27 \sin 3\beta - 0.05 \cos 3\beta - 0.16 \sin 4\beta + 0.11 \cos 4\beta$ , where  $\beta$  denotes the lunar position angle measured from the eastern part of the equator in the counter clockwise direction. The elliptical component of the profile is found to have its major axis inclined by approximately  $37^\circ$  to the lunar axis of rotation.

Goudas, C.L., 1966, Note on "Shape and Internal Structure of the moon" by Lamar and McGann: *Icarus*, V. 5, p. 99-101.

The mentioned paper is discussed. The statement that the lunar continents are 3 km higher than the maria is questioned.

Goudas, C.L., and Kopal, Z., 1966, Shape of the moon from the orbiter determination of its gravitational field: *Nature*, V. 212, p. 271.

An analysis of the perturbations of the American Orbiter I, revolving since August 14 in a 200 min orbit close to the moon, has led to a satisfactory determination of the principal characteristics of the lunar gravitational field. These are compared with previous predictions based on plausible physical assumptions, and show a close correspondence. Several other properties of the lunar globe are discussed with reference to results so far available.

Lamar, D.L., and McGann, J., 1966, Shape and internal structure of the moon: *Icarus*, V. 5, p. 10-23.

Studies of the libration of points on the moon's surface and the occultation of stars on the limb reveal a 10-km range in heights on the moon's surface. The continental areas are approximately 3 km higher than the maria. A concentration of material in the equatorial regions and around the axis must exist pointing toward the earth. The actual continental-maria distribution is opposite to that required to explain the moment-of-inertia data. The density variations and internal structures, as envisioned by Urey, Elsasser, and Rochester (1959), and a moon in isostatic equilibrium and thermal convection are calculated. It is found that either model of internal structure is consistent with our knowledge of the moon.

Levin, B.Yu., 1966, The structure of the moon: *Soviet Astronomy - A.J.*, V. 10, No. 3, p. 479-491.

This paper presents a survey dealing with the origin of the moon, the tidal evolution of the earth-moon system, the history of bombardment of the lunar surface and the thermal history of its interior, the figure of the moon, the density distribution along its radius, the composition of the moon, and the history of its atmosphere.

Michael, W.H., Jr., Tolson, R.H., and Gajcynski, J.P., 1966, Lunar orbiter: Tracking data indicate properties of moon's gravitational field: *Science*, V. 153, p. 1102-1103.

Preliminary investigations on the first U.S. satellite of the moon indicate that the lunar field has a large pear-shaped component.

Michelson, I., 1966, Augmented lunar tide heights in barycentric motion: *Monthly Notices of the Royal Astronomical Society*, V. 133, p. 17-20.

Lunar tide theory is generally written as if lunar centroid could be considered as an inertial reference. Earth-Moon barycenter is less objectionable, and elementary calculation shows that the "universal coefficient" is thereby increased a full order of magnitude--the factor is roughly one-third the Earth-Moon mass ratio. This is in substantial agreement with findings by M. Nahas.

Michelson, I., 1966, Reduced lunar equatorial principal inertia moment difference related to inclination angles: *The Astronomical Journal*, V. 71, p. 171.

Estimates of the mechanical ellipticity of the lunar equator furnished by the theory of the moon's physical librations in longitude have been subject to considerable revision and great uncertainty. In the past 150 yr accepted values of this quantity have been reduced in stages by roughly one full order of magnitude, while uncertainty limits are now taken as about 50% of the value itself. The greater values obtained from early observations, and now largely discredited, presupposed libration amplitudes that are now also regarded as excessive. Inconsistency with values deduced from liquid ellipsoid potentials induced Laplace to conclude that the moon could not have been primitively fluid.

When physical librations are analyzed by admitting the possibility of such small libration amplitudes as now seem probable, the sun's importance in determining lunar rotational motion is much enhanced. In addition to providing an improved physical basis for Cassini's laws, it is shown that the equatorial principal-moment difference does not require the separate treatment that it has customarily received. Both the largest (polar) difference and the equatorial difference are seen to be expressible in terms of the inclination angles of the moon's orbit and its equator, without reference to inequalities of orbital motion and related observations of doubtful accuracy used in the past. Short-period data from moon-based reflectors can be expected to facilitate greatly improved estimates of the constants of physical libration. (Abstract of a paper presented at the December 1965 meeting of the American Astronomical Society).

Middlehurst, B.M., 1966, An analysis of lunar events: Transactions of the American Geophysical Union, V. 47 No. 1, p. 150.

Recently, well substantiated reports of color changes and other evidence of lunar activity have led to increased interest in the possibility that the moon is not entirely inert. About 200 events, most in the 18th, 19th, and 20th centuries, are analyzed from the following points of view: (1) type of event, (2) lunar phase, (3) relative frequency and duration, (4) correlation with solar activity, (5) position in the lunar orbit around the earth, (6) positions on the face of the moon of the sites of the events. Evidence is presented suggesting that the onset of a lunar event may be associated with disturbance of the lunar crust. A correlation with lunar tides has been found. Physical conditions in the lunar surface layers are, however, almost unknown; therefore, many uncertainties remain. (Abstract of a paper presented at the April 1966 meeting of the American Geophysical Union).

Middlehurst, M., 1966, Transient lunar events: possible causes: Nature, V. 209, p. 602.

The author has analyzed lunar transient events from 1749 to 1964 with respect to monthly sunspot numbers and finds no correlation. However, the author finds that there are indications that internal lunar causes have been, and still may be significant, and that lunar events may be initiated by tidal cracking (near perigee--the corresponding time on earth is high tide) or at periods of maximal crustal relaxation (near apogee, which corresponds to low tide on the earth) with consequent release of hot or cold gases.

Mikhailov, A.A., 1966, Gravitational force and the moon's figure: Soviet Astronomy - A.J., V. 9, p. 819-823.

The figure of the moon is not a level surface corresponding to its rotation speed; the Clairaut theorem is consequently not applicable for deriving the normal force of gravity on the lunar surface. Since the moon is almost homogeneous, formulas can be used for the attraction of a triaxial ellipsoid by substituting for the lunar mass  $GM = 4,902,866 \cdot 10^9$  and the semiaxis values. We thereby obtain formulas for various values of the different moments of inertia associated with the constant  $f$  and yielding the normal gravitational force as a function of the latitude  $\phi$  and the longitude  $\lambda$ . The profile of the lunar limb is found from Goudas' formula for the expansion of the lunar topography on the visible lunar hemisphere using Frantz' measurements.

Runcorn, S.K., 1966, The figure of the moon: Transactions of the American Geophysical Union, V. 47, No. 3, p. 486.

Controversy on the reality of a lunar bulge has gone on for a century. Recently the heights of points on the lunar surface have been analyzed by Z. Kopal using spherical harmonics, and, because the fourth harmonic is larger than the second, talk of a "bulge" has been held to be meaningless. This result is shown to arise from the failure to use Baldwin's procedure of separating points on the maria from those on the uplands. When this is done the two mean surfaces so defined are approximately ellipsoidal, with ellipticities over twice that of the dynamical value. The significance of this result in terms of the moon's internal structure is discussed. It is inferred that convection, described by a second harmonic, is occurring inside the moon. (Abstract of a paper presented at the September 1966 meeting of the American Geophysical Union).

Salisbury, W.W., 1966, A method of translunar radio communication: Nature, V. 211, p. 950-951.

The author discusses the possibility of using sublunar surface materials as propagation medium for translunar communications, because extended radio coverage about the lithosphere will not be possible because of the lack of atmosphere. It is suggested that a small unmanned lunar satellite could be used as a vehicle to determine the feasibility of a miniature and simple system of translunar voice communication, and at the same time could considerably increase our knowledge of the internal structure of the moon.

Shimazu, Y., 1966, Survival time of lunar surface irregularities and viscosity distribution within the moon: *Icarus*, V. 5, p. 455-458.

The survival time of lunar surface irregularities is discussed. For simplicity, a two-layer model for which viscosity is constant in each layer is considered. Graphs are presented solving the problem for different viscosities.

Vand, V., 1966, Monro jets and the origin of tektites: *Nature*, V. 209, p. 496.

The author had previously proposed a detailed mechanism of a tektite jet formation through an implosion of a conical cavity lined with molten glass, which is formed immediately after impact, and showed that a jet of tektites can survive the upward atmospheric journey if of sufficient total mass.

Using the results of other authors on jets formed from imploding bubbles, he elucidates the operating mechanism and applies it to Riess Kessel, and speculates that the general inward motion of other crater materials caused by the passage of waves reflected from below will also be responsible for the formation of a central peak in some craters, if underlain by denser strata at favourable depth. The author also states that similar interpretation of central peaks of lunar craters might help in mapping such discontinuities under the lunar surface.

Zharkov, V.N., Berikashvili, V.Sh., and Osnach, A.I., 1966, Geophysical problems and lunar investigations: *Soviet Astronomy - A.J.*, V. 10, No. 3, p. 492-510.

In recent years geophysicists have vigorously undertaken a study of the applicability of geophysical methods for the study of the internal structure of the moon and planets. This review briefly sets forth a number of conclusions drawn by investigators on the basis of theory. Part I, "Lunar Seismic Experiment", considers the following problems: principal concepts of seismology, lunar seismic activity and its sources, distribution of seismic wave velocities in the moon, travel-time curves and amplitude distributions of body waves in the moon, natural oscillations of the moon and surface waves. This is followed by consideration of lunar tides in relation to different variants of lunar internal structure. Finally, the review considers the problem of a liquid core and a lunar magnetic field.

### 3.5.4 Changes

Blizard, J.B., 1966, Spatial distribution of lunar transient event regions: *Transactions of the American Geophysical Union*, V. 47, No. 3, p. 487.

Lunar transient events tend to occur when the moon is near perigee. It has been suggested that tidal force is a cause of fissuring, which leads to transient events. The tidal force normal to the surface was calculated for different active regions. A statistical analysis showed that active regions are six times more frequent per unit area near the moon's center than in the limb regions. There is a progressive decrease in events with distance from the center to the limb. The tidal force normal component is greatest near the center of the disk. The location of transient event regions by quadrant was also studied. An interpretation is that the transient event regions are located preferentially on or



near the maria, which show a similar distribution by quadrant. (Abstract of a paper presented at the September 1966 meeting of the American Geophysical Union).

Burley, J., and Middlehurst, B.M., 1966, Apparent lunar activity: Proceedings of the National Academy of Sciences, V. 55, p. 1007-1011.

The authors find a correlation of lunar activity with tidal disruption, and conclude that the events are probably due to internal causes. No correlation with sunspot numbers was discovered.

Cameron, W.S., 1966, Operation Moon-Blink: The Astronomical Journal, V. 71, p. 379.

Operation Moon-Blink is a project to develop, fabricate, and test James Edson's concept of using a blink technique to detect lunar color phenomena with a rotating two-color filter wheel. The filtered transmission is passed onto an image-converter tube whose face may be viewed or photographed directly. The whole unit is attached to the telescope at its focus. A color phenomenon is seen as a black, blinking area. In progress is the development of a multi-purpose detector, composed of a camera, polarimeter, spectrograph, and infrared detector, each to be successively rotated into the focal plane during an event. When complete, it will give the first multi-faceted assault on the nature of these phenomena.

I have received many other reports of transient phenomena, details of which are presented in tabular form. The last Moon-Blink observation was made on 15 November 1965. It marked the first completely successful Confirmation Network alert; two visual partial confirmations were received. Also, photographs and radio data were obtained. These observations are discussed in some detail. Other groups on the Moon-Blink Network have also been successful in photographing transitory phenomena in the Aristarchus region. (Abstract of a paper presented at the March 1966 meeting of the American Astronomical Society).

Dobar, W.L., 1966, Simulated basalt and granite magma upwelled in vacuum: Icarus, V. 5, p. 399-405.

The upwelling and solidification of a simulated basalt and granite magma in vacuum has produced a porous material not found in nature. The photometric curves of the upwelled samples show excellent correlation with the photometric curves of the lunar surface. The visible colors associated with the simulated magma during vacuum upwelling matches the visual observations of the color phenomena observed on the lunar surface in October and November of 1964.

Geake, J.E., and Walker, G., 1966, Reply to "Luminescence caused by proton impact with special reference to the Lunar Surface": Nature, V. 211, p. 471-472.

In this reply, the authors contend that Schutten and Van Dijk do not give enough information for Geake and Walker to attempt an explanation of their results, except to say that the results seem consistent with the use of high beam current density. Geake and Walker are surprised at Schutten and Van Dijk's selection of meteorites chosen for comparison, because of their low luminescence efficiency. They point out that the reason very little luminescence was observed is probably because the samples were damaged by the high beam current, which results in greatly reduced efficiency and a changed spectrum; as well as because the spectral range used did not include the region where highest efficiency had been observed.

Hynek, J.A., and Dunlap, J.R., 1966, A lunar transient phenomena detection program: The Astronomical Journal, V. 71, p. 389.

A program designed to detect and photographically record transient color or albedo changes which may take place on the lunar surface is in progress at the Corralitos Observatory near Las Cruces, New Mexico.

The image orthicon camera, in a closed circuit television chain, is placed at the Cassegrain focus of a 24-inch telescope. Interference filters, with sharp wavelength cutoff characteristics, are continuously and automatically alternated in the optical path. The resulting "blink" images in two or more regions of the visible spectrum are viewed on a large TV monitor which displays a 6 x 6 minute of arc lunar region. Each scan line corresponds to 0.5 arc. A separate telescope and television chain are employed to simultaneously monitor the moon in the near infrared from 0.7 to 1.1  $\mu$ .

Since initiation of the program, in October 1965, efforts of the Corralitos staff to detect any lunar surface changes have been negative. Suspected lunar changes, reported mainly through continuous monitoring of the short-wave radio "astro-net" have not been confirmed. The planet Jupiter, used frequently as a test and calibration source, shows a very pronounced blinking of the great red spot and more subtle but easily detectable changes in the equatorial and other regions of the planet. Star pairs, also used as test sources, display a "blink" image proportional to their spectral classification difference. (Abstract of a paper presented at the March 1966 meeting of the American Astronomical Society).

Middlehurst, B.M., 1966, An analysis of lunar events: Transactions of the American Geophysical Union, V. 47, No. 1, p. 150.

Recently, well substantiated reports of color changes and other evidence of lunar activity have led to increased interest in the possibility that the moon is not entirely inert. About 200 events, most in the 18th, 19th, and 20th centuries, are analyzed from the following points of view: (1) type of event, (2) lunar phase, (3) relative frequency and duration, (4) correlation with solar activity, (5) position in the lunar orbit around the earth, (6) positions on the face of the moon of the sites of the events. Evidence is presented suggesting that the onset of a lunar event may be associated with disturbance of the lunar crust. A correlation with lunar tides has been found. Physical conditions in the lunar surface layers are, however, almost unknown; therefore, many uncertainties remain. (Abstract of a paper presented at the April 1966 meeting of the American Geophysical Union).

Middlehurst, M., 1966, Transient lunar events: possible causes: Nature, V. 209, p. 602.

The author has analyzed lunar transient events from 1749 to 1964 with respect to monthly sunspot numbers and finds no correlation. However, the author finds that there are indications that internal lunar causes have been and still may be significant and that lunar events may be initiated by tidal cracking (near perigee--the corresponding time on earth is high tide) or at periods of maximal crustal relaxation (near apogee, which corresponds to low tide on the earth) with consequent release of hot or cold gases.

Nash, D.B., 1966, Proton-excited luminescence of silicates: experimental results and lunar implications: Journal of Geophysical Research, V. 71, p. 2517-2534.

Spectral energy distributions and excitation efficiencies as functions of mineral composition, irradiation time, proton energy, proton flux, sample geometry, and sample temperature have been determined from laboratory measurements of silicate luminescence spectrums of many silicates under continuous excitation by 5-keV protons is in the red when the mineral is first excited; the luminescence intensity decreases, and the maximum shifts from red to blue with time. This phenomenon is here described as a red flash. After the initial red flash, a second red flash,

subsequent intensity decay, and blue shift can be produced by a sudden increase of incident ion energy. In both cases the red flash has a principal decay period of about 15 to 20 minutes. The intensity of both the flash and aged luminescence response is directly proportional to incident ion energy and flux. Small particle size for powders, high roughness for solid surfaces, and low mineral temperature favor high luminescence intensity. These data qualitatively agree with the concept of solar-ion excitation as the origin of reported transient lunar reddening near Aristarchus and Kepler. However, these measurements show that the energy efficiency for proton excitation of silicate luminescence is between  $10^{-4}$  and  $10^{-5}$ ; this range is several orders of magnitude lower than values previously reported. In view of the known solar-ion flux, the low efficiencies indicate that luminescence on the sunlit lunar surface resulting from solar-ion excitation is far below the sensitivity of earth-based detection apparatus and that other energy sources or other explanations for the origin of lunar color flashes must be sought.

Ney, E.P., Woolf, N.J., and Collins, R.J., 1966, Mechanisms for lunar luminescence: *Journal of Geophysical Research*, V. 71, p. 1787-1793.

The visibility of luminescence on the moon depends on the competing processes that illuminate the moon and that provide energy for luminescence. It is shown that the most favorable times for seeing luminescence are at new moon, on the far side of the moon, and during rare dark eclipses. The luminosity and color of these rare eclipses are explained. Observations supposedly of luminescence during lunar day are criticized, and only the spectroscopic evidence is taken to support the reality of luminescence. Both direct and storage processes have been considered for converting energy to luminescence. Direct processes in lunar day cannot be energized by presently known sources of particles. If indirect processes occur they may give information about the dust particles at the extreme lunar surface.

Petrova, N.N., 1966, Spectrophotometric study of the lunar surface: *Soviet Astronomy* - A.J., V. 10, No. 1, p. 128-135.

Observations with the photoelectric spectrophotometer of the Astrophysical Institute of the Kazakh Academy of Sciences are reported for 11 areas on the lunar surface. The relative spectral distribution of the reflectivity is derived by comparing the lunar spectra with spectra of early-type stars and the sun. In general, the reflectivity varies almost linearly with wavelength; for similar inclinations, the same spectrum obtains for the brightness coefficients of certain terrestrial substances containing considerable quartz and other siliceous compounds. Direct comparison of spectra shows that lunar formations generally differ negligibly in color, but the curves for the spectral brightness ratios are not always monotonic, exhibiting several waves and humps. The humps in two spectral regions (at  $\lambda_{\text{max}} \approx 5305$  and  $6680 \text{ \AA}$ ) are interpreted as emissions excited by solar irradiation of the lunar surface. If the variable component of solar corpuscular radiation causes the observed emission variations, the flux estimated from the emission intensity would correspond to a very active sun, which is contrary to published data on solar activity during the period when maximum emission was observed. Photospheric ultraviolet energy would suffice to excite the observed emission, but the variability would then be inherent in the luminous material on the moon itself.

Righini, A., Jr., and Rigutti, M., 1966, Some results of research on lunar luminescence: *Icarus*, V. 5, p. 258-265.

Research on lunar luminescence has been done with a technique similar to that illustrated by Kopal and Rackham. No luminescence phenomena have been observed, but the analysis of the observations has pointed out that some precautions must be taken in order to obtain reliable photographic observations.

Roberts, G.L., 1966, Three-color photoelectric photometry of the moon: *Icarus*, V. 5, p. 555-564.

Preliminary results are described of a program of detailed high-resolution lunar photoelectric photometry. A three-beam photoelectric photometer designed specifically for lunar colorimetric studies is described briefly. Experiments designed to measure short time variations in lunar luminescence gave negative results. This is attributed to lack of solar activity.

Schutten, J., and Van Dijk, Th., 1966, Luminescence caused by proton impact with special reference to the lunar surface: *Nature*, V. 211, p. 470-471.

On the basis of absolute measurements made of the luminescence of meteorites excited by protons in the 30 keV range, the authors believe it is very improbable that even during solar flares, when the intensity of the solar wind is increased by a factor of 100, the observed excitation of lunar luminescence can be caused by proton bombardment. Their laboratory values differ considerably from those of Derham and Geake and this difference is attributed to two possible causes. 1) Because the target consists of insulating material, during proton bombardment a potential drop develops across the target leading to development of secondary electrons with 10% the efficiency of the protons. 2) Background pressure in the apparatus may be a second cause of luminescence due to ionization of the gas leading to creation of electrons. The authors conclude that luminous emission from the lunar surface is not due to solar wind but think it may be caused by electromagnetic radiation of short wavelength.

### 3.5.5 Surface Features

Anonymous, 1966, Lunar orbiter photographs earth and moon: *Sky and Telescope*, V. 32, p. 346-347 and fold out.

The photograph of the earth taken from the moon is presented as a 4 page fold out with notes.

Arthur, D.W.G., Pellicori, R.H., and Wood, C.A., 1966, The system of lunar craters, Quadrant IV: *Communications of the Lunar and Planetary Laboratory*, V. 5, p. 1-208, + 12 pages maps.

The designation, diameter, position, central peak information and state of completeness are listed for each discernible crater with a diameter exceeding 3.5 km in the fourth lunar quadrant. The catalog contains about 8000 items and is illustrated by a map in 11 sections. Names have been given to large or conspicuous craters in the limbs regions. Three previous parts were published as *Commun. L.P.L.* 30, 40, and 50.

Brinkmann, R.T., 1966, Lunar crater distribution from the Ranger 7 photographs: *Journal of Geophysical Research*, V. 71, p. 340.

Crater counts on the Ranger 7 photographs reaffirm the validity of Miller's suggestion that secondary craters are present in significant abundance in the smaller sizes. Fewer craters are detected than were predicted shortward of 100 meters, which may be the result of micrometeoroid erosion.

Cooke, S.R.B., 1966, An unusual lunar dome: *Sky and Telescope*, V. 32, p. 111.

A drawing of an unusual lunar dome, in *Oceans Procellarum*, with a "collapsed" area on one side is presented.



Cross, C.A., 1966, The size distribution of lunar craters: Monthly Notices of the Royal Astronomical Society, V. 131, p. 245-252.

A total of 1600 craters from .65 to 69,000 meters diameter have been measured, on Ranger photographs of three areas of the moon. The results show that in all three areas the frequency of crater occurrence is inversely proportional to the square of the crater diameter, and that this relation holds accurately over the whole size range. The overall crater frequency is shown to be lowest in Mare Tranquillitatis 1.4 times higher in Mare Nubium and 2.5 times greater in the Alphonsus region. The extrapolation of this distribution law to larger and smaller structures is examined.

Davies, J.G., Lovell, B., Pottchard, R.S., and Smith, F.G., 1966, Observation of the Russian Moon Probe Luna 9: Nature, V. 209, p. 848-850.

The article gives a short account of the observations made at Jodrell Bank of the landing phase and reception of television photographs from the first successful landing of scientific apparatus on the lunar surface. Several reconstructed lunar photographs are shown.

Elston, W.E., 1966, Ring-dike complexes: possible analogs of lunar craters: Transactions of the American Geophysical Union, V. 47, No. 1, p. 148.

Jeffrey's suggestion that large lunar craters resemble ring-dike complexes presents problems, because little is known about pre-erosion morphology of terrestrial ring-dike complexes. Volcanics preserved in their subsided central cauldrons link ring-dike complexes with rhyolite ash-flow provinces. The lunar ring-dike hypothesis overcomes the following difficulties of the impact and collapse caldera hypotheses: (1) No known terrestrial collapse caldera approaches the diameter of large lunar craters. (2) Certain neighboring lunar craters merge. (3) If some lunar craters formed non-catastrophically over  $10^7$  years, as did the Mogollon Plateau, conflicts over relative ages resolve. (4) Elongated, faulted, and rounded crater-wall segments capped by pitted spines (Alphonsus from Ranger 9) resemble neither impact ejecta nor rims of collapse calderas. They resemble the Valles rhyolite plug domes. (5) Lunar central peaks, pitted (Alpetragius, Regiomontanus) or smooth (Alphonsus), find their counterparts in the central peaks of the Mogollon Plateau and Valles structures, respectively. (Abstract of a paper presented at the April 1966 meeting of the American Geophysical Union).

Fielder, G., 1966, Tests for randomness in the distribution of lunar craters: Monthly Notices of the Royal Astronomical Society, V. 132, p. 413-422.

Two methods are used to avoid mixing different number-densities of craters in adjacent lunar regions before testing for randomness. In one method data is drawn from small regions of a given type of terrain. In the other only the most recent craters are selected.

Both analyses show that the craters cluster to a degree that exceeds that expected on the impact hypothesis. It is concluded that a significant proportion of the craters are of internal origin. In the case of the craters within Proteus, the proportion of endogenic craters is at least 38%.

Fielder, G., Wilson, L., and Guest, J.E., 1966, The moon from Luna 9: Nature, V. 209, p. 851-853.

The authors point out that perhaps the most important explanation of the difference between the American and Russian pictures is that ground resolution attained by Luna 9 is better by two orders of magnitude than that of any of the Ranger cameras. They also conclude from a study of a picture of a small area on the moon obtained

by Luna 9 that there is complete proof that at least part of the moon is not covered by an appreciable layer of unsintered dust and that some of the moon consists of lava flows.

- Fulmer, C.V., Saari, J.M., and Shorthill, R.W., 1966, Physical characteristics of some thermally anomalous lunar craters: Transactions of the American Geophysical Union, V. 47, No. 4, p. 628.

Infrared scanning during total lunar eclipse has revealed more than a thousand thermal anomalies. Some have been identified with major and minor rayed craters of various ages. In some cases thermal anomalies occur in local areas characterized by small non-rayed craters and small multiple craters, or in areas restricted to peripheral regions (lips) of major craters and local areas lacking visible craters. Specific localities characterized by anomalous cooling during lunar eclipse have been defined by contouring equal increments of signal received in the 10-12 micron band. Position information for each locality has been provided by superposition of a librated selenographic grid system and by transforming these contours to the standard Lunar Astronautical Charts. The contour position error averages about 2 sec of arc and the sensor resolution is approximately 8 sec of arc. The relation of thermal anomalies to crater phenomenology will be discussed. (Abstract of a paper presented at the September 1966 meeting of the American Geophysical Union).

- Fulmer, C., Saari, J.M., and Shorthill, R.W., 1966, Some physical characteristics of eclipse thermal anomalies in the Apollo band: Publications of the Astronomical Society of the Pacific, V. 78, p. 442-444.

The lunar disk was scanned in the infrared during the total lunar eclipse of December 19, 1964. Isothermal contours were constructed. The contours were transferred to the standard ACIC Lunar Atlas Charts for the equatorial region  $\pm 5^\circ$  latitude and  $\pm 30^\circ$  longitude. The rms location error is approximately 2.3 seconds of arc.

It was found that the thermal anomalies of this region are predominantly associated with craters, both rayed and non-rayed. The craters vary in size, shape, and depth. Furthermore, these craters span the entire age from Pre-Imbrian to Copernican although most of them in this area are either Copernican or Eratosthenian. A few anomalies are associated with multiple craters, and approximately five percent do not appear to be related with a visually detectable crater at earth-based telescopic resolution.

Two relatively large thermal anomalies are located along the trend of the Hyginus Rill. One anomaly includes the crater Hyginus and the central portion of the rill to the southeast. The second anomaly associated with this major structural feature is centered 25 kilometers to the northwest where the floor of the rill is occupied by a series of chain craters. Such craters are comparable to the maar-type volcanic craters characteristic of many rift-line volcanic regions on earth. (Abstract of a paper presented at a meeting of the Astronomical Society of the Pacific, June 1966).

- Gault, D.E., and Quaide, W.L., 1966, Meteoroid erosion and sedimentation on the lunar surface: Transactions of the American Geophysical Union, V. 47, No. 1, p. 148.

One of the most significant facts revealed by the Ranger photographs is the soft, subdued relief of the lunar surface at scales less than a few hundred meters. Theoretical and experimental studies indicate that the observed gently undulating surface can be explained as the natural consequence of an erosion and sedimentation process caused by meteoroid impact. An important implication arising from these studies is that the upper limit of the scale for the subdued characteristics is

related to the dimensions of the largest craters which saturate the surface. This, in turn, establishes a lower limit for the depth of a fragmental layer of impact crater ejecta. A conservative estimate of the thickness of this layer is 20 meters. (Abstract of a paper presented at the April 1966 meeting of the American Geophysical Union).

Gold, T., 1966, Probable mode of landing of Luna 9: *Nature*, V. 210, p. 150.

Guesses as to the mode of landing of Luna 9 are considered in terms of their implication to the nature of the lunar surface. The most puzzling feature appears to be the fact that the ground tends to give way after some extended period of time. A possible explanation of this is suggested in terms of the weight of the spacecraft resulting in many little slides and collapses in internal cavities, which eventually reduce the strength of the ground, and eventually let the vehicle settle.

Gold, T., and Hapke, B.W., 1966, Implications of the Luna 9 pictures: *Transactions of the American Geophysical Union*, V. 47, No. 2, p. 426.

The surface of the moon, cratered on a scale of centimeters as seen by Luna 9, can be interpreted as the surface of a fine-grained rock powder subjected to bombardment by material that includes similar powder. Laboratory demonstrations of such processes produced pictures that very closely resemble the landscape seen by Luna 9. The primary and secondary bombardment that the lunar surface must have received will thus fully account for its appearance, whatever the type of rock that was there originally, provided only that the material has been broken down into sufficiently fine particles. The degree of cohesion between the particles, or the amount of sintering that they may have suffered and therefore the firmness of the ground, cannot be judged from the appearance. The adhesion necessary to allow such a high degree of surface roughness to exist would be possessed by micron sized particles of any rock, though a coarser substance like sand would not maintain the observed forms. The movement of Luna 9 between two picture-taking sequences may have to be interpreted in terms of the nature of the lunar surface. (Abstract of a paper presented at the April 1966 meeting of the American Geophysical Union).

Hafner, W., 1966, Report on the lunar geological field conference, Bend, Oregon, August 22-28, 1965: *Geophysics*, V. 31, No. 4, p. 267-275.

This paper reviews the subject conference. Detailed descriptions are given of the geologic sites investigated. A summary is given of the papers and discussions on meteorite craters, volcanic features, lunar tectonism, and lunar surface properties.

Hapke, B., 1966, An improved theoretical lunar photometric function: *The Astronomical Journal*, V. 71, p. 333-339.

The theoretical photometric function for the lunar surface previously proposed by the author, which successfully predicted variations of brightness for areas between selenographic longitudes of  $\pm 60^\circ$ , has been improved so that it better agrees with observations in the limb regions. The modification consists of wrinkling the porous, open surface of the previous model into a series of steep-sided depressions. For formal mathematical reasons, the depressions used are cylindrical troughs whose axes are parallel to lines of luminance longitude. However, the primary requirement is that the surface must be densely covered ( $\sim 90\%$ ) with features whose walls make steep angles ( $24.5^\circ$ ) with the local horizontal, and that these walls must be visible even at glancing angles. This model is consistent with radar-reflection data which indicate that the moon is rough on a subcentimeter scale. Hence, the size of these depressions is inferred

to be centimeters and millimeters. These features are probably primary and secondary meteorite craters and ejecta debris, which saturate the lunar surface on a small scale.

Hartmann, W.K., 1966, Early lunar cratering: *Icarus*, V. 5, p. 406-418.

During the first seventh of lunar history, the cratering rate on the moon averaged roughly two hundred times the average post-mare rate. The peak rate may have been much higher. Crater densities are thus not proportional to age. The large, circular mare basins fit the diameter distribution of the "continental" craters and are thus identified with the pre-mare cratering. The true planetesimals from which the moon accreted were probably smaller than  $10^{18}$  gm, and may represent an intermediate stage in planetesimal growth. Of six hypothetical origins considered for the objects, a circumterrestrial swarm, probably related to the origin of the moon, appears the most likely. Observational tests for the hypotheses are listed.

Hartmann, W.K., 1966, Lunar basins, lunar lineaments, and the moon's far side: *Sky and Telescope*, V. 32, p. 128-131.

The author reviews the evidence from the Zond 3 probe and concludes that the pre-mare basins, thalassoids, and the craters are all genetically the same. Thalassoids, large basins with heavily cratered floors, are interpreted as unflooded mare-like basins. The author believes the radial systems surrounding the maria to be tectonic structures created by impact explosions.

The grid system of the moon and the marginally detectable grid systems of the earth and Mars are attributed to planetary rotation.

Herring, A.K., 1966, Observing the moon--Beer and Feuillée: *Sky and Telescope*, V. 31, p. 58.

A drawing of the area near the craters Beer and Feuillée is presented with observers notes.

Herring, A.K., 1966, Observing the moon--Bessarion B: *Sky and Telescope*, V. 31, p. 245.

A drawing of the vicinity of Bessarion B is presented with observers notes.

Herring, A.K., 1966, Observing the moon--Encke: *Sky and Telescope*, V. 32, p. 239.

A drawing of the crater Encke is presented with observers notes.

Herring, A.K., Observing the moon--Jansen B: *Sky and Telescope*, V. 32, p. 49.

A drawing and a photograph of the Jansen B area are presented together with observers comments.

Herring, A.K., 1966, Preliminary drawings of lunar limb areas, VI: *Communications of the Lunar and Planetary Laboratory*, V. 4, No. 66, p. 133-140.

The paper is the last in a series that presents a total of 12 interpretative drawings of the limb areas of the moon which are intended to supplement the "Rectified Lunar Atlas".

Heymann, D., Lipschutz, M.E., Nielsen, B., and Anders, E., 1966, Canyon Diablo meteorite: Metallographic and mass spectrometric study of 56 fragments: *Journal of Geophysical Research*, V. 71, p. 619-641.



In an attempt to reconstruct the history of the surviving Canyon Diablo fragments, 56 specimens were studied by metallography and mass spectrometry and 5 others by metallography only. Of these, 25 came from the rim of the crater, and 36 from the plains. Fifteen contained diamonds. On the basis of metallographically observable reheating effects, the samples were classified as strongly, moderately, and lightly shocked, corresponding to shock pressures of  $\geq 750$  kb, 130-750 kb, and  $< 130$  kb. The division among these categories was as follows. Plains: 0, 14, and 66%; rim: 72, 28, and 0%; diamond-bearing: 67, 33, and 0%. This bears out earlier observations by Nininger and the authors that rim (and diamond-bearing) specimens tend to be much more strongly reheated than plains specimens. Diamond-bearing and rim specimens also come from greater mean depths: 135 and 127 cm, in contrast to the depth of the plains specimens (81 cm). The throwout pattern for shocked material seems to have been highly directional, like the lunar ray craters.

Jaffe, L.D., 1966, Lunar overlay depth in Mare Tranquillitatus, Alphonsus, and nearby highlands: *Icarus*, V. 5, p. 545-550.

Photographs of lunar craters obtained by the spacecraft Ranger 8 and Ranger 9 have been compared with those of laboratory craters overlain with known amounts of granular material. Results are consistent with the interpretation that at least 5 meters of granular material, and probably considerably more, have been deposited on Mare Tranquillitatus, Alphonsus, and nearby highland areas, subsequent to the formation of most of the craters 55 meters in diameter or larger.

Kopal, Z., 1966, A possible cause of unequal distribution of the maria on the lunar globe: *Publications of the Astronomical Society of the Pacific*, V. 78, p. 444-445.

The presence of most of the maria on the near side of the moon has proved difficult of explanation by most theories for their origin.

Although the gravitational shielding of the moon by the earth is inadequate to produce the asymmetrical distribution by impacts, another type of earth-moon dynamical interaction which discriminates between the two hemispheres may provide the distribution. According to the backward extrapolation of the tidal evolution of the earth-moon system, some 2000 million years ago the moon should have been close enough to the earth to dip temporarily with its front side--but not the far side--into the terrestrial Roche limit. The observed conspicuous asymmetry in global distribution of the lunar maria appears indeed to be consistent with an assumption that the mare plains may constitute "scars" of the mechanical damage wrought on the lunar hemisphere which entered the Roche limit by disruptive tides of the earth. (Abstract of a paper presented at a meeting of the Astronomical Society of the Pacific, June 1966).

Kopal, Z., 1966, On the possible origin of the lunar maria: *Nature*, V. 210, p. 188.

Possible causes of the conspicuous disparity in the distribution of lunar maria on the two hemispheres of the globe are discussed. It is pointed out that such a distribution is consistent with an assumption the mare plains may constitute "scars" of mechanical damage wrought on the lunar hemisphere which entered the Roche limit by disruptive tides of the earth. The theory is developed suggesting lava may have been extruded to fill up the original scars and the source of adequate heat is discussed.

Kopal, Z., 1966, The nature of secondary craters photographed by Ranger VII: *Icarus*, V. 5, p. 201-213.

A mathematical theory of the ejection of secondary fragments from the focus of primary impacts on the moon has been developed. An application of the results

to the frequency distribution of the secondary lunar craters in the region of Mare Cognitum leads to a conclusion that the sum total of the mass required to produce all observed craters or craterlike formations in Mare Cognitum overlying Tycho's rays by secondary impacts of particles ejected from Tycho would--if spread evenly over the surface--cover the ground by a layer of debris about half a meter in thickness at the distance of 1000 km from the focus of ejection; and the volume of the material thus splashed out all over the moon would exceed the volume excavated by the primary impact at least 10 to 20 times.

On the strength of this evidence a hypothesis is advanced that a large fraction of depressions, smaller than 1 km in size, are in reality subsidence formations.

Kuiper, G.P., 1966, Interpretation of Ranger VII records: Communications of the Lunar and Planetary Laboratory, V. 4, No. 58, p. 1-70.

The interpretation of the photographs of Mare Cognitum is made in context of all available lunar data. Discussed are the relationship of secondary craters, crater rays, local and mare-wide patterns of ridges and the physical and mechanical structure of the known features of the lunar surface. The ranger records present a new class of objects, shallow depressions and dimple craters, and tree-bark pattern on high resolution pictures in a weak Tycho crater ray.

Hypotheses concerning the origin of lunar surface features are discussed.

Lipsky, Y.N., 1966, What Luna 9 told us about the moon: Sky and Telescope, V. 32, p. 257-260.

The Luna 9 mission is described, photographs and a discussion of results are presented. It is concluded that the bearing strength of the lunar soil is at least a few kilograms per square centimeter. The author feels the experiment refuted the dust theory of the lunar surface and showed that the effect of micro-meteorites on the surface has been overestimated.

Marcus, A.H., 1966, A stochastic model of the formation and survival of lunar craters II. Approximate distribution of diameter of all observable craters: Icarus, V. 5, p. 165-177.

It is assumed that the number density of lunar craters evolves because of the arrival of new craters and the obliteration of earlier craters by the formation of more recent ones nearby. Approximations are developed which permit the calculation of the expected number density. This result is applied to the meteoroidal impact hypothesis for the origin of lunar craters. It is shown that obliteration alone is not sufficient to explain observed crater diameter distributions.

Marcus, A.H., 1966, A stochastic model of the formation and survival of lunar craters III. Filling and disappearance of craters: Icarus, V. 5, p. 178-189.

A previous model is extended to include the effects of the disappearance of craters due to filling by dust or lava. These results are applied to the meteoroidal impact hypothesis of the origin of lunar craters. Good agreement is obtained with observed number densities on the lunar continents and maria. It is assumed that the rate of filling of craters on the continents corresponds to the rate of meteoritic accretion, and the rate of filling on the maria is 50 to 100 times larger than on the continents, corresponding to filling of mare craters by lava.

Marcus, A.H., 1966, A stochastic model of the formation and survival of lunar craters IV. On the non-randomness of crater centers: Icarus, V. 5, p. 190-200.

It is shown that even if the underlying distribution of craters is completely random, the distribution of centers of observable craters is not. In particular, in finite regions in which a very large crater is found, we would expect to find a dearth of small craters, since the large crater would have obliterated older small craters in its neighborhood.

Under the meteoroidal impact hypothesis, with disappearance of craters due to filling as well as obliteration, the coefficient of variation of density of small craters in regions of small size can be as large as 30%.

Another source of variation in crater counts is the grouping together of inhomogeneous regions, for example, maria whose crater densities differ by a factor of 2 or 3.

Empirical crater counts clearly show the negative correlation between density of small craters and the presence of large craters. It is concluded that there is no reason to reject the hypothesis of randomness of formation of craters of large and moderate size.

Marcus, A.H., 1966, A stochastic model of the formation and survival of lunar craters: *Icarus*, V. 5, p. 590-605.

Approximate upper and lower bounds are obtained for the expected number density of lunar craters by means of a model which takes into account the formation of primary and secondary craters and the destruction of craters by obliteration and filling. The shape of the observed distribution is the same as that of the predicted distribution, but the observed density of small craters is about 15 times larger than that predicted by analogy with terrestrial explosion craters. If the observed excess is real, then either some primary craters produce an unusually large number of secondaries, or else many of the smaller lunar craters are of internal origin.

Marcus, A., 1966, Comments on "Distribution of craters on the lunar surface": *Monthly Notices of the Royal Astronomical Society*, V. 134, p. 269-274.

In a recent study of the distribution of centers of lunar craters, Fielder found two apparent anomalies which he used as arguments against the meteoroidal impact hypothesis for the origin of lunar craters. First, the Poisson distribution gave a very bad fit to the number of crater centers in equiareal sectors of the continents and the maria, especially among craters smaller than 40 Km diameter. The second difficulty was a systematic excess in the number density of small craters in the trailing half of the moon. The author shows that these observations could also have been expected under the impact hypothesis, since the numbers of small and of large craters in a finite region are negatively correlated. Available crater statistics therefore neither preclude nor establish the impact or volcanic hypothesis for the origin of craters.

McConnell, R.K., Jr., and McClaine, L.A., 1966, Mechanics of magma migration: *Transactions of the American Geophysical Union*, V. 47, No. 1, p. 177.

In a dike through which magma is flowing, many features, such as the uniform width and constant size, may be explained by considering the balance between frictional heating and heat loss to the wall rock. If magma is driven under a fixed pressure gradient, any dike width is unstable, and, as long as the gradient is maintained, the dike must either enlarge or soon solidify. On the other hand, if the amount of melt moving through the dike per unit time is fixed, there will be a stable equilibrium width. The theory is shown to predict widths of feeder dikes that are consistent with field observations. If lunar igneous activity of a kind similar to that on earth has taken place, lunar dikes might be expected to

be about twice as wide as their terrestrial counterparts. (Abstract of a paper presented at the April 1966 meeting of the American Geophysical Union).

Moore, P., 1966, Origin of the lunar maria: *Nature*, V. 210, p. 1347.

The author comments on Kopai's (*Nature* 210, 188, 1966) hypothesis of the origin of maria and points out that to introduce a separate origin for the maria presupposes that they are of a nature basically different from that of the craters.

Morris, E.C., and Shoemaker, E.M., 1966, Craters and fragmental debris of the lunar surface around Surveyor 1: *Transactions of the American Geophysical Union*, V. 47, No. 4, p. 617.

The disturbance of the lunar surface by the Surveyor 1 footpads and the shapes of small natural craters in the field of view show that the lunar surface at the Surveyor 1 landing site is underlain by very weakly cohesive material. This material is probably composed of fragments of a wide range of size, similar to those observed directly at the surface. Near the spacecraft, the weakly cohesive material occurs as a layer that extends to an average depth of 1 to 2 meters, as indicated by the rim characteristics of craters that have been formed in the layer and of larger craters that have penetrated the layer. The raised rims of craters up to 3.3 meters across are relatively smooth, whereas raised rims of larger craters are covered with abundant coarse angular blocks that have been derived from beneath the weakly cohesive material. The observed thickness of the layer and the distribution of fragments and craters on the surface of the layer are in good agreement with the predicted thickness and surface characteristics of a fragmental debris layer expected to have been formed primarily by repetitive bombardment of the surface by lunar secondary ejecta. (Abstract of a paper presented at the September 1966 meeting of the American Geophysical Union).

Roberts, W.A., 1966, Lunar surface characteristics: A contemporary view: *Publications of the Astronomical Society of the Pacific*, V. 78, p. 448-449.

All the hypotheses concerning the origin of the moon cannot be true, but regardless of the birthplace of the moon and the method of formation, the body of the moon has been subject to the environment into which it was born. One of the environmental factors is a flux of micro- to macrometeorites. At present, the earth, and presumably the moon, is exposed to a flux of space debris, and the presence of probable fossil meteorite impact features on earth indicates that the present flux is probably an extension of a condition that has occurred throughout at least the later part of the history of the solar system. Meteorite impact at high velocity produces craters surrounded by brecciated target material. The quantity of atmosphere surrounding and protecting a planetary body determines to a large extent the size of meteorites that can penetrate to the planetary surface at high velocity. The moon is essentially unprotected. Some of the features seen in the earth-based photographs of the moon appear to be volcanic in nature. Volcanism on the moon would be restricted in areal and/or temporal distribution, unlike the ceaseless erosion and sculpturing process of the impact of space debris. Thus, volcanic and non-volcanic features will be altered and eroded by the meteorite flux to an extent proportional to the total areal density of impacting meteorites or, in effect, the age of the feature. The Surveyor 1 and Luna 9 pictures show views of the lunar terrain surrounding the experiment packages and detailed views of exposed rocks. The terrain illustrated by panoramic sequences is consistent with poorly sorted shock breccia from both primary and secondary craters formed in a layer of shock-brecciated fine-grained crystalline silicate rock. Apparent sorting suggests reworking of the breccia by several impacts. A detailed view of a rock by Surveyor shows a conjugate or orthogonal fracture system in a rock that appears to be agglomeratic--either



shock- or volcanic-cemented breccia. The rounded texture of the rock surface could indicate differential erosion by micrometeorites and secondary ejecta due to differential hardness of fragments and interfragmental materials. This texture would also be consistent with shock or thermal melting. A planar surface of this rock appears to have a texture consistent with a rock composed of weakly cemented fragments of various sizes. Such a rock could be shock-compacted breccia ejected from a nearby crater. (Abstract of a paper presented at a meeting of the Astronomical Society of the Pacific, June 1966).

Ronce, L.B., 1966, Meteoritic impact and volcanism: *Icarus*, V. 5, p. 515-520.

The possibility of volcanism triggered by meteoritic impact is analyzed theoretically by comparing volcanological and impact data. Field data on some terrestrial craters are also discussed. The conclusion is that volcanism triggered or localized by impact is possible. The hypothesis is proposed that lunar craters represent a spectrum of craters ranging from completely meteoritic craters, through meteoritic craters modified by volcanism, to completely volcanic craters. The data on Mars are meager, but suggest that Martian craters may owe their origin to the same processes.

Ronce, L.B., 1966, Structure of the crater Alphonsus: *Science*, V. 209, p. 182.

From a study of Ranger IX photographs, the author concludes that, regardless of the origin of the material forming the central spine and floor of the crater, both the general outline and the presence of the folds indicate that Alphonsus is a crater deformed by a strike-slip fault of the dextral type.

Saari, J.M., Shorthill, R.W., and Deaton, T.K., 1966, Infrared and visible images of the eclipsed moon: *Icarus*, V. 5, p. 635-659.

The moon was scanned with 10" arc resolution at 0.45 and 10-12 microns during the total lunar eclipse of December 19, 1964. It was found that the lunar surface exhibits a surprising amount of thermal inhomogeneity. Hundreds of thermal anomalies were observed, most of which can be identified with bright craters or white areas. Certain maria and portions of maria were found to be thermally enhanced over their environs during the eclipse.

Shoemaker, E.M., and Morris, E.C., 1966, Fine structure of the lunar surface at the Surveyor I landing site: *Transactions of the American Geophysical Union*, V. 47, No. 4, p. 617.

The terrain around Surveyor I is a gently undulating surface studded with craters ranging in diameter from a few centimeters to several hundred meters and with angular fragments ranging from less than a millimeter to several meters across. The size-frequency distribution of the craters is close to that predicted for the maria by extrapolation of the crater size-frequency distribution observed in the Ranger pictures.

The observed angular fragments occupy 7.6% of the surface area and have a volumetric median grain size of 130 mm. The volumetric median grain size of all fragmental material on the surface may be of the order of 1 millimeter. About one crater 6 meters in diameter or larger and one block 1 meter across or larger is found on each 100 m<sup>2</sup> of the lunar surface around Surveyor I. (Abstract of a paper presented at the September 1966 meeting of the American Geophysical Union).

Simpson, J.F., 1966, Additional evidence for the volcanic origin of lunar and Martian craters: *Earth and Planetary Science Letters*, V. 1, No. 3, p. 132-134.

This paper points out the similarity in frequency distribution of lunar and Martian craters with terrestrial volcanic craters, and the dissimilarity of these groups with terrestrial meteoritic craters. Surface density effects are also considered. The results of the study favor a volcanic origin of the bulk of the Martian and lunar craters.

Simpson, J.F., 1966, Evidence for the volcanic origin of lunar and Martian craters: *Earth and Planetary Science Letters*, V. 1, No. 3, p. 130-131.

This letter points out the relationship existing in the percentage distribution of crater diameters on the moon and Mars, which appears remarkably similar when normalized to uniform gravity. Crater diameters should vary approximately inversely with the value of  $g$  for any given cosmic body because for a given gas pressure the volume of rock removed will be a function of its weight (which is dependent on  $g$ ). This effect is enhanced by the tendency toward higher porosity and lower density of vesicular extrusive rocks formed at the surface in a low gravity environment. The percentage distribution of craters greater than 3 km in diameter is approximately 3.15 as large for lunar craters than for Martian craters.

Surveyor Scientific Evaluation and Analysis Team, 1966, Surveyor 1: Preliminary results: *Science*, V. 152, p. 1737-1750.

The terrain shown by Surveyor 1's photographs is described. Fragmental debris ranges in size from less than 1 mm to more than 1 m, and it extends to depth of at least 1 m. Lumps show that the material is at least slightly cohesive. Static bearing capacity of the soil is about  $4 \times 10^5$  dyne  $\text{cm}^{-2}$ , its cohesion is 1 to  $4 \times 10^3$  dyne  $\text{cm}^{-2}$ , its friction angle is between 30 and 40 degrees and its density is about 1.5 g  $\text{cm}^{-3}$ . However, it is also possible that the surface consists of a hard material overlain by a weak material to a depth of about 25 mm. Thermal properties reveal that the surface bears essentially no dust. The general surface is relatively smooth and nearly level on a kilometer scale. On a smaller scale the surface is littered with coarse blocks and fragments. The size distribution function resembles the distribution of crushed rocks, with a mean at approximately 1 mm. The albedo of the undisturbed surface is 7.7 percent, while the areas disturbed by the pads have a value of about 2 percent lower.

Thompson, T.W., and Dyce, R.B., 1966, Mapping of lunar radar reflectivity at 70 centimeters: *Journal of Geophysical Research*, V. 71, p. 4843-4853.

Radar observations of the lunar surface were made using the 10' beamwidth antenna at Arecibo, Puerto Rico, at a wavelength of 70 cm (430 Mc/s). Resolution of the surface of the order of 20 by 30 km was achieved, first, by resolving the echo in time delay and Doppler frequency shift and, second, by using the narrow antenna beamwidth to remove the ambiguity between hemispheres. Echo strengths measured in delay and frequency coordinates were then mapped onto photographs of the moon. The following were determined: (1) The lunar highlands of the southwest quadrant of the moon backscatter  $1\frac{1}{2}$  to 2 times as effectively per unit areas as the mare regions of the east and northeast quadrants of the moon. (2) The mountain ranges which surround the circular maria backscatter  $1\frac{1}{2}$  to 2 times as much power as the adjacent mare regions. (3) Some craters were found to backscatter as much as 10 times as much power as their environs. The craters which had enhanced backscattering were bright under a full moon illumination and were nearly always young.

Titulaer, C., 1966, Isophotes of the Aristarchus region of the moon: *Bulletin of the Astronomical Institutes of the Netherlands*, V. 18, p. 167-169.

Isophotometric measurements have been made on plates taken during the total eclipse of the moon, 19 December 1964. This paper gives the profiles of the isophotes and their relative intensities. It was not possible to determine the variation of intensity with time. 80 pictures of Aristarchus, the brightest object of the moon, have been taken through a yellow filter (5400 Å). The difference in intensity between the centre of Aristarchus and the surroundings is about a factor two at phase angles 107°.

Turkevich, A., and Rennilson, J.J., 1966, Location and altitude of Surveyor I on the lunar surface: Transactions of the American Geophysical Union, V. 47, No. 4, p. 616.

The location of Surveyor I on the lunar surface has been estimated by observation of horizon features with the television camera. These features were compared with telescopic photographs of the region around the landing site. The best estimate of the position of the spacecraft is 2.5°S, 43.5°W. Several celestial observations were conducted during the first lunar day to determine the altitude of the camera and the spacecraft. If the assumption is made that no spacecraft disfiguration occurred on landing, the tilt of the spacecraft is less than a degree in the SW direction. The horizon around the spacecraft is nearly level. (Abstract of a paper presented at the September 1966 meeting of the American Geophysical Union).

Vand, V., 1966, Monro jets and the origin of tektites: Nature, V. 209, p. 496.

The author had previously proposed a detailed mechanism of a tektite jet formation through an implosion of a conical cavity lined with molten glass which is formed immediately after impact, and showed that a jet of tektites can survive the upward atmospheric journey if of sufficient total mass.

Using the results of other authors on jets formed from imploding bubbles, he elucidates the operating mechanism and applies it to Riess Kessel, and speculates that the general inward motion of other crater materials caused by the passage of waves reflected from below will also be responsible for the formation of a central peak in some craters, if underlain by denser strata at favourable depth. The author also states that similar interpretation of central peaks of lunar craters might help in mapping such discontinuities under the lunar surface.

van Diggelen, J., 1966, The linear network of lunar surface features: Bulletin of the Astronomical Institutes of the Netherlands, V. 18, p. 311-322.

The investigation deals with a statistical method for determining the preferential directions shown by lunar surface formations, known as the lunar grid system. A strong system radially oriented with respect to Mare Imbrium has been found in some lunar regions. Nearly all systems mentioned by Fiedler (1963) could be confirmed by the statistical method.

Vonnegut, B., McConnell, R.K., Jr., and Allen, R.V., 1966, Evaporation of lava and its condensation from the vapour phase in terrestrial and lunar volcanism: Nature, V. 209, p. 445-448.

From observations made at the volcanoes on the Island of Surtsey during February 1964, and in the laboratory, the authors conclude that the formation of particulate matter by the condensation of vaporized components of hot lava is important in the origin of terrestrial volcanic clouds and atmospheric aerosols. The volcanic evaporation-condensation mechanism may also be of importance in the formation of the surface of the moon.

It thus appears that the volcanic evaporation-condensation mechanism should be added to micrometeorite impact and solar wind sputtering as a possible factor contributing to the evolution of the visible portion of the moon's surface.

Walker, E.H., 1966, Comments on paper by L.D. Jaffe, "Depth of the lunar dust": *Journal of Geophysical Research*, V. 71, p. 5007-5010.

It is pointed out that hypervelocity impact erosion is an active process which significantly changes the substrate, and is thus entirely different from the passive sedimentation that Jaffe used to modify his laboratory craters. As a result, Jaffe's treatment of the smoothed craters appearing in the Ranger 7 pictures neither establishes the presence of a significant layer of overlay, nor allows the determination of its thickness. (This letter is followed by a reply from Jaffe, pointing out that sedimentation ultimately occurs as a result of hypervelocity impact).

Watts, R.N., Jr., 1966, Lunar orbiter surveys the moon: *Sky and Telescope*, V. 32, p. 192-197.

A popular description of the Orbiter I mission. Several of the orbiter photographs are presented.

Watts, R.N., Jr., 1966, Pictures from the moon: *Sky and Telescope*, V. 32, p. 16-20.

A popular description of Surveyor I. Several of the photographs are presented.

Whitaker, E.A., 1966, Further observations on the Ranger VII records: *Communications of the Lunar and Planetary Laboratory*, V. 4, No. 59, p. 71-76.

The observations lead to the following conclusions:

1. Smooth conical lunar craters are presumably formed by impacting solid meteoritic bodies.
2. The larger ray systems appear to be more readily explainable on the basis of impacts with cometary nuclei.

Winter, D.F., 1966, Note on the non-uniform cooling behavior of the eclipsed moon: *Icarus*, V. 5, p. 551-553.

Fudeli's theory on the downslope migration of debris being the cause of the "hot spots" is discussed. The theory that the "hot spots" are due to an increase in roughness is favored.

### 3.5.6 Surface Materials

Aronson, J.R., Emslie, A.G., Allen, R.V., and McLinden, H.G., 1966, Far infrared studies of minerals for application in remote compositional mapping of the moon and planets: *Transactions of the American Geophysical Union*, V. 47, No. 1, p. 155.

The surface composition of the moon and planets, such as Mars and Mercury, with tenuous atmospheres can be measured remotely by infrared reflectance and emittance spectroscopy over a broad range of frequencies. The information in the far infrared region ( $50-667 \text{ cm}^{-1}$ ) is especially informative as to specific mineral composition, and is very desirable in order to disentangle the composite spectra resulting from complex mixtures. Experimental studies of far infrared spectra, at room and cryogenic temperatures, of possible lunar and planetary surface minerals have been performed. Theoretical and experimental studies of the factors that control spectral contrast in the spectra of particulate surfaces



and of the kind of mixing rules that must be used to disentangle the spectra of composite surfaces have been made. (Abstract of a paper presented at the April 1966 meeting of the American Geophysical Union).

Brown, W.E., Jr., 1966, Surveyor I radar reports: Transactions of the American Geophysical Union, V. 47, No. 4, p. 616.

Radar echo strength data from the lunar surface were telemetered from the Surveyor I spacecraft during the landing sequence. The three Surveyor I radars covered an altitude range of 350 km and operated on wavelengths of 2.25, 2.32, and 3.22 cm. The reflection surface was within 1 meter of the visible surface. The plumes of the vernier engines had no measurable effect upon the echo strengths, and one of the off-normal radar beams traversed a crater-like surface anomaly about 1 km wide and 2 km from the point of touchdown. The radar cross-section information obtained by Surveyor I is in good agreement with earth-based measurements obtained at about the same wavelength. (Abstract of a paper presented at the September 1966 meeting of the American Geophysical Union).

Bühler, F., Geiss, J., Meister, J., Eberhardt, P., Hüneke, J.C., and Singer, P., 1966, Trapping of the solar wind in solids. Part I. trapping probability of low energy He, Ne and Ar ions: Earth and Planetary Science Letters, V. 1, No. 5, p. 249-255.

The trapping probability in Al foils of He, Ne and Ar ions with energies between 0.46 and 7 KeV has been determined. Argon is trapped quantitatively for ion energies higher than 2.5 KeV. At 2.5 KeV the trapping probabilities of neon and helium are about 0.6, decreasing rapidly for lower energies with argon. The trapped gases are held quite firmly. These results show that an Al foil exposed to the solar wind would trap and retain a large fraction of these solar wind ions. There is little doubt that the solar wind will also be trapped in interplanetary dust grains and in the surface layers of asteroids and moons provided these have no atmosphere or magnetic field.

Christensen, E.M., 1966, Photo Interpretation of Surveyor I Interaction with the lunar material: Transactions of the American Geophysical Union, V. 47, No. 4, p. 617.

The photographs of the disturbances of the lunar surface, created by the Surveyor I spacecraft footpads and a crushable block during the landing, are valuable in studying the lunar surface mechanical properties. The two footpads that were visible to the camera created similar disturbances; i.e., an overthrow of fine material and a clumpy semi-circular ridge. The footpad penetrations are estimated to have been 1½ to 3 inches. The small area that is visible of an imprint by a crushable block assembly appears to indicate that a compression of the lunar material occurred, leaving a remaining edge with an angle to the horizon of at least 58°. No noticeable change in the disturbed material has been noted in the multitude of photographs taken over a period of seven weeks. (Abstract of a paper presented at the September 1966 meeting of the American Geophysical Union).

Clegg, P.E., Bastin, J.A., Gear, A.E., 1966, Heat transfer in lunar rock: Monthly Notices of the Royal Astronomical Society, V. 133, p. 63-66.

It is suggested that radiative transfer may play an important part in the mechanism of heat flow in the lunar surface and a simple treatment of this process is given. Rough estimates are made of the magnitude of the contribution of radiative transfer, and it is found that this process could account for a considerable fraction and perhaps almost all the heat flow deduced from infrared measurements. Furthermore, such a mechanism is of the right form to remove certain discrepancies which have been noted in infrared and microwave data.

Copeland, J., 1966, The two-layer model of the lunar surface: *Astrophysical Journal*, V. 145, p. 297-301.

Consideration is given to the two layer model by obtaining solutions to the heat-conduction equations for a homogeneous layer covering a homogeneous sub-surface. The cases of a transparent and a semi-transparent surface layer are considered.

Davidson, G., Kraner, H.W., Schroeder, G.L., and Carpenter, J.W., 1966, Enhanced radioactivity at the lunar surface: *Transactions of the American Geophysical Union*, V. 47, No. 1, p. 154-155.

The release of radioactive radon ( $Rn$ ,  $Rn^{222}$ ) and thoron ( $Tn$ ,  $Rn^{220}$ ) from the lunar surface provides a source for buildup of a thin radioactive surface layer on the moon. At the lunar surface released  $Rn$  and  $Tn$  will follow ballistic trajectories and form a radiogenic atmosphere, decaying with their respective half-periods of 3.8 days and 56 seconds. Half of the radioactive daughter products will recoil in the direction of the surface and form a radioactive surface layer. Assuming diffusion rates for  $Rn$  and  $Tn$  on the moon similar to those measured at the earth's surface, the equilibrium activity of this surface layer on the moon will be approximately  $1 \mu$  curie/ $m^2$ , consisting of alpha particles and gamma rays, at well defined energies, and beta rays. Some possible consequences of this activity as related to lunar exploration are discussed: (Abstract of a paper presented at the April 1966 meeting of the American Geophysical Union).

Davies, R.D., and Gardner, F.F., 1966, Linear polarization of the moon at 6, 11, and 21 cm wavelengths: *Australian Journal of Physics*, V. 19, p. 823-836.

The 210 ft. radio telescope at Parkes provides adequate resolution at wavelengths of 6, 11, and 21 cm for the derivation of the distribution of linear polarization across the disk of the moon. The polarization observations indicate an increase in dielectric constant with increasing wavelength.

The observed brightness distributions at all wavelengths indicate a rough surface. A roughness corresponding to a mean tilt of surface normals of about  $12^\circ$  is consistent with both the brightness and polarization distributions, and also with 68 cm radar observations, which sample a similar depth of lunar material.

The dielectric constant of the rough surface model at 6 and 11 cm wavelengths is significantly less than that deduced from the radar data. The discrepancy may be removed in a model where the surface layer is composed of a mixture of materials of different dielectric constants. For example, a mixture of 65%  $\epsilon = 1.6$  and 35%  $\epsilon = 5.0$  would give the observed polarization characteristics at 11 cm and the radar reflectivity at 68 cm.

Dobar, W.I., 1966, Simulated basalt and granite magma upwelled in vacuum: *Icarus*, V. 5, p. 399-405.

The upwelling and solidification of a simulated basalt and granite magma in vacuum has produced a porous material not found in nature. The photometric curves of the upwelled samples show excellent correlation with the photometric curves of the lunar surface. The visible colors associated with the simulated magma during vacuum upwelling matches the visual observations of the color phenomena observed on the lunar surface in October and November of 1964.

Dupes, W.D., and Alexander, S.S., 1966, The response of selected rock specimens to vacuum ultraviolet light: *Transactions of the American Geophysical Union*, V. 47, No. 1, p. 150.

In this investigation the reflectance of vacuum ultraviolet light from selected igneous rock specimens was measured in the spectral range from 550 to 1800 Å. Smoothly sawed but unpolished surfaces of the specimens were irradiated at a constant angle of incidence under uniform test conditions using a 1-meter vacuum ultraviolet scanning monochromator. In general, it was found that the specimens exhibit higher reflectivity at the shorter wavelengths in the range 550 to 1800 Å, and that each specimen has a characteristic response that may be related to the chemical composition of the sample. The responses among the rock types considered appear to be sufficiently distinct that the reflectance spectrum of incident ultraviolet light can be considered for remote identification of surface materials on extraterrestrial bodies, such as the moon. (Abstract of a paper presented at the April 1966 meeting of the American Geophysical Union).

Ebeoglu, D.B., 1966, Solar proton induced gamma rays on the lunar surface: Transactions of the American Geophysical Union, V. 47, No. 3, p. 487.

The Y-ray intensity on the lunar surface due to solar proton bombardment has been estimated using a Monte Carlo approach. The Y-ray spectrum emitted by radionuclides and excited stable nuclei created by the solar particles has been predicted as a function of depth. Examples of the lunar surface representing the volcanic origin theory, as well as the meteoritic impact hypothesis, have been used as models. The calculations are based on computer calculations of radionuclide and particle flux distributions on the lunar surface, which were previously compared with experimentally determined values. Point Y-ray source distributions and simple exponential attenuation have been assumed. (Abstract of a paper presented at the September 1966 meeting of the American Geophysical Union).

Ebeoglu, D.B., and Wainio, K.M., 1966, Solar proton activation on the lunar surface: Transactions of the American Geophysical Union, V. 47, No. 1, p. 154.

The nuclear activation of the surface of the moon, due to solar protons, has been estimated. Proton and neutron fluxes and the production rate of radionuclides have been calculated as a function of depth, and comparisons have been made among several models of the lunar crust. The purpose of the calculations has been to evaluate the effectiveness of lunar materials as a radiation shield and also to predict the particle flux reflected from the surface. The buildup of  $Mn^{54}$ ,  $Na^{22}$ ,  $C^{14}$ , and  $Be^7$  are given in compositions representing both the volcanic and meteoritic impact hypotheses of the lunar surface. The effect of the angular distribution of the protons on the radionuclide production rate and particle fluxes has also been investigated. Examples involving a monoenergetic beam of 400-Mev protons, as well as a solar proton spectrum, are included to permit direct comparisons with experimental irradiations of similar targets. (Abstract of a paper presented at the April 1966 meeting of the American Geophysical Union).

Ebeoglu, D.B., and Wainio, K.M., 1966, Solar proton activation of the lunar surface: Journal of Geophysical Research, V. 71, p. 5863-5872.

The nuclear activation on the surface of the moon due to solar protons has been estimated. Proton and neutron fluxes and the production rate of radionuclides have been calculated as a function of depth, and comparisons have been made between several models of the lunar crust. The purpose of the calculations has been to evaluate the effectiveness of lunar material as a radiation shield and also to predict the particle flux reflected from the surface. The build-up of  $Mn^{54}$ ,  $Na^{22}$ ,  $C^{14}$ , and  $Be^7$  are given in compositions representing both the volcanic and meteoritic-impact hypotheses for the lunar surface. The effect of the angular distribution of the protons on the radionuclide production rate and particle fluxes has also been investigated. Examples involving a monoenergetic



beam of 400-Mev protons as well as a solar proton spectrum are included, permitting direct comparisons with experimental irradiations of similar targets. The results show that the activation is strongly dependent on the spectrum and angular distribution of incident protons but relatively insensitive to the composition.

Egan, W.G., and Smith, L.L., 1966, Polarimetric measurements of simulated lunar surfaces: *The Astronomical Journal*, V. 71, p. 383-384.

Polarimetric studies of rough surfaces serve to delimit the range of their appropriate physical properties and geometries. In an effort to lay the basis for an analytical approach, the polarization properties of volcanic ash and furnace slag were investigated as a function of particle size, albedo and porosity, since current theories of polarization indicate that these properties are significant. These investigations were made on a large-scale polarimeter (4-in. diameter viewing area) in order that coarse specimens could be analyzed.

For both samples, it was found that the maximum percent polarization (positive) and the corresponding phase angle at zero and 60 deg viewing angles, the inversion angle and the minimum percent polarization (negative) varied as a function of porosity and albedo. It was found that the best fit to Crisium (Gehrels et al.) could be achieved with Haleakala volcanic ash with particle sizes between 37 and 88  $\mu$ , and furnace slag less than 37  $\mu$ ; Clavius could be fitted with the ash of sizes less than 37  $\mu$ , and the furnace slag less than 1  $\mu$ .

The polarimetric properties of the furnace slag, volcanic ash, and additional laboratory samples were investigated for wavelength dependence. It was found that the best color-polarimetric and best visual photometric match to Crisium were obtained with coarse chunks of the volcanic ash topped with less than 1  $\mu$  particles of itself. (Abstract of a paper presented at the March 1966 meeting of the American Astronomical Society).

Evans, J.V., and Hagfors, T., 1966, Study of radio echoes from the moon at 23 centimeters wavelength: *Journal of Geophysical Research*, V. 71, p. 4871-4889.

Short-pulse radio reflections have been studied to determine the average scattering behavior of the lunar surface at a wavelength of 23 cm. The intensities of both the polarized (expected) and depolarized components of the return have been measured. A precise determination of the total radar cross section of the moon  $\sigma_0$  using the Lincoln calibration sphere (LCS) satellite as a comparison standard yielded the results  $\sigma_0 = 0.065 \pm 0.008$  times the physical cross section ( $\pi a^2$ ). The observations reported here are compared with earlier measurements at 68- and 3.6-cm wavelength. It is concluded that, though the smoother parts of the moon's surface scatter in much the same fashion at 23-cm wavelength as at 68-cm wavelength, there appears to be an increase in the amount of surface covered with structure comparable in size to the wavelength. Attempts to account for the scattering theoretically are reviewed, and it is shown that no complete understanding has yet been achieved of the reflection properties of lunar and planetary surfaces containing structure both much larger than and comparable in size to the exploring wavelength. It is believed, however, that the mean surface slope of  $10^\circ$  is applicable to elements of the surface of the order of 5 to 10 wavelengths across and is therefore the slope that might be encountered by a landing vehicle.

Fielder, G., Wilson, L., and Guest, J.E., 1966, The moon from Luna 9: *Nature*, V. 209, p. 851-853.

The authors point out that perhaps the most important explanation of the difference between the American and Russian pictures is that ground resolution attained



by Luna 9 is better by two orders of magnitude than that of any of the Ranger cameras. They also conclude from a study of a picture of a small area on the moon obtained by Luna 9 that there is complete proof that at least part of the moon is not covered by an appreciable layer of unsintered dust and that some of the moon consists of lava flows.

Fudall, R.F., 1966, Implications of the non-uniform cooling behavior of the eclipsed moon: *Icarus*, V. 5, p. 536-544.

Recent infrared observations during a lunar eclipse have revealed the existence of hundreds of areas whose thermal behavior differs sharply from that of the surrounding terrain. The probable explanation for this behavior is a difference in the insulating properties of the material exposed in these areas. Specifically, a lack of insulating debris over all or parts of the anomalous areas is conceptually sound and explains all the known facts. An analysis of the features and associations of these "hot spots" suggests that the debris is lacking because of simple downslope movement on high angle slopes.

Gault, D.E., Quaide, W.L., Oberbeck, V.R., and Moore, A.J., 1966, Luna 9 photographs: Evidence for a fragmental surface layer: *Science*, V. 153, p. 985-988.

The morphological features of the lunar surface photographed by Luna 9 indicate a surficial layer of weakly cohesive to non-cohesive fragmental material. Most of this material is finer than a centimeter, probably finer than a millimeter.

Geake, J.E., and Walker, G., 1966, Reply to "Luminescence caused by proton impact with special reference to the lunar surface": *Nature*, V. 211, p. 471-472.

In this reply, the authors contend that Schutten and Van Dijk do not give enough information for Geake and Walker to attempt an explanation of their results, except to say that the results seem consistent with the use of high beam current density. Geake and Walker are surprised at Schutten and Van Dijk's selection of meteorites chosen for comparison, because of their low luminescence efficiency. They point out that the reason very little luminescence was observed is probably because the samples were damaged by the high beam current, which results in greatly reduced efficiency and a changed spectrum; as well as as because the spectral range used did not include the region where highest efficiency had been observed.

Gehrels, T., 1966, Some comments on Hapke's comments: *Icarus*, V. 5, p. 160-161.

Most observations in photometry and polarimetry of the moon and asteroids can be explained with a tenuous surface texture. The scattering elements or particles may be interconnected rather than freely suspended.

Gentry, R.V., 1966, Additional evidence of extinct radioactivity from pleochroic halos and the formation of the lunar crust: *Transactions of the American Geophysical Union*, V. 47, No. 3, p. 487.

Dwarf radioactive halos similar to the small bleached halos reported by Joly have been found in the Ytterby mica. The 5.2- $\mu$  radius halo was heretofore attributed to  $\text{Sm}^{147}$ , but energy considerations do not exclude the presently extinct isotope  $\text{Sm}^{148}$  as a parent nuclide of this halo. The 8.6- $\mu$  radius halo is attributed to the 3.18-Mev alpha from  $\text{Gd}^{148}$ , and a bleached ring halo of about 20- $\mu$  radius corresponds to an alpha emitter of about 5.5 Mev. This bleached ring has also been observed in certain polonium halos. Electron microprobe analysis of the central inclusions of some of these halos together with autoradiographic and fission track studies provide substantial evidence for naturally occurring extinct radioactivity. If similar radioactive halos are found in lunar crustal material,

there will be a method for determining the maximum time period between nucleosynthesis and formation of the lunar crust. (Abstract of a paper presented at the September 1966 meeting of the American Geophysical Union).

Gilvarry, J.J., 1966, Observability of indigenous organic matter on the moon: *Icarus*, V. 5, p. 228-236.

The theories of Gilvarry and Sagan implying the presence of indigenous organic matter on the moon are reviewed briefly, for comparison. The former postulates the presence in the lunar maria of organic remains derived from a pristine biota in a hydrosphere formed by exudation from the moon's interior and lasting several billion years. The latter assumes the presence of organic matter on the lunar highlands, now covered by meteoritic infall, formed by the action of solar ultraviolet light and other agencies on a reducing proto-atmosphere lasting significantly less than a billion years. However, the fact that meteoritic infall on a moon without an atmosphere causes a net loss of mass from that body is determinative for observability in the Surveyor and Apollo missions of the organic vestiges postulated in the two theories. On Gilvarry's model, a loss of mass from the lunar surface of at least 7 meters in depth is found for the effects of meteoritic impact and sputtering action (by the particles of the solar wind and flares) over the period of several billion years since the atmosphere and hydrosphere vanished.

Gold, T., 1966, Probable mode of landing of Luna 9: *Nature*, V. 210, p. 150.

Guesses as to the mode of landing of Luna 9 are considered in terms of their implication to the nature of the lunar surface. The most puzzling feature appears to be the fact that the ground tends to give way after some extended period of time. A possible explanation of this is suggested in terms of the weight of the space craft resulting in many little slides and collapses in internal cavities, which eventually reduce the strength of the ground and eventually let the vehicle settle.

Gold, T., and Hapke, B.W., 1966, Implications of the Luna 9 pictures: *Transactions of the American Geophysical Union*, V. 47, No. 2, p. 426.

The surface of the moon, cratered on a scale of centimeters as seen by Luna 9, can be interpreted as the surface of a fine-grained rock powder subjected to bombardment by material that includes similar powder. Laboratory demonstrations of such processes produced pictures that very closely resemble the landscape seen by Luna 9. The primary and secondary bombardment that the lunar surface must have received will thus fully account for its appearance, whatever the type of rock that was there originally, provided only that the material has been broken down into sufficiently fine particles. The degree of cohesion between the particles, or the amount of sintering that they may have suffered and therefore the firmness of the ground, cannot be judged from the appearance. The adhesion necessary to allow such a high degree of surface roughness to exist would be possessed by micron sized particles of any rock, though a coarser substance like sand would not maintain the observed forms. The movement of Luna 9 between two picture-taking sequences may have to be interpreted in terms of the nature of the lunar surface. (Abstract of a paper presented at the April 1966 meeting of the American Geophysical Union).

Gold, T., and Hapke, B.W., 1966, Luna 9 pictures: Implications: *Science*, V. 153, p. 290-293.

The Luna 9 pictures have not precluded the existence of a surface made up largely of very fine rock particles.

Greenman, N.N., Burklig, V.W., and Young, J.F., 1966, Ultraviolet reflectance measurements of possible lunar silicates: Transactions of the American Geophysical Union, V. 47, No. 1, p. 150.

The reflectance of granitic, gabbroic, and serpentinite rocks in the 2000-3000 Å range has been measured to determine whether they display characteristic spectra that could give compositional information about the lunar surface. Measurements were made of solid and granular samples, the latter of three different grain sizes with median diameters of 170-260, 11-16, and 8 microns. The reflectance in all cases was found to decline gradually from 3000 to 2500 Å and still more gradually from 2500 to 2000 Å. For the most part, the order of reflectance, from highest to lowest, was gabbroic, granitic, and serpentinite, but the differences were small. Typical values for vertical incidence were about 10-14% at 3000 Å and about 5-8% at 2000 Å. No consistent variation with grain size was detected. If sharply defined compositional differences exist in this band, they must be in the fine structure of the spectra and may be found only with spectroscopy of higher resolution than was used in these experiments. (Abstract of a paper presented at the April 1966 meeting of the American Geophysical Union).

Hafner, W., 1966, Report on the lunar geological field conference, Bend, Oregon, August 22-28, 1965: Geophysics, V. 31, No. 4, p. 267-275.

This paper reviews the subject conference. Detailed descriptions are given of the geologic sites investigated. A summary is given of the papers and discussions on meteorite craters, volcanic features, lunar tectonism, and lunar surface properties.

Hapke, B., 1966, An improved theoretical lunar photometric function: The Astronomical Journal, V. 71, p. 386.

The theoretical photometric function for the lunar surface previously proposed by the author (J. Geophys. Res. 68, 4571, 1963), which successfully predicted variations of brightness for areas between selenographic longitudes of  $\pm 60^\circ$ , has been improved so that it better agrees with observations in the limb regions. The modification consists of wrinkling the porous, open surface of the previous model into a series of steep-sided depressions. For formal mathematical reasons, the depressions used are cylindrical troughs whose axes are parallel to lines of luminance longitude. However, the primary requirement is that the surface must be densely covered (~90%) with features whose walls make steep angles ( $24.5^\circ$ ) with the local horizontal and that these walls must be partly visible even at glancing angles. This model is consistent with radar-reflection data which indicate that the moon is smooth on a scale of meters but is rough on a subcentimeter scale. Hence the size of these depressions is inferred to be centimeters and millimeters. These features are probably primary and secondary impact craters and ejecta debris, which saturate the lunar surface on this scale. The preceding conclusions were contained in a paper submitted to the Astronomical Journal in December 1965. The remarkable pictures of the lunar surface transmitted by Luna 9 appear to corroborate these predictions concerning the small-scale morphology of the lunar surface. (Abstract of a paper presented at the March 1966 meeting of the American Astronomical Society).

Hapke, B., 1966, Comments on paper by Philip Oetking, "Photometric studies of diffusely reflecting surfaces with applications to the brightness of the moon": Journal of Geophysical Research, V. 71, p. 2515.

Modification of photometric apparatus used in previous experiments so that all relevant instrumental angles were less than  $\frac{1}{2}^\circ$  resulted in the detection of the brightness surge reported by Oetking.

Hapke, B., 1966, On the composition of the lunar surface: Transactions of the American Geophysical Union, V. 47, No. 1, p. 149-150.

A large number of igneous rocks and meteoritic material were pulverized and irradiated by hydrogen ions to simulate the effects of meteorite and solar wind bombardment of the lunar surface. The optical properties of these materials were then studied and compared with those of the moon. Several varieties of basic rock powders duplicated lunar optical characteristics after irradiation, including certain ultrabasic rocks, basalts, and diorites. Highly acidic rocks, such as granites, syenites, and granodiorites, do not match the moon, nor do chondritic meteorites. From these observations, the following deductions can be made about the composition of the surface of the moon: (1) The lunar crust appears to be largely basic in composition. (2) The lunar surface apparently is not chondritic; hence, chondrites probably do not come from the moon, although achondrites may. The southern highland areas of the moon appear to be the unaltered remnants of the last stages of accretion, implying that at least part of the material from which the moon was accreted probably contained less Fe than chondrites, which is consistent with the density of the moon. (Abstract of a paper presented at the April 1966 meeting of the American Geophysical Union).

Hapke, B., 1966, Some comments on Gehrels' model of the lunar surface: Icarus, V. 5, p. 154-159.

Recently Gehrels and his associates have published new and important observations concerning the wavelength dependence of the optical properties of the lunar surface. To explain these properties Gehrels has put forward a new model of the lunar surface. This model consists of an optically-thin layer of micron-sized particles electrostatically suspended over a darker surface in such a manner that the average distance between particles is about 10 times their radii. The difficulties are twofold: (1) The electrostatic forces acting on the lunar surface are insufficient. (2) Such a layer would have optical properties which are quite different from those of the moon.

Hapke, B.W., and Gold, T., 1966, Luna 9 pictures and the lunar surface: The Astronomical Journal, V. 71, p. 857.

The small-scale morphology of the lunar surface seen in the Luna 9 pictures has been interpreted either as a porous volcanic rock froth or as a moderately cohesive soil saturated with primary and secondary impact craters. Without additional information it is not possible to differentiate between the two models. Such information is provided by radar, radio-thermal, infrared and optical investigations of the moon, which indicate that the lunar surface is almost everywhere covered with a porous material to a depth of at least several meters. The near-universal distribution of the material strongly implies that it is externally generated. The visible scattering and polarimetric evidence indicates that this material is largely fine rock dust. Craters have been generated in the laboratory in powders by both impacts and explosions. The resulting morphology bears a remarkable resemblance to that seen in the Luna 9 pictures. Features seen on both the laboratory and lunar surfaces include: rimmed craters, rimless craters, piles of gravel-like rubble, "rocks," steep slopes, and raised linear features. It is concluded that the landscapes shown in the Luna 9 pictures is largely dust of undetermined depth and undetermined degree of cohesion.

The Surveyor 1 photographs have shown that the surface near the landing site consists of dust (i.e., extremely fine-grained, moderately-cohesive rock powder). The similarity between both the appearance and the physical properties of the Luna 9 site and Surveyor 1 areas suggests that the Luna 9 site also consists of similar material.

Radar evidence indicates that the depth of the soil is at least several meters, and the detailed Surveyor photographs do not contradict this. (Abstract of a paper presented at the July 1966 meeting of the American Astronomical Society).

Hopfield, J.J., 1966, Mechanism of lunar polarization: *Science*, V. 151, p. 1380-1381.

A theoretical model to explain the negative branch of the lunar polarization curve is developed. The model is based on the effects of shadows produced by opaque dielectric obstacles.

Hunt, G.R., 1966, Rapid remote sensing by a "Spectrum Matching" technique, I, Description and discussion of the method: *Journal of Geophysical Research*, V. 71, p. 2919-2930.

A method of rapid remote sensing is described which is applicable for obtaining information about the compositions of materials from both terrestrial and extra-terrestrial sources. It is a method of infrared spectrum matching, in which the emission spectrum from the source is instrumentally compared with the reflection spectra of a set of polished samples of different compositions. The effects of other variables, such as temperature and surface condition, are explored, and the effect of an intervening attenuator is considered. It is found that despite the presence of other variables identification of compositional differences between targets can be made.

Irvine, W.M., 1966, The shadowing effect in diffuse reflection: *Journal of Geophysical Research*, V. 71, p. 2931-2937.

The theory of multiple scattering based on the equation of radiative transfer breaks down for directly backscattered radiation if the scattering particles are large enough and the medium dense enough for the particles to shadow one another. This "shadowing effect" can be incorporated as a correction into the usual radiative transfer theory. The resultant theory may be applicable to Saturn's rings and the lunar surface.

Jaffe, L.D., 1966, Lunar dust depth in Mare Cognitum: *Journal of Geophysical Research*, V. 71, p. 1095-1103.

A previously reported technique for preparing and imaging laboratory craters overlain by various thicknesses of granular material has been refined. The resulting photographs have been compared with those obtained by Ranger 7 spacecraft. Results support the earlier conclusion that the appearance of lunar craters in the Ranger photographs is consistent with the presence of at least 5 meters of granular overlay, and probably considerably more, in the area of Mare Cognitum.

Jaffe, L.D., 1966, Lunar overlay depth in Mare Tranquillitatus, Alphonsus, and nearby highlands: *Icarus*, V. 5, p. 545-550.

Photographs of lunar craters obtained by the spacecraft Ranger 8 and Ranger 9 have been compared with those of laboratory craters overlain with known amounts of granular material. Results are consistent with the interpretation that at least 5 meters of granular material, and probably considerably more, have been deposited on Mare Tranquillitatus, Alphonsus, and nearby highland areas, subsequent to the formation of most of the craters 55 meters in diameter or larger.

Jaffe, L.D., 1966, Scientific results of Surveyor 1--summary: *Transactions of the American Geophysical Union*, V. 47, No. 4, p. 617-618.

The lunar surface at the Surveyor 1 landing site is composed of granular material.

Most of this material consists of particles smaller than 1 mm. The size distribution extends up to blocks at least 1 meter in diameter. The local surface brightness temperatures generally agree with predictions from earth-based measurements, as does the local radar cross-section at 3-cm wavelength. The spacecraft pads penetrated at least 3 cm into the surface during landing, throwing out, pushing aside, and compressing surface material. The dynamic bearing resistance of the surface was  $4 \times 10^8$  to  $7 \times 10^8$  dynes/cm<sup>2</sup>. The surface material has appreciable cohesion; its mechanical behavior resembles that of a damp, fine-grained terrestrial soil. Photographs of the solar corona were made from the lunar surface and are being analyzed. (Abstract of a paper presented at the September 1966 meeting of the American Geophysical Union).

Jaffe, L.D., and Scott, R.F., 1966, Lunar surface strength: Implication of Luna 9 landing: *Science*, V. 153, p. 407-408.

From the ability of the lunar surface to support Luna 9, it is concluded that the surface can bear at least  $5 \times 10^8$  dyne cm<sup>-2</sup>. The landing dynamics gives a value of 1 to  $2 \times 10^8$  dyne cm<sup>-2</sup>, but this is uncertain because the landing parameters are not known.

Jones, R.H., 1966, Surveyor I landing dynamics: *Transactions of the American Geophysical Union*, V. 47, No. 4, p. 617.

The landing gear of the three-legged Surveyor spacecraft incorporates hydraulic orifice-damped shock absorbers and crushable aluminum honeycomb footpads and body blocks. Full scale tests have shown that, with known landing conditions, shock absorber force-time histories can be predicted with a high degree of accuracy. The excellent shock absorber strain gage data obtained from the Surveyor I mission have been compared with analytical results in an attempt to establish bounds on some surface mechanical properties. Good correlation has been achieved considering a landing between 11 and 12 ft/sec on a surface of 5-psi static bearing pressure and a density of 2.3 to 3.0 slugs per ft<sup>3</sup>. However, simulated landings on a "hard" surface also result in close agreement with measured force-time histories. Landing dynamics simulations alone are therefore unable to differentiate between a "hard" surface covered with a layer of very weak material, or some intermediate surface. Observations of some of the indigenous craters tend to substantiate a homogenous concept. (Abstract of a paper presented at the September 1966 meeting of the American Geophysical Union).

Katz, I., 1966, Wavelength dependence of the radar reflectivity of the earth and the moon: *Journal of Geophysical Research*, V. 71, p. 361-366.

Recent interest in the use of a multifrequency radar as a remote sensor for exploration of the earth and the moon has stimulated this study of the variation of radar backscattering with change in electromagnetic wavelength. The analysis of data has shown that radar cross sections of land and sea surfaces decrease with increasing wavelength and, on the average, follow approximately a  $\lambda^{-1}$  behavior, although the exponent may vary from +2 to -6 in individual cases. Snow-covered surfaces at all depression angles and sea surfaces at angles above 73° are the ones with positive values for the exponent. The wavelength dependence of the moon and the average values found on the earth in this study are quite similar. The combination of polarization and wavelength dependence versus depression angle may be characteristic features for distinguishing various terrain types by a multifrequency radar.

Kraner, H.W., Schroeder, G.L., Davidson, G., and Carpenter, J.W., 1966, Radioactivity of the lunar surface: *Science*, V. 152, p. 1235-1236.



Diffusion of radon and thoron from the lunar surface provides a mechanism for producing radioactivity on the lunar surface. If the diffusion is the same as on the earth's surface, the radioactivity would be of approximately 1 microcurie  $\text{m}^2$ .

Lettau, H.H., 1966, Dust on the moon's surface?: *Journal of Geophysical Research*, V. 71, p. 5469-5470.

Conclusions concerning the nature of the lunar surface layer based solely upon visual impressions from Ranger and Luna 9 photographs are unwarranted. Other and independent lines of evidence, such as the thermal radiation characteristics at various wavelengths, should also be used. The author concludes from these parameters that the lunar surface is probably porous, rather than covered by dust, and that solid basalt is present from 2 to 6 cm below the surface.

Linsky, J.L., 1966, Models of the lunar surface including temperature-dependent thermal properties: *Icarus*, V. 5, p. 606-634.

The thermal conditions on the lunar surface are considered on a gross scale in terms of models with temperature-dependent thermal properties, including radiative energy transport.

The postulated existence of radiative energy transport is consistent with a porous or frothy medium, in agreement with photometric and laboratory simulation experiments, as well as with recent radar depolarization measurements. A distance scale of 0.1-0.3 mm for the effective mean separation of radiating surfaces is suggested by this interpretation of the data.

Linsky, J., 1966, Models of the lunar surface with temperature-dependent thermal properties: *The Astronomical Journal*, V. 71, p. 168-169.

The author has written a computer program to solve the heat conduction equation and to compute radio brightness temperatures for a medium having conductive and radiative energy transport and characterized by arbitrary temperature- and depth-dependent thermal properties. This program will also solve periodic heat conduction problems of a more general nature.

A number of models were constructed with a range of temperature-dependent conductivities and specific heats, but each was consistent with the minimum surface temperature of 90°K observed by Low (*Astrophys. J.* 142, 806, 1965) at the morning terminator. All of these models predict infrared and radio brightness temperatures for eclipses and lunations which agree favorably with high-resolution data for the center of the lunar disk.

If there are no internal heat sources, a significant increase in the mean radio brightness temperature with wavelength occurs when the conductivity, but not the specific heat, increases with temperature. This increase in the mean radio brightness temperature results from the nonlinear nature of heat conduction under these circumstances, and is sufficient to explain the observed increase with wavelength described by Krotikov and Troitskii (*Soviet Phys.--U.S.S.R.* 6, 841, 1964), without requiring as a postulate an unusually high level of radioactivity in the moon. The general behavior of silicates at lunar temperatures and laboratory measurements of probable lunar materials suggest that radiative energy transport is the most probable mechanism to account for an increase in the conductivity with temperature. Several models in which radiative transfer and thermal conduction are of comparable importance at 350°K agree favorably with the data of Krotikov and Troitskii. The present findings support the hypothesis that porous or frothy material characterize the lunar surface at least to a depth of 20 cm, and are in agreement with radar depolarization studies. (Abstract of a paper presented at the December 1965 meeting of the American Astronomical Society).

Lipsky, Y.N., 1966, What Luna 9 told us about the moon: Sky and Telescope, V. 32, p. 257-260.

The Luna 9 mission is described, photographs and a discussion of results are presented. It is concluded that the bearing strength of the lunar soil is at least a few kilograms per square centimeter. The author feels the experiment refuted the dust theory of the lunar surface and showed that the effect of micrometeorites on the surface has been overestimated.

Lucas, J.W., Conel, J., Saari, J., Garipay, R., and Hagemeyer, W., 1966, Some lunar thermal characteristics from Surveyor I data: Transactions of the American Geophysical Union, V. 47, No. 4, p. 616.

Surveyor I has presented the first opportunity to obtain in situ estimates of some lunar surface thermal characteristics. Preliminary estimates have been made by analysis of the thermal engineering behavior of selected portions of the spacecraft during operation on the lunar surface. Local lunar surface brightness temperatures calculated from one thermal sensor are in good agreement near lunar noon and after sunset with earth-based predictions. The predictions were made assuming the lunar surface is a Lambertian emitter and has a thermal parameter value of 250 to 1000 in cgs units. The agreement indicates the lunar surface material near the spacecraft is highly insulating and is probably finely granulated. A discrepancy during the lunar morning between the Surveyor I and earth-based predictions is speculated to be due to directional thermal emission of the lunar surface. The thermal behavior of sun-dependent white surfaces on the spacecraft indicates that they remained free of any substantial amount of lunar dust. This conclusion is supported by TV pictures of the spacecraft which show only some small particles randomly distributed. (Abstract of a paper presented at the September 1966 meeting of the American Geophysical Union).

Matsushima, S., 1966, Apparent correlation between the lunar eclipse brightness and the solar wind: Nature, V. 211, p. 1027-1028.

An approximate calculation is performed which shows that the correlation found between the brightness of a lunar eclipse and the interplanetary index can be interpreted as arising from the effects of lunar luminescence.

Matsushima, S., 1966, Variation of lunar eclipse brightness and its association with the geomagnetic planetary index  $K_p$ : The Astronomical Journal, V. 71, p. 699-705.

A correlation is found between the brightness of the eclipsed moon and the geomagnetic planetary index  $K_p$ . The observed data consist of 20 photometric measurements in each of the  $B(\lambda 4700\text{\AA})$ ,  $G(\lambda 5300\text{\AA})$ , and  $R(\lambda 6200\text{\AA})$  colors for the 15 eclipses between 1932 and 1957. A plot of the logarithmic brightness of the eclipsed moon in each color against either 3 h or 24 h mean  $K_p$  at the time of each eclipse shows a monotonous increase with increasing  $K_p$ . A similar correlation is found in a plot of the B-G or B-R color index of the eclipsed moon vs  $K_p$ , implying that the eclipsed moon is more reddened when  $K_p$  is larger. On the other hand, no clear relationship is found between the eclipse brightness and the sunspot activity.

Using the empirical equation relating the mean plasma velocity and  $K_p$  derived by Snyder et al., the  $K_p$  value at each eclipse is converted to the plasma velocity. It is found that the logarithmic diagrams of the energy flux at the moon vs proton velocity show a linear increase with a slope of about 4 in all three colors. In order to interpret the above results as being due to variations in luminescent brightening caused by the direct bombardment of the solar wind, however, we find it necessary to assume about an order of magnitude larger

density of the solar proton than the value generally accepted. A number of luminescence observations so far published are reviewed on the basis of the  $K_p$  index. The dates of these observations do not always fall on the dates of high  $K_p$ . However, it should be noted that all of these observations were made on the moon outside of eclipse and the time durations appear to be very short. For the luminescent emission to be detectable over the ordinary moonlight requires the plasma flux to be at least three orders of magnitudes greater than the upper limit obtained from Snyder's equation. One explanation would be to assume that an extraordinarily active plasma may be emitted from the sun for a very short period of time which is not accessible to the system on which the parameter  $K_p$  is based, whereas Snyder's equation refers to the velocity fluctuations of the steady flow of the interplanetary plasma.

Matveev, Yu.G., Suchkin, G.L., and Troitskii, V.S., 1966, Change of lunitite density with depth in the surface layer: *Soviet Astronomy - A.J.*, V. 9, p. 626-630.

Comparison of radioastronomical and radar data for the coefficient of reflection of radio waves from the moon leads to the conclusion that there is a probable dependence of the coefficient of reflection on wavelength. It is shown that the determined frequency dependence of the coefficient of reflection, together with the firmly established fact of a difference in the values  $\gamma = (k_{pc})^{-2}$ , measured from the eclipse and phase variations of the surface temperature, can be attributed to an increase of the density  $\rho$  of lunitite by a factor of 1.5-2 within the upper layer. On the basis of this assumption, an electronic computer was used for making precise computations of the spectrum of the coefficient of reflection for an exponential change of the density of matter with depth for two different values of density and different thickness of the inhomogeneous layer. Comparison of computations with radar and radioastronomical data on the coefficient of reflection reveals that the density of lunitite increases with depth for a distance of about 4 cm and then remains constant, exceeding the surface density by a factor of 1.5. The value  $\alpha = k/\rho$ , characterizing the microstructure of lunitite, is estimated. It was found that this value is about  $2 \cdot 10^{-6}$  and falls between the values characteristic of finely dispersed unconsolidated and solid but porous terrestrial rocks.

Meloy, T.P., and Faust, L., 1966, Size and velocity distribution of ejecta from an impact crater: *Transactions of the American Geophysical Union*, V. 47, No. 1, p. 149.

A rotationally symmetric model of an impact crater was considered. It was assumed that the partition of energy in the compressional wave through the substrate was proportional to the energy in the wave. The Gaudin-Meloy size distribution law was used to compute the size distribution of the daughter fragments resulting from comminution of the rock substrate. The velocity of the ejecta particles was assumed to be proportional to the energy in the compressional wave and to the surface area of the particles. Integrating over the crater volume yields a size distribution and a velocity distribution of the fragment. This result is used to predict size distribution of fragments as a function of distance from the crater. (Abstract of a paper presented at the April 1966 meeting of the American Geophysical Union).

Meloy, T.P., and Faust, L., 1966, Size distribution and depth of dust on the lunar surface considering impact comminution alone: *Transactions of the American Geophysical Union*, V. 47, No. 1, p. 149.

Using the Meloy-Faust size and velocity distribution for fragments from impact craters, an estimate was made of the depth and size distribution of dust on the lunar surface as a function of time. Several meteoric bombardment rates were considered. Primary, secondary, tertiary bombardment is taken into consideration.

Degradation of fragments is considered. The results indicate a depth of dust of 25 feet with 50% of the mass of particles having a diameter of less than 40 microns of mass, and 99.9% of the mass having a diameter of 1 millimeter or less. The roughness of the surface due to blocks is low, since there is less than one block a meter (or larger) in size per square kilometer. (Abstract of a paper presented at the April 1966 meeting of the American Geophysical Union).

Mertz, L., 1965, Discussion of paper by E.A. Burns and R.J.P. Lyon, "Errors in the Measurement of the Lunar Temperature": *Journal of Geophysical Research*, V. 70, p. 999-1000.

Numerous cavities must occur in the surface, and the particles will in all probability be fine. Together these two characteristics would wipe out any resonance gaps in the spectral emissivity. The blackbody assumption of Pettit and Nicholson (1930) consequently remains valid. Indeed, it is discouraging that only in the few possible bare rock regions could resonances aid in determining the geologic composition of the moon.

Moron, J.M., Jr., and Staelin, D.H., 1966, Observations of the moon near 1-cm wavelength: *The Astronomical Journal*, V. 71, p. 865.

Observations of the moon were made with the 28-ft. antenna at Lincoln Laboratory, and a receiver with channels at 32.4, 29.5, 25.5, 23.5, and 21.9 GHz (Staelin and Barrett, *Astrophys. J.* 144, 1, 352). A total of 340 drift scans were taken between 15 June and 15 August 1964.

Because of long-term gain fluctuations, the harmonics of the equatorial brightness temperature were found from the slopes of the drift scans rather than their amplitudes. These slopes, computed by fitting a straight line to the center half of each scan, vary harmonically with time. The constants of proportionality between the harmonics of the brightness temperature and those of the slopes involve convolution integrals which are virtually independent of the lunar model. The presence of higher harmonics in the brightness temperature is more readily detected by this technique. The average lunar brightness temperature was assumed to be 217°K. The system was not otherwise calibrated. The first harmonic amplitudes are consistent with other published results. This is the lowest frequency at which the second harmonic has been measured and its amplitude appears to be higher than that predicted by a homogeneous model. The second and higher harmonics should yield information about the vertical stratification of the lunar surface.

With another receiver at 35.0 GHz drift scans across the center of the moon were made near transit alternately with vertical and horizontal polarization. The peak difference in antenna temperatures was 5.5% of the central temperature which implies an effective dielectric constant of 1.5. (Abstract of a paper presented at the July 1966 meeting of the American Astronomical Society).

Moroz, V.I., 1966, Infrared spectrophotometry of the moon and the Galilean satellites of Jupiter: *Soviet Astronomy - A.J.*, V. 9, p. 999-1006.

Spectra of selected sectors of the lunar surface in the region 0.8-3.8  $\mu$  were obtained using a 125-cm reflector and a prism infrared spectrometer with  $\lambda/\Delta\lambda$  from 20 (at 1.6  $\mu$ ) to 80 (at 3.4  $\mu$ ). Albedo increases with wavelength, at least to 2.2  $\mu$ , approximately identically for all the investigated sectors, including seas, continents and light craters. Among terrestrial rocks volcanic ash and scoria have a similar dependence of albedo on wavelength. Thermal emission makes a considerable contribution in the interval 3-4  $\mu$ . The value of the thermal excess was used in determining the temperature (395°K) of the subsolar point. The same spectrometer, with 125- and 260-cm reflectors, was used in observing the spectra of the Galilean satellites in the region 0.8-2.5  $\mu$ . The records of Europa and Ganymede show details characteristic of the reflection spectrum of a snow cover.

Morris, E.C., and Shoemaker, E.M., 1966, Craters and fragmental debris of the lunar surface around Surveyor 1: Transactions of the American Geophysical Union, V. 47, No. 4, p. 617.

The disturbance of the lunar surface by the Surveyor 1 footpads and the shapes of small natural craters in the field of view show that the lunar surface at the Surveyor 1 landing site is underlain by very weakly cohesive material. This material is probably composed of fragments of a wide range of size, similar to those observed directly at the surface. Near the spacecraft, the weakly cohesive material occurs as a layer that extends to an average depth of 1 to 2 meters, as indicated by the rim characteristics of craters that have been formed in the layer and of larger craters that have penetrated the layer. The raised rims of craters up to 3.3 meters across are relatively smooth, whereas raised rims of larger craters are covered with abundant coarse angular blocks that have been derived from beneath the weakly cohesive material. The observed thickness of the layer and the distribution of fragments and craters on the surface of the layer are in good agreement with the predicted thickness and surface characteristics of a fragmental debris layer expected to have been formed primarily by repetitive bombardment of the surface by lunar secondary ejecta. (Abstract of a paper presented at the September 1966 meeting of the American Geophysical Union).

Nash, D.B., 1966, Proton-excited luminescence of silicates: experimental results and lunar implications: Journal of Geophysical Research, V. 71, p. 2517-2534.

Spectral energy distributions and excitation efficiencies as functions of mineral composition, irradiation time, proton energy, proton flux, sample geometry, and sample temperature have been determined from laboratory measurements of silicate luminescence by low-energy proton excitation. The maximum of the luminescence spectrums of many silicates under continuous excitation by 5-keV protons is in the red when the mineral is first excited; the luminescence intensity decreases, and the maximum shifts from red to blue with time. This phenomenon is here described as a red flash. After the initial red flash, a second red flash, subsequent intensity decay, and blue shift can be produced by a sudden increase of incident ion energy. In both cases the red flash has a principal decay period of about 15 to 20 minutes. The intensity of both the flash and aged luminescence response is directly proportional to incident ion energy and flux. Small particle size for powders, high roughness for solid surfaces, and low mineral temperature favor high luminescence intensity. These data qualitatively agree with the concept of solar-ion excitation as the origin of reported transient lunar reddening near Aristarchus and Kepler. However, these measurements show that the energy efficiency for proton excitation of silicate luminescence is between  $10^{-4}$  and  $10^{-6}$ ; this range is several orders of magnitude lower than values previously reported. In view of the known solar-ion flux, the low efficiencies indicate that luminescence on the sunlit lunar surface resulting from solar-ion excitation is far below the sensitivity of earth-based detection apparatus and that other energy sources or other explanations for the origin of lunar color flashes must be sought.

Nash, D.B., 1966, Proton luminescence of feldspars and silica polymorphs and lunar applications: Transactions of the American Geophysical Union, V. 47, No. 1, p. 150.

Silica polymorphs and alkali and plagioclase feldspars luminesce under 5-keV proton excitation ( $10^{14}$   $H^+$ /cm<sup>2</sup>/sec) with intensities of an order of magnitude greater than those of other rock-forming silicates. Consequently, lunar luminescence should come largely from these phases, if lunar surface materials are similar to the earth's crust. To test this possibility, spectral and temporal variations in the luminescence response to simulated solar wind excitation of various species of these mineral groups have been investigated.



Excitation efficiencies for the silicas and feldspars are within the range  $2-7 \times 10^{-8}$ . Qualitatively, proton luminescence of these minerals is similar to observed lunar luminescence. The low excitation efficiencies, however, require solar particles fluxes a factor of  $10^8$  higher than those thought to exist at the lunar surface to provide the observed brightness of lunar luminescence. (Abstract of a paper presented at the April 1966 meeting of American Geophysical Union).

Ney, E.P., Woolf, N.J., and Collins, R.J., 1966, Mechanisms for lunar luminescence: *Journal of Geophysical Research*, V. 71, p. 1787-1793.

The visibility of luminescence on the moon depends on the competing processes that illuminate the moon and that provide energy for luminescence. It is shown that the most favorable times for seeing luminescence are at new moon, on the far side of the moon, and during rare dark eclipses. The luminosity and color of these rare eclipses are explained. Observations supposedly of luminescence during lunar day are criticized, and only the spectroscopic evidence is taken to support the reality of luminescence. Both direct and storage processes have been considered for converting energy to luminescence. Direct processes in lunar day cannot be energized by presently known sources of particles. If indirect processes occur they may give information about the dust particles at the extreme lunar surface.

Oetking, P., 1966, Photometric studies of diffusely reflecting surfaces with applications to the brightness of the moon: *Journal of Geophysical Research*, V. 71, p. 2505-2513.

A series of light reflectivity measurements has been made on a variety of samples in a search for materials or surface textures which might reproduce the photometric properties of the lunar surface, particularly the pronounced rise of reflectivity at small phase angles. It has been found that most terrestrial substances, including standard diffusing surfaces, when observed with an instrument of small aperture, show a prominent rise in reflectivity if the direction of observation is within  $45^\circ$  of the direction of the incident light. Experiments show that the height of the intensity peak entails complex interrelations of the particle size, shape, and optical properties of the reflector. The abrupt increase in the brightness of the lunar surface at zero phase may not be an unusual property of the moon but is one common to most substances.

Osgood, J.H., and Green, J., 1966, Sonic velocity and penetrability of simulated lunar rock dust: *Geophysics*, V. 31, No. 3, p. 536-561.

Theoretical considerations are given for the design of an ultrasonic pulsing system for non-cohesive dusts. Measurements of sonic velocity are reported for volcanic rocks of different textures. The data may be helpful in interpreting Surveyor results and evaluating lunar base requirements. Absolute measurements of shear strength were made at critical density obtained by vibrating the simulated lunar dust samples for specified time periods. For purposes of shear strength analysis, grain shapes may be grouped as spherical, prismatic, and vesiculate. Shear resistance curves are analyzed for each of these groups, and the vesiculate shapes have the highest shear strengths at critical density. Once sonic velocity and shear strength data are obtained by a lunar probe or astronaut, practical studies can be made on bearing capacity, trafficability, and lunar base construction.

Petrova, N.N., 1966, Spectrophotometric study of the lunar surface: *Soviet Astronomy - A.J.*, V. 10, No. 1, p. 128-135.

Observations with the photoelectric spectrophotometer of the Astrophysical Institute of the Kazakh Academy of Sciences are reported for 11 areas on the

lunar surface. The relative spectral distribution of the reflectivity is derived by comparing the lunar spectra with spectra of early-type stars and the sun. In general, the reflectivity varies almost linearly with wavelength; for similar inclinations, the same spectrum obtains for the brightness coefficients of certain terrestrial substances containing considerable quartz and other siliceous compounds. Direct comparison of spectra shows that lunar formations generally differ negligibly in color, but the curves for the spectral brightness ratios are not always monotonic, exhibiting several waves and humps. The humps in two spectral regions (at  $\lambda_{\text{max}} \approx 5305$  and  $6680 \text{ \AA}$ ) are interpreted as emissions excited by solar irradiation of the lunar surface. If the variable component of solar corpuscular radiation causes the observed emission variations, the flux estimated from the emission intensity would correspond to a very active sun, which is contrary to published data on solar activity during the period when maximum emission was observed. Photospheric ultraviolet energy would suffice to excite the observed emission, but the variability would then be inherent in the luminous material on the moon itself.

Righini, A., Jr., and Rigutti, M., 1966, Some results of research on lunar luminescence: *Icarus*, V. 5, p. 258-265.

Research on lunar luminescence has been done with a technique similar to that illustrated by Kopal and Rackham. No luminescence phenomena have been observed, but the analysis of the observations has pointed out that some precautions must be taken in order to obtain reliable photographic observations.

Rennilson, J.J., 1966, Selected colorimetric results from Surveyor I television: *Transactions of the American Geophysical Union*, V. 47, No. 4, p. 616.

Color is being measured from the Surveyor I television camera data to determine the visual appearance of the lunar surface and to search for color differences among the exposed rocks. Preliminary results indicate the surface is uniformly gray over large areas. Two rocks that were examined for color close to the spacecraft showed no easily detected difference in color from the general surface, even though they are strikingly different in texture and albedo. Further processing of the images is required to search for subtle color variations. (Abstract of a paper presented at the September 1966 meeting of the American Geophysical Union).

Rennilson, J.J., and Holt, H.E., 1966, Photometric properties and photoclinometry of the lunar surface from Surveyor I television: *Transactions of the American Geophysical Union*, V. 47, No. 4, p. 616.

The local photometric function of the lunar surface has been measured from Surveyor I television pictures. Our solution for the normal albedo of the lunar surface around the spacecraft, about 6% is estimated by extrapolation from the surface luminance measured at low phase angles. The photometric function derived from the Surveyor I television pictures is similar in form to the photometric functions of local areas on the moon measured photoelectrically at the telescope. The contribution to the telescopically measured photometric functions from topographic irregularities larger than about 10 cm is therefore minor. Topographic profiles have been computed from photometric measurements utilizing the photometric function derived from the Surveyor television pictures. This application of the new technique of lunar photoclinometry to spacecraft-acquired images is the first in which the local photometric function has been measured at a scale appropriate to the solution of the photoclinometric equations. (Abstract of a paper presented at the September 1966 meeting of the American Geophysical Union).

Roberts, W.A., 1966, Lunar surface characteristics: A contemporary view: *Publications of the Astronomical Society of the Pacific*, V. 78, p. 448-449.



All the hypotheses concerning the origin of the moon cannot be true, but regardless of the birthplace of the moon and the method of formation, the body of the moon has been subject to the environment into which it was born. One of the environmental factors is a flux of micro- to macrometeorites. At present, the earth, and presumably the moon, is exposed to a flux of space debris, and the presence of probable fossil meteorite impact features on earth indicates that the present flux is probably an extension of a condition that has occurred throughout at least the later part of the history of the solar system. Meteorite impact at high velocity produces craters surrounded by brecciated target material. The quantity of atmosphere surrounding and protecting a planetary body determines to a large extent the size of meteorites that can penetrate to the planetary surface at high velocity. The moon is essentially unprotected. Some of the features seen in the earth-based photographs of the moon appear to be volcanic in nature. Volcanism on the moon would be restricted in areal and/or temporal distribution, unlike the ceaseless erosion and sculpturing process of the impact of space debris. Thus, volcanic and nonvolcanic features will be altered and eroded by the meteorite flux to an extent proportional to the total areal density of impacting meteorites or, in effect, the age of the feature. The Surveyor 1 and Luna 9 pictures show views of the lunar terrain surrounding the experiment packages and detailed views of exposed rocks. The terrain illustrated by panoramic sequences is consistent with poorly sorted shock breccia from both primary and secondary craters formed in a layer of shock-brecciated fine-grained crystalline silicate rock. Apparent sorting suggests reworking of the breccia by several impacts. A detailed view of a rock by Surveyor shows a conjugate or orthogonal fracture system in a rock that appears to be agglomeratic--either shock- or volcanic-cemented breccia. The rounded texture of the rock surface could indicate differential erosion by micrometeorites and secondary ejecta due to differential hardness of fragments and interfragmental materials. This texture would also be consistent with shock or thermal melting. A planar surface of this rock appears to have a texture consistent with a rock composed of weakly cemented fragments of various sizes. Such a rock could be shock-compacted breccia ejected from a nearby crater. (Abstract of a paper presented at a meeting of the Astronomical Society of the Pacific, June 1966).

Roberts, G.L., 1966, Three-color photoelectric photometry of the moon: *Icarus*, V. 5, p. 555-564.

Preliminary results are described of a program of detailed high-resolution lunar photoelectric photometry. A three-beam photoelectric photometer designed specifically for lunar colorimetric studies is described briefly. Experiments designed to measure short time variations in lunar luminescence gave negative results. This is attributed to lack of solar activity.

Ronca, L.B., and Salisbury, J.W., 1966, Lunar history as suggested by the circularity index of lunar craters: *Icarus*, V. 5, p. 130-138.

A quantitative way of measuring the circularity of lunar craters, the circularity index, is defined. Frequency curves of the circularity indexes of 86 craters reveal that two populations of craters are definable, one more circular than the other. The most likely explanation proposed is that the subcircular craters were formed during a period of stress in the lunar crust.

Rosenberg, D.L., 1966, Modification of optical properties of the lunar surface by solar wind bombardment: *Transactions of the American Geophysical Union*, V. 47, No. 3, p. 486-487.

Various igneous and metamorphic rocks, glasses, compounds, metals, a meteorite, and a tektite were subjected to simulated solar wind bombardment. When in a powder form, the particle size and surface compaction were also controlled. For quantitative comparison with the moon, the samples were measured at various wave-

lengths as to albedo, photometric function, polarization of scattered light, and depolarization of incident polarized light. Powders are darkened and generally reddened by hydrogen ion bombardment. The spread in color of rock powders was far greater than that found on the moon, but solar wind sputtering may cause global mixing of lunar surface constituents. Polarization requires particles mostly less than 0.1 mm in size in the lunar surface layer, but no evidence requires a low-density surface layer. The lunar photometric function implies that the (powder) surface is very rough macroscopically. (Abstract of a paper presented at the September 1966 meeting of the American Geophysical Union).

Ryan, J.A., 1966, Adhesion of silicates in ultrahigh vacuum: *Journal of Geophysical Research*, V. 71, p. 4413-4425.

This paper presents results of a study of silicate adhesion. Single-crystal minerals have been contacted in vacuum ( $10^{-10}$  mm Hg). The contacting surfaces have usually been formed in air; however, in two cases the surfaces were formed at ultrahigh vacuum by cleavage. Adhesion force was measured as a function of load force, temperature, surface roughness, and crystalline orientation. Load forces up to  $10^3$  dynes were applied; adhesion forces as small as  $2 \times 10^{-2}$  dyne could be measured. Temperature was varied from  $-160^\circ\text{C}$  to  $+100^\circ\text{C}$ , roughness from about 10 microns peak to peak (p.t.p.) to optical flatness. Two types of adhesion behavior were found for the surfaces formed in air. The first appeared only under load, increasing rapidly with increasing load, was of relatively large magnitude (up to about  $4 \times 10^2$  dynes); and was present only at ultrahigh vacuum. When this type of adhesion was observed, extensive surface damage and material transfer were also noted. It is concluded that this type of behavior is caused by the action of the normal silicate atomic bonding forces. The second type was observed at zero load, showed little load dependence, was of relatively low magnitude, persisted in dry nitrogen (at atmospheric pressure), and did not produce surface damage or material transfer. It is concluded that this type of behavior is probably caused by the action of the dispersion forces. No indications of a temperature dependence for the adhesion were detected. The adhesion was found to be orders of magnitude larger for the samples cleaved in vacuum than for the samples formed in air, and a strong, long-range attractive force, indicative of surface charging, was noted.

Saari, J.M., Shorthill, R.W., and Deaton, T.K., 1966, Infrared and visible images of the eclipsed moon: *Icarus*, V. 5, p. 635-659.

The moon was scanned with  $10''$  arc resolution at 0.45 and 10-12 microns during the total lunar eclipse of December 19, 1964. It was found that the lunar surface exhibits a surprising amount of thermal inhomogeneity. Hundreds of thermal anomalies were observed, most of which can be identified with bright craters or white areas. Certain maria and portions of maria were found to be thermally enhanced over their environs during the eclipse.

Schutten, J., and Van Dijk, Th., 1966, Luminescence caused by proton impact with special reference to the lunar surface: *Nature*, V. 211, p. 470-471.

On the basis of absolute measurements made of the luminescence of meteorites excited by protons in the 30 keV range, the authors believe it is very improbable that even during solar flares, when the intensity of the solar wind is increased by a factor of 100, the observed excitation of lunar luminescence can be caused by proton bombardment. Their laboratory values differ considerably from those of Derham and Geake and this difference is attributed to two possible causes. 1) Because the target consists of insulating material, during proton bombardment a potential drop develops across the target leading to development of secondary electrons with  $10^3$  the efficiency of the protons. 2) Background pressure in the apparatus may be a second cause of luminescence due to ionization of the gas

leading to creation of electrons. The authors conclude that luminous emission from the lunar surface is not due to solar wind but think it may be caused by electromagnetic radiation of short wavelength.

Scott, R.F., 1966, Symposium on Surveyor I results: soil mechanics results: Transactions of the American Geophysical Union, V. 47, No. 4, p. 617.

Further work carried out since the first report of June 1966, indicates that little revision of the soil properties estimated previously is required. The properties calculated from the landing dynamics and penetration of footpads 2 and 3 were reviewed and are found to be compatible with those estimated from the appearance of small nearby craters. (Abstract of a paper presented at the September 1966 meeting of the American Geophysical Union).

Shoemaker, E.M., and Morris, E.C., 1966, Fine structure of the lunar surface at the Surveyor I landing site: Transactions of the American Geophysical Union, V. 47, No. 4, p. 617.

The terrain around Surveyor I is a gently undulating surface studded with craters ranging in diameter from a few centimeters to several hundred meters and with angular fragments ranging from less than a millimeter to several meters across. The size-frequency distribution of the craters is close to that predicted for the maria by extrapolation of the crater size-frequency distribution observed in the Ranger pictures.

The observed angular fragments occupy 7.6% of the surface area and have a volumetric median grain size of 130 mm. The volumetric median grain size of all fragmental material on the surface may be of the order of 1 millimeter. About one crater 6 meters in diameter or larger and one block 1 meter across or larger is found on each 100 m<sup>2</sup> of the lunar surface around Surveyor I. (Abstract of a paper presented at the September 1966 meeting of the American Geophysical Union).

Smoluchowski, R., 1966, Structure and coherency of the lunar dust layer: Journal of Geophysical Research, V. 71, p. 1569-1574.

Experiments show that corpuscular radiation such as solar wind can sinter fine dust by producing displaced atoms which diffuse toward the surface of the grain. The estimated rate of churning of the topmost layer of lunar dust excludes sintering through sputtering. It follows that the dust is probably not loose but is partly coherent (0.5 dyne per particle), which increases its mechanical strength and decreases its mobility. Lower layers of dust are compacted by meteorite bombardment, and a close-packed density is probably reached at a depth of a meter or so. Loads that will not commence to sink in loose and in sintered dust are calculated.

Spergel, M.S., 1966, Solar flare induced neutrons at the surface of the moon: Transactions of the American Geophysical Union, V. 47, No. 1, p. 154.

A theoretical calculation has been performed on the production, by solar flare protons, of neutrons within the lunar surface and the resulting neutron albedo flux at the lunar surface. The transport of the neutrons is approximated by a single, energy, independent, exponential attenuation function. The incident solar flare proton flux is represented by an exponential rigidity spectrum. Ionization losses for the incident solar protons are calculated from estimates of the range of the protons within the lunar surface. The medium is represented by an "average" chondritic material. The resulting neutron albedo is found for three different flares and for various values of the model's parameter. Reasonable choices of these parameters lead to neutron dosage levels that are well

below the NASA recommended maximum short mission dose levels. (Abstract of a paper presented at the April 1966 meeting of the American Geophysical Union).

Sun, K.H., and Gonzalez, J.L., 1966, Thermoluminescence of the moon: *Nature*, V. 212, p. 23-25.

The authors postulate that some of the luminescence behavior of the moon may be due to thermoluminescence caused by the release of energy, trapped during the lunar night, when the surface is heated rapidly by the sun at the terminator. Experiments were performed to demonstrate the feasibility of such a process, and the authors conclude that if the moon is covered with meteorites of the enstatite achondrite type, it is almost certain that red and blue thermoluminescence occurs at the terminator of the moon at dawn.

Surveyor Scientific Evaluation and Analysis Team, 1966, Surveyor 1: Preliminary results: *Science*, V. 152, p. 1737-1750.

The terrain shown by Surveyor 1's photographs is described. Fragmental debris ranges in size from less than 1 mm to more than 1 m, and it extends to depth of at least 1 m. Lumps show that the material is at least slightly cohesive. Static bearing capacity of the soil is about  $4 \times 10^8$  dyne  $\text{cm}^{-2}$ , its cohesion is 1 to  $4 \times 10^8$  dyne  $\text{cm}^{-2}$  m its friction angle is between 30 and 40 degrees and its density is about 1.5 g  $\text{cm}^{-3}$ . However, it is also possible that the surface consists of a hard material overlain by a weak material to a depth of about 25 mm. Thermal properties reveal that the surface bears essentially no dust. The general surface is relatively smooth and nearly level on a kilometer scale. On a smaller scale the surface is littered with coarse blocks and fragments. The size distribution function resembles the distribution of crushed rocks, with a mean at approximately 1 mm. The albedo of the undisturbed surface is 7.7 percent, while the areas disturbed by the pads have a value of about 2 percent lower.

Thompson, T.W., and Dyce, R.B., 1966, Mapping of lunar radar reflectivity at 70 centimeters: *Journal of Geophysical Research*, V. 71, p. 4843-4853.

Radar observations of the lunar surface were made using the 10' beamwidth antenna at Arecibo, Puerto Rico, at a wavelength of 70 cm (430 Mc/s). Resolution of the surface of the order of 20 by 30 km was achieved, first, by resolving the echo in time delay and Doppler frequency shift and, second, by using the narrow antenna beamwidth to remove the ambiguity between hemispheres. Echo strengths measured in delay and frequency coordinates were then mapped onto photographs of the moon. The following were determined: (1) The lunar highlands of the southwest quadrant of the moon backscatter  $1\frac{1}{2}$  to 2 times as effectively per unit area as the mare regions of the east and northeast quadrants of the moon. (2) The mountain ranges which surround the circular maria backscatter  $1\frac{1}{2}$  to 2 times as much power as the adjacent mare regions. (3) Some craters were found to backscatter as much as 10 times as much power as their environs. The craters which had enhanced backscattering were bright under a full moon illumination and were nearly always young.

Titulaer, C., 1966, Isophotes of the Aristarchus region of the moon: *Bulletin of the Astronomical Institutes of the Netherlands*, V. 18, p. 167-169.

Isophotometric measurements have been made on plates taken during the total eclipse of the moon, 19 December 1964. This paper gives the profiles of the isophotes and their relative intensities. It was not possible to determine the variation of intensity with time. 80 pictures of Aristarchus, the brightest object of the moon, have been taken through a yellow filter (5400 Å). The difference in intensity between the centre of Aristarchus and the surroundings is about a factor two at phase angles  $10^\circ$ .

Troitskii, V.S., 1966, Radio emission of the eclipsed moon: Soviet Astronomy - A.J., V. 9, p. 1007-1019.

A theoretical investigation of lunar radio emission at the time of a lunar eclipse was made. Relations are derived for computing the intensity of radio emission of the eclipsed moon. These computations show that the value of the maximum relative decrease of effective temperature is proportional to the value  $\kappa a$ , the product of the coefficient of attenuation of an electromagnetic wave and the square root of the thermal conductivity coefficient  $a = (k/\rho c)^{1/2}$ . Expressed through the directly measured lunar parameters, the inverse value of the maximum temperature change increases linearly with wavelength and is proportional to  $\sqrt{b/\epsilon^2}$ , where  $b = \tan \Delta/\rho$ ,  $\gamma = (k\rho c)^{-1/2}$ ,  $\tan \Delta$ ,  $\rho$ ,  $k$ ,  $c$ , and  $\epsilon$  are the angle of losses, density, thermal conductivity, heat capacity, and dielectric constant of the matter of the upper layer of the moon respectively. The experimental spectrum of this value corresponds fully to the theoretical spectrum and indicates that for the uppermost layer of matter with a thickness of 1-2 cm, where most of the thermal changes occur during an eclipse, the value  $\sqrt{b/\epsilon^2} = 6 \cdot 10^4$  and when  $\epsilon = 1.5$ ,  $\sqrt{b} = 7 \cdot 10^4$ . The same value was obtained earlier from lunation measurements. However, since  $\gamma = \gamma_1 = 1000$  for the upper layer, a value  $b_1 \approx 1.5 \cdot 10^{-2}$  is obtained for this layer, which exceeds by 1.2-2 times the specific losses for the deeper layers, determined from lunation measurements. This may be evidence that the uppermost centimeter of the surface layer is saturated by meteor matter having  $b_s \approx 2 \cdot 10^{-2}$ .

Tyler, G.L., 1966, The bistatic, continuous-wave radar method for the study of planetary surfaces: Journal of Geophysical Research, V. 71, p. 1559-1567.

A method is described for radar mapping of the surface of a planet. It is based on the use of a bistatic, continuous-wave mode of radar operation between the earth and a spacecraft orbiting or flying by the planet. The interference pattern resulting from a plane wave illuminating the planet and the fields scattered by the planet is analyzed. It is shown that the power in this pattern contains components corresponding to a linear superposition of the elementary wavelets scattered by the surface, multiplied by a phasor. The conditions under which the elementary wavelets may be recovered from a measurement of the interference pattern are given. Matched filter detection is then used to recover the amplitude of the local currents on the surface associated with each wavelet. The response to a point scatterer is calculated. Resolutions of a few wavelengths in range and azimuth can theoretically be obtained. Analogous applications to other geophysical problems are suggested.

Walker, E.H., 1966, Comments on paper by L.D. Jaffe, "Depth of the Lunar Dust": Journal of Geophysical Research, V. 71, p. 5007-5010.

It is pointed out that hypervelocity impact erosion is an active process which significantly changes the substrate, and is thus entirely different from the passive sedimentation that Jaffe used to modify his laboratory craters. As a result, Jaffe's treatment of the smoothed craters appearing in the Ranger 7 pictures neither establishes the presence of a significant layer of overlay, nor allows the determination of its thickness. (This letter is followed by a reply from Jaffe, pointing out that sedimentation ultimately occurs as a result of hypervelocity impact).

Watson, R.B., and Hapke, B.W., 1966, A comparison of the infrared spectra of the moon and simulated lunar surface materials: The Astrophysical Journal, V. 144, p. 364-368.

Reflection spectra of selected rock powders in the 1-2.5- $\mu$  wavelength range are compared with the Stratoscope III spectrum of Mare Tranquillitatis. The spectra

of natural powders are too bright and too flat to match the lunar reflectivity, which increases with wavelength in this range. However, irradiation by 2-keV  $H^+$  ions equivalent to approximately  $10^8$  years of solar-wind bombardment on the moon decreased the albedo and reddened the powders markedly in the infrared. Similar effects have been previously observed in the visible. A sample of powdered chondrite was not reddened by irradiation. The infrared reflectivities of the powders are too high even after irradiation, although their visible albedos are similar to the moon's; a possible explanation is that the radiation-altered layer is optically thick in the infrared on the lunar surface but not on the laboratory samples.

Winter, D.F., 1966, Note on the non-uniform cooling behavior of the eclipsed moon: *Icarus*, V. 5, p. 551-553.

Fudall's theory on the downslope migration of debris being the cause of the "hot spots" is discussed. The theory that the "hot spots" are due to an increase in roughness is favored.

Yagi, K., 1966, Discussion of paper by J.A. O'Keefe and E.W. Adams, "Tektite structure and lunar ash flows": *Journal of Geophysical Research*, V. 71, p. 5492-5493.

O'Keefe and Adams made theoretical calculations of the pressure, temperature, and voidage of ash flows on the mechanism of ash flows, he disagrees with some of the geological implications concerning the origin of tektites. In particular, the fabric of welded tuff should be rare on the moon and its presence in tektites should not be taken as an indication of a lunar origin. It also seems unlikely on geochemical grounds that tektites were formed from lunar ash flows, which should be similar in composition to the undifferentiated basaltic magma. O'Keefe and Lowman respond to these points in a reply which follows.

Zeller, E.J., Ronca, L.B., and Levy, P.W., 1966, Proton-induced hydroxyl formation on the lunar surface: *Journal of Geophysical Research*, V. 71, p. 4855-4860.

The interaction of both the particle and photon component of the solar wind with the lunar surface material is expected to produce diverse chemical reactions. Experimental evidence for proton-induced OH formation was obtained by bombarding a glass, chemically similar in composition to common silicate minerals, with high-energy protons. Rough calculations were made of the minimum proton-induced OH content in the lunar surface. If mixing or churning is not important, the upper centimeter could contain  $4 \times 10^{16}$  OH per  $cm^2$ . When protons below 40 Mev and the higher conversion rate are included in the computation, the estimated OH concentrations could increase by a factor of 10 or more. If surface mixing or churning has occurred, they should be divided by an average churning depth.

### 3.5.7 Temperature

Ashy, N., 1966, Energy balance on the lunar surface: *Publications of the Astronomical Society of the Pacific*, V. 78, p. 254-255.

Recalculation and intercomparison of energy balance observations indicates that, at the subsolar point, a reasonable value for reflected energy is  $0.106 \pm .01$  cal  $cm^{-2} min^{-1}$ . About  $1.88 \pm .02$  cal  $cm^{-2} min^{-1}$  is conducted into the surface.

Clegg, P.E., Bastin, J.A., Gear, A.E., 1966, Heat transfer in lunar rock: *Monthly Notices of the Royal Astronomical Society*, V. 133, p. 63-66.

It is suggested that radiative transfer may play an important part in the mechanism of heat flow in the lunar surface and a simple treatment of this process is given. Rough estimates are made of the magnitude of the contribution of radiative transfer,



and it is found that this process could account for a considerable fraction and perhaps almost all the heat flow deduced from infrared measurements. Furthermore, such a mechanism is of the right form to remove certain discrepancies which have been noted in infrared and microwave data.

Copeland, J., 1966, The two-layer model of the lunar surface: *Astrophysical Journal*, V. 145, p. 297-301.

Consideration is given to the two layer model by obtaining solutions to the heat-conduction equations for a homogeneous layer covering a homogeneous subsurface. The cases of a transparent and a semi-transparent surface layer are considered.

Fudali, R.F., 1966, Implications of the non-uniform cooling behavior of the eclipsed moon: *Icarus*, V. 5, p. 536-544.

Recent infrared observations during a lunar eclipse have revealed the existence of hundreds of areas whose thermal behavior differs sharply from that of the surrounding terrain. The probable explanation for this behavior is a difference in the insulating properties of the material exposed in these areas. Specifically, a lack of insulating debris over all or parts of the anomalous areas is conceptually sound and explains all the known facts. An analysis of the features and associations of these "hot spots" suggests that the debris is lacking because of simple downslope movement on high angle slopes.

Fulmer, C.V., Saari, J.M., and Shorthill, R.W., 1966, Physical characteristics of some thermally anomalous lunar craters: *Transactions of the American Geophysical Union*, V. 47, No. 4, p. 628.

Infrared scanning during total lunar eclipse has revealed more than a thousand thermal anomalies. Some have been identified with major and minor rayed craters of various ages. In some cases thermal anomalies occur in local areas characterized by small non-rayed craters and small multiple craters, or in areas restricted to peripheral regions (lips) of major craters and local areas lacking visible craters. Specific localities characterized by anomalous cooling during lunar eclipse have been defined by contouring equal increments of signal received in the 10-12 micron band. Position information for each locality has been provided by superposition of a librated selenographic grid system and by transforming these contours to the standard Lunar Astronautical Charts. The contour position error averages about 2 sec of arc and the sensor resolution is approximately 8 sec of arc. The relation of thermal anomalies to crater phenomenology will be discussed. (Abstract of a paper presented at the September 1966 meeting of the American Geophysical Union).

Fulmer, C., Saari, J.M., and Shorthill, R.W., 1966, Some physical characteristics of eclipse thermal anomalies in the Apollo band: *Publications of the Astronomical Society of the Pacific*, V. 78, p. 442-444.

The lunar disk was scanned in the infrared during the total lunar eclipse of December 19, 1964. Isothermal contours were constructed. The contours were transferred to the standard ACIC Lunar Atlas Charts for the equatorial region  $\pm 5^\circ$  latitude and  $\pm 30^\circ$  longitude. The rms location error is approximately 2.3 seconds of arc.

It was found that the thermal anomalies of this region are predominantly associated with craters, both rayed and non-rayed. The craters vary in size, shape, and depth. Furthermore, these craters span the entire age from Pre-Imbrian to Copernican although most of them in this area are either Copernican or Eratosthenian. A few anomalies are associated with multiple craters, and approximately five percent do not appear to be related with a visually detectable crater at earth-based telescopic resolution.

Two relatively large thermal anomalies are located along the trend of the Hyginus Rill. One anomaly includes the crater Hyginus and the central portion of the rill to the southeast. The second anomaly associated with this major structural feature is centered 25 kilometers to the northwest where the floor of the rill is occupied by a series of chain craters. Such craters are comparable to the maar-type volcanic craters characteristic of many rift-line volcanic regions on earth. (Abstract of a paper presented at a meeting of the Astronomical Society of the Pacific, June 1966).

Gaitskell, J.N., and Gear, A.E., 1966, Solar and lunar observations at submillimeter wavelengths: *Icarus*, V. 5, p. 237-244.

Observations of solar radiation in the spectral range 200 to 2000 microns are described. Some preliminary submillimeter lunar equatorial transits using the Fabry-Perot interferometer as an interference filter centered on a wavelength of 740 microns are also described.

Linsky, J.L., 1966, Models of the lunar surface including temperature-dependent thermal properties: *Icarus*, V. 5, p. 606-634.

The thermal conditions on the lunar surface are considered on a gross scale in terms of models with temperature-dependent thermal properties, including radiative energy transport.

The postulated existence of radiative energy transport is consistent with a porous or frothy medium, in agreement with photometric and laboratory simulation experiments, as well as with recent radar depolarization measurements. A distance scale of 0.1-0.3 mm for the effective mean separation of radiating surfaces is suggested by this interpretation of the data.

Linsky, J., 1966, Models of the lunar surface with temperature-dependent thermal properties: *The Astronomical Journal*, V. 71, p. 168-169.

The author has written a computer program to solve the heat conduction equation and to compute radio brightness temperatures for a medium having conductive and radiative energy transport and characterized by arbitrary temperature- and depth-dependent thermal properties. This program will also solve periodic heat conduction problems of a more general nature.

A number of models were constructed with a range of temperature-dependent conductivities and specific heats, but each was consistent with the minimum surface temperature of 90°K observed by Low (*Astrophys. J.* 142, 806, 1965) at the morning terminator. All of these models predict infrared and radio brightness temperatures for eclipses and lunations which agree favorably with high-resolution data for the center of the lunar disk.

If there are no internal heat sources, a significant increase in the mean radio brightness temperature with wavelength occurs when the conductivity, but not the specific heat, increases with temperature. This increase in the mean radio brightness temperature results from the non-linear nature of heat conduction under these circumstances, and is sufficient to explain the observed increase with wavelength described by Krotikov and Troitskii (*Soviet Phys.--U.S.S.R.* 6, 841, 1964), without requiring as a postulate an unusually high level of radioactivity in the moon. The general behavior of silicates at lunar temperatures and laboratory measurements of probable lunar materials suggest that radiative energy transport is the most probable mechanism to account for an increase in the conductivity with temperature. Several models in which radiative transfer and thermal conduction are of comparable importance at 350°K agree favorably with the data of Krotikov and Troitskii. The present findings support the hypothesis that porous or frothy

material characterize the lunar surface at least to a depth of 20 cm, and are in agreement with radar depolarization studies. (Abstract of a paper presented at the December 1965 meeting of the American Astronomical Society).

Lucas, J.W., Conel, J., Saari, J., Garipay, R., and Hagemeyer, W., 1966, Some lunar thermal characteristics from Surveyor I data: Transactions of the American Geophysical Union, V. 47, No. 4, p. 616.

Surveyor I has presented the first opportunity to obtain in situ estimates of some lunar surface thermal characteristics. Preliminary estimates have been made by analysis of the thermal engineering behavior of selected portions of the spacecraft during operation on the lunar surface. Local lunar surface brightness temperatures calculated from one thermal sensor are in good agreement near lunar noon and after sunset with earth-based predictions. The predictions were made assuming the lunar surface is a Lambertian emitter and has a thermal parameter value of 250 to 1000 in cgs units. The agreement indicates the lunar surface material near the spacecraft is highly insulating and is probably finely granulated. A discrepancy during the lunar morning between the Surveyor I and earth-based predictions is speculated to be due to directional thermal emission of the lunar surface. The thermal behavior of sun-dependent white surfaces on the spacecraft indicates that they remained free of any substantial amount of lunar dust. This conclusion is supported by TV pictures of the spacecraft which show only some small particles randomly distributed. (Abstract of a paper presented at the September 1966 meeting of the American Geophysical Union).

Mertz, L., 1965, Discussion of paper by E.A. Burns and R.J.P. Lyon, "Errors in the Measurement of the Lunar Temperature": Journal of Geophysical Research, V. 70, p. 999-1000.

Numerous cavities must occur in the surface, and the particles will in all probability be fine. Together these two characteristics would wipe out any resonance gaps in the spectral emissivity. The blackbody assumption of Pettit and Nicholson (1930) consequently remains valid. Indeed, it is discouraging that only in the few possible bare rock regions could resonances aid in determining the geologic composition of the moon.

Moron, J.M., Jr., and Staelin, D.H., 1966, Observations of the moon near 1-cm wavelength: The Astronomical Journal, V. 71, p. 865.

Observations of the moon were made with the 28-ft. antenna at Lincoln Laboratory and a receiver with channels at 32.4, 29.5, 25.5, 23.5, and 21.9 GHz (Staelin and Barlett, Astrophys. J. 144, 1, 352). A total of 340 drift scans were taken between 15 June and 15 August 1964.

Because of long-term gain fluctuations, the harmonics of the equatorial brightness temperature were found from the slopes of the drift scans rather than their amplitudes. These slopes, computed by fitting a straight line to the center half of each scan, vary harmonically with time. The constants of proportionality between the harmonics of the brightness temperature and those of the slopes involve convolution integrals which are virtually independent of the lunar model. The presence of higher harmonics in the brightness temperature is more readily detected by this technique. The average lunar brightness temperature was assumed to be 217°K. The system was not otherwise calibrated. The first harmonic amplitudes are consistent with other published results. This is the lowest frequency at which the second harmonic has been measured and its amplitude appears to be higher than that predicted by a homogeneous model. The second and higher harmonics should yield information about the vertical stratification of the lunar surface.

With another receiver at 35.0 GHz drift scans across the center of the moon were made near transit alternately with vertical and horizontal polarization. The peak difference in antenna temperatures was 5.5% of the central temperature which implies an effective dielectric constant of 1.5. (Abstract of a paper presented at the July 1966 meeting of the American Astronomical Society).

Plechkov, V.M., 1966, Observations of the June 1964 lunar eclipse at 1.8 cm at Gor'kii: Soviet Astronomy - A.J., V. 10, No. 1, p. 136-137.

Measurements are reported for the intensity of lunar radio emission at 1.8-cm wavelength during the eclipse of June 25, 1964. The intensity dropped by ~6% at the phase when the earth's shadow covered ~80% of the lunar disk. The rms error of measurement was ~3.5%.

Saari, J.M., and Shorthill, R.W., 1966, Hot spots on the moon: Sky and Telescope, V. 31, p. 327-331.

A popular article in which the authors describe their 10-12 micron wavelength observations of the eclipsed moon in 1964. They also present their results, a map and reconstructed infrared pictures showing many temperature anomalies.

Saari, J.M., and Shorthill, R.W., 1966, Studies of thermal features on the eclipsed moon: Publications of the Astronomical Society of the Pacific, V. 78, p. 451-453.

The lunar disk was scanned during the total eclipse of December 19, 1964, using a mercury-doped germanium detector with a 10-12 micron filter. The resolution of 1/100 lunar radius allowed correlation with lunar features. More than 1000 thermal anomalies have been located, most of which are identified with bright features. Figure 1 shows a recently revised map of 563 prominent thermal anomalies. Preliminary studies of the location of 1000 hot spots indicate a non-random distribution. An excess concentration was found in Mare Tranquillitatis and in an area centered on Bonpland.

Saari, J.M., Shorthill, R.W., and Deaton, T.K., 1966, Infrared and visible images of the eclipsed moon: Icarus, V. 5, p. 635-659.

The moon was scanned with 10" arc resolution at 0.45 and 10-12 microns during the total lunar eclipse of December 19, 1964. It was found that the lunar surface exhibits a surprising amount of thermal inhomogeneity. Hundreds of thermal anomalies were observed, most of which can be identified with bright craters or white areas. Certain maria and portions of maria were found to be thermally enhanced over their environs during the eclipse.

Selling, T.V., 1966, Observations of total eclipses of the moon at a wavelength of 1.82 centimeters: Journal of Geophysical Research, V. 71, p. 3339-3343.

Observations at a wavelength of 1.82 cm (16,500 Mc/s) with the University of Michigan's 85-foot radio telescope were made of the total lunar eclipses of December 30, 1963, June 25, 1964, and December 18, 1964. Results of the first two eclipses were inconclusive because of atmospheric and ground effects at the large zenith distances at which the eclipses occurred and inability to observe the entire eclipse. A full eclipse curve was obtained at small zenith distances on December 18, 1964. The measured decrease in emission during this eclipse was  $4.1 \pm 0.7\%$  of the central disk temperature after corrections for side-lobe effects. This corresponds to a change of  $10 \pm 2^\circ\text{K}$  for an assumed central surface brightness temperature of  $240^\circ\text{K}$ . Duration of the total eclipse phase of the center of the moon was 130 minutes. The delay in the minimum of the 1.82-cm eclipse curve from

the optical eclipse curve was not detectable within the observational uncertainty of 10 minutes. This is the longest wavelength at which a change has been reported in the radio emission from the moon during a lunar eclipse.

Troitskii, V.S., 1966, Radio emission of the eclipsed moon: *Soviet Astronomy - A.J.*, V. 9, p. 1007-1019.

A theoretical investigation of lunar radio emission at the time of a lunar eclipse was made. Relations are derived for computing the intensity of radio emission of the eclipsed moon. These computations show that the value of the maximum relative decrease of effective temperature is proportional to the value  $\kappa a$ , the product of the coefficient of attenuation of an electromagnetic wave and the square root of the thermal conductivity coefficient  $a = (k/\rho c)^{1/2}$ . Expressed through the directly measured lunar parameters, the inverse value of the maximum temperature change increases linearly with wavelength and is proportional to  $\gamma/b\epsilon^2$ , where  $b = \tan \Delta/\rho$ ,  $\gamma = (k\rho c)^{-1/2}$ ,  $\tan \Delta$ ,  $\rho$ ,  $k$ ,  $c$ , and  $\epsilon$  are the angle of losses, density, thermal conductivity, heat capacity, and dielectric constant of the matter of the upper layer of the moon respectively. The experimental spectrum of this value corresponds fully to the theoretical spectrum and indicates that for the uppermost layer of matter with a thickness of 1-2 cm, where most of the thermal changes occur during an eclipse, the value  $\gamma/b\epsilon^2 = 6 \cdot 10^4$  and when  $\epsilon = 1.5$ ,  $\gamma/b = 7 \cdot 10^4$ . The same value was obtained earlier from lunation measurements. However, since  $\gamma = \gamma_1 = 1000$  for the upper layer, a value  $b_1 \approx 1.5 \cdot 10^{-2}$  is obtained for this layer, which exceeds by 1.5-2 times the specific losses for the deeper layers, determined from lunation measurements. This may be evidence that the uppermost centimeter of the surface layer is saturated by meteor matter having  $b_2 \approx 2 \cdot 10^{-2}$ .

Winter, D.F., 1966, Note on the non-uniform cooling behavior of the eclipsed moon: *Icarus*, V. 5, p. 551-553.

Fudali's theory on the downslope migration of debris being the cause of the "hot spots" is discussed. The theory that the "hot spots" are due to an increase in roughness is favored.

### 3.5.8 Topography

Arthur, D.W.G., Pellicori, R.H., and Wood, C.A., 1966, The system of lunar craters, Quadrant IV: *Communications of the Lunar and Planetary Laboratory*, V. 5, p. 1-208, +12 pages maps.

The designation, diameter, position, central peak information and state of completeness are listed for each discernible crater with a diameter exceeding 3.5 km in the fourth lunar quadrant. The catalog contains about 8000 items and is illustrated by a map in 11 sections. Names have been given to large or conspicuous craters in the limb regions. Three previous parts were published as *Commun. L.P.L.* 30, 40, and 50.

Castin, J.A., 1966, Small scale lunar roughness: *Nature*, V. 212, p. 171-172.

The communication suggests that the centimetre and millimetre scale roughness of the lunar surface has been produced by the impact of small meteorites rather than by internal volcanic effects. This contention is supported by the arguments (a) that there is an apparent absence of horizontal directionality of small scale roughness photographed by recent soft landing experiments, and (b) from the known distribution of meteorites with size coupled with estimates of the age of the lunar surface. The roughness is a direct result of micrometeorite bombardment. The latter problem is briefly analyzed.

- Bray, T.A., and Goudas, C.L., 1966, A contour map based on the Selenodetic Control System of ACIC: *Icarus*, V. 5, p. 526-535.

The control system published in 1965 by ACIC has recently been augmented by more than 100 points. The analysis has led to no improvement in regard to the values of the two known harmonic coefficients of second order. This is probably caused by the uneven distribution of the additional data. Nevertheless, the contour map constructed on their basis exhibits substantial consistence with the one constructed from only the 196 points of the original system.

- Brown, W.E., Jr., 1966, Surveyor I radar report: *Transactions of the American Geophysical Union*, V. 47, No. 4, p. 616.

Radar echo strength data from the lunar surface were telemetered from the Surveyor I spacecraft during the landing sequence. The three Surveyor I radars covered an altitude range of 350 km and operated on wavelengths of 2.25, 2.32, and 3.22 cm. The reflection surface was within 1 meter of the visible surface and could have been the visible surface. The plumes of the vernier engines had no measurable effect upon the echo strengths, and one of the off-normal radar beams traversed a crater-like surface anomaly about 1 km wide and 2 km from the point of touchdown. The radar cross-section information obtained by Surveyor I is in good agreement with earth-based measurements obtained at about the same wavelength. (Abstract of a paper presented at the September 1966 meeting of the American Geophysical Union).

- Fung, A.K., and Moore, R.K., 1966, The correlation function in Kirchhoff's method of solution of scattering of waves from statistically rough surfaces: *Journal of Geophysical Research*, V. 71, p. 2939-2943.

The inconsistency of assuming that slope distribution, a Gaussian height distribution, and an exponential correlation function coexist is explained and avoided through the use of a better-behaved correlation function. This correlation function,  $\exp[-|g|/L + |g|/L \exp(-|g|/L)]$ , may vary in a Gaussian or an exponential fashion, or in a manner between the two. Thus, this theoretical function will probably fit many experimental correlation functions. The relationship among the slope distribution and the mean power returns obtained by both geometrical and physical optics theory is explained by the use of the new correlation function.

- Gault, D.E., and Quaide, W.L., 1966, Meteoroid erosion and sedimentation on the lunar surface: *Transactions of the American Geophysical Union*, V. 47, No. 1, p. 148.

One of the most significant facts revealed by the Ranger photographs is the soft, subdued relief of the lunar surface at scales less than a few hundred meters. Theoretical and experimental studies indicate that the observed gently undulating surface can be explained as the natural consequence of an erosion and sedimentation process caused by meteoroid impact. An important implication arising from these studies is that the upper limit of the scale for the subdued characteristics is related to the dimensions of the largest craters which saturate the surface. This, in turn, establishes a lower limit for the depth of a fragmental layer of impact crater ejecta. A conservative estimate of the thickness of this layer is 20 meters. (Abstract of a paper presented at the April 1966 meeting of the American Geophysical Union).

- Hagfors, T., 1966, Relationship of geometric optics and autocorrelation approaches to the analysis of lunar and planetary radar: *Journal of Geophysical Research*, V. 71, p. 379-383.



The formal relationship is established between the geometric optic approach and the autocorrelation approach to the analysis of lunar and planetary radar echoes for a Gaussian autocorrelation function when the surface has Gaussian height statistics and introduces deep phase modulation on the incident wave. Similarly it is inferred that such an analogy also holds whenever the surface undulations contain structure no smaller than the wavelength of observation divided by the rms slope of the surface. If an appreciable amount of small-scale structure is present, it is shown that (1) the range of scales responsible for the scattering will include an increasing amount of small-scale structure with increasing angle of incidence and (2) no simple relationship appears to exist between the distribution of apparent surface slopes and the power backscattered as a function of angle of incidence.

Jaeger, R.M., and Schuring, D.J., 1966, Spectrum analysis of terrain of Mare Cognitum: *Journal of Geophysical Research*, V. 71, p. 2023-2028.

The roughness of a portion of the lunar surface in Mare Cognitum is analyzed and compared with the roughness of the earth's surface in two previously measured areas. A two-dimensional random walk is taken on a contour topographic map produced from photograph P979 provided by Ranger 7. The resulting lunar elevation profile is treated as a realization of an ergodic, stationary time series and is analyzed in the spatial frequency domain by use of estimates of power-spectrum density. Similar estimates are presented for the Perryman test course at Aberdeen Proving Ground, for a grass runway, and for the Bonito lava flow, Arizona, to provide some basis for roughness comparison. The Aberdeen and Mare Cognitum spectrums are shown to be comparable in basic shape but significantly different in power in certain frequency ranges. An appendix presents a summary of the mathematical methods utilized.

Katz, I., 1966, Wavelength dependence of the radar reflectivity of the earth and the moon: *Journal of Geophysical Research*, V. 71, p. 361-366.

Recent interest in the use of a multifrequency radar as a remote sensor for exploration of the earth and the moon has stimulated this study of the variation of radar backscattering with change in electromagnetic wavelength. The analysis of data has shown that radar cross sections of land and sea surfaces decrease with increasing wavelength and, on the average, follow approximately a  $\lambda^{-1}$  behavior, although the exponent may vary from +2 to -6 in individual cases. Snow-covered surfaces at all depression angles and sea surfaces at angles above  $73^\circ$  are the ones with positive values for the exponent. The wavelength dependence of the moon and the average values found on the earth in this study are quite similar. The combination of polarization and wavelength dependence versus depression angle may be characteristic features for distinguishing various terrain types by a multifrequency radar.

Martin, J.J., 1966, Scattering from the moon and other rough surfaces: *Journal of Geophysical Research*, V. 71, p. 2687-2688.

The suggestion is made that the scattering of wave energy by rough surfaces is due (1) to specular points which may be counted and which have an average power associated with each of them and (2) to diffuse scattering which is proportional to projected area. Consequences of the hypothesis are: (1) the possibility that the power density spectrum returned from nearly normal incidence will have more high-frequency content than that returned from nearly grazing incidence due to scintillation and (2) the possibility that  $d(dp/dA)d\theta = 0$  at both  $0^\circ$  and  $90^\circ$  incidence, which may assist in interpreting experimental data.

Rennilson, J.J., and Holt, H.E., 1966, Photometric properties and photoclinometry of the lunar surface from Surveyor 1 television: *Transactions of the American Geophysical Union*, V. 47, No. 4, p. 616.

The local photometric function of the lunar surface has been measured from Surveyor I television pictures. Our solution for the normal albedo of the lunar surface around the spacecraft, about 6% is estimated by extrapolation from the surface luminance measured at low phase angles. The photometric function derived from the Surveyor I television pictures is similar in form to the photometric functions of local areas on the moon measured photoelectrically at the telescope. The contribution to the telescopically measured photometric functions from topographic irregularities larger than about 10 cm is therefore minor. Topographic profiles have been computed from photometric measurements utilizing the photometric function derived from the Surveyor television pictures. This application of the new technique of lunar photoclinometry to spacecraft-acquired images is the first in which the local photometric function has been measured at a scale appropriate to the solution of the photoclinometric equations. (Abstract of a paper presented at the September 1966 meeting of the American Geophysical Union).

Rindfleisch, T., 1966, Photometric method for lunar topography: Photogrammetric Engineering, V. 32, No. 2, p. 262-276.

A general and rigorous treatment is given of the photometric method for deriving surface elevation information from a single picture of the surface. In the course of the derivation a brief indication is given of possible photometric function symmetries yielding exact solutions to the problem. It is shown that the photometric properties of the lunar maria are sufficient to produce an exact solution but with inherent practical difficulty. The resulting equations are then specialized to the case of lunar photography and applied to the Ranger pictures as part of a digital processing procedure. Examples of the resulting elevation maps are given.

Ronce, L.B., 1966, Structure of the crater Alphonsus: Science, V. 209, p. 182.

From a study of Ranger IX photographs, the author concludes that, regardless of the origin of the material forming the central spine and floor of the crater, both the general outline and the presence of the folds indicate that Alphonsus is a crater deformed by a strike-slip fault of the dextral type.

### 3.6 Origin of the Solar System

Baldwin, R.B., 1966, On the origin of the moon: Journal of Geophysical Research, V. 71, p. 1936-1937.

It is suggested that the moon was originally situated at one of the two Lagrangian positions that precede and follow the earth by  $60^\circ$  in its orbit. Perturbations or secular changes in the planetary orbits may have caused the moon to be captured in a direct orbit at a distance of about 45 earth radii when the earth was rotating in about 10 hours.

Brown, R.L., 1966, The acquisition of the solar system: Transactions of the American Geophysical Union, V. 47, No. 3, p. 482.

The sun, as it moves at an angle through the main mass of stars and debris in its arm of the Milky Way, can acquire the bodies that now comprise the planets, planetoids, and some comets. Analysis of the relative motion of the sun and the mainstream of bodies and particles indicates that the greater momentum of the planets can be explained by the translation of greater linear velocity into the curvilinear motion of bodies forced to spiral with the sun as a consequence of that body's great gravitational attraction. Since the angle of approach of all bodies that have been captured by the sun must fall within certain critical limits,

the common plane and uniform direction of revolution of the planets, and the diversity of physical properties of the planets, considering that the planets were captured at different times from different clouds of material in our galactic arm, are also explained by this mechanism. The higher eccentricities and inclination of the orbits to the ecliptic can be explained on the basis of the relative angle of approach of the bodies, which, to be captured, must have nearly a common velocity. Parabolic and hyperbolic orbits of comets can be shown to be due to varying angles of approach and different velocities of bodies in the galactic arm. (Abstract of a paper presented at the September 1966 meeting of the American Geophysical Union).

Donahoe, F.J., 1966, On the abundance of earth-like planets: *Icarus*, V. 5, p. 303-304.

A moon-like satellite may be essential in the evolution of an earth-like planet.

Fesenkov, V.G., 1965, The role of meteorites in solving the problem of the origin of the solar system: *Akademiia Nauk SSSR Meteoritika*, No. 26, p. 69-76.

It is shown that the constitution of meteorites indicates that the solar system formed as a result of nucleogenesis (explosion of a supernova star) that took place about 5 b.y. ago. Any reasonable theory concerning the origin of the solar system should be based on this important conclusion.

Lyttleton, R.A., 1966, The effect on the lunar orbit of meteoritic accretion: *Icarus*, V. 5, p. 162-164.

Reduction of the lunar distance through meteoritic impacts depends only on the amount of incoming material and scarcely at all on how much may be exploded off the surface to escape. This is because the incoming material possesses negligible angular momentum on average, while outgoing material carries with it the same angular momentum per unit mass as the moon.

Ringwood, A.E., 1966, Chemical evolution of the terrestrial planets: *Geochimica et Cosmochimica Acta*, V. 30, p. 41-104.

The terrestrial planets are believed to have formed by accretion from an initially cold and chemically homogeneous cloud of dust and gas. The iron occurring in the dust particles of the cloud was present in a completely oxidized form. Either before or during accretion of dust into planets, partial reduction of oxidized iron to metal occurred. The role of oxidation-reduction equilibria during the formation of terrestrial planets is discussed and it is concluded that the differing zero-pressure densities of the planets are caused dominantly by differing mean states of oxidation which were established during the primary accretion processes. This interpretation avoids the necessity for assuming the occurrence of physical fractionation of metal from silicates in the solar nebula before accretion.

A detailed study is made of the evidence shed by chondritic meteorites upon oxidation-reduction equilibria occurring early in the history of the solar system. It is concluded that the different classes of chondrites have formed by an auto-reduction process operating upon primitive material similar in composition to the Type I carbonaceous chondrites. Reduction occurred when this material accreted into parent bodies which were heated internally, perhaps by extinct radioactivities. Under these conditions, trapped carbonaceous material reacted with oxidized iron to produce a metallic phase in situ. The chemistry of the reduction process which operated in chondrites is studied. The evidence strongly indicates that the principal reducing agent was carbon and not hydrogen. Furthermore, reduction occurred in a condensed environment and not in the dispersed solar nebula. The origins and chemical evolution of other terrestrial planets are discussed in the light of evidence yielded by the chondrites. The hypothesis is

advanced that each of the terrestrial planets formed by a single-stage auto-reduction process operating upon primitive material similar to the Type I carbonaceous chondrites. The origins of the Moon, Earth, Mars, Venus, and Mercury are developed in detail.

Ruskol, E.L., 1966, On the past history of the earth-moon system: *Icarus*, V. 5, p. 221-227.

New calculations of secular variations of lunar orbit owing to tidal friction are discussed. It is concluded that in the past the lunar orbit should be closer to the earth, more circular and less inclined with respect to the earth's equator than it is now. This is in favor of the formation of the moon in the vicinity of the earth.

Safronov, V.S., 1966, Sizes of the largest bodies falling onto the planets during their formation: *Soviet Astronomy - A.J.*, V. 9, p. 987-994.

Application of coagulation theory to the process of accumulation of the planets from solid matter leads to the conclusion that this matter was in the form of particles and bodies of different sizes. Falling onto the planets, the bodies imparted to them a rotational moment consisting of two components of different nature: a regular component ("direct" rotation), related to rotation of the system as a whole, and a random component, related to the random direction of velocity of the falling bodies relative to the planet and manifested in the inclinations of the axes of rotation of the planets. The largest bodies made the principal contribution to the random component of rotation. This article gives the derivation of expressions relating the values of the random component of rotation to the masses  $m_i$  of the largest bodies falling onto a planet of mass  $m$  on the assumption of an exponential distribution function of the sizes of the bodies. Table I gives the values  $m_i/m$  determined from a comparison of the theoretically computed angles of inclination of the axes of rotation of the planets and the observed values. The largest bodies falling onto the earth had masses of about  $10^{-3}$  of the earth's mass; that is, they were of the size of the largest asteroids. This same mechanism makes it possible to explain the anomalous rotation of Uranus if it is assumed that the random component of the rotation of Uranus was greater than the systematic component. The mass of the largest body falling onto the surface of Uranus in this case would have to be 0.05 of the mass of that planet.

Smalley, V.G., 1966, Time variance of the earth-moon distance: *Icarus*, V. 5, p. 491-504.

This paper shows that for Lyttleton's model, the terrestrial rate of accumulation of interplanetary debris was at least  $10^{10}$  gm/sec at the time the two bodies were drawn closer than their present distance of separation. It is further concluded that the maximum "capture" distance of the moon was 1.3 times the present distance. Velocity of approach profiles are also given for several possible initial conditions.

### 3.7 Planets

#### 3.7.1 General

Anderson, D.L., and Phinney, R.A., 1966, The early thermal history of the earth and the terrestrial planets: *Transactions of the American Geophysical Union*, V. 47, No. 1, p. 185.

Using a homogenized earth as a prototype planetary model and using new estimates of the earth's age and average radioactivity, it is possible to determine the thermal evolution of various-sized protoplanetary spheres up to the melting point. If the melting point of silicates and iron is exceeded in the lifetime of the planet, it

is assumed that the planet will outgas and will differentiate a core and a crust. Two protoplanetary models are considered; one has the same composition as the present earth and, therefore, contains free iron dispersed throughout the body; the other has this iron completely oxidized and is, therefore, an iron-rich silicate or a mixture of oxides. For both cases there exists a maximum-size planet, intermediate between the earth and Mars in mass, that can exist without differentiation. If the protoplanetary Mars and earth are identical in composition, Mars will not differentiate or outgas significantly but the earth will. The thermal calculations are, therefore, consistent with data of Mars regarding its shape, magnetic field, radiation belts, atmosphere, and surface coloration. The Martian surface and interior are probably similar to those of the primitive earth. The study of Mars, therefore, can provide clues to the very early properties of the earth. (Abstract of a paper presented at the April 1966 meeting of the American Geophysical Union).

Barabashov, N.P., Garazha, V.I., and Dudinov, V.N., 1966, Determination of corrections to photometric cross sections of planets: *Soviet Astronomy - A.J.*, V. 10, No. 1, p. 113-116.

A noteworthy method suggested 'by Koval' [10] to correct for distortions in the brightness distribution over a planetary disk is examined. Although this method is often used in physics and radio engineering, its applications are limited and it is incapable of correcting the brightness at points very close to the limb. The disparity reported by Koval' in the brightness distribution over the disk of Mars arises from inadequate allowance for uncertainties in solving Eq. (1).

Chamberlain, J.W., and McElroy, M.B., 1966, Diffuse reflection by an inhomogeneous planetary atmosphere: *The Astrophysical Journal*, V. 144, p. 1148-1158.

An approximate solution is developed for the diffuse reflection by an inhomogeneous atmosphere--specifically one in which the albedo for single scattering decreases exponentially with optical depth. The approach consists of finding a homogeneous atmosphere that closely mimics the intensities reflected by the inhomogeneous one. The solution for the diffusely reflected radiation is conveniently expressed in terms of an effective Chandrasekhar H-function. This H-function specifies an effective mean albedo for the entire atmosphere.

Goldreich, P., 1966, Dynamics of planet-satellite system: *Transactions of the American Geophysical Union*, V. 47, No. 1, p. 155.

The origin of natural satellites is discussed as a part of a general dynamical theory of planets and satellites. New calculations of the evolution of the earth-moon system are described. The tidal effective  $Q$ 's of the major planets are shown to be several orders of magnitude larger than that of the earth. (Abstract of a paper presented at the April 1966 meeting of the American Geophysical Union).

Goldreich, P., 1966, Final spin states of planets and satellites: *The Astronomical Journal*, V. 71, p. 1-7.

The spin of a planet or satellite which is losing angular momentum through tidal friction may approach one of at least two distinct final state will be one of synchronous rotation. If the tidal phase lag is independent of the amplitude and frequency of the tide, then synchronous rotation will result when  $[3(B-A)/C] \geq (9.5\pi e^2)$ . If this inequality is not satisfied, the body will end up spinning with a mean angular velocity which is somewhat larger than its orbital mean motion. This criterion is only slightly altered if the phase lag varies with amplitude and/or frequency. It is easily seen that the moon fails to satisfy the condition for synchronous rotation with the present value of its orbital eccentricity. However, the moon could have attained synchronous rotation if its mean orbital eccentricity was less than 0.041 at some time in the past.

No analytical treatment of commensurate spin states other than synchronous rotation is included in the present investigation. However, the results of a separate study of these commensurate spins are briefly described.

Goldreich, P., and Peale, S.J., 1966, Resonant spins in the solar system: Transactions of the American Geophysical Union, V. 47, No. 1, p. 155.

The effects of gravitational torques on spinning non-axisymmetric planets and satellites are investigated in detail. A stability criterion is derived for the maintenance of a planetary or satellite spin angular velocity which is commensurate with its mean motion. Spin angular velocities that are half and whole integral multiples of orbital angular velocities are shown to be stable for even very slight deviations from axial symmetry. An analytical method is developed for determining the probability of a planet's or satellite's being captured into such a resonant spin state, as the spin is decreased by tidal friction. The dependence of this capture probability on orbital eccentricity is also discussed. Numerical results are given for Mercury and the moon. A similar analysis gives a stability criterion for a Venusian spin that is resonant with the synodic motion of Venus. (Abstract of a paper presented at the April 1966 meeting of the American Geophysical Union).

Goldreich, P., and Soter, S., 1966,  $Q$  in the solar system: Icarus, V. 5, p. 375-389.

Secular changes brought about by tidal friction in the solar system are reviewed. The presence or absence of specific changes is used to bound the values of  $Q$  (the specific dissipation function) appropriate for the planets and satellites. It is shown that the values of  $Q$  separate sharply into two groups. Values in the range from 10 to 500 are found for the terrestrial planets and satellites of the major planets. On the other hand,  $Q$  for the major planets is always larger than  $6 \times 10^4$ . It is difficult to reconcile these large  $Q$ 's with the much smaller values obtained in laboratory tests of solids. Lyttleton's hypothesis that Pluto is an escaped satellite of Neptune is critically examined. Using the  $Q$ 's we obtain for the major planets and their satellites, we show that any eccentricity that Triton's orbit may have possessed after a near encounter with Pluto would have been subsequently damped, thus accounting for its present near-circular orbit.

Hadjidemetriou, J.D., 1966, Analytic solutions of the two-body problem with variable mass: Icarus, V. 5, p. 34-36.

The system of equations defining the variation of the orbital elements in the two-body problem with variable mass has been solved analytically for various laws of mass loss. There are two cases in which the eccentricity is a periodic function of the eccentric anomaly with a period of  $2\pi$ . In all cases the secular variation of the eccentricity is very small, but there are oscillations with variable amplitude.

Hagfors, T., 1966, Relationship of geometric optics and autocorrelation approaches to the analysis of lunar and planetary radar: Journal of Geophysical Research, V. 71, p. 379-383.

The formal relationship is established between the geometrioptic approach and the autocorrelation approach to the analysis of lunar and planetary radar echoes for a Gaussian autocorrelation function when the surface has Gaussian height statistics and introduces deep phase modulation on the incident wave. Similarly it is inferred that such an analogy also holds whenever the surface undulations contain structure no smaller than the wavelength of observation divided by the rms slope of the surface. If an appreciable amount of small-scale structure is present, it is shown that (1) the range of scales responsible for the scattering will include an increasing amount of small-scale structure with increasing angle of incidence and (2) no simple relationship appears to exist between the distribution of apparent



surface slopes and the power backscattered as a function of angle of incidence.

Hide, R., 1966, Planetary magnetic fields: Planetary and Space Science, V. 14, No. 7, p. 579-586.

Present knowledge and modern theories of the earth's main magnetic field are outlined and the state of knowledge of the magnetic fields of the other planets is sketched. Little is known of planetary magnetic fields other than for the earth and Jupiter, although magnetometer data from Mariner II and Mariner IV may set an upper limit to the magnetic fields of Venus and Mars, respectively. Lunick II data indicates the surface magnetic field of the moon may be less than  $10^{-8}$  G. Decameter wavelength radiation has been observed from Jupiter and Saturn only. The effect of the solar wind interacting with planetary magnetic fields is briefly mentioned.

O'Leary, B.T., 1966, On the occurrence and nature of planets outside the solar system: Icarus, V. 5, p. 419-436.

The topic of the occurrence of planets outside the solar system is discussed in detail. It is found that many independent approaches are possible. They stem from present astrometric observations, future observations from space, physical theories on the evolution of stars and planets, theories on the origin of the solar system, problems of the unseen mass in the solar neighborhood and in certain galaxies, statistics of the mass-frequency functions of stars and of solar system bodies, and statistics and theories of the angular momenta of stellar systems. From the astrometric investigations alone it is now known that at least six of the nearest one hundred stars have planetary companions of mass greater than that of Jupiter.

Rank, D.H., Fink, U., and Wiggins, T.A., 1966, Measurements on spectra of gases of planetary interest. II.  $H_2$ ,  $CO_2$ ,  $NH_3$ , and  $CH_4$ : Astrophysical Journal, V. 143, p. 980.

An empirical curve of growth on the S(1) line of the I-O hydrogen quadrupole band was obtained. With this curve the laboratory and planetary hydrogen quadrupole spectra can be corrected for saturation. Self-broadening and nitrogen-broadening together with intensity measurements were made on the 121-000  $CO_2$  band. The region of the ammonia band around  $6450 \text{ \AA}$  was observed, and nitrogen-broadening coefficients for eighteen selected lines were obtained. The self- and hydrogen-broadening coefficients for several low J-lines of the  $2_{12}$  methane band at  $1.67 \mu$  were measured.

Roemer, E., Thomas, M., and Lloyd, R., 1966, Observations of comets, minor planets, and Jupiter VIII: The Astronomical Journal, V. 71, p. 591-601.

Accurate positions and descriptive notes are presented for 24 comets, 11 minor planets, and the eighth satellite of Jupiter.

Sekera, Z., 1966, Recent developments in the theory of radiative transfer in planetary atmospheres: Review of Geophysics, V. 4, No. 1, p. 101-111.

The review of the recent advances made in the western part of the world in the theory of radiative transfer relates to the studies of the only physically realistic models of a planetary atmosphere in which both multiple scattering and polarization are taken fully into consideration. In the mathematical formulation of radiative transfer problems, the meaningful advances have been made in the emphasis on better physical interpretation of the mathematical analysis and of the parameters used. Chapman's approach is demonstrated in the derivation of the equation for the inhomogeneous case of imperfect scattering. The solution of the integrodifferential equations for the reflection and transmission matrices are indicated.

Trafton, L., 1966, Model atmospheres of the major planets: *The Astronomical Journal*, V. 71, p. 183.

Model atmospheres of the major planets have been constructed by using recently discovered sources for the dominant thermal opacity. These sources are the pressure-induced absorption in molecular hydrogen and the pressure-induced enhancement resulting from the mixing of molecular hydrogen and helium. They are responsible for most of the greenhouse effect observed in the upper atmosphere of each major planet. These model atmospheres are non-gray and were constructed in hydrostatic equilibrium. They incorporate a first-order correction to account for convection. The thermal opacity of ammonia does not play a significant role in the atmosphere of any major planet except Jupiter and here, it was found to play a relatively small role. Each planet is represented by several models having different values of the effective temperature and  $\text{He}/\text{H}_2$  ratio. These quantities were considered as free parameters to be determined by fitting the models to the observations. Most of the models indicate the existence of a tenuous fog or mist overlying a cloud zone.

In the case of the Jovian models, it was necessary to include the  $10\text{-}\mu$  band of ammonia in order to explain the observed limb darkening in the 8 to  $14\mu$  region of the spectrum. It was also necessary to include helium in order to explain the scale height observations. Jovian models which are compatible with all the observations have high effective temperatures indicating that Jupiter has an internal heat source yielding greater than about one-tenth of the incident solar flux. In addition, an upper limit of about two on the  $\text{He}/\text{H}_2$  ratio is implied by the Jovian models. (Abstract of a paper presented at the December 1965 meeting of the American Astronomical Society).

Tyler, G.L., 1966, The bistatic, continuous-wave radar method for the study of planetary surfaces: *Journal of Geophysical Research*, V. 71, p. 1559-1567.

A method is described for radar mapping of the surface of a planet. It is based on the use of a bistatic, continuous-wave mode of radar operation between the earth and a spacecraft orbiting or flying by the planet. The interference pattern resulting from a plane wave illuminating the planet and the fields scattered by the planet is analyzed. It is shown that the power in this pattern contains components corresponding to a linear superposition of the elementary wavelets scattered by the surface, multiplied by a phasor. The conditions under which the elementary wavelets may be recovered from a measurement of the interference pattern are given. Matched filter detection is then used to recover the amplitude of the local currents on the surface associated with each wavelet. The response to a point scatterer is calculated. Resolutions of a few wavelengths in range and azimuth can theoretically be obtained. Analogous applications to other geophysical problems are suggested.

Wildt, R., 1966, The greenhouse effect in a gray planetary atmosphere: *Icarus*, V. 5, p. 24-33.

Hopf's analytical solution is illustrated for several values of the greenhouse parameter, i.e., the ratio of gray absorption coefficients for insulating and escaping radiation, assumed to be constant at all depths.

### 3.7.2 Asteroids

Bühler, F., Geiss, J., Meister, J., Eberhardt, P., Huneke, J.C., and Singer, P., 1966, Trapping of the solar wind in solids. Part I. Trapping probability of low energy He, Ne and Ar ions: *Earth and Planetary Science Letters*, V. 1, No. 5, p. 249-255.

The trapping probability in Al foils of He, Ne and Ar ions with energies between 0.46 and 7 KeV has been determined. Argon is trapped quantitatively for ion energies higher than 2.5 KeV. At 2.5 KeV the trapping probabilities of neon and helium are about 0.6, decreasing rapidly for lower energies with argon. The trapped gases are held quite firmly. These results show that an Al foil exposed to the solar wind would trap and retain a large fraction of these solar wind ions. There is little doubt that the solar wind will also be trapped in interplanetary dust grains and in the surface layers of asteroids and moons provided these have no atmosphere or magnetic field.

Kiang, T., 1966, Bias-free statistics of orbital elements of asteroids: *Icarus*, V. 5, p. 437-449.

The problem of observational selection of data on asteroid orbits is considered. Three selection factors (brightness, latitude, and seasonal) are taken into account, but the brightness factor is given an overriding priority. It is then inferred that observational selection has given rise to (i) an overabundance of small inclinations and a second harmonic in the frequency distribution of nodes, among asteroids fainter than magnitude 15, and (ii) an overabundance of large eccentricities among those fainter than magnitude 16. There is a significant (positive) correlation between proper eccentricity and proper inclination which suggests the former existence of a resisting medium.

Malsch, W., 1966, Beobachtungen von Planetoiden 1965: *Astronomische Nachrichten*, V. 289, p. 194.

Gives a table of observation data of planetoids during 1965. (In German).

Roemer, E., and Lloyd, R.E., 1966, Observations of comets, minor planets, and satellites: *The Astronomical Journal*, V. 71, p. 433-457.

Accurate positions and descriptive notes are presented for 38 comets, 33 minor planets, 5 faint natural satellites, and Pluto, for which astrometric reduction of the series of Flagstaff observations has been completed.

### 3.7.3 Jupiter

Baart, E.E., Barrow, C.H., and Lee, R.T., 1966, Burst structure of Jupiter's decametric radiation: *The Astronomical Journal*, V. 71, p. 377-378.

The structure of the bursts of decametric radiation from Jupiter has been investigated using chart speeds up to 50 mm/sec and time constants down to 5 m sec. To make identification of short pulses more certain observations have been made of the left- and right-handed components of the radiation at 16, 18, and 22 Mc/sec, and of the total power at 14 Mc/sec. The polarization measurements have been made using a hybrid ring and separate receivers for the two senses of polarization to avoid the uncertainties which might arise from switching techniques. In addition, the total power was recorded at 18 Mc/sec by using an array having a null in the direction of Jupiter. This antenna served as a monitor to identify static pulses which could have the same appearance as millisecond pulses from Jupiter. A phase-switching interferometer was operated at 18 Mc/sec throughout observing periods as an additional means of identifying that Jupiter was active during the period. Several distinct forms of burst structure have been observed. In particular, pulses as short as or shorter than 10 m sec, with different forms of grouping, have been observed on numerous occasions. These pulses appear to be associated with "sources" B and C rather than "source" A on Jupiter. Different forms of burst structure may occur on different frequencies at the same time, and on occasions different polarizations occur simultaneously on different frequencies. (Abstract of a paper presented at the March 1966 meeting of the American Astronomical Society).

Baart, E.E., Barrow, C.H., and Lee, R.T., 1966, Millisecond radio pulses from Jupiter: *Nature*, V. 211, p. 808.

Observations were made of the left- and right-handed components of the radiation at 16, 18 and 22 Mc/s, and of the total power at 14 Mc/s.

Jupiter radio storms were observed on ninety-two occasions on 62 days during the period November 21, 1965-March 17, 1966.

It seems to be most unlikely that the I-pulses were not connected with Jupiter because (a) I-pulses were received on aeriels pointing towards Jupiter but not on an aerial with a null in that direction. (b) The I-pulses were only observed as part of a normal Jupiter storm and were usually preceded and/or succeeded by N-bursts at the same frequency. (c) The bandwidth of the I-pulses was always less than 4 Mc/s and individual pulses never occurred simultaneously on the different frequencies. (d) The I-pulse radiation seems to be correlated with two central meridian longitude regions of Jupiter.

In view of the foregoing it would seem to be most unlikely that these I-pulses were not connected with Jupiter in some manner.

Barber, D., 1966, The polarization, periodicity and angular diameter of the radiation from Jupiter at 610 Mc/s: *Monthly Notices of the Royal Astronomical Society*, V. 133, p. 285-308.

The radiation from Jupiter at 610 MHz (49 cm) has been investigated, values are given for the flux density and the degree of polarization, the data have shown the presence of the beaming of the radiation into Jupiter's magnetic equatorial plane for the first time at a wavelength as long as 49 cm. The shape of the radiation pattern has been found to be asymmetrical about zero magnetic declination. The equatorial diameter of the emitting region has been determined and the data has also shown a periodic variation in the projected diameter as the source oscillates due to the inclination of Jupiter's magnetic axis to the axis of rotation. This has enabled an independent value for the inclination angle to be obtained.

Berge, G.L., 1966, An interferometric study of Jupiter's decimeter radio emission: *Astrophysical Journal*, V. 144, p. 767-798.

An interferometric study of the decimeter radio emission from the planet Jupiter has recently been carried out at the Owens Valley Radio Observatory. Using the two 90-foot paraboloids as an interference polarimeter, observations have been made with various east-west spacings ranging from 300 to 4700  $\lambda$  at 10.4 cm and 300 to 2300  $\lambda$  at 21.2 cm and also with some critical north-south spacings at 10.6 cm. The visibility functions obtained are in agreement with earlier measurements, which gave the polar and equatorial dimensions as 1 and 3 planetary diameters, respectively, but they are more complete and extend to larger base lines. They permit the fitting of a rather detailed model for the decimeter brightness distribution. The observations are consistent with a symmetrical synchrotron emission source having the polarization properties one would expect with a dipole magnetic field. It probably is centered quite closely on the planetary disk, which is itself seen as a thermal radio source.

The observations also indicate the presence of a small circularly polarized component in the radiation which varies in magnitude and sense as Jupiter rotates. The disk emission at 10.4 cm is about twice the thermal emission one would expect for a temperature of 1300K.

The implications of the various results are discussed.

- Bigg, E.K., 1966, Periodicities in Jupiter's decametric radiation: Planetary and Space Science, V. 14, No. 8, p. 741-758.

A systematic search for periodicities in Jupiter's decametric radio emission and methods of assessing their statistical and physical significances are described. It is shown that no independent effects of the satellites Ganymede (III), Callisto (IV), and Amalthea (V) are detectable, while Europa (II) has a small apparent effect, reducing the emission when the satellite is  $40^\circ$  past the sun-Jupiter line. Claims that simultaneous conjunctions of satellites, I, II, III, or that the magnetic longitude of Io (I), have an effect upon the emission are shown to be questionable. A hypothesis of the origin of the radiation is presented which is designed to explain the partially independent influences on it of Io and the magnetic field.

- Binder, A.B., and Cruikshank, D.P., 1966, Photometric search for atmospheres on Europa and Ganymede: Icarus, V. 5, p. 7-9.

Observations of the eclipse disappearances and reappearances of JII and JIII were made to detect possible atmospheres on these satellites revealed by excess brightness on eclipse reappearance. An observation of an eclipse reappearance of JII showed a brightness anomaly of  $0.03 \pm 0.01$  stellar magnitudes. Two high-quality observations of JIII showed no brightness anomaly greater than 0.01 stellar magnitudes.

- Clark, T.A., and Dulk, G.A., 1966, Observations of Jupiter at 8.9 and 10 MHz: The Astronomical Journal, V. 71, p. 158.

At Boulder, Colorado, from August 1964 through February 1965, the authors have obtained synoptic observations of the radiation from Jupiter at 8.9 and 10 MHz.

The observations indicated emission probabilities of 0.95 at 8.9 MHz and 0.75 at 10 MHz at levels greater than three times the rms noise fluctuations. At 10 MHz, the 3-rms criterion represents a flux of  $2.0 \pm 0.5 \times 10^4$  flux units (1 flux unit =  $10^{-26} \text{ W m}^{-2} \text{ Hz}^{-1}$ ). More recent observations with greater sensitivity at 10 MHz indicate that there is continuous emission at a minimum level of about 5-10 000 flux units. The very high emission probabilities are similar to those found by Ellis at 4.8 MHz and also seem consistent with the low-level flux profiles observed by Stone, Alexander, and Erickson at 26.3 MHz. As a function of Jupiter longitude, there was enhanced emission intensity at  $\lambda_{III} = 200^\circ$  and  $0^\circ$  and depressed emission intensity near  $140^\circ$ . As a function of Io phase, enhancements occurred at  $\phi_{Io} = 80^\circ$  and  $240^\circ$ , with a lesser peak at  $\phi_{Io} = 330^\circ$ . When examined simultaneously as a function of Jupiter longitude and Io phase,  $\lambda_{III} = 0^\circ$ ,  $\phi_{Io} = 80^\circ$  (the fourth source) and  $\lambda_{III} = 270-300^\circ$ ,  $\phi = 0^\circ$  appear prominently. The latter region is not particularly prominent at higher frequencies. (Abstract of a paper presented at the December 1966 meeting of the American Astronomical Society).

- Danielson, R.E., 1966, The infrared spectrum of Jupiter: Astrophysical Journal, V. 143, p. 949.

During the second flight of Stratoscope II, the infrared reflection spectrum of Jupiter was traced from 0.8 to  $3.1\mu$  at a balloon altitude of 84,000 feet. Deep absorption features caused largely by  $\text{CH}_4$  occur at 0.85, 0.99, 1.15, 1.37, and  $1.7\mu$ . A deep, broad absorption feature centered at  $2.25\mu$  appears to be primarily due to the collision-induced I-O band of  $\text{H}_2$  at  $2.4\mu$ . A large absorption at  $3\mu$  is attributed to  $\text{NH}_3$ .

- Davies, R.D., and Williams, D., 1966, Observations of the continuum emission from Venus, Mars, Jupiter, and Saturn at 21.2 cm wavelength: Planetary and Space Science, V. 14, No. 1, p. 15-32.

The effective brightness temperature at 21.2 cm wavelengths determined for the planets studied are: Venus,  $591 \pm 300\text{K}$ ; Mars,  $271 \pm 760\text{K}$ ; Saturn,  $286 \pm 370\text{K}$ . The brightness temperature from Venus does not vary significantly over the wavelength range 3-21 cm, which appears to indicate that this radiation comes from the surface of the planet. Polarization studies of the 21.2 cm emission from Jupiter showed a rotation period of  $9^{\text{h}}55^{\text{m}}29^{\text{s}}50 \pm 0^{\text{s}}29$ , in close agreement with the period of the decameter radiation. Possible emission mechanisms are discussed briefly.

DeMarcus, W.C., 1966, Jupiter's Great Red Spot: *Nature*, V. 209, p. 62.

The authors suggest a novel and alternative explanation of Jupiter's Great Red Spot to the explanation that it is either a floating body or a "Taylor column". The explanation is based on a theoretical prediction by Van der Waals, and it is that the red spot is merely a region where phase separation occurs under the condition that the two distinct phases have the same density, but different compositions, so that the red spot region would be buoyantly neutral with respect to its surroundings--i.e. a thermodynamic Cartesian diver.

Dickel, J.R., 1966, Observations of Jupiter at a frequency of 610.5 MHz: *The Astronomical Journal*, V. 71, p. 159-160.

A total of 37 measurements of Jupiter have been made at a frequency of 610.5 MHz with a 400-ft radio telescope. The results give a mean flux density for the planet of  $5.2 \pm 1.0$  flux units [ $10^{-26} \text{ W m}^{-2} (\text{Hz})^{-1}$ ] for a normalized distance to Jupiter of 4.04 a.u. The telescope receives left-hand circular polarization so that the radiation recorded will not include possible right-hand circularly polarized components which may be generated in the Jovian magnetosphere. The radiation appears to vary by almost 25% with the rotation of Jupiter. The intensity reaches its minimum value when the magnetic pole in the northern hemisphere, at about  $\lambda^{\text{III}} = 200^{\circ}$ , lies on the central meridian. This variation is consistent with the beaming of the radiation into the plane of Jupiter's magnetic equator. The results can be combined with other measurements in order to determine the spectrum of the radiation and the physical properties of the Jovian magnetosphere. (Abstract of a paper presented at the December 1965 meeting of the American Astronomical Society).

Dulk, G.A., and Eddy, J.A., 1966, A new search for visual aurorae on Jupiter: *The Astronomical Journal*, V. 71, p. 160.

The nature of decametric radio emission from Jupiter and the known properties of its magnetic field suggest that energetic electrons frequently impinge on its upper atmosphere. These events, occurring at the time of decametric emission, should ionize atmospheric constituents and cause a visible recombination emission spectrum. This Jupiter auroral emission has long been suspected but never observed. Past attempts to observe the effect in hydrogen- $\alpha$  have mostly used filter monochromators, with bandpass 15-20Å, or low-dispersion spectrographs. The recent finding that Io controls much of the radio emission (Bigg, *Nature* 20, 1008, 1964) enables one to predict the time and place of probable aurorae on Jupiter (Dulk, *Science* 148, 1585, 1965) and thus increases the chance of detection. Auroral activity is likely to occur on magnetic field lines connecting Io to Jupiter, at times and places favorable for detection several times per week, with duration 3 to 5 h. The authors have reinstituted the optical search for these events using the coude spectrograph at the 84-in. telescope at the Kitt Peak National Observatory. Auroral emission expected is a narrow, weak perturbation in the reflected absorption lines, Doppler-shifted from line center by planetary rotation. With spectral resolution of 0.1Å, a 1.2 kilorayleigh aurora should be detectable in H $\alpha$ , and approximately 10 kilorayleigh aurora elsewhere in the spectrum. Spectra were obtained on three favorable nights in November 1965 with negative results. We con-



clude that either no aurora brighter than 1.2 kilorayleigh was present or the spectrograph slit was incorrectly placed on the planet. Nearly concurrent filtergrams were obtained with a 5Å HP interference filter which has a 1000 kilorayleigh auroral threshold. (Abstract of a paper presented at the December 1965 meeting of the American Astronomical Society).

Duncan, R.A., 1966, Comments on the modulation of Jovian decametric emission by Jupiter's satellites: *Planetary and Space Science*, V. 14, No. 3, p. 173-176.

The first Galilean satellite, Io, sensibly modulates only high frequency Jovian decametric emissions; it has almost no effect below 30 Mc/s. The outer Galilean satellites cause no perceptible modulation at any frequency.

Duncan, R.A., 1966, Factors controlling Jovian decametric emission: *Planetary and Space Science*, V. 14, No. 12, p. 1291-1301.

Only those Jovian decametric storms whose maximum radio-frequency reaches or exceeds 30 Mc/s. exhibit the strong well-known pattern of peak occurrence at Io phases 90° and 230°. The majority of storms, those which fail to reach 30 Mc/s, exhibit a weaker and more complex pattern.

The maximum radio-frequency of storms also determines the pattern of occurrences with Jovian longitude. The current belief that Jupiter's radio rotation period has lengthened during the last few years is probably erroneous.

Fung, P.C.W., 1966, Excitation of cyclotron radiation in the forward subliminous mode and its application to Jupiter's decametric emissions: *Planetary and Space Science*, V. 14, No. 6, p. 469-481.

In this study the growth rate of a "forward-subliminous-mode" electromagnetic wave excited in a helical stream-plasma system is calculated for general wave-normal angle  $\theta$ , with parameters appropriate to the Jovian magnetosphere. It is found that for the fundamental harmonic, the growth rate maximizes at  $\theta_m$  which ranges from about 40 to 50 degrees (with respect to the static magnetic field vector) for pitch angles and energies of electron streams considered appropriate for Jupiter. The growth rate of the second and third harmonics are also discussed. The application of the amplification theory to Jupiter's decametric burst radiation is discussed and found to support the cyclotron theory of Ellis for this radiation.

Gulkis, S., and Carr, T.D., 1966, Asymmetrical stop zones in Jupiter's exosphere: *Nature*, V. 210, p. 1104-1105.

It is shown that if the models of Cerenkov emission, Doppler shifted cyclotron emission, or the "escaped-whistler" are indeed responsible for the bursts of radio noise from Jupiter, then the stop zone asymmetries must be one of the factors producing the characteristic variations of occurrence probability with central meridian longitude. Beaming of the escaping radiation into thin sheets is probably another contributing factor. Thus, if the probability of escape of radiation from a given region of Jupiter toward the earth is high, then the field orientation must be suitable to produce a beam in the right direction.

Gulkis, S., and Carr, T.D., 1966, Radio rotation period of Jupiter: *Science*, V. 154, p. 257-259.

Observations of Jupiter at 18 megacycles per second indicate that the apparent rotation period drifts cyclically about a constant mean value. The drift period appears to be 11.9 years, the same as the orbital period. It is explained on the basis of beaming of the escaping radiation at an angle 6 degrees north of the magnetic equator.

- Gulkis, S., and Carr, T.D., 1966, Radio rotation period of Jupiter: The Astronomical Journal, V. 71, p. 856-857.

It has been concluded from a re-examination of the results of 18 Mc/sec observations of Jupiter that the apparent rotation period drifts cyclically about a constant mean value. The most probable drift period appears to be 11.9 yr, Jupiter's orbital period. The mean rotation period during one orbital period is about 0.3% longer than the System III (1957.0) period. This is in close agreement with the rotation period deduced from decimetric observations, and probably represents the true rotation period of the magnetic field. The cyclic drift in the rotation period of source A at 18 Mc/sec is explained on the basis of beaming of the escaping radiation at an angle  $60^\circ$  north of the magnetic equator. The apparent rotation period of source A depends on the rate of change of the Jovicentric declination of the earth. (Abstract of a paper presented at the July 1966 meeting of the American Astronomical Society).

- Hide, R., 1966, On the circulation of the atmospheres of Jupiter and Saturn: Planetary and Space Science, V. 14, No. 8, p. 669-675.

The planetary-scale atmospheric circulations of Jupiter and Saturn are discussed in terms of basic fluid dynamics. Owing to the great size of these planets, effects of rotation are even more pronounced than in the case of the earth. There is evidence in the case of Jupiter that hydromagnetic effects may have to be taken into account.

- Hide, R., and Ibbetson, A., 1966, An experimental study of "Taylor columns": Icarus, V. 5, p. 279-290.

According to the "Taylor column" hypothesis of Jupiter's Great Red Spot, the planet rotates so rapidly that hydrodynamical disturbances at great depths within its atmosphere, possibly due to a "topographical feature" of the surface underlying the atmosphere, can penetrate upward as far as the visible surface.

Systematic experiments have been carried out on Taylor columns produced by moving solid objects through a liquid in a rotating cylindrical tank. They show that the theoretical criterion is probably correct, and indicate how it is affected by viscosity.

- Hughes, M.P., 1966, Planetary observations at a wavelength of 6 cm: Planetary and Space Science, V. 14, No. 10, p. 1017-1022.

Radiometric measurements of Venus at a wavelength of 6 cm made in the period from November 1965 through March 1966 indicate that the disk temperature reached a minimum of  $630 \pm 30^\circ\text{K}$  soon after inferior conjunction. An observation of Mars near opposition in 1965 gave a disk temperature of  $190 \pm 60^\circ\text{K}$ , the same as that reported by Kellermann. The disk temperature of Jupiter remained essentially constant at  $291 \pm 25^\circ\text{K}$  from March 1965 through March 1966. Saturn was found to have a disk temperature of  $190 \pm 45^\circ\text{K}$ , which is slightly higher than anticipated.

- Hynek, J.A., and Dunlap, J.R., 1966, A lunar transient phenomena detection program: The Astronomical Journal, V. 71, p. 389.

A program designed to detect and photographically record transient color or albedo changes which may take place on the lunar surface is in progress at the Corralitos Observatory near Las Cruces, New Mexico.

The image orthicon camera, in a closed circuit television chain, is placed at the Cassegrain focus of a 24-inch telescope. Interference filters, with sharp wavelength cutoff characteristics, are continuously and automatically alternated in the

optical path. The resulting "blink" images in two or more regions of the visible spectrum are viewed on a large TV monitor which displays a 6 x 6 minute of arc lunar region. Each scan line corresponds to 0.95 arc. A separate telescope and television chain are employed to simultaneously monitor the moon in the near infrared from 0.7 to 1.1 $\mu$ .

Since initiation of the program, in October 1965, efforts of the Corralitos staff to detect any lunar surface changes have been negative. Suspected lunar changes, reported mainly through continuous monitoring of the short-wave radio "astro-net" have not been confirmed. The planet Jupiter, used frequently as a test and calibration source, shows a very pronounced blinking of the great red spot and more subtle but easily detectable changes in the equatorial and other regions of the planet. Star pairs, also used as test sources, display a "blink" image proportional to their spectral classification difference. (Abstract of a paper presented at the March 1966 meeting of the American Astronomical Society).

Kalinyak, A.A., 1966, Data on the spectra of the Galilean satellites of Jupiter: Soviet Astronomy - A.J., V. 9, p. 824-826.

Spectral observations of the Galilean satellites of Jupiter made in 1963 at the Crimean Astrophysical Observatory give evidence of new lines in the satellite spectra, which differ from those of the solar Fraunhofer spectrum. A list of the most intense lines for three satellites, Io(I), Europa(II), and Ganymede(III), is presented.

Kellerman, K.I., and Pauling-Toth, I.I.K., 1966, Observations of the radio emission of Uranus, Neptune, and other planets at 1.9 cm: The Astrophysical Journal, V. 145, p. 954-957.

The radio emission from Venus, Jupiter, Saturn, Uranus, Neptune, and Pluto has been investigated with the 140-foot radio telescope of the National Radio Astronomy Observatory at an effective wavelength of 1.9 cm.

The effective temperatures of the four major planets at 1.9 cm are all near 200°K, although their distance from the sun ranges from 5.2 to 30 a.u. At this wavelength the main source of opacity is probably due to the ammonia inversion line near 1.25 cm. Since the ammonia will not exist in a gaseous state in the cooler upper regions of the atmosphere, the level where  $\tau \sim 1$  on all the planets corresponds to a fixed effective temperature near the freezing point of ammonia, which is 195°K.

Low, F.J., 1966, Observations of Venus, Jupiter and Saturn at  $\lambda 20\mu$ : The Astronomical Journal, V. 71, p. 191.

The first observations of the planets at  $20\mu$  were reported by Low (Lowell Observatory Bulletin 128, 184, 1965). Using the same radiometer, which cuts on at 17.5 $\mu$  and is uniformly sensitive to about 25 $\mu$ , further observations have been made with angular resolutions between 4 and 35 arc sec. Under the assumption that Mars radiates as a blackbody, its brightness temperature at  $20\mu$  was taken as  $2250 \pm 50^\circ\text{K}$ , the value measured for the disk at  $10\mu$ . This yielded a temperature for Venus at  $20\mu$  of  $248 \pm 100^\circ\text{K}$ , significantly above the  $10\mu$  value of  $221 \pm 100^\circ\text{K}$  but in good agreement with solar heating. Using Mars and Venus as standards, it was possible to observe Saturn with angular resolutions both large and small compared to its disk. Correcting for the obscuration of the rings, which were found to be much colder than the planet, the mean disk brightness temperature was  $95 \pm 30^\circ\text{K}$ , quite close to the measured value of  $93^\circ\text{K}$  at  $10\mu$  (Low, F.J., Astron. J. 69, 550, 1964). Scans of Jupiter show a hot equatorial band,  $150 \pm 50^\circ\text{K}$ , covering about half the disk; the poles are about  $130^\circ\text{K}$ . Although the equatorial scans show significant limb darkening, the east and west limbs are equal in temperature to within the accuracy of measurement.

The total amount of energy Jupiter receives from the sun is less than the observed radiation between 10 and 25  $\mu$  and would produce an effective temperature of only 105°K. Thus, an internal supply of energy must be present. The Jovian temperature measured at 1 mm is  $155 \pm 15^\circ\text{K}$  (Low, F.J., and Davidson, A.W., *Astrophys. J.* 142, 1278, 1965). If the brightness temperature between 25  $\mu$  and 1 mm does not drop below 140°K, the total power radiated by Jupiter is more than 3 times the insolation. A similar conclusion may be drawn for Saturn; however, since only a small fraction of its total energy is observed, its excess brightness temperature at 20  $\mu$  may be caused by a greenhouse effect. (Abstract of a paper presented at the March 1966 meeting of the American Astronomical Society).

McAdam, W.B., 1966, The extent of the emission region on Jupiter at 408 Mc/s: *Planetary and Space Science*, V. 14, No. 11, p. 1041-1046.

Observations of the emission region on Jupiter have been made with the E-W arm of the 1-mile Mills Cross. The extended Van Allen belt has been resolved in right ascension by the 88" arc fan beam, and a model of the brightness distribution compared with the more detailed models obtained at higher frequencies. Most emission comes from within 1.6 Jovian radii of the centre, but there is a region at 6 radii that contributes 16-20 percent of the flux.

McCulloch, P.M., and Ellis, G.R.A., 1966, Observations of Jupiter's decametric radio emissions: *Planetary and Space Science*, V. 14, No. 4, p. 347-359.

Observations of the mean power of Jupiter's decametric radio emissions at six frequencies, 4.7, 15.7, 18.7, 21.5, 24.5, and 28.0 Mc/s, have been used to prepare histograms of relative power and probability of occurrence at each frequency. The variation of the mean flux density of the emissions was determined as a function of frequency, and was found to increase monotonically with decreasing frequency down to 4.7 Mc/s. The location of Jupiter's magnetic poles is discussed. The data at four of the six frequencies was examined for influence of the Jovian Satellite Io and contour diagrams of the emission were plotted.

Miller, A.C., and Griffin, J., 1966, 1414 Mc/sec Jupiter observations: *The Astronomical Journal*, V. 71, p. 744-746.

Jupiter was observed at a frequency of 1414 Mc/sec on 28 nights from 10 September to 17 December 1963 using a crystal mixer receiver with a linearly polarized rotating feed horn installed in NRL's 84-ft. radio telescope. Rotating feed measurements gave, for 244 rotations, an average equivalent blackbody temperature of  $25900 \pm 2000^\circ\text{K}$  (s.e.) and a fractional polarization of  $0.23 \pm 0.03$  (s.e.) at an average position angle of  $6190 \pm 290$  (s.e.) for the maximum intensity. The average of 241 drift curves taken with the E plane of the feed horn oriented at the position angle of the Jovian optical equator gave a temperature of  $3250 \pm 200^\circ\text{K}$  (s.e.). Observed equatorial and polar fluxes of 5.5 and  $3.4 \times 10^{-22} \text{ W m}^{-2} \text{ cps}^{-1}$ , normalized to 5 a.u., agree within  $\pm 0.2$  flux units with previous NRL measurements made near 1400 Mc/sec. The temperatures and fluxes are based on an assumed value for Virgo A of  $198 \times 10^{-28} \text{ (mks)}$ .

Moroz, V.I., 1966, The spectra of Jupiter and Saturn in the 1.0-2.5  $\mu$  region: *Soviet Astronomy - A.J.*, V. 10, No. 3, p. 457-468.

Spectra of Jupiter, Saturn's disk, and Saturn's rings in the region 1-2.5  $\mu$  have been obtained at resolutions  $\lambda/\Delta\lambda \approx 500, 150$ , and 20 respectively. They are analyzed on a "simple reflection" model, with the cloud-layer boundary assumed optically equivalent to a solid surface. The  $\text{CH}_4$  content above Jupiter's cloud layer is apparently  $< 150 \text{ m. atm}$ . The 1-0 band of  $\text{H}_2$  probably contributes significantly to the absorption near 2  $\mu$ . Saturn's cloud layer most likely consists of  $\text{CH}_4$  ice particles; the rings,  $\text{H}_2\text{O}$  ice particles.

- Moroz, V.I., 1966, Infrared spectrophotometry of the moon and the Galilean satellites of Jupiter: Soviet Astronomy - A.J., V. 9, p. 999-1006.

Spectra of selected sectors of the lunar surface in the region  $0.8-3.8\mu$  were obtained using a 125-cm reflector and a prism infrared spectrometer with  $\lambda/\Delta\lambda$  from 20 (at  $1.6\mu$ ) to 80 (at  $3.4\mu$ ). Albedo increases with wavelength, at least to  $2.2\mu$ , approximately identically for all the investigated sectors, including seas, continents and light craters. Among terrestrial rocks volcanic ash and scoria have a similar dependence of albedo on wavelength. Thermal emission makes a considerable contribution in the interval  $3-4\mu$ . The value of the thermal excess was used in determining the temperature (395°K) of the subsolar point. The same spectrometer, with 125- and 260-cm reflectors, was used in observing the spectra of the Galilean satellites in the region  $0.8-2.5\mu$ . The records of Europa and Ganymede show details characteristic of the reflection spectrum of a snow cover.

- Olivarez, J., 1966, Unusual widespread colors on Jupiter: Sky and Telescope, V. 31, p. 306-307.

The observer reports various anomalous hues on Jupiter for his observations of the last three years.

- Olsson, C.N., and Smith, A.G., 1966, Decametric radio pulses from Jupiter: Characteristics: Science, V. 153, p. 289-290.

The decametric radio bursts from Jupiter occasionally contain pulses of millisecond duration. These pulses have a Jovian longitude distribution different from pulses of longer duration. Also the two types of pulses are differently affected by the position of the innermost satellite.

- Owen, T., 1966, An identification of the 6800-Å methane band in the spectrum of Uranus and a determination of atmospheric temperature: Astrophysical Journal, V. 146, p. 611.

By considering the relative intensities of the R branch lines in the 4 overtone of the  $\nu_3$  vibration of methane, the author calculates that the mean temperature of the visible atmosphere of Uranus is  $600 \pm 150$ K. Additionally he points out that the same band can be detected in the spectra of Jupiter and Saturn.

- Reese, E.J., and Smith, B.A., 1966, A rapidly moving spot on Jupiter's North Temperate Belt: Icarus, V. 5, p. 248-257.

A very rapid drift in the longitude of a small dark spot on the south edge of Jupiter's North Temperate Belt (NTBs) has been determined. The mean daily drift of the spot was  $-90.4056$  relative to System II, and  $-10.7756$  relative to System I. This corresponds to a mean rotation period of  $9^h 49^m 18^s.5$ . A more detailed study of its motion disclosed a nearly sinusoidal displacement with respect to its mean position. A period of 300 days and an amplitude of  $4^\circ$  in longitude would best describe this oscillatory motion. The center of the spot remained stationary near zenographic latitude  $+24^\circ$ , within the probable error of the measures. This solitary spot apparently represents the fifth observed outbreak of activity in the well-known but rarely observed North Temperate Current "C", a current which has produced the shortest rotation periods ever recorded on Jupiter.

- Reese, E.J., and Solberg, H.G., Jr., 1966, Recent measures of the latitude and longitude of Jupiter's Red Spot: Icarus, V. 5, p. 266-273.

The latitude and longitude of Jupiter's Red Spot were measured from photographic plates. The longitudes measured from photographs have been found to be an order

of magnitude more accurate than the longitudes obtained from visual estimates of central meridian transit times. The significantly improved accuracy of photographic observations made possible the detection of rapid, short-term changes in longitude. The Red Spot slowly oscillated in latitude, remaining within 1% of its mean latitude of  $-22.94^\circ$  for the reported interval.

Riihimäki, J.J., 1966, High-resolution spectra of decametric radio bursts from Jupiter: *Nature*, V. 209, p. 387-388.

Fine structure in the dynamic spectra of decametric radiation from Jupiter were recorded during the 1964 apparition. Most recordings showed similar variations of intensity with time from channel to channel, indicating radiation bandwidths of the order of 500 kc/s or more, but on 14 nights recordings were obtained in which the variations were not similar at all, indicating fine structure composed of pulses with bandwidths of the order of 50 kc/s or less.

It is possible that these observations indicate some variations in the spectral fine structure depending on the positions of the radio system and the satellite Io. Others have discussed the Jovian decametric emissions presuming some kind of exospheric disturbances; the extension of the present experiment to weaker radio storms would probably have some interest in studying the nature of the disturbances produced by the satellite.

Riihimäki, J.J., 1966, Spectral types of decametric radiation from Jupiter: *Nature*, V. 212, p. 1338-1339.

There are indications that three types of dynamic spectra of high resolution, as well as burst which have bandwidths of the order of 50 kc/s., are contained in the Jovian decametric emission. These three types of spectra are discussed separately. It is suggested that the classification of the radio bursts from Jupiter should be based on the characteristics of their high resolution dynamic spectra.

Roberts, J.A., and Ekers, R.D., 1966, The position of Jupiter's Van Allen belt: *Icarus*, V. 5, p. 149-153.

This paper reports a series of measurements of the location of the centroid of the 11.3-cm Jovian radio emission relative to a nearby radio source whose position is known from a lunar occultation. The mean position of the centroid of the Jovian emission is close to the center of the planet.

Roemer, E., Thomas, M., and Lloyd, R., 1966, Observations of comets, minor planets, and Jupiter VIII: *The Astronomical Journal*, V. 71, p. 591-601.

Accurate positions and descriptive notes are presented for 24 comets, 11 minor planets, and the eighth satellite of Jupiter.

Sastry, Ch.V., 1966, Short-term correlations of decameter radio emission from Jupiter and solar activity: *The Astronomical Journal*, V. 71, p. 179.

An analysis of decameter radio emission from Jupiter and solar activity over the past 10 yr by the Chree method of superposed epochs showed that there is a significant increase in the radio emission from Jupiter following enhanced solar activity during the past sunspot maximum. The indices used to represent solar activity are (1) geomagnetic planetary index  $A_p$ , (2) solar radio flux at centimeter wavelengths.

It is pointed out that due to the directivity of the source on Jupiter, the effect of the satellite Io and the observing procedures the Jupiter data contain



periodicities which are not inherent in the source. These periodicities are estimated in the following way. A two-dimensional histogram giving the occurrence probability as a function of LCM (system III) and the position of the satellite Io is calculated using all the available data. For an assumed 4 h observing function each day the theoretical probability of observing Jupiter based on the two-dimensional histogram is calculated for a number of days. A power spectrum analysis of these theoretical probabilities showed that there can be a number of periodicities in Jupiter data with periods ranging from 2 to 30 days. It is well known that solar data exhibit similar periodicities. The observed correlations may be due to the existence of similar periodicities in both time series. To test this hypothesis the probability of observing Jupiter for each day, for which observing times are available, during the period 1957 through 1961 is calculated using the two-dimensional histogram. These theoretical probabilities are correlated with the solar indices for the same period. The correlation curves thus obtained are similar to the correlation curves obtained by using the days on which Jupiter emission is detected. On the basis of these results it is suggested that there is no conclusive evidence that decameter radio emission from Jupiter and solar activity are related. (Abstract of a paper presented at the December 1965 meeting of the American Astronomical Society).

Six, N.F., Jr., Holmes, J.R., Lebo, G.R., Smith, A.G., and Carr, T.D., 1966, Periodicities in the Jovian decametric radio emission: *The Astronomical Journal*, V. 71, p. 398.

Autocorrelation and power spectrum analyses have been made of the decameter-wave-length radio emission from Jupiter received at stations in Florida and in Chile at the frequencies 15, 18, and 22.2 MHz during the apparitions of 1960, 1961, 1962, and 1963. The authenticity of the various periodic components has been decided by determining which periods appear from year to year, from frequency to frequency, and from station to station. The most dominant periods in the 21 samples analyzed are 3-4, 17-18, and 34-35 days. Periods of 7-8, 11-12, 19-20, and 24-25 days also appeared in a majority of the samples. We have attempted to find physical periods which match these, in order to perhaps uncover related phenomena. The Jovian emission is known to be correlated with (1) the system III longitude of the central meridian and (2) the position of the satellite Io. The 3.5-day syzygy period of Io and V and the 7-day syzygy period of Io, Europa, and Ganymede account for many of the periodic components in the emission. Autocorrelation studies have been performed on various solar indices to determine what periodic components exist in them besides the solar rotation period. The indices investigated were the 2800-MHz flux, sunspot number, and solar flare importance number for the years 1961-1963. Legitimate periodic components at 7-9, 10-11, and 32-35 days appear to be present. (Abstract of a paper presented at the March 1966 meeting of the American Astronomical Society).

Slee, O.B., and Higgins, C.S., 1966, The apparent sizes of the Jovian decametric radio sources: *Australian Journal of Physics*, V. 19, p. 167-180.

During 1963 and 1964 measurements were made of the angular sizes of the sources of Jovian radio bursts, at a frequency of 19.7 Mc/s, using interferometers with spacings up to 12700  $\lambda$ . The measured source sizes were mostly in the range 10-15 sec of arc, but it seems likely that these apparent sizes are produced by interplanetary scattering and that the intrinsic size may be much smaller.

It is suggested that many of the "bursts" received from Jupiter are produced by a diffraction or focusing process in interplanetary space and so may be analogous to the interplanetary scintillations recently reported by Hewish, Scott, and Wills (1964). If so, the real angular size of the Jupiter source would probably be less than 1 sec of arc.

Spinrad, H., and Giver, L.P., 1966, Jupiter and Saturn: Planetary line inclinations: *Publications of the Astronomical Society of the Pacific*, V. 78, p. 175-177.

Observations have been continued of planetary line inclinations ( $\text{CH}_4$  and  $\text{NH}_3$  on Jupiter,  $\text{CH}_4$  on Saturn) previously found to be suspiciously anomalous on equatorial spectrograms. New results from Lick spectrograms show that no anomaly was present in 1964 and 1965. These results do not differ significantly from the expected 50% from Doppler-shift calculations. So far, no satisfactory model of these planets has been proposed to explain the sometimes anomalous line inclination.

Staellin, D.H., and Neal, R.W., 1966, Observations of Venus and Jupiter near 1-cm wavelength: *The Astronomical Journal*, V. 71, p. 872.

A search for spectral features on Venus and Jupiter was made from January to March 1966. Five Dicke-type radiometers were connected simultaneously to the antenna feed by means of frequency-selecting filters. They operated at 19.0, 21.0, 22.235, 23.5, and 25.5 GHz. The following results were obtained:

Venus			rms error	Jupiter			rms error
Freq. (GHz)	T <sub>B</sub> (°K)	Rel. (%)	Abs. (%)	T <sub>B</sub> (°K)	Rel. (%)	Abs. (%)	
19.0	477	+8	+12	105	+20	+20	
21.0	451	+4	+9	106	+9	+10	
22.235	436	+4	+9	98	+10	+11	
23.5	418	+4	+9	116	+8	+9	
25.5	400	+4	+9	123	+7	+9	

(Abstract of a paper presented at the July 1966 meeting of the American Astronomical Society).

Telfel, V.G., 1966, Spectrophotometry of the methane absorption bands at 0.7-1.0  $\mu$  on the disk of Jupiter: *Soviet Astronomy - A.J.*, V. 10, No. 1, p. 121-123.

The intensity of the  $\text{CH}_4$  infrared absorption bands at 7250, 8610 + 8860, and 9900  $\text{\AA}$  has been measured on spectrograms of various zones on Jupiter obtained with an electronic image converter. In the equatorial zone the  $\text{CH}_4$  absorption does not intensify but declines slightly toward the limb; it increases slightly at intermediate latitudes, but declines toward the poles. The absorption varies far less than implied by the ordinary secant effect in a one-layer absorbing model atmosphere. The equatorial-temperate variation could arise from a differing height for the top of the cloud deck, with  $\Delta h$  only 2-4 km for a one-layer model, 5-10 km for a two-layer model. Pressure effects must be considered if the two-layer model is to explain the constant absorption observed in the equatorial zone and its decline near the limb.

Tolbert, C.W., 1966, Observed millimeter wavelength brightness temperatures of Mars, Jupiter, and Saturn: *The Astronomical Journal*, V. 71, p. 30-32.

Analyses of observations of 35, 70, and 94 Gc radiation from Mars, Jupiter, and Saturn made with a 16-ft. antenna yield brightness temperatures for Mars of 230 (+42, -42)°K and 240(+72, -48)°K at 35 and 94 Gc, respectively; for Jupiter, 113 (+11, -11)°K, 105(+18, -12)°K and 111(+22, -11)°K at 35, 70 and 94 Gc, respectively. The antenna temperatures from which the brightness temperatures were calculated were obtained by averaging the responses of right ascension scans of the antenna beam across the planets. The observing and data reducing techniques are herein described and the averaged antenna temperatures shown.

Trafton, L., 1966, Model atmospheres of the major planets: *The Astronomical Journal*, V. 71, p. 183.

Model atmospheres of the major planets have been constructed by using recently discovered sources for the dominant thermal opacity. These sources are the pressure-induced absorption in molecular hydrogen and the pressure-induced enhancement resulting from the mixing of molecular hydrogen and helium. They are responsible for most of the greenhouse effect observed in the upper atmosphere of each major planet. These model atmospheres are non-gray and were constructed in hydrostatic equilibrium. They incorporate a first-order correction to account for convection. The thermal opacity of ammonia does not play a significant role in the atmosphere of any major planet except Jupiter and here, it was found to play a relatively small role. Each planet is represented by several models having different values of the effective temperature and  $\text{He}/\text{H}_2$  ratio. These quantities were considered as free parameters to be determined by fitting the models to the observations. Most of the models indicate the existence of a tenuous fog or mist overlying a cloud zone.

In the case of the Jovian models, it was necessary to include the 10- $\mu$  band of ammonia in order to explain the observed limb darkening in the 8 to 14  $\mu$  region of the spectrum. It was also necessary to include helium in order to explain the scale height observations. Jovian models which are compatible with all the observations have high effective temperatures indicating that Jupiter has an internal heat source yielding greater than about one-tenth of the incident solar flux. In addition, an upper limit of about two on the  $\text{He}/\text{H}_2$  ratio is implied by the Jovian models. (Abstract of a paper presented at the December 1965 meeting of the American Astronomical Society).

Warwick, J.W., 1966, New information on Jupiter's magnetic field: Transactions of the American Geophysical Union, V. 47, No. 1, p. 44.

Several refined observations recently made of Jupiter's radiation belt radio emission show that the centroid of the emission lies close to the mass centroid of the planet itself. The data strongly oppose the decentered dipole model of Jupiter's magnetic field. On the other hand, the recent discovery of Io's decisive influence over much of the ionospheric radio emission allows us to reaffirm the existence of important asymmetries in the field geometry with respect to the mass of the planet. These two types of data appear, therefore, to be in conflict with one another. One way to resolve the paradox involves modeling the field by a strong quadrupole magnetic field in addition to a dipole term, both poles centered within the planet. This proposal can explain the relatively small asymmetry of the radiation belt emission and, as well, the large asymmetry of ionospheric emission. (Abstract of a paper presented at the April 1966 meeting of the American Geophysical Union).

Welch, W.J., Thornton, D.D., and Lohman, R., 1966, Observations of Jupiter, Saturn, and Mercury: Astrophysical Journal, V. 144, p. 799-809.

Observations of the radio emission from Jupiter, Saturn, and Mercury at 1.53-cm wavelength are reported. The disk temperature of Saturn was found to be 0.94 times that of Jupiter at this wavelength. Mercury, observed at an average phase angle of 125°, was found to have a disk temperature three times that of Jupiter. With Jupiter's disk temperature assumed to be 1500K at this wavelength, the temperatures of Saturn and Mercury are 1410 and 4500K, respectively. The similarity in the emission from Jupiter and Saturn at this wavelength can be explained if one supposes that ammonia gas is the chief source of microwave thermal radiation from both planets (due to the ammonia absorption band centered at 1.28 cm) and that the gas is saturated near the cloud tops of both planets.

The possibility that emission from Saturn's rings may contribute to the radio "disk" temperature of Saturn is briefly considered. If the particles in the ring are many centimeters in diameter and perfectly absorbing, the rings contribute

about 250K to the "disk" temperature. If their mean radius is about 300u, a probable size obtained by Franklin and Cook, their microwave extinction cross-section is small and the ring particles will not emit significant microwave energy.

Witting, J., 1966, Satellite roles in radio emission from Jupiter: *The Astronomical Journal*, V. 71, p. 187.

Jupiter I is known to influence quite strongly the probability of decameter wavelength radio emission from Jupiter. It is shown that the direct scattering of electrons of 40 keV by the satellite produces particle lifetimes of the order of months, probably much longer than lifetimes required by the intensity of the bursts. It is also shown, however, that Alfvén waves which propagate along magnetic fields without radial attenuation can be generated by the moving satellite. This might provide a mechanism for triggering plasma instabilities leading to decameter bursts.

Radio emission from Jupiter at decimeter wavelengths implies a radiation belt of relativistic electrons near the orbit of Jupiter V. It is shown that Jupiter V scatters relativistic electrons out of the belt in less than 2 yr, either by direct impact or reflection from large-amplitude Alfvén waves generated by the moving satellite. This lifetime is small compared to the lifetime of highly relativistic electrons against radio emission. This implies either that electron densities are larger than those given by Chang and Davis (1962) or that the magnetic field near Jupiter V is greater than 1 G. If large-amplitude Alfvén waves are present, they provide a means of accelerating electrons through Fermi acceleration, such that electron energies follow a power law spectrum having exponent of the order of -1, which is consistent with decimeter observations. (Abstract of a paper presented at the December 1965 meeting of the American Astronomical Society).

Zabriske, F.R., Solomon, W.A., and Hagen, J.P., Jr., 1966, Radiation from Jupiter at long wavelengths: *The Astronomical Journal*, V. 71, p. 877.

During the 1964 apparition of Jupiter, observations were made at several frequencies between 3.5 and 7.3 Mc/sec. Analysis of these records shows about 32 events that are probably Jupiter. To be seen with certainty on our records for a typical night, the flux density must exceed  $2 \times 10^{-21} \text{ W m}^{-2} \text{ cps}^{-1}$ , although some nights are much better. This is a large flux and probably explains our low occurrence probability.

Certain other details appear: emission, in two cases only, can be traced down to 3.5 Mc/sec. However, the flux density falls to one-tenth or less that recorded above 5 Mc/sec. The longitude profile shows a broad maximum between  $300^\circ$  and  $50^\circ$ , a secondary peak near  $150^\circ$ , and a quiet zone between  $200^\circ$  and  $240^\circ$ . When radiation is observed from the broad peak, the satellite Io has a strong tendency to lie between  $210^\circ$  and  $250^\circ$  from superior conjunction. Radiation from  $150^\circ$  peak does not show this tendency, but the statistical sample is small. (Abstract of a paper presented at the July 1966 meeting of the American Astronomical Society).

Zheleznyakov, V.V., 1966, The origin of Jovian radio emission: *Soviet Astronomy - A.J.*, V. 9, p. 617-625.

The hypothesis of the origin of the decameter radio emission of Jupiter, in which the source of the Jovian radio emission bursts are plasma waves excited in the planetary ionosphere, is discussed. The simplest variant of the hypothesis, which does not take the Jovian magnetic field into account and ensures the generation of radio emission at frequencies  $\omega \sim \omega_p$  where  $\omega_p$  is the plasma frequency, is possible only for extremely small values of the recombination coefficient  $\alpha_{\text{eff}} \sim 10^{-13} - 10^{-14} \text{ cm}^3$  (necessary for creating an ionospheric electron concentration of

$N \sim 10^7$  el/cm<sup>3</sup>). However, in actuality  $\alpha_{\text{eff}}$  cannot decrease below  $10^{-12}$  cm<sup>3</sup>, that is, below the value of the coefficient of radiative recombination. Allowance for a magnetic field makes it possible to decrease the value  $N$  and accordingly increase  $\alpha_{\text{eff}}$  to reasonable limits; the necessary values of the frequency of radio emission in this case  $\omega \sim \omega_H$  ( $\omega_H$  is the gyrofrequency) are obtained when the strength of the magnetic field in the ionosphere is quite great (several oersteds). The observed characteristics of Jovian dekameter radio emission can be explained if  $N \sim 3 \cdot 10^5$  el/cm<sup>3</sup>. In particular, this value  $N$  is adequate to explain the directional character of the Jovian bursts associated with the gyroresonance absorption of extraordinary radio emission in the upper layers of the planetary ionosphere (at the level where  $\omega \approx 2\omega_H$ ). The predominant emission of extraordinary waves ensures a mechanism of transformation of plasma waves in the region of sharp decreases of density of ionospheric plasma of the shock-wave type. It is noted that plasma waves at the frequencies  $\omega \approx \omega_H$  can be excited by the "anisotropy" of temperatures or by "two-stream" instability at shock-wave fronts. In conclusion, arguments are given against the cyclotron mechanism and in favor of the synchrotron mechanism of Jovian dekameter radio emission.

### 3.7.4 Mars

Alkezweeny, A.J., and Hobbs, P.V., 1966, The reflection spectrum of ice in the near infrared: *Journal of Geophysical Research*, V. 71, p. 1083-1086.

The reflection spectrum of ice has been measured as a function of angle of incidence in the wavelength interval 2.5 to 5 $\mu$ . The results show two bands, one at 3.05 $\mu$  and the other at 4.5 $\mu$ ; the latter has not been observed previously in the reflection spectrum of ice. At 3.05 $\mu$ , values for the real part of the refractive index and the extinction coefficient of 1.396 and 0.39, respectively, are found to give good agreement with the experimental results. A theoretical explanation is given for the effect of temperature on the reflection coefficient of ice.

Anderson, D.L., and Kovach, R.L., 1966, The interiors of the moon and terrestrial planets: *Transactions of the American Geophysical Union*, V. 47, No. 1, p. 155.

Present information regarding the composition and strength of the interior of the earth is used to discuss the interiors of the moon and terrestrial planets. Results strongly suggest homogeneity of the Fe/Si ratio in the inner part of the solar system. The mass versus density function is determined for iron-rich silicate planets with different degrees of oxidation, and the results are compared with the terrestrial planets. The properties of Mars, Venus, and the earth are all consistent with the assumption of early uniformity of the solar system. The data for Mars slightly favor the hypothesis that Mars is more oxidized than the earth, but the uncertainty in the radius of Mars also allows the composition to be the same as the earth's. Contrary to current thoughts, the shape of the moon implies that it is weaker than the earth; this is consistent with thermal calculations. Using the earth's mantle as a model, the density and elastic properties are calculated for the interior of the moon. Density and velocity decrease with depth throughout most of the moon. (Abstract of a paper presented at the April 1966 meeting of the American Geophysical Union).

Anderson, D.L., and Phinney, R.A., 1966, The early thermal history of the earth and the terrestrial planets: *Transactions of the American Geophysical Union*, V. 47, No. 1, p. 185.

Using a homogenized earth as a prototype planetary model and using new estimates of the earth's age and average radioactivity, it is possible to determine the thermal evolution of various-sized protoplanetary spheres up to the melting point. If the melting point of silicates and iron is exceeded in the lifetime of the planet, it

is assumed that the planet will outgas and will differentiate a core and a crust. Two protoplanetary models are considered: one has the same composition as the present earth and, therefore, contains free iron dispersed throughout the body; the other has this iron completely oxidized and is, therefore, an iron-rich silicate or a mixture of oxides. For both cases there exists a maximum-size planet, intermediate between the earth and Mars in mass, that can exist without differentiation. If the protoplanetary Mars and earth are identical in composition, Mars will not differentiate or outgas significantly but the earth will. The thermal calculations are, therefore, consistent with data of Mars regarding its shape, magnetic field, radiation belts, atmosphere, and surface coloration. The Martian surface and interior are probably similar to those of the primitive earth. The study of Mars, therefore, can provide clues to the very early properties of the earth. (Abstract of a paper presented at the April 1966 meeting of the American Geophysical Union).

Aronson, J.R., Emslie, A.G., Allen, R.V., and McLinden, H.G., 1966, Far infrared studies of minerals for application in remote compositional mapping of the moon and planets: Transactions of the American Geophysical Union, V. 47, No. 1, p. 155.

The surface composition of the moon and planets, such as Mars and Mercury, with tenuous atmospheres can be measured remotely by infrared reflectance and emittance spectroscopy over a broad range of frequencies. The information in the far infrared region ( $50\text{--}667\text{ cm}^{-1}$ ) is especially informative as to specific mineral composition, and is very desirable in order to disentangle the composite spectra resulting from complex mixtures. Experimental studies of far infrared spectra, at room and cryogenic temperatures, of possible lunar and planetary surface minerals have been performed. Theoretical and experimental studies of the factors that control spectral contrast in the spectra of particulate surfaces and of the kind of mixing rules that must be used to disentangle the spectra of composite surfaces have been made. (Abstract of a paper presented at the April 1966 meeting of the American Geophysical Union).

Belton, J.S., and Hunten, D.M., 1966, Abundance and temperature of  $\text{CO}_2$  in the Martian atmosphere: The Astronomical Journal, V. 71, p. 156.

Spectrophotometric observations of the R branch of the weak  $\nu_1 + 2\nu_2 + 3\nu_3$  band of  $\text{CO}_2$  at  $1.05\mu$  in the spectrum of Mars yield an atmospheric abundance of  $69 \pm 26$  (atm  $\cdot$  m)STP. Taken together with the results of Gray's (1965) analysis of the strong bands of  $\text{CO}_2$  at  $2.0\mu$ , this abundance indicates a surface pressure in the range of 3–13 mbar. Individual lines in the branch have been resolved up to  $J = 28$  and their intensity distribution indicates a rotational temperature of  $194^\circ\text{K}$ . The head region alone yields a somewhat higher temperature of  $210^\circ\text{K}$ . The observations were also analyzed with the help of a polytropic model atmosphere. The most satisfactory fit to the data was found for a mean surface temperature of  $270^\circ\text{K}$  over the illuminated disk and a lapse rate of  $5^\circ\text{K/km}$ .

A brief discussion of the compatibility of the present observations with others that are available concludes the paper. (Abstract of a paper presented at the December 1965 meeting of the American Astronomical Society).

Belton, J.S., and Hunten, M., 1966, The abundance and temperature of  $\text{CO}_2$  in the Martian atmosphere: Astrophysical Journal, V. 145, p. 454–467.

Spectrophotometric observations of the R branch of the weak  $\nu_1 + 2\nu_2 + 3\nu_3$  band of  $\text{CO}_2$  at  $1.05\mu$  in the spectrum of Mars yield an atmospheric abundance of  $68 \pm 26$  m-atm(STP). Taken together with the results of Gray's analysis of the strong bands of  $\text{CO}_2$  at  $2\mu$ , this abundance indicates a surface pressure in the range of 5–13 mb. Individual lines in the R branch have been resolved up to  $J = 28$ , and



their intensity distribution indicates a rotational temperature of  $194^{\circ}\text{K}$ . The head region alone yields a somewhat higher temperature of  $210^{\circ}\text{K}$ . The observations were also analyzed with the help of a polytropic model atmosphere. The most satisfactory fit to the data was found for a maximum air temperature at the surface of  $270^{\circ}\text{K}$  and a lapse rate of  $50^{\circ}\text{K km}^{-1}$ . The paper is concluded with a brief discussion of the compatibility of the present observations with others that are available.

Binder, A.B., 1966, Mariner IV: Analysis of preliminary photographs: *Science*, V. 152, p. 1053-1055.

It is deduced that the Martian surface is from  $2.2$  to  $3 \times 10^9$  years old. This result implies that in the early history large-scale erosion occurred. Of 69 Martian craters greater than  $10$  km, 13 have central peaks, in good agreement with lunar statistics. This may indicate that the central peak is the result of impact rather than volcanism.

Binder, A.B., and Cruikshank, D.P., 1966, Lithological and mineralogical investigation of the surface of Mars: *Icarus*, V. 5, p. 521-525.

Laboratory comparisons indicate that the infrared color profile of the Martian deserts matches that of a naturally occurring limonite stain which forms and is preserved on igneous rocks in a terrestrial desert environment. The colorimetry of the Martian dark regions is found to be different from the colorimetry of basalt.

Binder, A.B., and Cruikshank, D.P., 1966, The composition of the surface layer of Mars: *Communications of the Lunar and Planetary Laboratory*, V. 4, No. 64, p. 111-120, +2 pages photographs.

A comparison of the infrared spectra of the bright areas of Mars with that of terrestrial rock samples shows evidence that the deserts consist of rock outcrops and probably rock fragments of all sizes, coated for the most part with a hard surface stain of limonite.

Bullen, K.E., 1966, On the constitution of Mars III: *Monthly Notices of the Royal Astronomical Society*, V. 133, p. 229-238.

Results pertinent to the assumption that Mars and the earth have certain common features in their composition are assembled and discussed. Reference is made to problems arising from changes of phase and chemical composition in the earth's mantle. The limitations of a procedure via an Emden equation are pointed out and contrasted with other procedures. It is shown that, up to a point recent calculations by Lyttleton may be regarded as involving a variant of the earth model B. When the strictures forced by the Emden equation are taken into account, Lyttleton's results are broadly equivalent to earlier conclusions of Ramsey and the writer on Mars. Questions on: (a) the presence of a core in Mars, and (b) the use of a quadratic law of incompressibility against pressure, are discussed and certain misconceptions corrected. Attention is drawn to certain implications of the value which Lyttleton arrives at for the pressure at the boundary between the two zones of his Mars model. Finally some comments are made on questions of scientific inference in this field.

Chamberlain, J.W., and McElroy, M.B., 1966, Martian atmosphere: The Mariner Occultation Experiment: *Science*, V. 152, p. 21-25.

A model of the Martian atmosphere is presented, consisting of 44 percent  $\text{CO}_2$ , provided it is not strongly dissociated, and 56 percent  $\text{N}_2$ . The major ionization is in the E region, produced by solar x-rays.

Charlson, R.J., 1966, Some thoughts on noctilucent clouds: Transactions of the American Geophysical Union, V. 47, No. 4, p. 628-629.

Noctilucent clouds occur near the mesopause at a height of about 80 km and are best seen between 45°N and 70°N latitudes. The purpose of this paper is to present a theoretical model of these clouds based on the simple hypothesis that they are relatively ordinary and may involve only nuclei and water. It is not necessary to invoke assumptions of esoteric chemical compounds and/or physical processes in order to explain this beautiful nocturnal phenomenon. Conclusions based on this model will be discussed in connection with the visual appearance of the clouds. The possible extension of this simple model to atmospheric phenomena on other planets (e.g., Mars) will be examined briefly. (Abstract of a paper presented at the September 1966 meeting of the American Geophysical Union).

Cohen, A.J., 1966, Martian canal system: The Astronomical Journal, V. 71, p. 849.

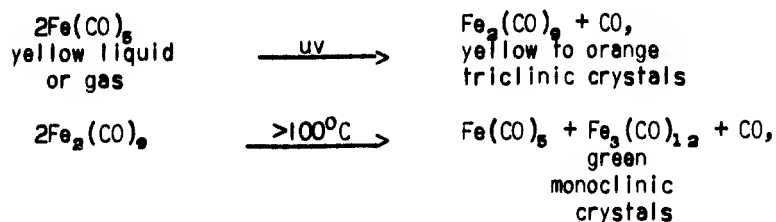
The Martian canal system is an illusion probably caused by observation of combinations of arcuate and elliptical rays from numerous impact craters on the surface. Presence of arcuate and elliptical rays completely covering areas seen in several Mariner IV photographs confirms this possibility as well as the impact nature of the craters. The presence of large numbers of rays compared to the lunar surface may indicate almost total lack of outgassing on the Martian surface. Presence of complex overlapping ray systems on Mars indicates the seasonal colors are due to changes in superficial coatings of inorganic complexes and frozen gases.

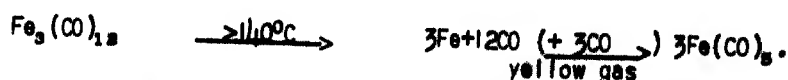
The relatively small number of impact craters observed on Mariner IV pictures and therefore the possible young age ( $\sim 8 \times 10^8$  yr) of the observed craters could indicate a rather recent ice cover of molecules of low atomic number atoms on the Martian surface. Earlier impacts in the ice would by now have been largely obscured due to the large diameter: depth ratio of impact structures. A primordial ice cover would help account for the lack of surface relief on Mars. Detailed observation of arcuate and elliptical ray structures on the Martian surface was facilitated by use of optically filtered Mariner IV photographs. (Abstract of a paper presented at the July 1966 meeting of the American Astronomical Society).

Cohen, A.J., 1966, Seasonal color changes on Mars: The Astronomical Journal, V. 71, p. 849-850.

The atmosphere, seasonal color changes, polar ice caps, and "dust storms" on the Martian surface may be all explained by various molecules, compounds and complexes of permutations among iron, carbon, and oxygen. The atmosphere is almost certainly made of carbon dioxide along with dissociation products.

A seasonal chemical cycle closely explaining Lowell's color changes observed in 1903 as well as the "yellow dust clouds" may be written as follows:





This model is capable of laboratory test and would preclude even the most rudimentary life on Mars. (Abstract of a paper presented at the July 1966 meeting of the American Astronomical Society).

Connes, J., Connes, P., and Kaplan, L.D., 1966, Mars: New absorption bands in the spectrum: *Science*, V. 153, p. 739-740.

New absorption bands have been found in the near infrared by Fourier spectroscopy. They are tentatively identified as due to reduced gases in the Martian atmosphere.

Coulson, K.L., Gray, E.L., and Bouricius, G.M.B., 1966, Effect of surface reflection on planetary albedo: *Icarus*, V. 5, p. 139-148.

The intensity and polarization of the sunlight which would be directed to space from the top of a molecular atmosphere is computed for wavelengths of 4920 and 6430 Å, under the assumption that the surface material is either red clay soil or white quartz sand. It is shown that the most important component of the outward radiation is that which is due to solar radiation which has been transmitted directly downward through the atmosphere, reflected from the surface, and then transmitted directly back out through the atmosphere.

Davies, R.D., and Williams, D., 1966, Observations of the continuum emission from Venus, Mars, Jupiter, and Saturn at 21.2 cm wavelength: *Planetary and Space Science*, V. 14, No. 1, p. 15-32.

The effective brightness temperature at 21.2 cm wavelengths determined for the planets studied are: Venus,  $591 \pm 30^\circ\text{K}$ ; Mars,  $271 \pm 76^\circ\text{K}$ ; Saturn,  $286 \pm 37^\circ\text{K}$ . The brightness temperature from Venus does not vary significantly over the wavelength range 3-21 cm, which appears to indicate that this radiation comes from the surface of the planet. Polarization studies of the 21.2 cm emission from Jupiter showed a rotation period of  $9^{\text{h}}55^{\text{m}}29^{\text{s}}50 + 0^{\text{s}}29$ , in close agreement with the period of the decameter radiation. Possible emission mechanisms are discussed briefly.

Donahue, T.M., 1966, Upper atmosphere and ionosphere of Mars: *Science*, V. 152, p. 763-764.

For Mariner IV's occultation experiment it is deduced that the single-layer ionosphere at 125 km is on F1 region. The  $\text{CO}_2$  density must be about  $10^{11}$  molecules per cubic centimeter.

A model with an exospheric temperature of  $4000^\circ\text{K}$ , a modest degree of  $\text{CO}_2$  dissociation, and diffusive separation above 70 Km is possible.

Dryer, M., and Heckman, G.R., 1966, Application of the hypersonic analog to Mars' magnetic field: *Transactions of the American Geophysical Union*, V. 47, No. 1, p. 155-156.

The hypersonic analog, used to infer the upper limit of the Martian magnetic moment, is shown to have several implications regarding its application to earth. It is tentatively assumed that the 5-γ increase reported by the Mariner 4 magnetometer experiments was a shock wave indication on July 15, 1965, at 0123 UTE. A magnetopause model, based on Imp 1 data, is used with a magnetoacoustic Mach number of 3.8. It is concluded, on the basis of the limited preliminary data published thus far, that Mars' shock was possibly detected; if it is true,

$M_0/M_e \leq 2 \times 10^{-4}$ . Implied for further analog application is the use of the magnetoacoustic Mach number together with a specific heat ratio lower than the values of 2 and  $5/3$  used previously. (Abstract of a paper presented at the April 1966 meeting of the American Geophysical Union).

Dyce, R.B., 1966, Radar observations of Mars at 70 cm: Transactions of the American Geophysical Union, V. 47, No. 2, p. 427.

Pulse radar observations of the planet Mars were made over a seven-month period centered on the opposition of March 1965. The cross section was variable (3 to 13% of the geometrical area) and tended to be high when dark region of Mars passed under the radar reflection region. Spectral investigations have now shown that this effect may be attributed to a narrow bandwidth component superimposed on a relatively steady wideband component. Some crude deductions about the surface variability can be made. (Abstract of a paper presented at the April 1966 meeting of the American Geophysical Union).

Epstein, E.E., 1966, Disk temperatures of Mercury and Mars at 3.4 mm: The Astrophysical Journal, V. 143, p. 597.

Observations of Mercury and Mars were made in April 1965 at 3.4 mm (88 GHz). When all corrections have been applied, a temperature of  $190^\circ \pm 40^\circ\text{K}$  was arrived at for Mars. For Mercury the average values arrived at was  $220^\circ \pm 35^\circ\text{K}$ . The corresponding average illuminated fraction was 0.10.

Fish, F.F., Jr., 1966, The stability of goethite on Mars: Journal of Geophysical Research, V. 71, p. 3063-3068.

Polarization and visible and infrared reflectivity studies of Mars and of various minerals and rocks have been interpreted as implying that a significant part of the Martian surface material is finely divided limonite--a mixture of iron oxides and hydroxides--but principally the monohydrate, goethite. In this paper, the thermodynamic stability of goethite under Martian surface conditions is examined using the available experimental data. It is concluded that hematite ( $\text{Fe}_2\text{O}_3$ ) rather than goethite ( $\text{HFeO}_2$ ) is the stable form on the Martian surface.

Fjeldbo, G., Fjeldbo, W.C., and Eshleman, V.R., 1966, Models for the atmosphere of Mars based on the Mariner 4 occultation experiment: Journal of Geophysical Research, V. 71, p. 2307-2316.

Several possible atmospheric models are investigated based on data from the radio occultation experiment, and one is shown to be more likely than the others. Profiles in height of the constituent number densities, electron number density, temperature, pressure, and mass density are derived. The analysis indicates that Mars has a tenuous carbon dioxide lower atmosphere with a temperature of only about  $180^\circ\text{K}$  near the surface, and an atomic oxygen upper atmosphere with a temperature of only about  $80^\circ\text{K}$ . Frozen carbon dioxide particles may be an almost permanent feature of the atmosphere at intermediate altitudes. The main daytime ionospheric layer has its peak density at 120 km, and is most likely a Bradbury ( $\text{F}_2$ ) layer with the principal ion ( $\text{O}^+$ ) being lost through  $\text{O}^+ + \text{CO}_2 \rightarrow \text{O}_2^+ + \text{CO}$ . The atmospheric mass density decreases nearly ten orders of magnitude from the surface to the base of the exosphere at 140 km, thus remaining several orders of magnitude below the density of the earth's atmosphere at corresponding altitudes despite the lower gravity.

Fjeldbo, G., Fjeldbo, W.C., and Von Eshleman, R., 1966, Atmosphere of Mars: Mariner IV models compared: Science, V. 153, p. 1518-1523.

Three classes of models for the atmosphere of Mars differ in identifying the main ionospheric layer as being a  $F_2$ ,  $F_1$  or E layer. Theory and observations are in best agreement with an  $F_2$  model. An  $F_1$  model is possible if photo-dissociation is much less than what expected. The E model appears unlikely, as it requires unlikely assumption about the values and changes with height of the effective recombination coefficient and the average ion mass.

Gray, L.D., 1966, Transmission of the atmosphere of Mars in the region of  $2\mu$ : Icarus, V. 5, p. 390-398.

The random Elsasser band model is used to compute the transmission of the atmospheres of earth and Mars for the  $2\mu$  bands of carbon dioxide. Comparison of calculated values for transmission of sunlight through both atmospheres indicates that  $mp_0 = 500 \pm 100$  meter-atm mbar where  $m$  is the amount of  $CO_2$  in one air mass and  $p_0$  is the "effective" surface pressure. For  $m_0 = 60$  to  $85$  meter-atm, the above value of  $mp_0$  leads to  $p_{s0} = 7.1 \pm 2.2$  mbar for the surface pressure of the Martian atmosphere.

Gross, S.H., McGovern, W.E., and Rasool, S.I., 1966, Mars: Upper atmosphere: Science, V. 151, p. 1216-1221.

The thermal structure of the Martian upper atmosphere is theoretically calculated to be pure  $CO_2$  with a temperature between 4000K and 7000K.

Harrison, A.E., 1966, Stereo visualization techniques: Transactions of the American Geophysical Union, V. 47, No. 4, p. 629.

An exaggerated - stereo model is useful as a means of enhancing visual experience and improving the interpretation of the terrain being examined. The ideas are most useful when interpreting horizontal photography with short baselines and an excess of visual clues, but are also applicable to vertical aerial photography, moon photography and the Mariner photographs of Mars. Interchanging the left and right pictures produces an "inside-out" stereo view, which is often quite useful in suppressing the ordinary visual clues and emphasizing the parallax information needed for producing the stereo model. When the Mariner photographs are viewed in this manner, the bottom of a Martian crater appears as a flat, round plateau with sloping edges. (Abstract of a paper presented at the September 1966 meeting of the American Geophysical Union).

Harrison, H., 1966, Metastable oxygen atoms and Martian model atmospheres: Transactions of the American Geophysical Union, V. 47, No. 4, p. 629.

If one starts with a set of chemical equations, their kinetic orders and rates, the approximation of photochemical steady-state, and some boundary values for temperature and composition, it is a straight-forward exercise to calculate vertical distribution profiles for the chemical species expected on Mars. The value of the resulting model depends crucially upon the completeness of the set of reactions; to omit an important one is ruinous. The photolysis of  $CO_2$  in the uv may, or may not, yield oxygen atoms in the metastable  $^1S$  and  $^1D$  electronic states. The evidence and arguments are discussed. If produced, these metastables may fluoresce, quench, or react. A model atmosphere is constructed that includes these processes and the effects of their rather large rate uncertainties; an estimate is made of their contribution to the Martian dayglow. (Abstract of a paper presented at the September 1966 meeting of the American Geophysical Union).

Hartmann, W.K., 1966, Lunar basins, lunar lineaments, and the moon's far side: Sky and Telescope, V. 32, p. 128-131.

The author reviews the evidence from the Zond 3 probe and concludes that the pre-mare basins, thalassoids, and the craters are all genetically the same. Thalassoids, large basins with heavily cratered floors, are interpreted as unflooded mare-like basins. The author believes the radial systems surrounding the maria to be tectonic structures created by impact explosions.

The grid system of the moon and the marginally detectable grid systems of the earth and Mars are attributed to planetary rotation.

Hartmann, W.K., 1966, Martian cratering: Communications of the Lunar and Planetary Laboratory, V. 4, No. 65, p. 121-131.

Independent counts of Martian and lunar craters are used in a new analysis of the Mariner IV records.

The observations suggest that there has been substantial erosion on Mars and that fundamental conclusions about Mars erosion history cannot be drawn from the ages of the large craters only.

Hartmann, W.K., 1966, Martian cratering: Icarus, V. 5, p. 565-576.

New counts of Martian and lunar craters are used in a new analysis of the Mariner IV photographs. The difference in impact velocities on the two planets, neglected by other authors, is found to introduce an appreciable effect. The age of a Martian surface layer capable of retaining craters larger than 50-km diameter is found to be about  $4 \times 10^9$  years, within a factor of about 2. The crater retention time for a structure of about 1-km diameter is estimated to be on the order of  $10^9$  years, and it appears that an erosive process flattens large-scale relief at a rate of about  $10^{-4}$  cm/year.

Horowitz, N.H., 1966, The search for extraterrestrial life: Science, V. 151, p. 789-792.

Present knowledge on the Martian environment and on the origin of the planets does not preclude the possibility of Martian life.

Hughes, M.P., 1966, Planetary observations at a wavelength of 6 cm: Planetary and Space Science, V. 14, No. 10, p. 1017-1022.

Radiometric measurements of Venus at a wavelength of 6 cm made in the period from November 1965 through March 1966 indicate that the disk temperature reached a minimum of  $630 \pm 30^\circ\text{K}$  soon after inferior conjunction. An observation of Mars near opposition in 1965 gave a disk temperature of  $190 \pm 60^\circ\text{K}$ , the same as that reported by Kellermann. The disk temperature of Jupiter remained essentially constant at  $291 \pm 25^\circ\text{K}$  from March 1965 through March 1966. Saturn was found to have a disk temperature of  $190 \pm 45^\circ\text{K}$ , which is slightly higher than anticipated.

Kellermann, K.I., 1966, The thermal radio emission from Mercury, Venus, Mars, Saturn, and Uranus: Icarus, V. 5, p. 478-490.

No appreciable phase variation was found in the 11-cm radiation from Mercury, indicating that there is little temperature difference between the illuminated and dark hemispheres. The effective surface temperature at 11 cm is between  $250^\circ$  and  $300^\circ\text{K}$ .

The observations of Venus indicate a slight decrease in effective temperature from about  $600^\circ\text{K}$  at centimeter wavelengths to about  $500^\circ\text{K}$  at decimeter wavelengths. Little or no change with phase angle was found in the apparent temperature at 11 cm.



Observations of Mars at 6, 11, and 21 cm indicate effective temperatures near 200°K, in good agreement with the infrared measurements.

The apparent temperature of Saturn was found to increase at longer wavelengths, reaching nearly 200°K at 11 cm and 300°K at 21 cm.

Uranus was found to have an equivalent temperature of  $1300 \pm 400$  K at 11 cm which, like Saturn, is about twice that expected from solar heating.

Kutuza, B.G., Losovskii, B.Ya., and Salomonovich, A.E., 1966, Observations of the radio emission of Mars at 8 mm: Soviet Astronomy - A.J., V. 10, No. 1, p. 190-191.

Results of observations of radio emission from Mars at 8-mm wavelength which were made with the PT-22 radio telescope at the Institute of Physics in March 1965 are given. The brightness temperature averaged over the visible disk is  $225 \pm 10$  K.

Leighton, R.B., and Murray, B.C., 1966, Behavior of carbon dioxide and other volatiles on Mars: Science, V. 153, p. 136-153.

It is concluded that the polar caps consist of frozen  $\text{CO}_2$ . This study was based on the following points: 1)  $\text{CO}_2$  is a major constituent of the Martian atmosphere; 2) The blanketing effects of the atmosphere is small; 3) Heat transport by the atmosphere is small; 4) The far infrared emissivity of Martian soil and solid  $\text{CO}_2$  are near unity; 5) In the visible the reflectivity of Mars is 0.15, and of frozen  $\text{CO}_2$  is 0.65; 6) Water is a minor constituent of the Martian atmosphere.

Leovy, C., 1966, Mars ice caps: Science, V. 154, p. 1178-1179.

Minimum atmospheric temperatures required to prevent  $\text{CO}_2$  condensation in the Mars polar cap are higher than those obtained from a computer experiment designed to simulate general circulation in the Mars atmosphere.

Leovy, C., 1966, Note on thermal properties of Mars: Icarus, V. 5, p. 1-5.

The variation of infrared emission from the surface of Mars with local time on Mars is here interpreted in terms of a simplified theory of diurnal temperature variations, in which the effect of the atmosphere is included. The results suggest a very low thermal conductivity for the upper few centimeters of the Martian ground. Such low conductivities appear to be possible only if the material composing these layers is very fine powder having a characteristic size of not more than a few microns.

McCall, G.J.H., 1966, Implication of the Mariner IX photography of Mars: Nature, V. 211, p. 1384-1385.

The author contends that the unresolved controversy concerning the formation of craters has simply been extended from the moon to Mars by the Mariner IX probe. Various authors assessing the data have reached the conclusion that the craters on Mars were formed by hypervelocity impact rather than volcanism. The present paper discusses the evidence for volcanism rather than impact being the cause of the Martian cratering.

Miyamoto, S., 1966, Martian atmosphere and crust: Icarus, V. 5, p. 360-374.

It is shown that we can derive some knowledge about surface relief indirectly from cloud observations. In the Martian summer, energy flows from the summer hemisphere to the winter hemisphere and the prevailing wind over middle latitudes turns from spring westerlies to summer easterlies. Crater morphology revealed by

the Mariner IV photographs suggests that craters are one of the characteristic features of the original crust of terrestria-type planets, and that Martian deserts and maria correspond to the terra and maria of the moon and the continents and oceans of our earth, respectively. Canals are interpreted as tectonic lines. It may be shown how wind erosion destroys most of the tectonic lines but develops some of them into canals when they are properly located along the courses of vapor migration.

Neubauer, F.M., 1966, Thermal convection in the Martian atmosphere: *Journal of Geophysical Research*, V. 71, p. 244-245.

Formation of dust clouds observed in the Martian atmosphere can be explained by the action of dust devils larger than 100 meters in diameter. The condition for the onset of thermal convection is the existence of an unstable temperature profile. The daily variation of the atmospheric temperature profile shows that the Martian atmosphere is more favorable for the initiation of dust devils than the earth's atmosphere. The calculations indicate that dust devils on Mars produce wind velocities only slightly lower than those on earth.

Norton, R.B., Ferguson, E.E., Fehsenfeld, F.C., and Schmeltekopf, A.L., 1966, Ion-neutral reactions in the Martian ionosphere: *Planetary and Space Science*, V. 14, No. 10, p. 969-978.

A number of reactions that might be important in the Martian ionosphere have been studied and their rate coefficients have been measured with a pulsed flowing afterglow system. One of the most important of these is  $O^+ + CO_2 \rightarrow O_2 + CO$ , which has a rate coefficient of about  $10^{-10} \text{ cm}^3 \text{ sec}^{-1}$ . The ion chemistry is discussed and model ionospheres are constructed and compared with the Mariner IV electron concentration. Two interpretations seem possible: (1) the ions are mostly atomic (probably  $O^+$ ) and the peak electron concentration occurs at a neutral concentration of about  $10^9 \text{ cm}^{-3}$ , and (2) the ions are mostly molecular (possibly with  $O_2^+$  dominant) and the peak electron concentration occurs at a neutral concentration of about  $5 \times 10^{10} \text{ cm}^{-3}$ . The atomic ion model implies a rather low temperature which may prove to be a problem. The molecular ion model requires the neutral atmosphere to be mostly molecular near the electron density maximum which would probably indicate that mixing is important to greater altitudes than previously assumed.

Oncley, P.B., and Fulmer, C., 1966, The Martian "Canali" as meteoritic crater rays: *Transactions of the American Geophysical Union*, V. 47, No. 3, p. 482.

The Mariner 4 photographs have brought awareness of the role of crater-forming impacts in the history of the surface of Mars. In hindsight, lunar photographs, whose resolution has been degraded to compare with astronomical images of Mars, show a distinct similarity between the lunar rayed craters and the Martian "oases" and "canali". Possible explanations are presented for the fact that the Martian markings are darker than the general albedo, while the lunar rays are lighter. Certain implications are drawn concerning the composition and nature of the Martian surface. (Abstract of a paper presented at the September 1966 meeting of the American Geophysical Union).

Öpik, E.J., 1966, The Martian surface: *Science*, V. 153, p. 255-265.

A volcanic origin of the Martian craters is to be completely excluded. Craters larger than 20 km survived erosion from the beginning of the Martian surface, therefore a dense atmosphere never existed. The large amplitude in temperature indicates that the upper soil is of a porous, unconsolidated structure. Survival of vegetation, if it exists, must depend on the low nighttime temperature and deposition of hoarfrost, which could melt to droplets after sunrise, before evaporating. The "canals" may be cracks in the crust, radiating from the point

of impact. Limb darkening of the planet in green, yellow and red light indicates absorption by atmospheric haze, aerosols, and dust.

Ottermann, J., and Bronner, F.E., 1966, Martian wave of darkening: A frost phenomenon: *Science*, V. 153, p. 56-60.

It is suggested that the optical darkening is due to microrelief features caused by frost.

Owen, T., 1966, The composition and surface pressure of the Martian atmosphere: results from the 1965 opposition: *Astrophysical Journal*, V. 146, p. 259-270.

Observations of the photographic spectrum of Mars obtained at the most recent opposition in March 1965, are presented and discussed. The absence of any trace of the  $\text{NO}_2$  absorption at  $4480\text{\AA}$  confirms previous upper limits set on the abundance of this gas. Observations of the weak  $\text{CO}_2$  bands at  $8689\text{\AA}$  and  $10488\text{\AA}$  lead to a derivation of  $65 \pm 20$  m-atm for the abundance of  $\text{CO}_2$  in the Martian atmosphere. This abundance is used with new observations of the strong  $\text{CO}_2$  bands at  $1.6\mu$  made by Kuiper to derive a value for the surface pressure of 9 mb. The uncertainty in this determination ranges from 5 to 20 mb, the lower values being considered most probable. A discussion of these results in the context of the origin and development of the Martian atmosphere suggests that, with the exception of water vapor, the present atmospheric composition may be very similar to that of the primitive, outgassed terrestrial atmosphere.

Robinson, J.C., 1966, Ground-based photography of the Mariner IV region of Mars: *Icarus*, V. 5, p. 245-247.

The large "desert" area between longitudes  $90^\circ$  and  $240^\circ$  was partially obscured during the greater part of the 1965 apparition. The Mariner IV probe photographed the western limits of this region, where the haze tended to clear off by noon of each day, reforming in late afternoon. Surface features in this region include a number of oases and canals. The large Proponitis I oasis was found to be considerably further south than expected.

Ronca, L.B., 1966, Meteoritic impact and volcanism: *Icarus*, V. 5, p. 515-520.

The possibility of volcanism triggered by meteoritic impact is analyzed theoretically by comparing volcanological and impact data. Field data on some terrestrial craters are also discussed. The conclusion is that volcanism triggered or localized by impact is possible. The hypothesis is proposed that lunar craters represent a spectrum of craters ranging from completely meteoritic craters, through meteoritic craters modified by volcanism, to completely volcanic craters. The data on Mars are meager, but suggest that Martian craters may owe their origin to the same processes.

Sagan, C., and Pollack, J.B., 1966, An inorganic model of Martian phenomena: *The Astronomical Journal*, V. 71, p. 178.

Recent work showing that the optical detection of life on earth over inter-planetary distances is extremely difficult has led us to re-examine the Martian seasonal changes and related phenomena, to see whether plausible inorganic models explaining these observations can be devised. We assume that the entire planet, except for the polar caps, is covered with a layer of pulverized limonite, with mean particle dimensions  $\sim 0.1$  mm, in accordance with polarimetric and spectrometric observations. Elevation differences will lead to a particle size segregation, as suggested by Rea. The smaller particles will be preferentially present in the lowlands. The visible reflectivity of the highlands, with relatively more large particles, will be less. If the lowlands have mean particle sizes  $\sim 0.3$  that of the

highlands, the average reflectivity differences between Martian bright and dark areas can be understood; but the dark areas must have systematically higher elevations. Wind patterns, which are expected to change markedly with the seasons, will force greater periodic variations in mean particle size for the windswept highlands than for the lowlands, as is the case in some terrestrial deserts. This particle size modulation can account quantitatively for the observed seasonal variation in albedo and polarization. The model also explains in a straightforward manner the secular changes, the "blue haze", the blue clearings, and the relatively high radar reflectivity of the Martian dark areas. Since it assumes only winds, pulverized limonite, elevation differences and dust storms, we believe the model is promising; but while providing an inorganic explanation of gross Martian phenomena previously attributed to life, it does not of course in any way exclude life on Mars. (Abstract of a paper presented at the December 1965 meeting of the American Astronomical Society).

Sagan, C., and Pollack, J.B., 1966, Elevation differences on Mars: Special Report No. 224, Smithsonian Astrophysical Observatory, Cambridge, Massachusetts.

Observations of apparent frost phenomena occurring preferentially in the Martian bright areas has, in the past, led to the conclusion that the bright areas are elevations. From the quasi-specular component of the radar power reflectivity, and from the radar Doppler spectra, both as a function of the Martian longitude, the Martian dark areas are now found to have systematically higher elevations than the adjacent bright areas. Mean slopes of a few degrees are deduced, and elevation differences up to 17 km are inferred. These results may help to explain the discrepancy between the dynamical and the optical oblateness of Mars as well as the discrepancy between ground-based infrared spectrometric and Mariner 4 occultation values of Martian surface pressures.

Sagan, C., and Pollack, J.B., 1966, Elevation differences on Mars: The Astronomical Journal, V. 71, p. 869.

Observations of apparent frost phenomena, occurring preferentially in the Martian bright areas, have in the past led to the conclusion that the bright areas are elevations. The argument hinges on the implicit assumption that near midday highlands should be at lower temperatures than lowlands. On the earth this assumption is valid, because of adiabatic cooling of rising air, a diminished greenhouse effect, and a greater inclination of surfaces to the sun's rays for highlands than for lowlands. It is shown that these factors are unlikely to be important on Mars, and that the polar cap recession data, in particular, suggest that the dark areas are highlands.

From the quasi-specular component of the radar power reflectivity, and from the radar Doppler spectra, both as a function of Martian longitude, the Martian dark areas are found to have systematically higher elevations than the adjacent bright areas (Sagan, C., Pollack, J.B., and Goldstein, R.M., to be published). This evidence is reviewed. Slopes of a few degrees are deduced, and elevation differences up to 17 km are inferred. The picture of Mars which emerges is similar to that expected for the earth if oceans were removed, water erosion non-existent, and the relief amplified by the ratio of the gravitational accelerations on the two planets. These results may bear on the discrepancies between ground-based spectrometric and Mariner IV occultation values of Martian surface pressure, and on those between the optical and dynamical oblateness of Mars. They suggest that pressures ~20 mbar are typical of the centers of bright areas, while 6 mbar is a typical dark area pressure. (Abstract of a paper presented at the July 1966 meeting of the American Astronomical Society).

Sagan, C., and Pollack, J.B., 1966, On the nature of the canals of Mars: Nature, V. 212, p. 117-121.

In the light of the new evidence supplied by the Mariner IV photographs and radar Doppler spectroscopic results at 12.5 cm, the authors review and discuss all the proposed theories concerning the Martian canals. They suggest that the canals are ridge systems or associated mountain chains in analogy to similar linear features found in the terrestrial ocean basins, in particular, such as mid-Atlantic ridge, and explain their seasonal variability in terms of scouring of fine particles in one season and deposition in another.

Sagan, C., Pollack, J.B., and Goldstein, R.M., 1966, Radar Doppler spectroscopy of Mars. I. Elevation differences between bright and dark areas: Special Report No. 221, Smithsonian Astrophysical Observatory, Cambridge, Massachusetts.

From the quasi-specular component of the radar power reflectivity as a function of Martian longitude, and from radar Doppler spectra also as a function of longitude, the Martian dark areas have been found to have systematically higher elevation than the adjacent bright areas. Slopes of a few degrees are deduced, and elevation differences up to a few km are inferred. These slopes and elevations are similar to those expected for the earth if oceans and water erosion were removed and the acceleration due to gravity decreased by a factor of 2.5. It is further found that some areas that characteristically undergo marked secular changes have very shallow slopes ( $1-2^\circ$ ) and elevations  $\sim 6$  km; classical canals have steeper slopes ( $>4^\circ$ ) but elevations of the same order; and large dark areas such as Syrtis Major and Moeris Locus may have elevations between 10 and 20 km.

Salisbury, J.W., 1966, The light and dark areas of Mars: *Icarus*, V. 5, p. 291-298.

Evidence provided by Mariner, together with evidence from other sources, indicates that the bulk of the surface material in light areas is probably pulverized Martian crustal rock. Where this material has been exposed on the surface for long periods of time, even the tenuous Martian atmosphere is expected to produce surficial chemical weathering.

A review of the various hypotheses which have been advanced to explain the origin of the dark areas indicates that both organic and non-organic hypotheses are consistent with the observations. It is suggested that internal water might play an important role in the creation of dark areas, through either organic or non-organic means. It appears, lacking conclusive evidence for any darkening mechanism, that still more alternative hypotheses might usefully be sought.

Shawhan, S.D., 1966, Ionization rate and electron density profile for the Martian ionosphere based on Mariner 4 observations: *Transactions of the American Geophysical Union*, V. 47, No. 2, p. 427.

Several properties of the Martian atmosphere and ionosphere as deduced from the Mariner 4 occultation experiment are used with Chapman ionized layer theory to calculate an ionization rate and an electron density profile for the Martian ionosphere. From the observed surface number density ( $1.9 \times 10^{17}$  mol  $\text{cm}^{-3}$ ) and surface temperature (1800K), assuming that  $\text{CO}_2$  is the major constituent in the lower atmosphere, an ion production profile is calculated for solar radiation between 10 angstroms and 850 angstroms for two models. Agreement is noted with the preliminary analysis of Mariner 4 data for both models. An electron density profile is presented assuming a constant radiative recombination coefficient of  $1.75 \times 10^{-7}$   $\text{cm}^3 \text{sec}^{-1} \text{ion}^{-1}$ . (Abstract of a paper presented at the April 1966 meeting of the American Geophysical Union).

Simpson, J.F., 1966, Additional evidence for the volcanic origin of lunar and Martian craters: *Earth and Planetary Science Letters*, V. 1, No. 3, p. 132-134.

This paper points out the similarity in frequency distribution of lunar and Martian craters with terrestrial volcanic craters, and the dissimilarity of these groups with terrestrial meteoritic craters. Surface density effects are also considered. The results of the study favor a volcanic origin of the bulk of the Martian and lunar craters.

Simpson, J.F., 1966, Evidence for the volcanic origin of lunar and Martian craters: *Earth and Planetary Science Letters*, V. 1, No. 3, p. 130-131.

This letter points out the relationship existing in the percentage distribution of crater diameters on the moon and Mars, which appears remarkably similar when normalized to uniform gravity. Crater diameters should vary approximately inversely with the value of  $g$  for any given cosmic body because for a given gas pressure the volume of rock removed will be a function of its weight (which is dependent on  $g$ ). This effect is enhanced by the tendency toward higher porosity and lower density of vesicular extrusive rocks formed at the surface in a low gravity environment. The percentage distribution of craters greater than 3 km in diameter is approximately 3.15 as large for lunar craters than for Martian craters.

Smith, N., and Beutler, A.E., 1966, A model Martian atmosphere and ionosphere: *Transactions of the American Geophysical Union*, V. 47, No. 1, p. 156.

The results of the Mariner 4 experiment indicate that  $\text{CO}_2$  is probably the only significant constituent of the lower Martian atmosphere. Assuming this, we have derived an equilibrium model atmosphere and ionosphere of Mars for the subsolar region and at sunspot maximum. A temperature profile resulted from consideration of radiation balance between the troposphere and mesosphere, vibrational relaxation of  $\text{CO}_2$ , and the heat released by photodissociation and ionization processes. The resulting ionosphere is bimodal, the lower peak being predominantly  $\text{O}_2^+$ . The upper peak, predominantly  $\text{O}^+$ , is due to the transition between chemical and diffusive equilibrium, and may thus be considered an  $\text{F}_2$  peak. The difference between this ionosphere and that observed by Mariner 4 can be resolved by considering a rapid decay of the  $\text{F}_2$  peak with increasing solar zenith angles, due in part to an expected decrease in temperature and in part because  $\text{O}^+$  decreases much more rapidly than  $\text{O}_2^+$  with decreasing ionizing flux density. (Abstract of a paper presented at the April 1966 meeting of the American Geophysical Union).

Smith, W.B., Shapiro, I.I., and Ash, M.E., 1966, Preliminary results from processing radar and optical planetary observations: *The Astronomical Journal*, V. 71, p. 871-872.

Preliminary values of a number of astronomical constants have been obtained from the simultaneous processing of planetary radar data spanning the interval from 1959 to July 1966 and of U.S. Naval Observatory optical data extending from 1950 to 1965. Results obtained using general relativity (Newtonian) theory with their formal standard errors are: a.u., 499.004786 (499.004785)  $\pm$  0.000005 light-sec; Mercury radius, 2434 (2440)  $\pm$  2 km; Venus radius, 6056 (6055)  $\pm$  1 km; Mercury mass, 6021000 (6029000)  $\pm$  53000; Venus mass, 408250 (408450)  $\pm$  120; earth plus moon mass, 328900 (328950)  $\pm$  60; Mars mass, 3111000 (3107000)  $\pm$  9000; earth-moon mass ratio, 81.3030 (81.3024)  $\pm$  0.005. The planetary masses are given as inverses in terms of the solar mass. (Abstract of a paper presented at the July 1966 meeting of the American Astronomical Society).

Spinrad, H., Schorn, R.A., Moore, R., Giver, L.P., and Smith, H.J., 1966, High-dispersion spectroscopic observations of Mars I. The  $\text{CO}_2$  content and surface pressure: *Astrophysical Journal*, V. 146, p. 331-338.

From high-dispersion infrared McDonald and Lick Observatories' spectrograms of Mars we have determined a  $\text{CO}_2$  abundance of  $90 \pm 27$  (estimated error) m-atm (STP)



at 200°K, chosen as a representative lower-atmosphere temperature. The weak  $5_{\mu}$   $\text{CO}_2$  lines near  $\lambda 8700 \text{ \AA}$  are used. An abundance of 90- m-atm of  $\text{CO}_2$  gives a surface partial pressure of 6.6 mb. The observation and reductions are discussed.

By comparing the weak-line  $\text{CO}_2$  abundance with Sinton's and Kuiper's measures of the saturated 1.6- and 2.0- $\mu$  bands a total surface pressure of  $P_s = 8 \pm 4$  (estimated error) mb from the 1.6- $\mu$  band and  $P_s = 16 \pm 8$  mb from the 2.0- $\mu$  band is found. The technique of analyses follows Kaplan, Munch, and Spinrad and Owen and Kuiper. The lower pressure (1.6- $\mu$  data) is to be preferred. A compromise value is  $P_s = 10 \pm 5$  mb. The result is compared to the Mariner IV occultation data which yield  $P_s = 5$  or 6 mb if the temperature of the lower Martian atmosphere is 180°K. The difference in surface pressure is not substantial; the occultation results coupled with our  $\text{CO}_2$  abundance suggest an almost pure  $\text{CO}_2$  atmosphere for Mars.

Tolbert, C.W., 1966, Observed millimeter wavelength brightness temperatures of Mars, Jupiter, and Saturn: The Astronomical Journal, V. 71, p. 30-32.

Analyses of observations of 35, 70, and 94 Gc radiation from Mars, Jupiter, and Saturn made with a 16-ft. antenna yield brightness temperatures for Mars of  $230(+42, -42)^{\circ}\text{K}$  and  $240(+72, -48)^{\circ}\text{K}$  at 35 and 94 Gc, respectively; for Jupiter,  $113(+11, -11)^{\circ}\text{K}$ ,  $105(+18, -12)^{\circ}\text{K}$  and  $111(+22, -11)^{\circ}\text{K}$  at 35, 70, and 94 Gc, respectively. The antenna temperatures from which the brightness temperatures were calculated were obtained by averaging the responses of right ascension scans of the antenna beam across the planets. The observing and data reducing techniques are herein described and the averaged antenna temperatures shown.

Tombaugh, C.W., 1966, Evidence that the dark areas on Mars are elevated mountain ridges: Nature, V. 209, p. 1338.

The author cannot reconcile the statement that the dark areas are elevated land, and states that the total of all the operative effects, and the limitation of detail under the best seeing conditions, makes an abrupt topographic difference of 20,000 ft. or less impossible to detect. He considers his earlier suggestion that the round dark oases represent asteroid impact craters is confirmed by the Mariner 4 pictures.

Tull, R.G., 1966, The reflectivity spectrum of Mars in the near-infrared: Icarus, V. 5, p. 505-514.

Spectral scans have been obtained of Mars and a region on the moon in the range 0.5 $\mu$  to 1.2 $\mu$  at the 82-inch telescope. The monochromatic Russell-Bond albedo is found to rise to a maximum of 39% at 0.8 $\mu$ . A shallow minimum occurs near 1 $\mu$ , followed by a rise to 49% at 1.52 $\mu$ . Apparently the albedo is still rising at 1.52 $\mu$ . The radiometric albedo is found to be 0.287.

Earlier conclusions that the surface layer of Mars consists largely of limonite are not inconsistent with these observations, as indicated by laboratory reflectivity spectra.

Younkin, R.L., 1966, A search for limonite near-infrared spectral features on Mars: The Astrophysical Journal, V. 144, p. 809, 818.

Previous authors have found limonite to be the only mineral whose polarization, color, and albedo duplicate those of the bright areas of Mars in the visual spectral region. Recent measurements of spectral reflectance show in the near-infrared that powdered limonite exhibits two characteristics, a wide-band absorption with minimum reflectance in the 8200-9500  $\text{\AA}$  region and, just beyond

this absorption, a rise in reflectance.

Spectrophotometric measurements from 0.5 to 1.1  $\mu$  have been made at Mount Wilson of the integral intensity of the disk of Mars and of a bright area and a dark area. Comparison of the intensities of the two areas gives no indication of any difference in limonite content. The integral intensity has been reduced to relative reflectance by means of the energy distribution of  $\alpha$  Lyr, and independently it has been compared directly to the intensity of the lunar crater Plato. An upper limit of 2 per cent may be placed on the strength of the limonite spectral features in the reflectance of Mars.

### 3.7.5 Mercury

Aronson, J.R., Emslie, A.G., Allen, R.V., and McLinden, H.G., 1966, Far infrared studies of minerals for application in remote compositional mapping of the moon and planets: Transactions of the American Geophysical Union, V. 47, No. 1, p. 155.

The surface composition of the moon and planets, such as Mars and Mercury, with tenuous atmospheres can be measured remotely by infrared reflectance and emittance spectroscopy over a broad range of frequencies. The information in the far infrared region (50-667  $\text{cm}^{-1}$ ) is especially informative as to specific mineral composition, and is very desirable in order to disentangle the composite spectra resulting from complex mixtures. Experimental studies of far infrared spectra, at room and cryogenic temperatures, of possible lunar and planetary surface minerals have been performed. Theoretical and experimental studies of the factors that control spectral contrast in the spectra of particulate surfaces and of the kind of mixing rules that must be used to disentangle the spectra of composite surfaces have been made. (Abstract of a paper presented at the April 1966 meeting of the American Geophysical Union).

Colombo, G., and Shapiro, I., 1965, The rotation of the planet Mercury: Astrophysical Journal, V. 145, p. 296-307.

Reliable radar observations and some of the generally unreliable optical observations of Mercury are consistent with its rotating in a direct fashion with a period just two-thirds of its orbital period. This possibility may be understood as a consequence of the combined solar torques exerted on tidal deformations and on a permanent asymmetry in Mercury's equatorial plane, as suggested by Colombo. A simple model illustrating this superharmonic resonance phenomenon is developed in some detail; several alternative paths by which Mercury could have reached its present state of motion are discussed briefly.

Cruikshank, D.P., 1966, Possible luminescence events on Mercury: Nature, V. 209, p. 701.

The author has carefully observed fluctuations in intensity of portions of the surface of Mercury. Because of the short period of these fluctuations he suggests that, because of the great similarities between the moon and Mercury (pointed out by many investigators), and the probable luminescence phenomena on the moon, it may be possible to interpret changes on Mercury as the effects of luminescence of the surface materials.

Epstein, E.E., 1966, Mercury: Anomalous absence from the 3.4 millimeter radio emission of variation with phase: Science, V. 151, p. 445-447.

No significant variations with phase were noticed on the 3.4 millimeter emission of Mercury. Brightness temperature was calculated to be only about 200°K.

Epstein, E.E., 1966, Mercury: Anomalous absence of a variation with phase in the 3.4 mm radio emission: *The Astronomical Journal*, V. 71, p. 161.

The dark-side brightness temperature of  $220 \pm 35^\circ\text{K}$  which we recorded at 3.4 mm (88 GHz) during the April 1965 inferior conjunction of Mercury and the brightness temperatures recorded at longer wavelengths led us to expect a large variation with phase in the 3-mm emission of Mercury. This expectation was based on the assumption that Mercury's surface layers behave as do those of the moon. We made observations on 34 days at 3.4 mm with the 15-ft., 3 arc min beamwidth antenna of the Space Radio Systems Facility of Aerospace Corporation from 16 July through 17 October 1965; these observations cover almost a complete revolution of Mercury. We also made frequent observations of Venus and Jupiter to verify the overall system reliability. In addition, special observations indicated that there were no detectable effects in the Mercury data due to antenna sidelobe reception of solar radiation.

The Mercury brightness temperatures were only  $\approx 200^\circ\text{K}$ , even when as much as 95% of the illuminated hemisphere was visible, and exhibited no significant variation with phase. (Abstract of a paper presented at the December 1965 meeting of the American Astronomical Society).

Epstein, E.E., 1966, Disk temperatures of Mercury and Mars at 3.4 mm: *The Astrophysical Journal*, V. 143, p. 597.

Observations of Mercury and Mars were made in April 1965 at 3.4 mm (88 GHz). When all corrections have been applied, a temperature of  $190^\circ \pm 40^\circ\text{K}$  was arrived at for Mars. For Mercury, the average values arrived at was  $220^\circ \pm 35^\circ\text{K}$ . The corresponding average illuminated fraction was 0.10.

Goldreich, P., and Peale, S.J., 1966, Resonant spins in the solar systems: *Transactions of the American Geophysical Union*, V. 47, No. 1, p. 155.

The effects of gravitational torques on spinning non-axisymmetric planets and satellites are investigated in detail. A stability criterion is derived for the maintenance of a planetary or satellite spin angular velocity which is commensurate with its mean motion. Spin angular velocities that are half and whole integral multiples of orbital angular velocities are shown to be stable for even very slight deviations from axial symmetry. An analytical method is developed for determining the probability of a planet's or satellite's being captured into such a resonant spin state, as the spin is decreased by tidal friction. The dependence of this capture probability on orbital eccentricity is also discussed. Numerical results are given for Mercury and the moon. A similar analysis gives a stability criterion for a Venusian spin that is resonant with the synodic motion of Venus. (Abstract of a paper presented at the April 1966 meeting of the American Geophysical Union).

Jefferys, W.H., 1966, Rotation of the planet Mercury: *Science*, V. 152, p. 201-202.

It is shown that it is possible for Mercury's rotation to be locked into a 2:3 resonance with its revolution.

Kellermann, K.I., 1966, The thermal radio emission from Mercury, Venus, Mars, Saturn, and Uranus: *Icarus*, V. 5, p. 478-490.

No appreciable phase variation was found in the 11-cm radiation from Mercury, indicating that there is little temperature difference between the illuminated and dark hemispheres. The effective surface temperature at 11 cm is between  $250^\circ$  and  $300^\circ\text{K}$ .

The observations of Venus indicate a slight decrease in effective temperature from about 600°K at centimeter wavelengths to about 500°K at decimeter wavelengths. Little or no change with phase angle was found in the apparent temperature at 11 cm.

Observations of Mars at 6, 11, and 21 cm indicate effective temperatures near 200°K, in good agreement with the infrared measurements.

The apparent temperature of Saturn was found to increase at longer wavelengths, reaching nearly 200°K at 11 cm and 300°K at 21 cm.

Uranus was found to have an equivalent temperature of  $130^{\circ} \pm 40^{\circ}\text{K}$  at 11 cm which, like Saturn, is about twice that expected from solar heating.

Laslett, L.J., and Sessler, A.M., 1966, Rotation of Mercury: *Science*, V. 151, p. 1384-1385.

The rotation of Mercury is shown to be explainable by the dynamics of a rigid ellipsoidal planet.

Liu, Han-Shou, 1966, The libration of Mercury: *Journal of Geophysical Research*, V. 71, p. 3099-3100.

As a follow-on to a previous analysis of the resonance-locked rotation of Mercury, the author presents the numerical solution of the librational motion.

Plagemann, S., 1965, A model of the internal constitution and temperature of the planet Mercury: *Journal of Geophysical Research*, V. 70, p. 985-993.

The internal structure of Mercury is assumed to be similar to that of the earth. A review of the astronomical data gives the mean radius as 2446 km and the mean density as 5.31 g/cm<sup>3</sup>. Mercury must thus have both a core and a mantle. An iterative procedure gives a core radius of 2112 km. The pressure, density, and gravity are calculated for a small mantle and core. Numerical integration of the equation of hydrostatic equilibrium yields 7.37 g/cm<sup>3</sup> as the density and  $0.327 \times 10^{12}$  dynes/cm<sup>2</sup> as the pressure at the center of the planet. From the structural model of Mercury the temperature distribution in the interior is calculated. Two extreme values of the temperature are calculated because of the uncertainty in the heat generation and thermal conductivity terms. The highest temperature (1380°K) occurs on the sunward side of Mercury at the core-mantle boundary. This indicates that neither the core nor the mantle is molten.

Sagan, C., 1966, The photometric properties of Mercury: *The Astrophysical Journal*, V. 144, p. 1218, 1221.

The striking similarities between photometric properties of surfaces of Mercury and the moon suggest a common cause. The solar proton wind cannot penetrate the atmosphere of Mercury implied by spectrometric and polarimetric observations, and contemporary solar cosmic ray protons have insufficient intensity to account for the observed properties within the age of the solar system. An alternative source of proton-irradiated powders is accretion of interplanetary dust slowly falling through the thin mercurian atmosphere.

Smith, W.B., Shapiro, I.I., and Ash, M.E., 1966, Preliminary results from processing radar and optical planetary observations: *The Astronomical Journal*, V. 71, p. 871-872.

Preliminary values of a number of astronomical constants have been obtained from the simultaneous processing of planetary radar data spanning the interval from

1959 to July 1966 and of U.S. Naval Observatory optical data extending from 1950 to 1965. Results obtained using general relativity (Newtonian) theory with their formal standard errors are: a.u., 499.004786 (499.004785) + 0.000005 light-sec; Mercury radius, 2434 (2440) + 2 km; Venus radius, 6056 (6055) + 1 km; Mercury mass, 6021000 (6029000) + 53000; Venus mass, 408250 (408450) + 120; earth plus moon mass, 328900 (328950) + 60; Mars mass, 3111000 (3107000) + 9000; earth-moon mass ratio, 81.3030 (81.3024) + 0.05. The planetary masses are given as inverses in terms of the solar mass. (Abstract of a paper presented at the July 1966 meeting of the American Astronomical Society).

Soter, S.L., 1966, Mercury: Infrared evidence of non-synchronous rotation: *Science*, V. 153, No. 3740, p.1112-1113.

The asymmetry of the infrared phase curve is interpreted to mean direct rotation.

Welch, W.J., Thornton, D.D., and Lohman, R., 1966, Observations of Jupiter, Saturn, and Mercury: *Astrophysical Journal*, V. 144, p. 799-809.

Observations of the radio emission from Jupiter, Saturn, and Mercury at 1.53-cm wavelength are reported. The disk temperature of Saturn was found to be 0.94 times that of Jupiter at this wavelength. Mercury, observed at an average phase angle of 125°, was found to have a disk temperature three times that of Jupiter. With Jupiter's disk temperature assumed to be 150°K at this wavelength, the temperatures of Saturn and Mercury are 141° and 450°K, respectively. The similarity in the emission from Jupiter and Saturn at this wavelength can be explained if one supposed that ammonia gas is the chief source of microwave thermal radiation from both planets (due to the ammonia absorption band centered at 1.28 cm) and that the gas is saturated near the cloud tops of both planets.

The possibility that emission from Saturn's rings may contribute to the radio "disk" temperature of Saturn is briefly considered. If the particles in the ring are many centimeters in diameter and perfectly absorbing, the rings contribute about 25°K to the "disk" temperature. If their mean radius is about 300μ, a probable size obtained by Franklin and Cook, their microwave extinction cross-section is small and the ring particles will not emit significant microwave energy.

### 3.7.6 Neptune

Kellermann, K.I., and Pauling-Toth, I.I.K., 1966, Observations of the radio emission of Uranus, Neptune, and other planets at 1.9 cm: *The Astrophysical Journal*, V. 145, p. 954-957.

The radio emission from Venus, Jupiter, Saturn, Uranus, Neptune, and Pluto has been investigated with the 140-foot radio telescope of the National Radio Astronomy Observatory at an effective wavelength of 1.9 cm.

The effective temperatures of the four major planets at 1.9 cm are all near 200°K, although their distance from the sun ranges from 5.2 to 30 a.u. At this wavelength the main source of opacity is probably due to the ammonia inversion line near 1.25 cm. Since the ammonia will not exist in a gaseous state in the cooler upper regions of the atmosphere, the level where  $\tau \sim 1$  on all the planets corresponds to a fixed effective temperature near the freezing point of ammonia, which is 195°K.

Kellermann, K.I., and Pauling-Toth, I.I.K., 1966, The detection of the thermal radio emission from Uranus and Neptune at 1.9 cm: *The Astronomical Journal*, V. 71, p. 390.

The thermal radio emission from Uranus and Neptune has been measured at a wavelength of 1.9 cm. The measurements were made by positioning the antenna in such a way that

the planet was alternately in the main beam or in a reference beam 6' away. In each position the difference between the two beams was integrated for 30-sec periods.

The antenna gain was calibrated from observations of Venus, Jupiter, and Saturn which were taken to have temperatures of 500°K, 180°K, and 200°K, respectively. The measured blackbody disk temperatures for Uranus and Neptune were  $220^\circ \pm 35^\circ$  and  $180^\circ \pm 40^\circ$ K, respectively. In both cases the major error is due to a 5% uncertainty in the calibration. The error due to receiver noise fluctuations was less than ten percent for each planet. The 1.9-cm value for the temperature of Uranus reported here is somewhat greater than a previous measurement at 11.3 cm made at CSIRO which gave a temperature of  $130^\circ \pm 40^\circ$ K, and is more than twice the temperature expected of a blackbody in thermal equilibrium. There have been no previous measurements of the temperature of Neptune reported either at radio or at infrared wavelengths. The 1.9 cm temperature is again considerably greater than the expected equilibrium value of about 40°K. These high effective temperatures, observed at radio frequencies, suggest either the presence of a greenhouse effect in the atmospheres of Uranus and Neptune or a strong source of internal heating.

An attempt has also been made to detect the thermal emission from the planet Pluto, and an upper limit of 500°K can be placed on its temperature if it is assumed that its radius is equal to that of the earth. (Abstract of a paper presented at the March 1966 meeting of the American Astronomical Society).

### 3.7.7 Pluto

Halliday, I., and Hardie, R.H., 1966, An upper limit for the diameter of Pluto: Publications of the Astronomical Society of the Pacific, V. 78, p. 113-124.

Based on near-occultation observations, an extreme upper limit of 6800 km can be assigned to the diameter of Pluto with a confidence of 95%. On this basis, an extreme lower limit can be assigned for its albedo of 0.1.

Kellermann, K.I., and Pauling-Toth, I.I.K., 1966, Observations of the radio emission of Uranus, Neptune, and other planets at 1.9 cm: The Astrophysical Journal, V. 145, p. 954-957.

The radio emission from Venus, Jupiter, Saturn, Uranus, Neptune, and Pluto has been investigated with the 140-foot radio telescope of the National Radio Astronomy Observatory at an effective wavelength of 1.9 cm.

The effective temperatures of the four major planets at 1.9 cm are all near 200°K, although their distance from the sun ranges from 5.2 to 30 a.u. At this wavelength the main source of opacity is probably due to the ammonia inversion line near 1.25 cm. Since the ammonia will not exist in a gaseous state in the cooler upper regions of the atmosphere, the level where  $\tau \sim 1$  on all the planets corresponds to a fixed effective temperature near the freezing point of ammonia, which is 195°K.

Rubashevskii, A.E., 1966, A method for determining the diameter of Pluto from occultation observations (remarks on Halliday's paper): Soviet Astronomy - A.J., V. 10, No. 1, p. 124-127.

The epoch of an occultation can be established by observing very close approaches of Pluto to faint stars. This procedure can yield improved values for the diameter and mean density of the planet. Precise determination of Pluto's motion during close approach to an occulted star may yield its dimensions from observation of one contact only. Even a modest telescope could furnish a diameter accurate to 0".12

from a single contact. The method has several advantages over Halliday's for deriving the size of Pluto.

### 3.7.8 Saturn

Cook, A.F., and Franklin, F.A., 1966, Particle sizes in Saturn's rings: The Astronomical Journal, V. 71, p. 851.

Saturn's rings exhibit a vertical thickness which is two or more orders of magnitude greater than the thickness expected from thermal motions (Franklin, F.A., and Cook, A.F., Astron. J. 70, 704, 1965). In order to explain this difference, we propose that the ring particles carry electrostatic charges and that the accompanying electrostatic forces will be sufficient to maintain the required thickness. We find that the charges on the particles must be negative and propose that the ambient net space charge is due to positive sodium ions produced by sunlight. The analysis suggests that particle radii lie between 300 and 700  $\mu$ , with ion densities between  $2 \times 10^4$  and  $3 \times 10^5$   $\text{cm}^{-3}$ . The corresponding neutral sodium concentrations yield equivalent widths of about 1  $\text{\AA}$  for the D lines on the damping portion of the curve of growth. (Abstract of a paper presented at the July 1966 meeting of the American Astronomical Society).

Cook, A.F., and Franklin, F.A., 1966, Rediscussion of Maxwell's Adams Prize Essay on the Stability of Saturn's rings. II: The Astronomical Journal, V. 71, p. 10-19.

The authors conclude a study of the stability of Saturn's rings by investigating the properties of a model stabilized by gravitational dilution and random particle motions. Comparison of present results with those of an earlier paper (Cook and Franklin 1964) indicates that of the two stabilizing mechanisms the latter is the more significant. An examination of all models which we have presented shows that the rings are gravitationally stable against infinitesimal disturbances if the average density is less than  $\sim 0.18$   $\text{g/cm}^3$ , but unstable if it is greater than  $\sim 1.04$   $\text{g/cm}^3$ .

Davies, R.D., and Williams, D., 1966, Observations of the continuum emission from Venus, Mars, Jupiter, and Saturn at 21.2 cm wavelength: Planetary and Space Science, V. 14, No. 1, p. 15-32.

The effective brightness temperature at 21.2 cm wavelengths determined for the planets studied are: Venus,  $591 \pm 30^\circ\text{K}$ ; Mars,  $271 \pm 76^\circ\text{K}$ ; Saturn,  $286 \pm 37^\circ\text{K}$ . The brightness temperature from Venus does not vary significantly over the wavelength range 3-21 cm, which appears to indicate that this radiation comes from the surface of the planet. Polarization studies of the 21.2 cm emission from Jupiter showed a rotation period of  $9^{\text{h}}55^{\text{m}}29^{\text{s}}.50 \pm 0^{\text{s}}.29$ , in close agreement with the period of the decimeter radiation. Possible emission mechanisms are discussed briefly.

Giver, L.P., and Spinrad, H., 1966, Molecular hydrogen features in the spectra of Saturn and Uranus: Icarus, V. 5, p. 586-589.

The S(1) and S(0) lines of the (4,0) overtone quadrupole rotation-vibration band of molecular hydrogen have been measured on two Lick Observatory 120-inch Coude spectrograms of Uranus; the ratio of the equivalent widths of these two lines results in a temperature of  $124^\circ \pm 30^\circ\text{K}$ . The same lines have been measured on one Lick spectrogram of Saturn taken in September 1964, and the resulting rotational temperature is  $126^\circ \pm 30^\circ\text{K}$ . An average of  $103^\circ \pm 20^\circ\text{K}$  was determined from these lines on three Mt. Wilson and Palomar Coude spectrograms taken in 1962.



Hide, R., 1966, On the circulation of the atmosphere of Jupiter and Saturn: *Planetary Space Science*, V. 14, No. 8, p. 669-675.

The planetary-scale atmospheric circulations of Jupiter and Saturn are discussed in terms of basic fluid dynamics. Owing to the great size of these planets, effects of rotation are even more pronounced than in the case of the earth. There is evidence in the case of Jupiter that hydromagnetic effects may have to be taken into account.

Hughes, M.P., 1966, Planetary observations at a wavelength of 6 cm: *Planetary and Space Science*, V. 14, No. 10, p. 1017-1022.

Radiometric measurements of Venus at a wavelength of 6 cm made in the period from November 1965 through March 1966 indicate that the disk temperature reached a minimum of  $630 \pm 30^\circ\text{K}$  soon after inferior conjunction. An observation of Mars near opposition in 1965 gave a disk temperature of  $190 \pm 60^\circ\text{K}$ , the same as that reported by Kellermann. The disk temperature of Jupiter remained essentially constant at  $291 \pm 25^\circ\text{K}$  from March 1965 through March 1966. Saturn was found to have a disk temperature of  $190 \pm 45^\circ\text{K}$ , which is slightly higher than anticipated.

Irvine, W.M., 1966, The shadowing effect in diffuse reflection: *Journal of Geophysical Research*, V. 71, p. 2931-2937.

The theory of multiple scattering based on the equation of radiative transfer breaks down for directly backscattered radiation if the scattering particles are large enough and the medium dense enough for the particles to shadow one another. This "shadowing effect" can be incorporated as a correction into the usual radiative transfer theory. The resultant theory may be applicable to Saturn's rings and the lunar surface.

Kellermann, K.I., and Pauling-Toth, I.I.K., 1966, Observations of the radio emission of Uranus, Neptune, and other planets at 1.9 cm: *The Astrophysical Journal*, V. 145, p. 954-957.

The radio emission from Venus, Jupiter, Saturn, Uranus, Neptune, and Pluto has been investigated with the 140-foot radio telescope of the National Radio Astronomy Observatory at an effective wavelength of 1.9 cm.

The effective temperatures of the four major planets at 1.9 cm are all near  $200^\circ\text{K}$ , although their distance from the sun ranges from 5.2 to 30 a.u. At this wavelength the main source of opacity is probably due to the ammonia inversion line near 1.25 cm. Since the ammonia will not exist in a gaseous state in the cooler upper regions of the atmosphere, the level where  $\tau \sim 1$  on all the planets corresponds to a fixed effective temperature near the freezing point of ammonia, which is  $195^\circ\text{K}$ .

Kellermann, K.I., 1966, The thermal radio emission from Mercury, Venus, Mars, Saturn, and Uranus: *Icarus*, V. 5, p. 478-490.

No appreciable phase variation was found in the 11-cm radiation from Mercury, indicating that there is little temperature difference between the illuminated and dark hemispheres. The effective surface temperature at 11 cm is between  $250^\circ$  and  $300^\circ\text{K}$ .

The observations of Venus indicate a slight decrease in effective temperature from about  $600^\circ\text{K}$  at centimeter wavelengths to about  $500^\circ\text{K}$  at decimeter wavelengths. Little or no change with phase angle was found in the apparent temperature at 11 cm.

The apparent temperature of Saturn was found to increase at longer wavelengths, reaching nearly 200°K at 11 cm and 300°K at 21 cm.

Uranus was found to have an equivalent temperature of  $130^\circ \pm 40^\circ\text{K}$  at 11 cm which, like Saturn, is about twice that expected from solar heating.

Low, F.J., 1966, Observations of Venus, Jupiter, and Saturn at  $\lambda 20\mu$ : The Astronomical Journal, V. 71, p. 191.

The first observations of the planets at  $20\mu$  were reported by Low (Lowell Observatory Bulletin 128, 184, 1965). Using the same radiometer, which cuts on at  $17.5\mu$  and is uniformly sensitive to about  $25\mu$ , further observations have been made with angular resolutions between 4 and 35 arc sec. Under the assumption that Mars radiates as a blackbody, its brightness temperature at  $20\mu$  was taken as  $225^\circ \pm 5^\circ\text{K}$ , the value measured for the disk at  $10\mu$ . This yielded a temperature for Venus at  $20\mu$  of  $248 \pm 10^\circ\text{K}$ , significantly above the  $10\mu$  value of  $221 \pm 10^\circ\text{K}$  but in good agreement with solar heating. Using Mars and Venus as standards, it was possible to observe Saturn with angular resolutions both large and small compared to its disk. Correcting for the obscuration of the rings, which were found to be much colder than the planet, the mean disk brightness temperature was  $95 \pm 3^\circ\text{K}$  quite close to the measured value of  $93^\circ\text{K}$  at  $10\mu$  (Low, F.J., Astron. J. 69, 550, 1964). Scans of Jupiter show a hot equatorial band,  $150 \pm 5^\circ\text{K}$ , covering about half the disk; the poles are about  $130^\circ\text{K}$ . Although the equatorial scans show significant limb darkening, the east and west limbs are equal in temperature to within the accuracy of measurement.

The total amount of energy Jupiter receives from the sun is less than the observed radiation between 10 and  $25\mu$  and would produce an effective temperature of only  $105^\circ\text{K}$ . Thus, an internal supply of energy must be present. The Jovian temperature measured at 1 mm is  $155 \pm 15^\circ\text{K}$  (Low, F.J., and Davidson, A.W., Astrophys. J. 142, 1278, 1965). If the brightness temperature between  $25\mu$  and 1 mm does not drop below  $140^\circ\text{K}$ , the total power radiated by Jupiter is more than 3 times the insolation. A similar conclusion may be drawn for Saturn; however, since only a small fraction of its total energy is observed, its excess brightness temperature at  $20\mu$  may be caused by a greenhouse effect. (Abstract of a paper presented at the March 1966 meeting of the American Astronomical Society).

Mertz, L., and Coleman, I., 1966, Infrared spectrum of Saturn's ring: The Astronomical Journal, V. 71, p. 747-748.

The infrared spectrum of Saturn's ring is found to show a strong absorption feature at  $1.66\mu$ . The spectrum is not consistent with the current ice hypothesis, and it is suggested that the ring material is (or is covered with) paraformaldehyde.

Moroz, V.I., 1966, The spectra of Jupiter and Saturn in the 1.0-2.5 $\mu$  region: Soviet Astronomy - A.J., V. 10, No. 3, p. 457-468.

Spectra of Jupiter, Saturn's disk, and Saturn's rings in the region 1-2.5 $\mu$  have been obtained at resolutions  $\lambda/\Delta\lambda \approx 500, 150$ , and 20 respectively. They are analyzed on a "simple reflection" model, with the cloud-layer boundary assumed optically equivalent to a solid surface. The  $\text{CH}_4$  content above Jupiter's cloud layer is apparently  $<150 \text{ m} \cdot \text{atm}$ . The 1-0 band of  $\text{H}_2$  probably contributes significantly to the absorption near  $2\mu$ . Saturn's cloud layer most likely consists of  $\text{CH}_4$  ice particles; the rings,  $\text{H}_2\text{O}$  ice particles.

Owen, T., 1966, An identification of the 6800-Å methane band in the spectrum of Uranus and a determination of atmospheric temperature: Astrophysical Journal, V. 146, p. 611.

By considering the relative intensities of the R branch lines in the 4 overtone of the  $\nu_3$  vibration of methane, the author calculates that the mean temperature of the visible atmosphere of Uranus is  $600 \pm 15^\circ\text{K}$ . Additionally he points out that the same band can be detected in the spectra of Jupiter and Saturn.

Spinrad, H., and Giver, L.P., 1966, Jupiter and Saturn: Planetary line inclinations: Publications of the Astronomical Society of the Pacific, V. 78, p. 175-177.

Observations have been continued of planetary line inclinations ( $\text{CH}_4$  and  $\text{NH}_3$  on Jupiter,  $\text{CH}_4$  on Saturn) previously found to be suspiciously anomalous on equatorial spectrograms. New results from Lick spectrograms show that no anomaly was present in 1964 and 1965. These results do not differ significantly from the expected 50% from Doppler-shift calculations. So far, no satisfactory model of these planets has been proposed to explain the sometimes anomalous line inclination.

Tolbert, C.W., 1966, Observed millimeter wavelength brightness temperatures of Mars, Jupiter, and Saturn: The Astronomical Journal, V. 71, p. 30-32.

Analyses of observations of 35, 70, and 94 Gc radiation from Mars, Jupiter, and Saturn made with a 16-ft. antenna yield brightness temperatures for Mars of  $230(+12, -12)^\circ\text{K}$  and  $240(+72, -118)^\circ\text{K}$  at 35 and 94 Gc, respectively; for Jupiter,  $113(+11, -11)^\circ\text{K}$ ,  $105(+18, -12)^\circ\text{K}$  and  $111(+22, -11)^\circ\text{K}$  at 35, 70, and 94 Gc, respectively. The antenna temperatures from which the brightness temperatures were calculated were obtained by averaging the responses of right ascension scans of the antenna beam across the planets. The observing and data reducing techniques are herein described and the averaged antenna temperatures shown.

Welch, W.J., Thornton, D.D., and Lohman, R., 1966, Observations of Jupiter, Saturn, and Mercury: Astrophysical Journal, V. 144, p. 799-809.

Observations of the radio emission from Jupiter, Saturn, and Mercury at 1.53-cm wavelength are reported. The disk temperature of Saturn was found to be 0.94 times that of Jupiter at this wavelength. Mercury, observed at an average phase angle of  $125^\circ$ , was found to have a disk temperature three times that of Jupiter. With Jupiter's disk temperature assumed to be  $150^\circ\text{K}$  at this wavelength, the temperatures of Saturn and Mercury are  $141^\circ$  and  $450^\circ\text{K}$ , respectively. The similarity in the emission from Jupiter and Saturn at this wavelength can be explained if one supposed that ammonia gas is the chief source of microwave thermal radiation from both planets (due to the ammonia absorption band centered at 1.28 cm) and that the gas is saturated near the cloud tops of both planets.

The possibility that emission from Saturn's rings may contribute to the radio "disk" temperature of Saturn is briefly considered. If the particles in the ring are many centimeters in diameter and perfectly absorbing, the rings contribute about  $25^\circ\text{K}$  to the "disk" temperature. If their mean radius is about 3004, a probable size obtained by Franklin and Cook, their microwave extinction cross-section is small and the ring particles will not emit significant microwave energy.

Yabushita, S., 1966, Stability analysis of Saturn's rings with differential rotation: Monthly Notices of the Royal Astronomical Society, V. 133, p. 247-263.

A method is presented for calculating the potential due to an arbitrary thin gravitating ring by making use of cylindrical functions. Equilibrium configuration of the ring is defined in such a way that the centrifugal force exactly balances the self-gravitation of the ring plus the gravitation due to the planet which is taken as spherical. By taking into account the differential rotation obtained in this manner mathematical analysis of the stability of motion about the equilibrium configuration is carried out by making use of the equations

of hydrodynamics. Frequencies of the free oscillations are shown to be given as eigen values of a certain infinite matrix and the eigen value problem is then solved. The upper limit to the mass of the ring which is stable against axisymmetric perturbations is given for several model rings. If the density distribution of the ring is taken as a linear combination of the zeroth order Bessel functions of the first and second kind such that the density vanishes at the inner ( $r = a$ ) and outer ( $r = b$ ) boundaries. The limiting mass turns out to be 0.0386  $M_g$ , 0.0109  $M_g$ , and 0.00209  $M_g$ , for  $a/b = 0.2$ ,  $a/b = 0.5$  and  $a/b = 0.75$  respectively, where  $M_g$  is Saturn's mass, these values differ considerably from that obtained by Maxwell for a rigidly rotating ring where the effect of the edges are entirely neglected. Stability criterion for a different density distribution is also discussed.

Younkin, R.L., and Münch, G., 1966, Visible and near-infrared spectrophotometry of Saturn's rings: *The Astronomical Journal*, V. 71, p. 188.

Measurements of the narrow-band spectral energy distribution of the rings of Saturn have been made at the Mount Wilson Observatory using the 60-in. reflector and the Fastie-Ebert spectrometer. Spectral scans from 0.51 to 1.1 $\mu$  were made of a segment of the rings at the western end of the semi-major axis.

The energy distribution was determined at 54 points in this wavelength region. The color sensitivity of the system was determined from scans of  $\alpha$  Lyr and the  $\alpha$  Lyr energy distribution of Oke. The relative reflectance of the rings was calculated by use of the solar intensity values of Labs and Neckel, converted to solar flux by the ratios of Minnaert.

The reflectance of the rings is very nearly constant from 0.78 to 1.05 $\mu$ . Shortward of this region it falls slowly to 0.60 $\mu$ , then more rapidly to a value at 0.51 $\mu$  some 0.45 below the maximum. There is a slight decrease in reflectance (0.703-0.705) from 1.05 to 1.08 $\mu$ . This is marginally outside of the experimental error. Owen has recently reported a drop in the reflectance of the rings from 1.04 to 1.09 $\mu$ , which he identified as due to water ice. This drop was determined on the basis of a drop in the ratio of the intensity of the rings to the intensity of Saturn in this region. Separate measurements at Mount Wilson of the reflectance of Saturn show a continuous strong absorption from 0.97 to 1.0 $\mu$ . This unfortuitous coincidence yields a large drop in the ratio beyond 1.0 $\mu$  which will completely mask any possible ice absorption which by the results above will be only a few percent at most. (Abstract of a paper presented at the December 1965 meeting of the American Astronomical Society).

### 3.7.9 Uranus

Giver, L.P., and Spinrad, H., 1966, Molecular hydrogen features in the spectra of Saturn and Uranus: *Icarus*, V. 5, p. 586-589.

The S(1) and S(0) lines of the (4,0) overtone quadrupole rotation-vibration band of molecular hydrogen have been measured on two Lick Observatory 120-inch Coudé spectrograms of Uranus; the ratio of the equivalent widths of these two lines results in a temperature of  $124^\circ \pm 30^\circ K$ . The same lines have been measured on one Lick spectrogram of Saturn taken in September 1964, and the resulting rotational temperature is  $126^\circ \pm 30^\circ K$ . An average of  $103^\circ \pm 20^\circ K$  was determined from these lines on three Mt. Wilson and Palomar Coudé spectrograms taken in 1962.

Kellermann, K.I., 1966, The thermal radio emission from Mercury, Venus, Mars, Saturn, and Uranus: *Icarus*, V. 5, p. 478-490.

No appreciable phase variation was found in the 11-cm radiation from Mercury, indicating that there is little temperature difference between the illuminated

and dark hemispheres. The effective surface temperature at 11 cm is between 250° and 300°K.

The observations of Venus indicate a slight decrease in effective temperature from about 600°K at centimeter wavelengths to about 500°K at decimeter wavelengths. Little or no change with phase angle was found in the apparent temperature at 11 cm.

Observations of Mars at 6, 11, and 21 cm indicate effective temperatures near 200°K, in good agreement with the infrared measurements.

The apparent temperature of Saturn was found to increase at longer wavelengths, reaching nearly 200°K at 11 cm and 300°K at 21 cm.

Uranus was found to have an equivalent temperature of  $1300 \pm 400$ °K at 11 cm which, like Saturn, is about twice that expected from solar heating.

Kellermann, K.I., and Pauling-Toth, I.I.K., 1966, Observations of the radio emission of Uranus, Neptune, and other planets at 1.9 cm: *The Astrophysical Journal*, V. 145, p. 954-957.

The radio emission from Venus, Jupiter, Saturn, Uranus, Neptune, and Pluto has been investigated with the 140-foot radio telescope of the National Radio Astronomy Observatory at an effective wavelength of 1.9 cm.

The effective temperatures of the four major planets at 1.9 cm are all near 200°K, although their distance from the sun ranges from 5.2 to 30 a.u. At this wavelength the main source of opacity is probably due to the ammonia inversion line near 1.25 cm. Since the ammonia will not exist in a gaseous state in the cooler upper regions of the atmosphere, the level where  $\tau \sim 1$  on all the planets corresponds to a fixed effective temperature near the freezing point of ammonia, which is 195°K.

Kellermann, K.I., and Pauling-Toth, I.I.K., 1966, The detection of the thermal radio emission from Uranus and Neptune at 1.9 cm: *The Astronomical Journal*, V. 71, p. 390.

The thermal radio emission from Uranus and Neptune has been measured at a wavelength of 1.9 cm. The measurements were made by positioning the antenna in such a way that the planet was alternately in the main beam or in a reference beam 6' away. In each position the difference between the two beams was integrated for 30-sec periods.

The antenna gain was calibrated from observations of Venus, Jupiter, and Saturn which were taken to have temperatures of 500°, 180°, and 200°K, respectively. The measured blackbody disk temperatures for Uranus and Neptune were  $2200 \pm 350$ ° and  $1800 \pm 400$ °K, respectively. In both cases the major error is due to a 15% uncertainty in the calibration. The error due to receiver noise fluctuations was less than ten percent for each planet.

The 1.9-cm value for the temperature of Uranus reported here is somewhat greater than a previous measurement at 11.3 cm made at CSIRO which gave a temperature of  $1300 \pm 400$ °K, and is more than twice the temperature expected of a blackbody in thermal equilibrium. There have been no previous measurements of the temperature of Neptune reported either at radio or at infrared wavelengths. The 1.9-cm is again considerably greater than the expected equilibrium value of about 40°K. These high effective temperatures, observed at radio frequencies, suggest either the presence of a greenhouse effect in the atmospheres of Uranus and Neptune or a strong source of internal heating.

An attempt has also been made to detect the thermal emission from the planet Pluto, and an upper limit of 500°K can be placed on its temperature if it is assumed that its radius is equal to that of the earth. (Abstract of a paper presented at the March 1966 meeting of the American Astronomical Society).

Klein, M.J., and Selig, T.V., 1966, Radio emission from Uranus at 8 Gc/s: *Astrophysical Journal*, V. 146, p. 599.

To determine a more accurate measurement of the brightness temperature and to obtain a second point on its microwave spectrum, a total of 593 scans of Uranus on 11 separate nights between January 24 and March 21, 1966, at a frequency of 8 Gc/s ( $\lambda 3.75$  cm) were taken. The measured brightness temperature and its mean error were  $159^\circ \pm 16^\circ\text{K}$ . The observations were made with the University of Michigan's 85-foot radio telescope using a wide-band (1000 Mc/s) tunnel diode radiometer (Selig 1964).

Low, F.J., 1966, The infrared brightness temperature of Uranus: *Astrophysical Journal*, V. 146, p. 326.

The effective disk temperature of a planet in radiative equilibrium with the Sun is given approximately by either  $T_E(\text{Max}) = 394 (1 - A)^{1/4}$ , if it keeps the same face to the Sun long enough to reach local equilibrium, or by  $T_E(\text{Av}) = T_E(\text{Max})/1.4$ , if the solar heating is averaged over a day and night period short compared to the time for local equilibrium to be reached.

At the present epoch, the polar axis of Uranus, which lies almost in the orbital plane, is nearly perpendicular to the line from the planet to the Sun and, because of the planet's rapid rotation, we would expect a radiometric temperature close to  $T_E(\text{Av})$ . At present the planet is near perihelion; at aphelion the temperature should be 5 per cent lower because of the greater distance to the Sun.

From the above we would expect an effective temperature of about  $50^\circ\text{K}$  for Uranus with a peak in its spectral energy curve near  $60\mu$ .

Owen, T., 1966, An identification of the 6800-Å methane band in the spectrum of Uranus and a determination of atmospheric temperature: *Astrophysical Journal*, V. 146, p. 611.

By considering the relative intensities of the R branch lines in the 4 overtone of the  $\nu_2$  vibration of methane, the author calculates that the mean temperature of the visible atmosphere of Uranus is  $60^\circ \pm 15^\circ\text{K}$ . Additionally he points out that the same band can be detected in the spectra of Jupiter and Saturn.

Safronov, V.S., 1966, Sizes of the largest bodies falling onto the planets during their formation: *Soviet Astronomy - A.J.*, V. 9, p. 987-994.

Application of coagulation theory to the process of accumulation of the planets from solid matter leads to the conclusion that this matter was in the form of particles and bodies of different sizes. Falling onto the planets, the bodies imparted to them a rotational moment consisting of two components of different nature: a regular component ("direct" rotation), related to rotation of the system as a whole, and a random component, related to the random direction of velocity of the falling bodies relative to the planet and manifested in the inclinations of the axes of rotation of the planets. The largest bodies made the principal contribution to the random component of rotation. This article gives the derivation of expressions relating the values of the random component of rotation to the masses  $m_i$  of the largest bodies falling onto a planet of mass  $m$  on the assumption of an exponential distribution function of the sizes of the bodies. Table 1 gives the values  $m_i/m$  determined from a comparison of the theoretically computed angles of inclination of the axes of rotation of the planets and the observed values. The largest bodies falling onto the earth had masses of about  $10^{-3}$  of the earth's mass; that is, they were of the size of the largest asteroids. This same mechanism makes it possible to explain the anomalous rotation of Uranus if it is assumed that the random component of the rotation of Uranus was greater than the systematic component. The mass of the largest body falling onto the surface of Uranus in this case would have to be 0.05 of the mass of that planet.

## 3.7.10 Venus

Anderson, D.L., and Kovach, R.L., 1966, The interiors of the moon and terrestrial planets: Transactions of the American Geophysical Union, V. 47, No. 1, p. 155.

Present information regarding the composition and strength of the interior of the earth is used to discuss the interiors of the moon and terrestrial planets. Results strongly suggest homogeneity of the Fe/Si ratio in the inner part of the solar system. The mass versus density function is determined for iron-rich silicate planets with different degrees of oxidation, and the results are compared with the terrestrial planets. The properties of Mars, Venus, and the earth are all consistent with the assumption of early uniformity of the solar system. The data for Mars slightly favor the hypothesis that Mars is more oxidized than the earth, but the uncertainty in the radius of Mars also allows the composition to be the same as the earth's. Contrary to current thoughts, the shape of the moon implies that it is weaker than the earth; this is consistent with thermal calculations. Using the earth's mantle as a model, the density and elastic properties are calculated for the interior of the moon. Density and velocity decrease with depth throughout most of the moon. (Abstract of a paper presented at the April 1966 meeting of the American Geophysical Union).

Applebaum, D.C., Hartek, P., Reeves, R.R., Jr., and Thompson, B.A., 1966, Some comments on the Venus temperature: Journal of Geophysical Research, V. 71, p. 5541-5545.

The observed microwave emission from Venus has been widely attributed to a high surface temperature for the planet. A lack of realistic models to account for such a high temperature has led to a search for alternative interpretations for the emission. The paper describes experiments in which anomalous signals have been observed in the X-band region from glow discharges through  $\text{CO}_2$  and  $\text{SO}_2$ . Although this type of emission may not necessarily be the source of the microwave emission from Venus, the fact that it occurs points out the need for caution in basing conclusions about the surface temperature on microwave observations.

Arking, A., and Potter, J., 1966, Calculated light curves for models of the Venus atmosphere: The Astronomical Journal, V. 71, p. 154.

The microwave observations of Venus have led to widely differing interpretations of the Venus atmosphere--from a dry  $\text{N}_2 + \text{CO}_2$  mixture at several hundred atmospheres surface pressure to a very wet, precipitating cloud model at a few atmospheres. The implications of these models with respect to scattering of solar radiation in the visible spectrum have been examined by obtaining numerical solutions to the anisotropic multiple scattering problem for thick but finite atmospheres. Results of these calculations for various models are presented and compared with photometric observations of Venus. (Abstract of a paper presented at the December 1965 meeting of the American Astronomical Society).

Basharinov, A.E., and Kutuza, B.G., 1966, The nature of the cloud layer on Venus from microwave observations: Soviet Astronomy - A.J., V. 10, No. 1, p. 117-120.

The hypothesis that the cloud layer of Venus contains super-cooled water droplets is supported by extrapolation of absorption data at 8-mm wavelength to millimeter and centimeter wavelengths, as derived from the phase dependence of the radio-brightness temperature. The extrapolated value for the temperature agrees with measurements for the night side of Venus. The water content of the cloud layer is about 0.1-0.3 g/cm<sup>2</sup>; absorption in the layer is  $\leq 1.5$  dB at centimeter wavelengths, and  $\leq 5$  dB for wavelengths higher than 3 mm.

Belton, M.J.S., and Hunten, D.M., 1966, Water vapor in the atmosphere of Venus: Astrophysical Journal, V. 146, p. 307.



The authors have detected the presence of water-vapor lines in the spectrum of Venus, Doppler-shifted from the normal wavelengths of 8189.27 and 8193.00 Å.

The spectra were taken in November 1965, and May 1966, by photoelectric scanning of the Venus spectrum formed by the 40-foot spectrograph of the McMath Solar Telescope.

In order to disentangle the Venus lines from their strong telluric counterparts during each observing period spectra were taken of both Venus and the Sun.

A preliminary estimate of the absorption in the red wing of the 8189 Å line suggests an effective pressure of about 5 atm.

Carpenter, R.L., 1966, Preliminary results of 12.5 cm radar observations of Venus during its 1966 conjunction: *The Astronomical Journal*, V. 71, p. 848.

Venus was observed with the 85-ft. dish, planetary radar system at the NASA/JPL Deep Space Instrumentation Facility at Goldstone, California. The transmitter power and frequency were 100 kW and 2388 Mc, respectively. Both polarized and depolarized cw spectra were obtained. They show features similar to those observed in 1962 and 1964 which are believed to be the result of different surface structures on Venus. If this is the case, their motions can be used to determine the planet's rotation period. A preliminary comparison of the features over three successive conjunctions suggest that Venus' sidereal period is  $243 \pm 1$  days retrograde. This result is remarkable because it overlaps 243.16 days retrograde, that period where Venus would present the same face toward the earth every conjunction. (Abstract of a paper presented at the July 1966 meeting of the American Astronomical Society).

Carpenter, R.L., 1966, Study of Venus by cw radar--1964 results: *The Astronomical Journal*, V. 71, p. 142-152.

During the 1964 conjunction of Venus, the planet was observed by radar on a daily basis with an 85-ft. dish. The wavelength was 12.5 cm and the transmitter power was 100 kW. The results of one phase of the program are discussed--those of the high-resolution cw radar spectra. The polarized reflectivity obtained is  $0.114 \pm 0.01$ . The depolarized reflectivity is  $0.0067 \pm 0.0005$ . The estimated average dielectric constant of Venus' surface is  $3.75 \pm 0.3$ . The base bandwidth of the spectra gives a retrograde sidereal rotation of 250 days  $\pm 4$ ,  $-7$  days. The direction of the north polar axis is estimated to be  $\alpha = 255^\circ \pm 10^\circ$ ,  $-4^\circ$  and  $\delta = 68^\circ \pm 4^\circ$ . This places the axis within  $10^\circ$  of the orbit pole. Several spectral features were found and their positions on Venus' surface is derived. A comparison of the 1964 features with the features observed in 1962 suggests that the rotation of Venus may be nearer to 244 days retrograde rather than 250 days given by the base bandwidth measurements.

Copeland, J., 1966, Observations of Venus at 8.6 mm wavelength near inferior conjunction: *Astrophysical Journal*, V. 143, p. 996-1000.

This note reports the results of some radio observations of the planet Venus at 8.6 mm wavelength near the inferior conjunction of 1964. The reduced data contain anomalous variations which are larger than would be expected from phase alone so that a reliable measure of brightness-temperature dependence on phase angle could not be made. Of more interest is the fact that the anomalous variations in brightness temperature appear to be correlated with solar activity.

Danielson, R.E., and Solomon, D.M., 1966, Role of collision-induced transitions in the Venus greenhouse effect: *The Astronomical Journal*, V. 71, p. 382-383.

The infrared opacity of collision-induced transitions in  $N_2$  and  $CO_2$  has been estimated for  $T = 6000K$  from laboratory tracings obtained at room temperature. Assuming a 10%  $CO_2$ , 90%  $N_2$  atmosphere on Venus having a surface pressure of 100 atm and a surface temperature of 6000K, the optical depth of the Venus atmosphere is in excess of 500 bands: (1)  $N_2$ , rot.-trans. ( $\sim 200\text{ cm}^{-1}$ ), (2)  $CO_2$ ,  $2\nu_2^0$  ( $1286\text{ cm}^{-1}$ ). Optical depths of the order of 50 occur at the centers of the following weaker bands resulting from collision induced simultaneous transitions: (5)  $N_2$ ,  $(1-0)-CO_2$ ,  $\nu_2$  ( $1664\text{ cm}^{-1}$ ), (6)  $N_2$ ,  $(1-0) + CO_2$ ,  $\nu_2$  ( $2998\text{ cm}^{-1}$ ), (7)  $N_2$ ,  $(1-0) + CO_2$ ,  $\nu_2$  ( $4680\text{ cm}^{-1}$ ). In addition to the induced bands, many allowed  $CO_2$  bands contribute strongly to the infrared opacity. The opacity in the wings of the above bands depends on the profiles of the lines making up the bands. Conservative estimates of these line profiles yield sufficiently wide bands that they overlap to produce a harmonic mean opacity (based on the Planck distribution at 6000K) greater than 50. On the other hand, the opacity due to Rayleigh scattering is sufficiently small to allow a significant fraction of the solar radiation to penetrate to the surface.

Thus, it appears possible to produce a greenhouse effect on Venus which is sufficient to maintain a 6000K surface temperature by a deep  $CO_2$ ,  $N_2$  atmosphere. The required surface pressure is reduced if the relative abundance of  $CO_2$  is larger than 10%. Furthermore, it does not seem that  $H_2O$  is necessary to produce a greenhouse model on Venus, although a small amount of water vapor would substantially add to the infrared opacity without producing a cloud layer thick enough to prevent penetration of incident solar radiation to the surface. (Abstract of a paper presented at the March 1966 meeting of the American Astronomical Society).

Davies, R.D., and Williams, D., 1966, Observations of the continuum emission from Venus, Mars, Jupiter, and Saturn at 21.2 cm wavelength: Planetary and Space Science, V. 4, No. 1, p. 15-32.

The effective brightness temperature at 21.2 cm wavelengths determined for the planets studied are: Venus,  $591 \pm 30^\circ K$ ; Mars,  $271 \pm 76^\circ K$ ; Saturn,  $286 \pm 37^\circ K$ . The brightness temperature from Venus does not vary significantly over the wavelength range 3-21 cm, which appears to indicate that this radiation comes from the surface of the planet. Polarization studies of the 21.2 cm emission from Jupiter showed a rotation period of  $9^h 55^m 29^s 50 \pm 0^s 29$ , in close agreement with the period of the decimeter radiation. Possible emission mechanisms are discussed briefly.

Dickel, J.R., 1966, Measurement of the temperature of Venus at a wavelength of 3.75 cm for a full cycle of planetary phase angles: Icarus, V. 5, p. 305-308.

Observations of Venus have been made at a wavelength of 3.75 cm. The observations span a full cycle of planetary phase angle in order to determine the dependence of temperature on phase angle. The results give a mean temperature of 6460K and suggest a variation of temperature with solar illumination.

Dickel, J.R., 1966, Microwave spectrum of Venus: The Astronomical Journal, V. 71, p. 852-853.

Venus was observed at a wavelength of 6 cm on four days during February 1966 using the 140-ft. radio telescope at the National Radio Astronomy Observatory. The observations consisted of a series of on-offs which included baselines surrounding the planet. The feed system consisted of a linearly polarized feed probe which was switched versus either a sky horn for total intensity measurements or an orthogonal feed probe for polarization measurements. The feed could be rotated to any given position angle.

Although Venus was reasonable far from the zenith during the period of observation, it was only  $10^\circ$  south of the source Hydra A. Measurements of Hydra A by Dr. I.I.K. Pauling-Toth, Dr. K.I. Kellermann, and Dr. C.V. Sastry were therefore used for

calibration purposes. They adopted a flux density for Hydra A of 13.0 flux units at 6 cm. All observations were kept within two hours of the meridian.

The observations were made shortly after inferior conjunction of Venus at a mean phase angle of  $215^\circ$ , and the measured brightness temperature of Venus at 6 cm was  $706 \pm 45^\circ\text{K}$  (mean error). This value is definitely greater than the temperature recorded near inferior conjunction at both shorter and longer wavelengths showing that the temperature does appear to reach a maximum value near this wavelength. The actual mean value of the brightness temperature is probably somewhat higher than the value recorded because of the phase variation of the observed temperature. There is some evidence for a degree of polarization less than 0.5%. (Abstract of a paper presented at the July 1966 meeting of the American Astronomical Society).

Evans, J.V., and Ingalls, R.P., 1966, Radar observations of Venus at 23- and 3.8-cm wavelength: *The Astronomical Journal*, V. 71, p. 854.

During the early part of 1966 the Lincoln Laboratory Millstone Hill Radar ( $\lambda = 23$  cm) and Haystack Radar ( $\lambda = 3.8$  cm) were employed to observe the planet Venus. The cross section observed at the longer wavelength was about 15% of the projected area of the disk. This is in agreement with earlier measurements (Evans et al., 1965) but at the shorter wavelength the cross section was only one-tenth as much. This finding supports the low value for the cross section reported by Karp et al. (1964), though in contrast to these workers the echo spectrum is found to be comparatively narrow, suggesting the solid surface as the reflecting agent. No echo power can be observed outside the frequency limits expected on the basis of the known rotation rate and the center Doppler shift measured using the  $\lambda = 23$  cm radar. If any energy is reflected by the atmosphere it appears to be only a small portion of the total. Confirmation that the surface is the scattering agent has been provided by near simultaneous ranging experiments at the two frequencies, which showed that the echo delay times agreed to  $5 \mu\text{sec}$ , which is well within the experimental accuracy. The depolarized component of the echoes was observed at both wavelengths and found to be of the order of 14 dB weaker than the expected component. The implications of these results concerning model atmospheres for Venus are discussed. (Abstract of a paper presented at the July 1966 meeting of the American Association for the Advancement of Science).

Evans, J.V., Ingalls, R.P., Rainville, L.P., and Silva, R.R., 1966, Radar observations of Venus at 3.8-cm wavelength: *The Astronomical Journal*, V. 71, p. 902-915.

During the early part of 1966 the Lincoln Laboratory Haystack Radar ( $\lambda = 3.8$  cm) was employed to observe the planet Venus. The radar cross section observed at this wavelength was only about one-tenth as much as has been reported at wavelengths of 12 cm or longer. Separate observations of the planet Mercury yielded cross sections similar to those previously obtained at longer wavelengths and lent confidence that the radar equipment was functioning properly. Thus, our measurements support the low value for the cross section reported by Karp et al. (1964). The echo spectrum is found to be comparatively narrow, suggesting the solid surface as the reflecting agent. No echo power can be observed outside the frequency limits expected on the basis of the known rotation rate and the center Doppler shift measured using a separate  $\lambda = 23$  cm radar. If any energy is reflected by the atmosphere it appears to be only a small portion of the total. Confirmation that the surface is the scattering agent has been provided by near simultaneous ranging experiments at two frequencies, which showed that the echo delay times agreed to  $5 \mu\text{sec}$ , i.e., well within the experimental accuracy. The depolarized component of the echoes was observed and found to be of the order of 14 dB weaker than the expected component. An analysis of the scattering law for the planet has been made, and when compared with the law observed at longer wavelengths indicates that about 4-6 dB two-way vertical

absorption occurs in the atmosphere of Venus. Variations in the observed cross section with time (by as much as a factor of 2) support the view that atmospheric attenuation is responsible at least in part for the low cross section observed. A comparison of the positions of anomalously reflecting regions observed in these observations with the positions reported by Carpenter (1966) during the 1964 inferior conjunction permits the Venus rotation period to be established as  $244 \pm$  a few days.

Evans, J.V., Brockelman, R.A., Dupont, E.N., Hanson, L.B., and Reid, W.A., 1966, Radar observations of Venus at 23 cm in 1965/1966: *The Astronomical Journal*, V. 71, p. 897-901.

During late 1965 and early 1966 the Lincoln Laboratory Millstone Hill radar was employed to make flight time and Doppler shift measurements of signals reflected from the planet Venus. The flight time to Venus was determined twice weekly over a six-month period to an accuracy of  $\pm 10 \mu$  sec, and to somewhat poorer accuracy beyond this interval. The scattering behavior of the planet was redetermined and found to agree with that observed in 1964. The depolarization of the signals introduced on reflection was observed and it was determined that the echo power in the orthogonal circular sense is some 15 dB weaker than that in the expected sense.

Goldreich, P., and Peale, S.J., 1966, Resonant rotation of Venus?: *Nature*, V. 209, p. 1117.

Previously these authors discussed stable resonant spins for a planet in an eccentric orbit and found that a necessary condition for capture into a resonance was the existence of a significant term in the tidal torque, which would damp librations about the commensurate spin value. For Venus a similar condition must be met by a total additional torque. As yet they have been unable to find any physical basis for the existence of such a torque.

Goldreich, P., and Peale, S.J., 1966, Resonant spins in the solar systems: *Transactions of the American Geophysical Union*, V. 47, No. 1, p. 155.

The effects of gravitational torques on spinning non-axisymmetric planets and satellites are investigated in detail. A stability criterion is derived for the maintenance of a planetary or satellite spin angular velocity which is commensurate with its mean motion. Spin angular velocities that are half and whole integral multiples of orbital angular velocities are shown to be stable for even very slight deviations from axial symmetry. An analytical method is developed for determining the probability of a planet's or satellite's being captured into such a resonant spin state, as the spin is decreased by tidal friction. The dependence of this capture probability on orbital eccentricity is also discussed. Numerical results are given for Mercury and the moon. A similar analysis gives a stability criterion for a Venusian spin that is resonant with the synodic motion of Venus. (Abstract of a paper presented at the April 1966 meeting of the American Geophysical Union).

Goody, R.M., and Robinson, A.R., 1966, A discussion of the deep circulation of the atmosphere of Venus: *Astrophysical Journal*, V. 146, p. 339-355.

If high temperatures ( $\sim 600^\circ\text{K}$ ) exist at the base of the Venus cloud layer, the question arises as to whether deep penetration of solar radiation is the only possible mechanism for their maintenance. A model in which the atmosphere is completely opaque to both solar and planetary radiation but which is in motion on account of the differential heating between subsolar and antisolar points is examined.

The nature of the solution depends upon the magnitudes of the turbulent eddy coefficients of viscosity and thermal conductivity. It is argued that the geometry

of the system favors moderate vertical mixing coefficients ( $\sim 10^4 \text{ cm}^2 \text{ s}^{-1}$ ) and that the inflow of solar energy is large enough to maintain an essentially non-linear boundary layer near to the cloud tops. This flow has to be supported by an upwelling motion over most of the planet, whose velocity is of such a magnitude that the deep interior currents are adiabatic.

Ho, W., Kaufman, I.I., and Thaddeus, P., 1966, Laboratory measurement of microwave absorption in models of the atmosphere of Venus: *Journal of Geophysical Research*, V. 71, p. 5091-5108.

Coefficients of induced absorption in model atmospheres containing  $\text{CO}_2$ ,  $\text{N}_2$ , A, and Ne, needed to calculate the properties of the lower atmosphere of Venus from the radio observations on the assumption that the atmosphere is dry and massive, have been measured in the temperature range 240-500°K to pressures as high as 130 atm. Since the microwave region lies on the low-absorption coefficient is proportional to the square of the frequency, and all measurements have been made at one frequency, 9260 Mc/s. Absorption due to small amounts of water vapor in  $\text{N}_2$  has also been studied at 9260 Mc/s, over a comparable pressure range, and over the temperature interval 393-473°K. It is concluded that (a) water vapor can account for the microwave spectrum only if water is several orders of magnitude more abundant than the infrared studies suggest and that (b) if induced absorption in a  $\text{CO}_2$ - $\text{N}_2$  atmosphere is responsible for the spectrum, if  $\text{CO}_2$  is a relatively minor constituent of the atmosphere, and if the lapse rate is close to the adiabatic, then the ground pressure must lie in the range 100-300 atm.

Hughes, M.P., 1966, Planetary observations at a wavelength of 6 cm: *Planetary and Space Science*, V. 14, No. 10, p. 1017-1022.

Radiometric measurements of Venus at a wavelength of 6 cm made in the period from November 1965 through March 1966 indicate that the disk temperature reached a minimum of  $630 \pm 30^\circ\text{K}$  soon after inferior conjunction. An observation of Mars near opposition in 1965 gave a disk temperature of  $190 \pm 60^\circ\text{K}$ , the same as that reported by Kellermann. The disk temperature of Jupiter remained essentially constant at  $291 \pm 25^\circ\text{K}$  from March 1965 through March 1966. Saturn was found to have a disk temperature of  $190 \pm 45^\circ\text{K}$ , which is slightly higher than anticipated.

Kellermann, K.I., 1966, The thermal radio emission from Mercury, Venus, Mars, Saturn, and Uranus: *Icarus*, V. 5, p. 478-490.

No appreciable phase variation was found in the 11-cm radiation from Mercury, indicating that there is little temperature difference between the illuminated and dark hemispheres. The effective surface temperature at 11 cm is between 250° and 300°K.

The observations of Venus indicate a slight decrease in effective temperature from about 600°K at centimeter wavelengths to about 500°K at decimeter wavelengths. Little or no change with phase angle was found in the apparent temperature at 11 cm.

Observations of Mars at 6, 11, and 21 cm indicate effective temperatures near 200°K, in good agreement with the infrared measurements.

The apparent temperature of Saturn was found to increase at longer wavelengths, reaching nearly 200°K at 11 cm and 300°K at 21 cm.

Uranus was found to have an equivalent temperature of  $130^\circ \pm 40^\circ\text{K}$  at 11 cm which, like Saturn, is about twice that expected from solar heating.

Kellermann, K.I., 1966, and Pauling-Toth, I.I.K., 1966, Observations of the radio emission of Uranus, Neptune, and other planets at 1.9 cm: *The Astrophysical Journal*, V. 145, p. 954-957.

The radio emission from Venus, Jupiter, Saturn, Uranus, Neptune, and Pluto has been investigated with the 140-foot radio telescope of the National Radio Astronomy Observatory at an effective wavelength of 1.9 cm.

The effective temperatures of the four major planets at 1.9 cm are all near 200°K, although their distance from the sun ranges from 5.2 to 30 a.u. At this wavelength the main source of opacity is probably due to the ammonia inversion line near 1.25 cm. Since the ammonia will not exist in a gaseous state in the cooler upper regions of the atmosphere, the level where  $\tau \sim 1$  on all the planets corresponds to a fixed effective temperature near the freezing point of ammonia, which is 195°K.

Koval, A.G., Koppe, V.T., and Fogel, Ya.M., 1966, CO, CO<sub>2</sub>, and NO emission spectra excited by 13-keV electrons: Soviet Astronomy - A.J., V. 10, No. 1, p. 165-175.

Emission spectra have been obtained for rarefied CO, CO<sub>2</sub>, and NO gases excited by electrons of 13-keV energy. Relative intensities are derived for all the emission bands in each spectrum. A comparison is made with the spectra of CO and CO<sub>2</sub> excited by 37-keV protons, and with the night-sky spectrum of Venus.

Kuz'min, A.D., 1966, Measurements of the brightness temperature of the illuminated side of Venus at 10.6 cm: Soviet Astronomy - A.J., V. 9, p. 995-998.

The brightness temperature of Venus, averaged over the visible disk, was measured at 10.6 cm near the superior conjunction ( $k = 0.84$ ) and found to be 550°K. Comparison with measurements made using the same apparatus and the same reference source 3C 48 revealed that the phase variation of the brightness temperature of Venus at this wavelength does not exceed 2.5%. The result does not agree with measurements of phase variation of 3.15 cm, emission of the planetary surface within the framework of the Troitskii theory, and the depths of penetration of the electrical wave; and apparently indicates a need for taking absorption in the Venusian atmosphere at the 3-cm wavelength into account.

Kuz'min, A.D., and Dent, W.A., 1966, The brightness temperature and polarization of Venus at 3.75-cm wavelength: Soviet Astronomy - A.J., V. 10, No. 3, p. 544-545.

Results are presented of measurements of the brightness temperature and polarization of the brightness temperature and polarization of the integrated radio emission of Venus at 3.75-cm wavelength, as obtained in August-September 1964 with the 26-m radio telescope of the University of Michigan. The instrumentation is described briefly. Near the angle  $\phi = 85^\circ$  the brightness temperature of Venus was measured as  $659 \pm 65^\circ\text{K}$ . A 1% upper limit was found for the polarization of the integrated radio emission.

Leftus, V., 1966, Radio emission of Venus at 3 cm and the solar activity: Nature, V. 211, p. 176.

An investigation was made of the possible dependence of the Venusian temperature on the instantaneous solar activity. The longitude differences of the earth and Venus were respected. A resulting value for the temperature, reduced to the conditions without solar activity, of 475°K is arrived at.

Low, F.J., 1966, Observations of Venus, Jupiter and Saturn at  $\lambda 20 \mu$ : The Astronomical Journal, V. 71, p. 191.

The first observations of the planets at  $20 \mu$  were reported by Low (Lowell Observatory Bulletin 128, 184, 1965). Using the same radiometer, which cuts on at  $17.5 \mu$  and is uniformly sensitive to about  $25 \mu$ , further observations have been made with angular resolutions between 4 and 35 arc sec. Under the assumption that Mars radiates as a blackbody, its brightness temperature at  $20 \mu$

was taken as  $225^{\circ} \pm 5^{\circ}\text{K}$ , the value measured for the disk at  $10\ \mu$ . This yielded a temperature for Venus at  $20\ \mu$  of  $248 \pm 10^{\circ}\text{K}$ , significantly above the  $10\text{-}\mu$  value of  $221 \pm 10^{\circ}\text{K}$  but in good agreement with solar heating. Using Mars and Venus as standards, it was possible to observe Saturn with angular resolutions both large and small compared to its disk. Correcting for the obscuration of the rings, which were found to be much colder than the planet, the mean disk brightness temperature was  $95 \pm 3^{\circ}\text{K}$ , quite close to the measured value of  $93^{\circ}\text{K}$  at  $10\ \mu$  (Low, F.J., *Astron. J.* 69, 550, 1964). Scans of Jupiter show a hot equatorial band,  $150 \pm 5^{\circ}\text{K}$ , covering about half the disk; the poles are about  $130^{\circ}\text{K}$ . Although the equatorial scans show significant limb darkening, the east and west limbs are equal in temperature to within the accuracy of measurement.

The total amount of energy Jupiter receives from the sun is less than the observed radiation between  $10$  and  $25\ \mu$  and would produce an effective temperature of only  $105^{\circ}\text{K}$ . Thus, an internal supply of energy must be present. The Jovian temperature measured at  $1\ \text{mm}$  is  $155 \pm 15^{\circ}\text{K}$  (Low, F.J., and Davidson, A.W., *Astrophys. J.* 142, 1278, 1965). If the brightness temperature between  $25\ \mu$  and  $1\ \text{mm}$  does not drop below  $140^{\circ}\text{K}$ , the total power radiated by Jupiter is more than 3 times the insolation. A similar conclusion may be drawn for Saturn; however, since only a small fraction of its total energy is observed, its excess brightness temperature at  $20\ \mu$  may be caused by a greenhouse effect. (Abstract of a paper presented at the March 1966 meeting of the American Astronomical Society).

Ohring, G., 1966, Water-vapor mixing ratios near the cloudtops of Venus: *Icarus*, V. 5, p. 329-333.

It has been argued that the observed amounts of water vapor in the Cytherean atmosphere are incompatible with the presence of an aqueous cloud. These arguments have been based upon a comparison of the water mixing ratios derived from the observations and the required saturation mixing ratio. In the present paper, it is shown that if the Cytherean water-vapor mixing ratio decreases with altitude in an isothermal atmosphere at rates comparable to those in the earth's upper troposphere, some of the observed amounts of water vapor, at the present state of our knowledge, are compatible with the presence of aqueous clouds on Venus.

O'Leary, B.T., 1966, Photometry of a Venus halo effect: *Transactions of the American Geophysical Union*, V. 47, No. 1, p. 156.

The commonly observed terrestrial halo consists primarily of a luminous ring  $22^{\circ}$  from the sun or moon and is due to hexagonal ice crystals that doubly refract light in the direction of minimum deviation in a manner analogous to prisms. This angle depends on the index of refraction of the crystal substance and on the crystal shape. A theory is proposed by which a halo effect may be disentangled from the photometric phase function of Venus. Three independent observations of Venus near the halo angle a few years ago have marginally shown the effect to occur both in magnitude and in color. A positive result would indicate the following: an unambiguous proof of ice as a constituent of the Venus cloud layer. The sizes of the crystals must be somewhat greater than a wavelength of light. The approximate abundance of the crystals could be derived. The crystal shapes would be largely hexagonal, and more detailed models of the Venus cloud layer could be constructed. (Abstract of a paper presented at the April 1966 meeting of the American Geophysical Union).

O'Leary, B.T., 1966, The presence of ice in the Venus atmosphere as inferred from a halo effect: *Publications of the Astronomical Society of the Pacific*, V. 78, p. 447-448.



Photometry of Venus was performed at Kitt Peak National Observatory in three colors, (B, V, and R) between phase angles  $153^\circ$  and  $165^\circ$  before and after inferior conjunction of 1966. These results along with an interpretive study of the photometric, colorimetric, and polarimetric characteristics of Venus as it passes through these phase angles suggest a halo effect of brightness amplitude 0.05 magnitude. The most common terrestrial halo phenomenon is a luminous ring located  $22^\circ$  from the sun or moon and is due to the presence of hexagonal ice crystals in the atmosphere. Although the existence of a Venus halo effect cannot now be definitely established, it is suggested by many types of observations and is not inconsistent with any observation. A halo effect would be definite proof of ice as a constituent of the Venus cloud layer because of the uniqueness of the angle and brightness, color, and polarization curves corresponding to an index of refraction of 1.31 and a hexagonal shape. The amplitude of the effect shows that, at most, a small fraction (a few percent) of the tops of the Venus clouds would consist of these halo-producing crystals. (Abstract of a paper presented at a meeting of the Astronomical Society of the Pacific, June 1966).

O'Leary, T.O., 1966, The presence of ice in the Venus atmosphere as inferred from a halo effect: *Astrophysical Journal*, V. 144, p. 754-766.

Photometry of the integrated light of Venus was performed at Kitt Peak National Observatory in three colors (B, V, and R) between phase angles  $153^\circ$  and  $165^\circ$  before and after inferior conjunction of 1966. These results along with an interpretive study of the photometric, colorimetric, and polarimetric characteristics of Venus as it passes through these phase angles suggest a halo effect of brightness dispersions of about 0.05 mag. brighter than the background phase-curve at predicted halo maximum and about 0.04 mag. fainter than the background phase-curve at predicted halo minimum. The corresponding polarizations of Venus observed near the halo maximum and minimum agree both in quantity and in direction with the predictions of Fresnel's laws of reflection as applied to the  $22^\circ$  halo.

A halo effect would indicate definite proof of ice as a constituent of the Venus cloud layer because of the uniqueness of the angle and the curves of brightness, color, and polarization corresponding to an index of refraction of 1.31 and a hexagonal shape. The findings then tentatively indicate confirmation of  $H_2O$  in the Venus atmosphere and a temperature and pressure environment at the cloud tops conducive to the formation of ice.

Plummer, W.T., and Strong, J., 1966, Conditions on the planet Venus: *Transactions of the American Geophysical Union*, V. 47, No. 1, p. 156.

Recent information about the composition of the Venus clouds and a new interpretation of radio brightness measurements have led to a model for the planet that is not unfavorable to life. Surface pressure and temperatures are discussed, and a scheme is proposed for the atmospheric circulation. The available observational material is shown to be consistent with this model, and some suggestions are made for future work. (Abstract of a paper presented at the April 1966 meeting of the American Geophysical Union).

Plummer, W., and Strong, J., 1966, A new estimate of the surface temperatures of Venus: *The Astrophysical Journal*, V. 144, p. 423.

The authors consider it premature to assign precise temperatures to various parts of Venus on the basis of present data, but point out that previous high estimates are not well supported.

Sagan, C., and Pollack, J.B., 1966, On the nature of the clouds and the origin of the surface temperature of Venus: *The Astronomical Journal*, V. 71, p. 178-179.

The authors have solved the combined anisotropic non-conservative multiple scattering radiative transfer problem in the Schuster-Schwarzschild approximation and the related Mie theory problem for ice crystals, and have succeeded in reproducing the visible and near-infrared albedo variation of Venus, as determined by Strong and others, after appropriate allowance has been made for telluric and Cytherean gaseous absorbers. Ice crystals with mean radii  $\sim 7.5 \mu$  match the observations satisfactorily; water droplets at  $T > 280^\circ\text{K}$  do not. This spherical particle radius is consistent with polarimetric observations, which refer to somewhat higher altitudes.

With surface pressures  $\sim 30$  atm, and the upper limits  $\text{H}_2\text{O} \sim 100 \text{ g cm}^{-2}$  and  $\text{CO}_2 \sim 10^6 \text{ cm-atm}$ , cloudless greenhouse models can account for almost all of the high surface temperature. With the same surface pressure but lower limits on  $\text{H}_2\text{O}$  and  $\text{CO}_2$ , clouds are required to close infrared radiation leaks through atmospheric windows. We find that the same ice clouds which explain the observed albedos can, because they are poorly absorbing and strongly forward-scattering in the visible, but strongly absorbing and nearly isotropically scattering in the infrared, provide the additional opacity needed to construct consistent Venus greenhouse models. With their underlying atmosphere, the same clouds--primarily ice crystals, with water droplets towards their bottoms--account, with no further assumptions, and within observational error, for the general millimeter spectrum, the millimeter phase effect, the Mariner II microwave limb-darkening, and the infrared limb-darkening of Venus. (Abstract of a paper presented at the December 1965 meeting of the American Astronomical Society).

Samuelson, R.E., 1966, Greenhouse effect in semi-infinite scattering atmospheres: *The Astronomical Journal*, V. 71, p. 179.

The method of discrete ordinates is extended to describe the steady state intensity distribution of thermal radiation and the corresponding depth-dependent thermal structure of a plane-parallel semi-infinite particulate medium in radiative equilibrium in the presence of an outside point source of visible radiation. The greenhouse factor  $B(\tau)/F(0)$  is found to approach a finite limit as  $\tau \rightarrow \infty$ . Phase functions and albedos for single scattering in the infrared are computed for a wide variety of complex indices of refraction and particle size distributions in accordance with the Mie theory. Three sets of single scattering parameters in the infrared are chosen from these computations to be representative of a wide range of physically interesting conditions. Appropriate visible radiation single scattering parameters are selected accordingly, and the equation of transfer solved, in accordance with the theory, for the temperature profile and the law of darkening relevant for each of the models. Numerical calculations show that the diffuse field of visible radiation generated by multiple scattering processes is extremely effective in heating the lower regions of a particulate atmosphere. In particular, with albedos for single scattering in the visible of  $\omega_0^v = 0.99$  and in the infrared of  $\omega_0^i = 0.5$ , and for equal particle cross sections in both wavelength regions, it is found that surface temperatures of  $T_s \sim 700^\circ\text{K}$  and effective temperatures of  $T_E \sim 400^\circ\text{K}$  may be obtained. In this model the sun is assumed to be at normal incidence and at a distance comparable to that relevant for Venus. For slightly more realistic single scattering parameters than those considered in this study, it would appear that the large differences in temperature between the surface and the effective level of infrared radiation of Venus, as inferred from the infrared and microwave observations, can be mostly accounted for. (Abstract of a paper presented at the December 1965 meeting of the American Astronomical Society).

Smith, W.B., Shapiro, I.I., and Ash, M.E., 1966, Preliminary results from processing radar and optical planetary observations: *The Astronomical Journal*, V. 71, p. 871-872.

Preliminary values of a number of astronomical constants have been obtained from the simultaneous processing of planetary radar data spanning the interval from 1959 to July 1966 and of U.S. Naval Observatory optical data extending from 1950 to 1965. Results obtained using general relativity (Newtonian) theory with their formal standard errors are: a.u.,  $499.004786 (499.004785) + 0.000005$  light-sec; Mercury radius,  $2434 (2440) + 2$  km; Venus radius,  $6056 (6056) + 1$  km; Mercury mass,  $6021000 (6029000) + 53000$ ; Venus mass,  $408250 (408450) + 120$ ; earth plus moon mass,  $328900 (328950) + 60$ ; Mars mass,  $3111000 (3107000) + 9000$ ; earth-moon mass ratio,  $81.3030 (81.3024) + 0.005$ . The planetary masses are given as inverses in terms of the solar mass. (Abstract of a paper presented at the July 1966 meeting of the American Astronomical Society).

Spinrad, H., 1966, Resolution of the  $\text{CO}_2$  "hot band" in the Venus spectrum: The Astrophysical Journal, V. 145, p. 943-945.

A series of weak absorption lines at  $8736-8768 \text{ \AA}$  in the Venusian spectrum are identified as hot bands of  $\text{CO}_2$ , and this indicates a  $\text{CO}_2$  rotational temperature of near  $450^\circ\text{K}$ . Thus, the hot bands originate deep in the Venus cloud layer, far below the "cloud tops" at  $230^\circ\text{K}$ , the usually quoted infrared temperature.

Spinrad, H., and Shawl, S.J., 1966, Water vapor on Venus--a confirmation: Astrophysical Journal, V. 146, p. 328.

On three Lick Observatory coude spectrograms of Venus the authors have found several Doppler-displaced lines of water vapor originating in the atmosphere of Venus. The Cytherean absorption lines are quite weak, and a dispersion of  $1.9 \text{ \AA/mm}$  was required to detect them. This work confirms the Venus  $\text{H}_2\text{O}$  detection by balloon of Bottema, Plummer, and Strong (1964) and the recent ground-based photoelectric observations by Belton and Hunten (1966).

Staelin, D.H., and Barrett, A.H., 1966, Spectral observations of Venus near 1-centimeter wavelength: The Astrophysical Journal, V. 144, p. 352.

During June and July 1964, measurements of Venus were made with a five-channel microwave radiometer operating at wavelengths of 0.93, 1.02, 1.18, 1.28, and 1.37 cm simultaneously. A single-channel radiometer at 1.42-cm wavelength was used separately. The antenna was a 28-foot paraboloid located at Lincoln Laboratory, Massachusetts Institute of Technology. The spectrum of Venus was determined by comparison with the moon. The antenna patterns measured at each frequency were used to relate the observations of the moon and Venus. The absorption in the terrestrial atmosphere was determined by solar extinction measurements and by measurements of ground-level humidity. The average observed brightness temperatures and relative rms uncertainties for thirteen separate experiments were:  $430^\circ \pm 24^\circ\text{K}$ ,  $463^\circ \pm 32^\circ\text{K}$ ,  $428^\circ \pm 20^\circ\text{K}$ ,  $450^\circ \pm 23^\circ\text{K}$ ,  $404^\circ \pm 28^\circ\text{K}$ , and  $572^\circ \pm 82^\circ\text{K}$ , in order of increasing wavelength. The results suggest that near 1.3-cm wavelength there was a resonant absorption feature that was most prominent within a few weeks of inferior conjunction, and that disappeared approximately five weeks after conjunction. This time variation is consistent with the results of other observers. The suggested feature is near the wavelength of a strong water-vapor resonance.

Staelin, D.H., and Neal, R.W., 1966, Observations of Venus and Jupiter near 1-cm wavelength: The Astronomical Journal, V. 71, p. 872.

A search for spectral features on Venus and Jupiter was made from January to March 1966. Five Dicke-type radiometers were connected simultaneously to the antenna feed by means of frequency-selecting filters. They operated at 19.0, 21.0, 22.235, 23.5, and 25.5 GHz. The following results were obtained:

Freq. (GHz)	Venus			Jupiter		
	<T <sub>B</sub> > (°K)	Rel. (%)	Abs. (%)	<T <sub>B</sub> > (°K)	Rel. (%)	Abs. (%)
19.0	477	+8	+12	105	+20	+20
21.0	451	+4	+9	106	+9	+10
22.235	436	+4	+9	98	+10	+11
23.5	418	+4	+9	116	+8	+9
25.5	400	+4	+9	123	+7	+9

(Abstract of a paper presented at the July 1966 meeting of the American Astronomical Society).

Walker, R.G., and Sagan, C., 1966, The ionospheric model of the Venus microwave emission: An obituary: *Icarus*, V. 5, p. 105-123.

In the ionospheric model of Venus, the observed microwave radiation is attributed to free-free emission of electrons in a dense Cytherean ionosphere. The present paper discusses the mechanisms for formation of such a dense ionosphere, both in the original formulation of Jones and in later formulations which introduce holes in the ionosphere to achieve consistency with the observed radar reflectivities. Ionization by solar ultraviolet radiation and by the solar proton wind, as measured near Venus by Mariner 2, are considered. If dissociative recombination prevails, characteristic values of the electron density are  $n_e \sim 10^8 \text{ cm}^{-3}$  over a region of 50-km thickness. If radiative recombination prevailed,  $n_e \sim 10^9 \text{ cm}^{-3}$  would result, but even this is too small for the ionospheric model to be a valid explanation of the Venus microwave emission. The ionospheric model is accordingly rejected. We conclude that the observed microwave emission arises from the Cytherean surface.

Westphal, J.A., 1966, The 10-micron limb darkening of Venus: *Journal of Geophysical Research*, V. 71, p. 2693-2696.

Observations of 8- to 14- $\mu$  flux from diametric scans of Venus with the 200-inch Hale telescope have been made. The reduced data indicate an unexpected brightening near the Cytherean limb. The data show a more complicated atmospheric structure than postulated by published models. Horizontal inhomogeneity of the emission complicates the interpretation.

Zander, R., 1966, Spectral scattering properties of ice clouds and hoarfrost: *Journal of Geophysical Research*, V. 71, p. 375-378.

The infrared reflectivity of ice clouds, hoarfrost, and many other constituents was measured in the infrared. This paper relates the strong similarity in the over-all spectral scattering for ice clouds and frost deposits. Infrared reflectivity of ice and water clouds is of importance in estimating the effective total albedo of the earth, since half of the energy in the solar constant lies in the infrared, as well as in determining the composition of the clouds of Venus.

### 3.8 Tektites

Baker, G., 1966, External form and structure of some hollow australites: *Geochimica et Cosmochimica Acta*, V. 30, p. 607-615.

Thirteen hollow australites, 1.15-3.25 cm in diameter, range in weight from 0.717 to 12.539 g. Most are weathered by abrasion and/or by natural solution etching, but the internal cavity remains intact in each specimen. The volumes

of the internal cavities range from 0.002 cm<sup>3</sup> in the smallest form, to 4.0 cm<sup>3</sup> in the largest form, and the specific gravity values of the hollow specimens range from 2.420 in the second smallest form to 1.357 in the largest form. Although specific gravity values generally decrease towards the larger, heavier specimens with their usually larger internal cavities, specimens in the 2.2-5.8 g weight range show slight departures from this trend according to the size of the internal cavity relative to the amount of enclosing tektite glass. Thus, specimens of similar weight and size do not always have internal cavities of similar size, and a somewhat larger specimen does not always have a larger internal cavity than a somewhat smaller specimen.

Baker, G., 1966, Hollow australite button with Flange, Hordern Vale, Otway Peninsula, Western Victoria: *Meteoritics*, V. 3, p. 35-53.

A relatively thin walled hollow australite button recently discovered in an unbroken condition on the surface of a shallow sand pit in the Otway Ranges, Victoria, contains a double internal cavity with a total calculated volume of approximately four cubic centimeters. A little over half of a well developed circumferential flange is still attached to the hollow core of the specimen, the missing portion having been removed by terrestrial erosion. The front surface reveals a well preserved aerodynamic sculpture pattern such that the orientation of the specimen during hypersonic atmospheric transit can be accurately determined to show its aerodynamically stable flight position.

Such double bubbles are unique among Australian tektites, whether in the fractured or well preserved state, and it is equally as uncommon to find an unbroken hollow australite core with remnants of still attached circumferential flange.

Barnes, V.E., and Russell, R.V., 1966, Devitrification of glass around collapsed bubbles in tektites: *Geochimica et Cosmochimica Acta*, V. 30, p. 143-152.

Devitrification was first observed around partly collapsed bubbles (vacuoles) in Santa Mesa philippinites heated by the fire which destroyed Manila near the end of World War II. This localization of devitrification furnishes independent evidence that bubbles in normal tektites were formed by water vapor and that the very low pressure in normal tektite bubbles resulted from the absorption in or reaction of the water vapor with the surrounding tektite glass. Although tektites are essentially anhydrous they do contain a trace of water, in fact more than enough to form all the bubbles found in tektites. Experiments show that a similar amount of devitrification and partial collapse of bubbles takes place in philippinites when heated about 4 days at a temperature of 825°C. Under identical conditions of time and temperature australites, indochinites and javanites showed equivalent amounts of change in shorter times. Bidasites showed no change in 7 days. Neither collapse nor devitrification took place around bubbles in Muong Nong-type tektites, indicating that water vapor was not an important constituent of the gas forming these bubbles and that the pressure in the bubbles approaches equilibrium with atmospheric pressure.

Booker, J.R., and Harrison, C.G.A., 1966, Magnetic properties of tektites: *Transactions of the American Geophysical Union*, V. 47, No. 1, p. 144-145.

The intensity of magnetization in most tektites is less than  $10^{-7}$  emu/g. However, they have a measurable susceptibility of the order of  $5 \times 10^{-6}$  emu/g. After heating in a field of 0.5 oersted, tektites show a remarkable increase in magnetization, which suggests that they were formed in a magnetic field considerably smaller in strength than the earth's field. (Abstract of a paper presented at the April 1966 meeting of the American Geophysical Union).

Brett, R., 1966, Metallic spherules in impactite and tektite glasses: Transactions of the American Geophysical Union, V. 47, No. 1, p. 145.

Electron-microprobe analyses indicate that Ni-Fe spherules within impactite glass bombs from the Canyon Diablo area, Arizona, contain from 20 to 65 weight % Ni. Spherules from impactite glass at Wabar, Saudi Arabia, contain 12-41 weight % Ni. The parent meteorites contain 7-8 weight % Ni. Microprobe analysis indicates that the glass surrounding the spherules is enriched in iron. The glass surrounding tektite spherules is not enriched in Fe. Therefore, some mechanism is considerably enriching the metal and glass in nickel and iron, respectively, in impactites, but not in tektites. It is proposed that spherules in impactite glasses were partially oxidized before incorporation into impactite bombs. After incorporation, the almost Ni-free Fe oxide diffused into the glass, thus enriching it in Fe. Spherules in tektites were not oxidized because the tektites were formed in an atmosphere with extremely low fugacity of oxygen. A less likely alternative is that the spherules were incorporated into the tektite glass instantaneously so that oxidation was prevented. (Abstract of a paper presented at the April 1966 meeting of the American Geophysical Union).

Centolanzi, F.J., and Chapman, D.R., 1966, Vapor pressure of tektite glass and its bearing on tektite trajectories determined from aerodynamic analysis: Journal of Geophysical Research, V. 71, p. 1735-1749.

Various experiments have been conducted to resolve a large discrepancy between two measurements that have been reported for the vapor pressure of tektite glass. This discrepancy significantly affects the trajectories and mode of tektite origin as determined from calculations of aerodynamic ablation. Measurements in a furnace of vaporization rate relative to that of four different standards ( $\text{SiO}_2$ ,  $\text{TiO}_2$ , Au, Ag) yield mutually concordant results for tektite vapor pressure. Also, measurements in an arc jet of the stagnation temperature, the rate of surface recession, and the mass loss during aerodynamic ablation are in mutual agreement with the results from vaporization rate measurements.

Further observations of flash boiling occurring under certain experimental conditions, and not occurring under others, provide a bracketing of tektite vapor pressure that is also compatible with the other measurements. Over the temperature range of the present experiments, 1700 to 3000°K, a least-squares fit to the data is represented by  $P(\text{atm}) = \exp[18.5 - 57,400/T(^{\circ}\text{K})]$ . These various experimental results demonstrate that previous measurements by other investigators of the pressure for incipient bubbling do not represent tektite vapor pressure but, instead, some bubble pressure that at certain temperatures is as much as a million times higher than the vapor pressure. Some recent aerodynamic calculations of very shallow, grazing tektite trajectories, which were based on bubble-pressure measurements, are therefore invalid; other calculations of relatively steep, direct-entry trajectories are not affected significantly by the new vapor-pressure data.

Chao, E.C.T., Dwornik, E.J., and Merrill, C.W., 1966, Nickel-iron spherules from Aouelloul glass: Science, V. 154, p. 759-765.

Nickel-iron spherules were found in glass associated with the Aouelloul Crater. It is concluded that the glass is of terrestrial origin.

Clarke, R.S., Jr., Wosinski, J.F., Marvin, R.F., and Friedman, I., 1966, Potassium-argon ages of artificial tektite glass: Transactions of the American Geophysical Union, V. 47, No. 1, p. 144.

It is reasonable to assume that tektites were formed by melting pre-existing material that contained geologically old K and a related amount of  $^{40}\text{Ar}$ . The assumption that all  $^{40}\text{Ar}$  is expelled from the melt at the time of formation is

made in calculating the K-Ar ages of tektites. Potassic glasses of average tektite composition were prepared from geologically old raw materials. One batch contained K in the form of a Precambrian feldspar, while the second contained K in an Ordovician sandstone that contained appreciable feldspar. Several glasses were made from the batches using different heat treatments and apparent K-Ar ages were measured. Apparent ages ranged from zero to over 1 m.y. The data indicate that the assumption of complete loss of  $^{40}\text{Ar}$  may not be completely valid, and the interpretation of K-Ar dating as applied to tektites may need re-evaluation. (Abstract of a paper presented at the April 1966 meeting of the American Geophysical Union).

Cobb, J.C., 1966, A trace element study of tektites: Transactions of the American Geophysical Union, V. 47, No. 1, p. 145.

Tektite samples from various localities have been analyzed by neutron activation followed by gamma counting on a lithium drifted germanium detector. The resolution of this detector is such that many elements can be measured by gamma counting without any chemical processing of the sample. Elements detected in this way include: Fe, Na, Mn, Cr, Th, Sc, Co, Hf, Sb, as well as the lanthanide elements La, Ce, Sm, Eu, Yb, and Lu. Abundances of these elements among the various tektite groups will be compared.

David, E., 1966, Meteorite impacts and the ejection mechanism of tektites: Earth and Planetary Science Letters, V. 1, No. 2, p. 75-76.

The possibility that tektites could be formed by meteorite impact on the surface of the earth has been frequently rejected because no mechanism has been found which explains the large distances over which the tektites appear to travel. This paper presents a description of meteoritic impact according to which the ejection of collision fragment out of the atmosphere is possible, and which therefore can explain the large distances of tektites travel. The horizontal expansion of the compressed, overheated impact vapor against the air of normal density stops within ten kilometers. Vertically the barometric decrease of air density soon exceeds the pressure decrease of the expanding rock vapor which shoots out into free space in a large cone, with a streaming velocity of at least 3 km/s. Fortuitously favorable injection conditions combined with an event which needs not surpass the Reis event in order of magnitude might have given rise to the enormous quantity of the southeast Asian-Australian tektites.

Faul, H., 1966, Tektites are terrestrial: Science, V. 152, p. 1341-1345.

Geochronologic evidence is presented in favor of the theory of terrestrial origin of tektites from large impact craters. Ivory Coast tektites are related to the Bosumtwi crater, and Moldavites to the Ries crater. No crater has been found for the North American and Australasian tektites.

Gentry, R.V., 1966, Antimatter meteorite explosions relative to fission track ages of tektites: Transactions of the American Geophysical Union, V. 47, No. 4, p. 618.

Previous attempts to account for the considerable variation of fission track ages in the Georgia and Australian tektite fields have been on the basis of post-arrival heating events. If tektites are assumed to have originated with antimatter meteorite explosions (lunar or terrestrial), then another source of error in fission track ages is possible. Using nuclear explosion data, calculations show that small but significant amounts of certain short half-life spontaneous fissionable nuclides may be produced by the interaction of the high neutron flux from an antimatter burst with the  $\text{U}^{238}$  fraction in the vaporized material. Subsequent incorporation of these short half-life nuclides into molten tektites material would then produce large background fission track densities. Thus, anomalously high fission track ages would result in some tektites. If this



hypothesis is correct it would tend to support geological evidence of recent tektite infalls. Electron microprobe analysis of several unusual structures in biotite is discussed relative to antimatter burst phenomena. (Abstract of a paper presented at the September 1966 meeting of the American Geophysical Union).

Johnson, R.H., 1966, Flow instabilities relating to the surface markings of tektites: *Journal of Geophysical Research*, V. 71, p. 945-949.

Experimental study has shown that the instability of the hypersonic shock layer flow over blunt bodies with surface cavities is coupled to the dynamic stability of the body. The ablative action in the cavities and the body motion induced by the cavity flow may possibly provide evidence of aerodynamic origin of surface markings on some tektites.

King, E.A., Jr., 1966, Baddeleyite inclusion in a Georgia tektite: *Transactions of the American Geophysical Union*, V. 47, No. 1, p. 145.

A baddeleyite inclusion has been identified in Georgia tektite DGA-1 by electron microprobe and X-ray diffraction techniques. The grain is an idiomorphic pseudomorph of baddeleyite and an unidentified silica phase after zircon, and is completely enclosed in the tektite glass. This inclusion differs markedly from the baddeleyite inclusion identified in the Martha's Vineyard tektite by Clarke and Wosinski. The inclusion in DGA-1 is almost identical to baddeleyite studied by El Goresy in the Aquelloul and Ries impact glasses, and is additional evidence of the impact origin of tektites. (Abstract of a paper presented at the April 1966 meeting of the American Geophysical Union).

King, E.A., Jr., 1966, Major element composition of Georgia tektites: *Nature*, V. 210, p. 828.

A new analysis of a Georgia tektite (DGA-2) is presented. On the basis of the Georgia tektite analyses now available, the Georgia tektites are found to be very similar in their major elemental composition to silica-rich bediasites. The Georgia tektites show decreasing contents of alumina, ferrous iron, and possibly titania with increasing silica. The variation of soda with potash defines a trend that does not overlap values observed in any bediasite yet analyzed. In view of the identical potassium-argon ages, close chemical similarity, and general geographic association, the North American tektites are probably the product of a single event. However, the Georgia tektites and the specimen from Martha's Vineyard can be classed as a distinct subgroup characterized by low soda: potash ratios.

Levengood, W.C., 1966, Internal elastic energy variations in tektites: *Journal of Geophysical Research*, V. 71, p. 613-618.

Four varieties of tektites were quantitatively examined for stress response effects using a technique based on surface defect formation. A parameter of surface flaw length was shown to increase linearly with the square root of applied load on an indenter tool. A critical stress  $\sigma_c$  for defect formation was calculated from the slopes of the empirical curves. An intercept constant  $b$  gave an indication of the yield in the tektite structures during the initial loading. As a group the  $\sigma_c$  and  $b$  values were similar in the tektites, the values indicating a less ordered structure than in a natural obsidian and more order than in commercial glasses. Both  $\sigma_c$  and the constant  $b$  were found to change systematically with the K/Ar ages of the tektites. The nature of these variations suggest the formation of ordered, clustered groupings in the glass network which increase with the geologic age of the tektite. The general similarities in the structures of the tektites indicate a common environment of formation.

Lin, S.C., 1966, Cometary impact and the origin of tektites: *Journal of Geophysical Research*, V. 71, p. 2427-2437.

The possibility of a terrestrial origin of tektites is re-examined in the light of recent aerodynamic evidence presented by Chapman, Larson, and Anderson. It is found that even though existing evidence points strongly toward a lunar origin as most probable for Australasian tektites, there still exists the possibility that these small glassy objects originated on the earth. In particular, it is conceivable that a sufficiently energetic cometary collision of the type hypothesized earlier by Urey could momentarily blow a bubble through the earth's atmosphere and hence propel small objects over intercontinental distances. The minimum mass of a comet head required to accomplish such a feat is estimated to be about  $5 \times 10^{17}$  grams. Some obvious questions which remain to be answered in order to support such a model of tektite origin are discussed.

O'Keefe, J.A., 1966, Lunar questions discussed at Pasadena: *Sky and Telescope*, V. 31, p. 10-12.

A popular summary of a conference held in September 1965: Various authors discussed the origin of the craters, the heat balance of the moon, the origin of tektites and other lunar problems.

O'Keefe, J.A., 1966, Muong Nong tektites and lunar ash flows: *The Astronomical Journal*, V. 71, p. 393-394.

Barnes has pointed out that the parent material from which tektites came is probably closely represented by what he calls the Muong Nong type. He has also drawn attention to the presence of angular voids in these tektites. The meaning of the angular voids is probably that the material consists of fragments incompletely welded together. This fact makes possible a test of theories of the origin of tektites.

If tektites are terrestrial, then the fragments should correspond at least in their chemical constitution to typical particles of soil or sedimentary rock (they cannot be terrestrial igneous rock because of differences in chemistry). If they are of lunar origin, the theories of O'Keefe and Cameron indicate that they should be particles of volcanic ash constituting a welded tuff.

Tracings made with the electron microprobe show that the material is homogeneous over large areas with the exception of inclusions of silica which form a few percent of the mass. The chemistry of the glass does not correspond to any known ordinary mineral; yet it could not have been produced by the melting of a sedimentary rock because the angular voids show us that the Muong Nong material was glass before the impact took place.

Their structure under the microprobe resembles a terrestrial welded tuff except that the borders of the separate bits of ash (shards) are more difficult to distinguish because of the absence of devitrification. (Abstract of a paper presented at the March 1966 meeting of the American Astronomical Society).

Philpotts, J.A., and Pinson, W.H., Jr., 1966, New data on the chemical composition and origin of moldavites: *Geochimica et Cosmochimica Acta*, V. 30, p. 253-266.

Twenty-three new major-element analyses of moldavites are reported. The samples include seventeen Bohemian and six Moravian tektites. The Rb and Sr contents and the Rb/Sr ratios are also reported for the 23 specimens. The densities and refractive index values range from 2.3312 to 2.3718 g/cm<sup>3</sup> and from 1.486 to 1.495, respectively. In contrast to the australites, the moldavites display significant negative correlations between the alkali metals (Na and Rb) and the alkaline earths.

The relationships in the chemical compositions of moldavites appear to be unlike those of sedimentary or igneous rocks. It is suggested that the observed variations in composition are largely due to fractional volatilization. The wide range of Rb/Sr ratios in conjunction with the uniformity of the Sr isotopic composition supports this theory.

Seeger, C.R., 1966, Sound wave velocities in some tektites and natural glasses: Transactions of the American Geophysical Union, V. 47, No. 1, p. 144.

Sound wave velocities (compressional and surface) have been measured in eleven tektites (two philippinites, two indochinites, one australite, and six moldavites). Also, two "americanite" glasses (Peru), and samples of Aquelloul Crater glass, Darwin glass, and Libyan Desert glass have been measured. The measurements on tektites show the same lack of variation as other properties (e.g., density and chemical composition); the compressional wave velocities vary by only about 6%. The other natural glasses show slightly greater variations. This is an additional indication of the unity of origin of the tektites. The technique may have other petrologic applications. (Abstract of a paper presented at the April 1966 meeting of the American Geophysical Union).

Shima, M., 1966, Glassy spherules (microtektites?) found in ice at Scott Base, Antarctica: Journal of Geophysical Research, V. 71, p. 3595-3596.

In the precipitate of melted ice collected on December 20, 1964, near Scott Base, Antarctica, glassy spherules were found under the microscope. The composition, shape, and refractive index of some of these spherules suggest that they are microtektites.

Shute, B.E., 1966, Geocentric initial conditions of trajectories originating at the moon's surface: The Astronomical Journal, V. 71, p. 602-609.

A reduced form of the patch conic method has been employed to determine the initial elements of a particle launched or ejected from the moon's surface with any arbitrary starting conditions. The reduction was obtained by considering the selenocentric velocity asymptotes. Explicit and tractable analytic functions have been derived for the geocentric energy, the Jacobi constant, the angular momentum, standard orbital elements, and conditions for moon-to-earth trajectories. Percents of randomly ejected material which initially strike earth, are in retrograde orbits, or go into heliocentric orbits have been obtained. The results are compared with results obtained by a numerical integration program for several different situations.

Shute, B.E., 1966, Geocentric initial conditions of trajectories originating at the moon's surface: The Astronomical Journal, V. 71, p. 870-871.

A reduced form of the patch conic method has been employed to determine the initial orbital elements of a particle launched or ejected from the moon's surface with any arbitrary starting conditions. The reduction was obtained by considering the selenocentric velocity asymptotes. Explicit and tractable analytic functions have been derived for the geocentric energy, the Jacobi constant, the angular momentum, standard orbital elements, and conditions for moon-to-earth trajectories. A minimum value of 2.51 km/sec ejection velocity is necessary for moon-to-earth trajectories, provided that the selenocentric velocity asymptote is opposed to the direction of the moon's motion. As the ejection velocity increases, the region where the velocity asymptotes may be located moves along the plane of the moon's orbit about the earth toward the earth-moon line. The maximum percent of material thrown into a direct moon-to-earth trajectory is 3.3% at a value of 2.62 km/sec ejection velocity. (Abstract of a paper presented at the July 1966 meeting of the American Astronomical Society).

Shute, B.E., 1966, Moon-to-earth trajectories and the origin of tektites: Transactions of the American Geophysical Union, V. 47, No. 3, p. 486.

Two hypotheses of the mode of tektite arrival on earth have been proposed, supposing a lunar origin: (1) they are formed on the moon's surface, during crater formation, (2) they are formed in the earth's atmosphere during a grazing entry of a large parent body. Analytic means have been used to investigate typical fall patterns of direct moon-to-earth trajectories from the crater Tycho. The indicated geographical spreads are consistent if a jet confined to  $2^\circ$  in azimuth and elevation angle is assumed at the crater origin. It does not appear that the entry angle into the earth's atmosphere will correspond uniformly to the location of fall as assumed in Chapman's discussion of the Australasian strewn field. The evidence provided by the theory of moon-to-earth trajectories tends to support the parent body hypothesis. (Abstract of a paper presented at the September 1966 meeting of the American Geophysical Union).

Tatlock, D.B., 1966, Some alkali and titania analyses of tektites before and after G-I precision monitoring: *Geochimica et Cosmochimica Acta*, V. 30, p. 123-128.

A comparison of 55 older analyses of Australasian tektites with 110 modern precisely monitored analyses suggests that more than half of the older alkali and titania determinations are decidedly inaccurate and misleading. Deviations of the older analyses from the restricted values of the modern analyses are comparable to the imprecisions shown by early analyses of G-I granite and W-I diabase. This suggests that a high percentage of older alkali and titania analyses, such as those of Washington's tables, are of questionable quality.

Taylor, H.P., Jr., and Epstein, S., 1966, Oxygen isotope studies of Ivory Coast tektites and impactite glass from the Bosumtwi Crater, Ghana: *Science*, V. 153, p. 173-175.

Comparison between oxygen isotope ratios of Ivory Coast tektites and Bosumtwi Crater glass suggests a terrestrial origin of these tektites.

Taylor, S.R., 1966, Australites, Henbury impact glass and subgreywacke: a comparison of the abundances of 51 elements: *Geochimica et Cosmochimica Acta*, V. 30, p. 1121-1136.

Data are presented for 51 elements in two subgreywackes and a meteorite impact glass from Henbury, Australia, and for five australites covering the range in composition for this group of tektites. There are no significant differences in composition between the impact glass and the parental subgreywackes, and no effective alteration in concentration has taken place during melting for the elements studied. The australites are closely similar in composition to the Henbury glass and sedimentary rocks, except that Ca and Sr are enriched, and the chalcophile elements Cu, Pb, Sn, Tl, In and Bi are depleted in the tektites. From analogy with the impact glass-sediment relations, these variations are considered to be present in the tektite parent material, which otherwise is equivalent in composition to terrestrial subgreywacke.

Vand, V., 1966, Monro jets and the origin of tektites: *Nature*, V. 209, p. 496.

The author had previously proposed a detailed mechanism of a tektite jet formation through an implosion of a conical cavity lined with molten glass which is formed immediately after impact, and showed that a jet of tektites can survive the upward atmospheric journey if of sufficient total mass.

Using the results of other authors on jets formed from imploding bubbles, he elucidates the operating mechanism and applies it to Riess Kessel, and speculates that the general inward motion of other crater materials caused by the passage of

waves reflected from below will also be responsible for the formation of a central peak in some craters, if underlain by denser strata at favourable depth. The author also states that similar interpretation of central peaks of lunar craters might help in mapping such discontinuities under the lunar surface.

Vorob'yev, G.G., 1964, New finds and new tektite deposits in southern Bohemia: *Akademiia Nauk SSSR Meteoritika*, No. 25, p. 178-187.

This report is compiled from information furnished by members of the Young People's Astronomy Circle in Ceske-Budejovice, Czechoslovakia. Fourteen more tektite deposits have been found in southern Bohemia, in addition to the 40 known ones. Their locations are shown on a sketch map. A total of 294 specimens, altogether weighing 1,087 g, have been found to date. The tektite localities are up to several hundred meters in extent; typically the tektites are found in soil, sand, and gravel in fields and meadows or along rivers and lakes. They are waterworn to varying degrees. There is some indication that the tektites found west and south of Ceske-Budejovice are different. More detailed work on the Bohemian field is necessary in order to ascertain the conditions of occurrence and of origin of these tektites. (From *Geophysical Abstracts*, No. 217).

Wampler, J.M., Smith, D.H., and Cameron, A.E., 1966, Isotopic comparison of lead from Ivory Coast tektites and Bosumtwi Crater materials: *Transactions of the American Geophysical Union*, V. 47, No. 1, p. 145.

Lead from samples of two Ivory Coast tektites has the isotopic composition:  $Pb^{206}/Pb^{207} = 1.184$ ,  $Pb^{206}/Pb^{208} = 0.494$ ,  $Pb^{208}/Pb^{204} = 18.1$ . Whereas lead from tektites of other groups is quite similar to relatively young terrestrial lead samples, the Ivory Coast tektite lead is slightly higher in  $Pb^{204}$  and lower in  $Pb^{206}$  than most terrestrial lead samples with a similar  $Pb^{206}/Pb^{207}$  ratio. The hypothesis that Ivory Coast tektites are derived from terrestrial materials at Lake Bosumtwi, Ghana, is examined. Although none of the Lake Bosumtwi samples contained lead identical to that of the tektites, the qualitative similarities support the hypothesis that the tektite material is of terrestrial origin. (Abstract of a paper presented at the April 1966 meeting of the American Geophysical Union).

Yagi, K., 1966, Discussion of paper by J.A. O'Keefe and E.W. Adams, "Tektite structure lunar ash flows": *Journal of Geophysical Research*, V. 71, p. 5492-5493.

O'Keefe and Adams made theoretical calculations of the pressure, temperature, and voidage of ash flows on the earth and on the moon. Although the author commends their theoretical work on the mechanism of ash flows, he disagrees with some of the geological implications concerning the origin of tektites. In particular, the fabric of welded tuff should be rare on the moon and its presence in tektites should not be taken as an indication of a lunar origin. It also seems unlikely on geochemical grounds that tektites were formed for lunar ash flows, which should be similar in composition to the acid differentiate of a basaltic magma. O'Keefe and Lowman respond to these points in a reply which follows.

Unclassified  
Security Classification

DOCUMENT CONTROL DATA - R&D		
(Security classification of title, body of abstract and indexing annotation must be entered when the overall report is classified)		
1. ORIGINATING ACTIVITY (Corporate author) Air Force Cambridge Research Laboratories (CRF) United States Air Force Bedford, Massachusetts 01730		2a. REPORT SECURITY CLASSIFICATION <u>Unclassified</u> 2b. GROUP
3. REPORT TITLE BIBLIOGRAPHY OF LUNAR AND PLANETARY RESEARCH Supplement No. 2 -- 1966		
4. DESCRIPTIVE NOTES (Type of report and inclusive dates) Scientific. Interim.		
5. AUTHOR(S) (Last name, first name, initial) J. W. Salisbury, Editor		
6. REPORT DATE September 1967	7a. TOTAL NO. OF PAGES 235	7b. NO. OF REFS
8a. CONTRACT OR GRANT NO.	9a. ORIGINATOR'S REPORT NUMBER(S) AFCRL-67-0518	
a. PROJECT AND TASK NO. 8602-01-01	9b. OTHER REPORT NO(S) (Any other numbers that may be assigned this report) Special Report No. 67	
c. DOD ELEMENT 6144501F		
d. DOD SUBELEMENT 681311		
10. AVAILABILITY/LIMITATION NOTICES Distribution of this document is unlimited. It may be released to the Clearinghouse, Department of Commerce, for sale to the general public.		
11. SUPPLEMENTARY NOTES TECH, OTHER	12. SPONSORING MILITARY ACTIVITY Air Force Cambridge Research Laboratories (CRF) United States Air Force Bedford, Massachusetts 01730	
13. ABSTRACT <p>A bibliography of lunar and planetary research articles published during 1966 is presented with both subject and author listings. The major subject categories are: astrobiology, comets, meteorite craters and cratering effects meteors and meteorites, the moon, origin of the solar system, the planets, and tektites. Each article is abstracted.</p>		

DD FORM 1473  
1 JAN 64

Unclassified  
Security Classification

Unclassified

Security Classification

14.	KEY WORDS	LINK A		LINK B		LINK C	
		ROLE	WT	ROLE	WT	ROLE	WT
	Planetology Moon Planets Meteorites Tektites Astrobiology						

Unclassified

Security Classification